Characterization of the Hewitt Lake and Leta Arm groups, Indin Lake Greenstone Belt, Northwest Territories

Tshepiso Moipane Sekhula

A thesis submitted in partial fulfillment of the requirements

of the degree of Master of Science

Department of Geology

Lakehead University

July 2025

Abstract

Exposures of the Leta Arm (LA) group and southwestern Hewitt Lake (HL) group volcanic rocks in the northeast-trending 2670-2629 Ma Indin Lake Supracrustal Belt (ILSB) of the western Slave Craton were studied to understand their composition, petrogenesis and tectonic setting. This was achieved by integrating petrology, mineral chemistry, whole-rock geochemistry, U-Pb zircon geochronology, and Sm/Nd isotope analyses. Samples were collected through a combination of surface geological mapping and sampling of historic drill core from different lithologies within the central ILSB volcanic rocks.

The ≤2670 Ma HL group is amphibole-rich and comprises mafic and intermediate rocks of basaltic and andesitic composition whereas the 2668-2673 Ma LA group is pyroxene-rich and contains mafic through felsic units ranging from basalt to rhyolite. Alteration was mainly the result of metamorphic processes based on the abundance of ferro-hornblende, actinolite, carbonates, sericite, epidote and minor biotite, quartz, rutile and Fe-Ti oxides. Metamorphic conditions vary from greenschist to amphibolite facies and revealed an interplay of prograde and minor retrograde metamorphism based on amphibole chemistry and the textural relations with primary phases in the rocks. Metamorphism was regional and accompanied by plastic deformation resulting in the formation of high temperature microstructures.

Mafic tholeiites of the western HL and LA groups likely formed in an oceanic plateau based on their flat REE on primitive mantle-normalized spider plots, positive to minor Nb anomalies and low La/Sm_N values of <2. The eastern LA group basalts and felsic to intermediate rocks are characterized by LREE enrichment (La/Sm_N up to 5.47), positive Th anomalies, negative Ti and

Nb anomalies as well as both positive and negative Zr-Hf anomalies. These characteristics are typical of arc-type rocks formed by metasomatism of a mantle wedge above a subducting slab. Low Gd/Yb_N values < 2.80 in both groups suggest melting at shallow depths in the absence of garnet, possibly suggesting an oceanic rather than continental arc setting. Positive ε_{Nd} values suggest that the rocks did not interact significantly with older crust. The variable negative Nb anomalies in the arc rocks could be the result of crustal contamination or a subduction zone signature as slab-derived fluids stabilize Nb-bearing phases in the slab, leading to depletions of Nb in the metasomatized mantle. The Coterill tonalites may have been the source of contamination and the broadly similar age to the volcanic rocks would allow for modification of the whole rock signature without modifying the isotopic make-up of the LA and HL rocks.

Data from this study was used to revise the existing tectonic model for the ILSB volcanic rocks. The new model places the initial formation of the western basalts in an oceanic plateau which collided with a west-moving crustal block and clogged the subduction zone due to its buoyant nature with a new subductions zone forming behind the plateau. Arc magmas from the subducting slab erupted through and onto the plateau to form primitive arc tholeiites and the intermediate to felsic rocks observed in the ILSB.

Acknowledgments

Firstly, I would like to thank my supervisor Pete Hollings for guiding and mentoring me during my studies. Thank you for being patient and understanding. It was not easy, but you made it possible for me to get this far. I extend my appreciation to John McBride and the STLLR Gold Inc team for funding and summer jobs. Working with you has been very insightful.

I am grateful for the funding provided by NSERC (Natural Sciences and Engineering Research Council of Canada) and conference opportunities by the NTGS (Northwest Territories Geological Survey) and NAPEG (Northwest Territories and Nunavut Association of Professional Engineers and Geoscientists). I am very grateful for their assistance as it made a huge difference. I would also like to thank Dr. Jonas Valiunas and Kristi Tavener for their efficiency in thin section preparations. My writing sessions and consistency would not have been as great without the help of Dr. Moses Angombe who constantly motivated me to test my limits during this research. Thanks to Turner Green and my colleagues at Lakehead University for the discussions and helping me understand my data better.

To my family, friends and loved ones, thank you for your greatest support and nurturing love. You have motivated me to see this research through, and I cannot thank you enough.

Table of Contents

List of Figures

List of Tables

1. Introduction

1.1. Background

The Indin Lake Supracrustal Belt (ILSB) hosts numerous mineral occurrences some of which have been mined, such as the Colomac gold deposit (Morgan, 1991; Pehrsson & Kerswill, 1996; Pehrsson, 1998; Poulsen et al., 2000; Anhaeusser, 2014). Several studies have been conducted on the ILSB and other gold deposits in the Northwest Territories (NWT) by the Geological Survey of Canada (GSC) as part of the Exploration Science and TECHnology (EXTECH) program (Anglin & Wright, 2006 and references therein). In addition, a PhD study by Pehrsson (1998) led to a publication that brought many insights into the evolution of the belt and bracketed the age of the ILSB between 2670 and 2630 Ma (Pehrsson & Villeneuve, 1999). The study also generated an improved geological map of the area and reconstructed the tectono-metamorphic history of the belt. Exploration continues to this day to fill knowledge gaps, discover new deposits and extend known ones.

1.2. Problem statement

Despite earlier work, geochronological and geochemical information on the ILSB volcanic rocks is still sparse. There is a lack of detailed insights into the petrogenetic attributes such as their magma source, the tectonic setting in which they formed, and modification processes such as contamination or alteration. A link between mineral-hosting sills and volcanic rocks of the belt is still unclear and this limits exploration. Only the rocks in the Colomac area, the most endowed part of the belt bounded by mafic to felsic rocks of the Leta Arm group, are relatively well constrained although with minimal geochronology. A lack of detailed information on the ILSB

means there is a need for advanced studies given the extent of the belt. This thesis provides constraints on some of the missing geological aspects in the belt by utilizing advanced techniques. The data provides new insights into the magma source, timing of volcanism, tectonic setting, mineralisation and its associated host rocks.

1.3. Aims and objectives

The aim of this study was to reconstruct the petrogenetic history of the Leta Arm and southwestern Hewitt Lake groups using an integration of field mapping, core logging, whole-rock geochemistry, U-Pb TIMS (Thermal Ionization Mass Spectrometry) geochronology, mineral chemistry by Electron Probe Microanalyzer (EPMA), and radiogenic Sm-Nd isotopes. The study aimed to constrain the Colomac sill by establishing a link between host volcanic rocks and their association with the ILSB assemblages. This was achieved by:

- Characterising the geochemistry of lithostratigraphic groups
- Determining hornblende compositions in the two groups
- Characterising the magma source and tectonic setting
- Constraining the timing of volcanism
- Constraining the degree of contamination
- Developing a revised geological map

1.4. Location and access

The study area is located approximately 220 km northwest of Yellowknife, Northwest Territories, Canada within the 930 km^2 STLLR Gold Incorporated property (64°24'N and 115°06’W, Fig. 1.1). The area is accessible by aircraft in the summer whereas in the winter, access is by a combination

of all-season and winter roads. The all-season road starts from Yellowknife through Behchokǫ̀ and Whatì which transitions to a 245 km-long winter road that branches off at Matteberry Lake leading to Indin Lake (Robb, 1997).

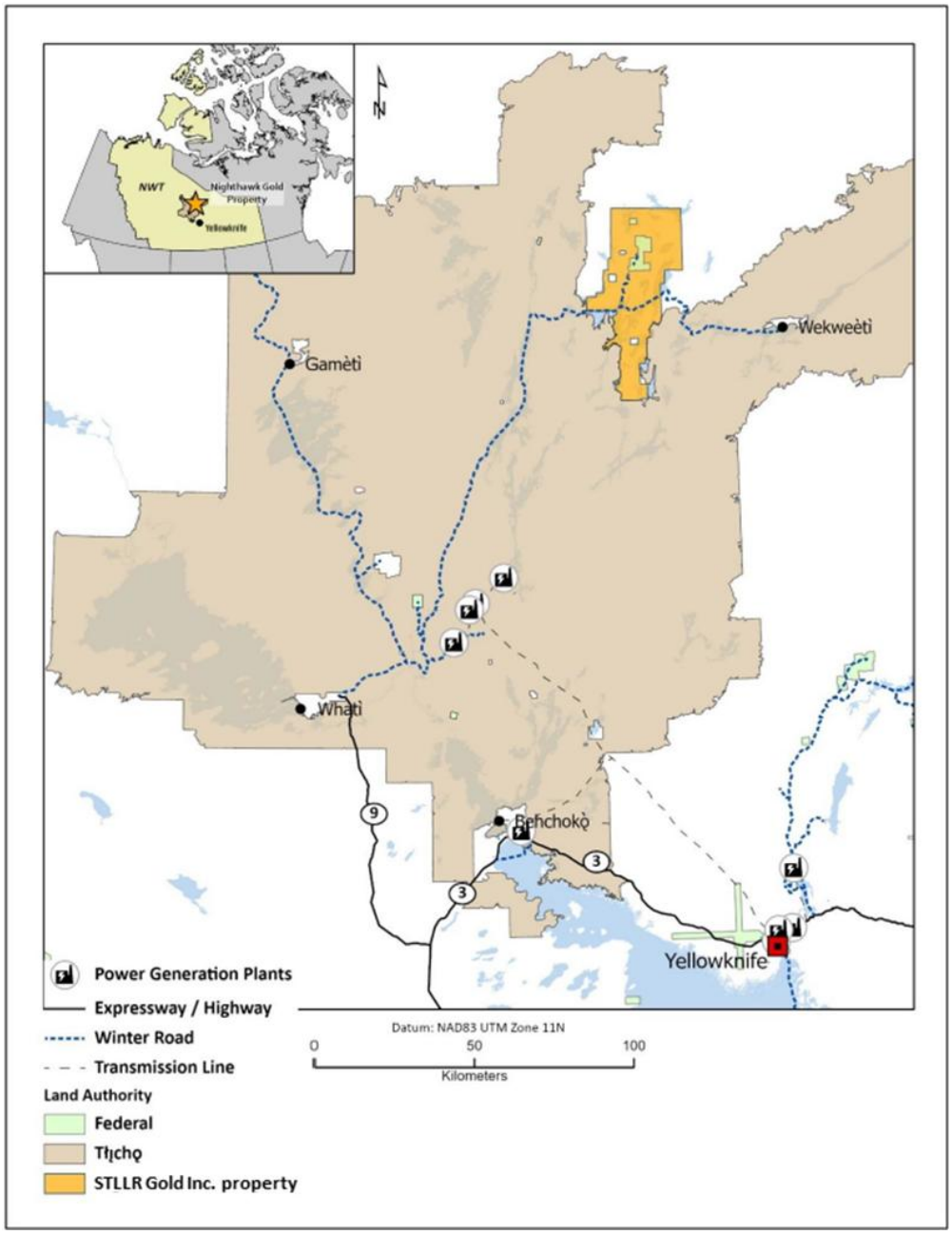

Figure 1.1. A) Location map of the ILSB within the STLLR Gold Inc. (orange area) with reference to the Northwest Territories, Canada. The map shows access roads to the ILSB (Lund, 2023; STLLR Gold Inc., 2023).

2. Geology of the Indin Lake Supracrustal Belt

2.1. The Slave Province

The Slave Province is a heterogeneous granite-greenstone sequence that encompasses supracrustal volcano-sedimentary rocks and a suite of voluminous (>60%) syn- to post-volcanic granitoids (Fig. 2.1, Van Breemen et al., 1992; Pehrsson et al., 1995; Villeneuve et al., 1997). The sequence includes and is underlain by metavolcanic and metasedimentary rocks of the 2600-2720 Ma

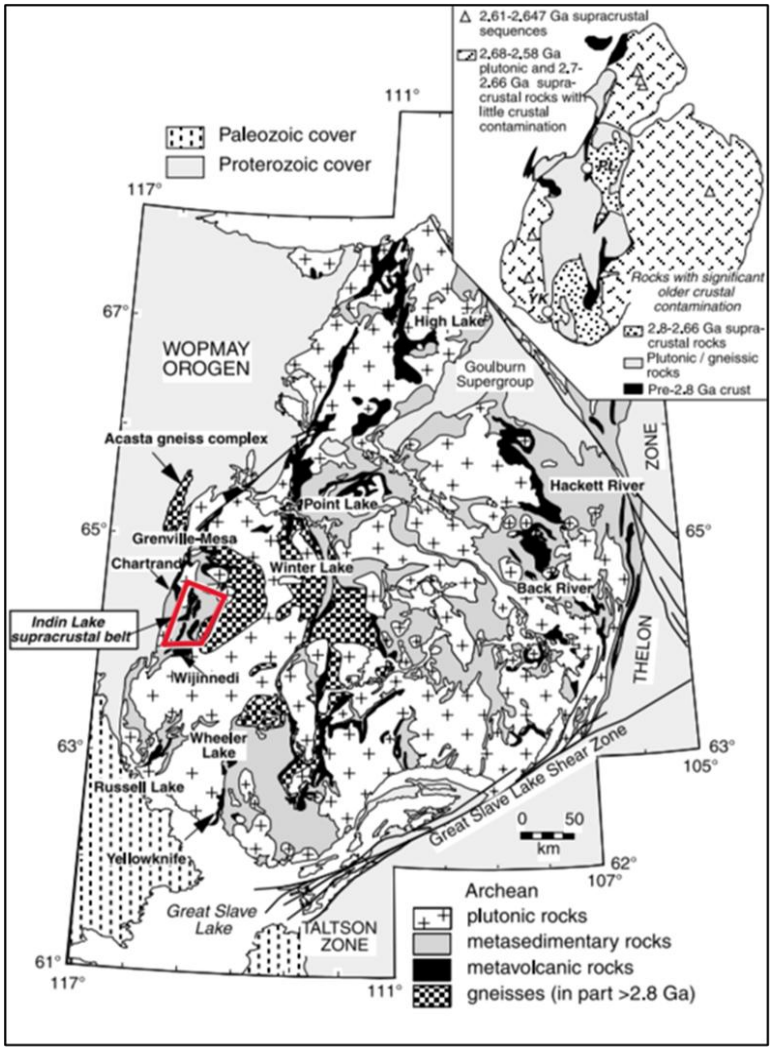

Figure 2.1. Geological map of the Slave Province and location of the ILSB (Hoffman, 1989; Pehrsson, 1998; Pehrsson & Villeneuve, 1999).

Yellowknife Supergroup (Henderson, 1972; Pehrsson, 1998). The Yellowknife supergroup is underlain by 2700 to 2650 Ma gneisses and granitoids that vary in composition from a suite of tonalite-trondhjemite-granodiorite (TTGs) to diorite (Pehrsson, 1996; Pehrsson, 1998) The oldest rocks in the Slave Province are >2800 Ma (e.g., the Acasta gneiss complex) and include tonalitic to granitic gneisses which are only found in some parts of the western and central Slave Province (Fig. 2.1; Villeneuve et al., 1997; Pehrsson, 1998). The central Slave Province is characterized as basement-cover high-strain zones, with basement rocks reaching up to 3.3 Ga in age (Bleeker et al., 1999). The southwestern margin of the Slave Province hosts the Indin Lake Supracrustal Belt bounded by rocks of the Grenville-Messa to the north, Winter Lake to the east and Wijinnedi to the south (Fig. 2.1; Hoffman, 1989; Pehrsson, 1998).

2.2. The Indin Lake Supracrustal Belt (ILSB)

The ILSB is a NE-trending sequence of metamorphosed and deformed volcano-sedimentary rocks with an aerial extent of ~2200 km^2 (Fig. 2.2; Frith, 1993; Pehrsson & Villeneuve, 1999; Poulsen et al., 2000; Anhaeusser, 2014). Rocks in the area encompass units of Archean ages, representing some of the oldest lithologies in the NWT (Pehrsson, 1998). Mafic to felsic metavolcanic rocks of the ILSB are intercalated with and conformably overlain by metasedimentary rocks (Frith, 1993). The stratigraphy of the belt is divided into three groups based on their extent, age, composition and volcanic facies (Figs. 2.2 & 2.3; Pehrsson, 1998). The ILSB is bounded by the Cotterill gneiss complex to the east along the Daran Lake fault (D3 fault) and Archean granitoid plutons and migmatites to the north and west (Fig. 2.2; Pehrsson & Kerswill, 1996; Pehrsson & Villeneuve, 1999). The 2680 ± 3 Ma Coterill complex to the east of the ILSB extends over 90 km^2 and is made up of a heterogeneous mixture of monzogranite, amphibolite, paragneiss and orthogneisses which together with the ILSB are intruded by syntectonic biotite-tonalite bodies (Pehrsson, 1998).

2.2.1. Lithogeochemistry of volcano-sedimentary rocks of the ILSB

The lowermost undated unit in the ILSB is the Hewitt Lake group which occurs as a 50 km long x 750 m thick homogeneous unit that is more laterally continuous than the other groups (Pehrsson, 1998). It is distinguished by its extensive carbonate alteration together with facies ranging from syn-volcanic gabbroic sills, submarine mafic flows and minor calc-alkaline felsic volcanic (<20%), and epiclastic rocks. Felsic volcanic rocks form discontinuous lenses interbedded with mafic flows (Pehrsson & Villeneuve, 1999). Quartz-feldspar porphyry dykes and hypabyssal sills intrude the mafic volcanic rocks and are interpreted to be the source of magma for the felsic volcanic rocks (Pehrsson, 1998; Pehrsson & Villeneuve, 1999). The Hewitt Lake group is crosscut by a 2670 ± 2 Ma porphyry sill constraining the minimum age of the assemblage (Fig. 2.2; Pehrsson, 1998).

Overlying the Hewitt Lake group along a contact marked by polymictic volcanogenic conglomerate is the Leta Arm group with U-Pb zircon ages ranging between 2671 +8/-7 Ma and 2668 +5/-3 Ma acquired from felsic units (Fig. 2.2; Pehrsson & Villeneuve, 1999). It shows more heterogeneity associated with sudden lateral and vertical facies changes (Fig. 2.3; Pehrsson, 1995; Pehrsson, 1998; Pehrsson & Villeneuve, 1999). Lithologies include tholeiitic and calc-alkaline mafic through felsic volcanic rocks, and gabbro to quartz diorite syn-volcanic intrusions (Pehrsson, 1998).

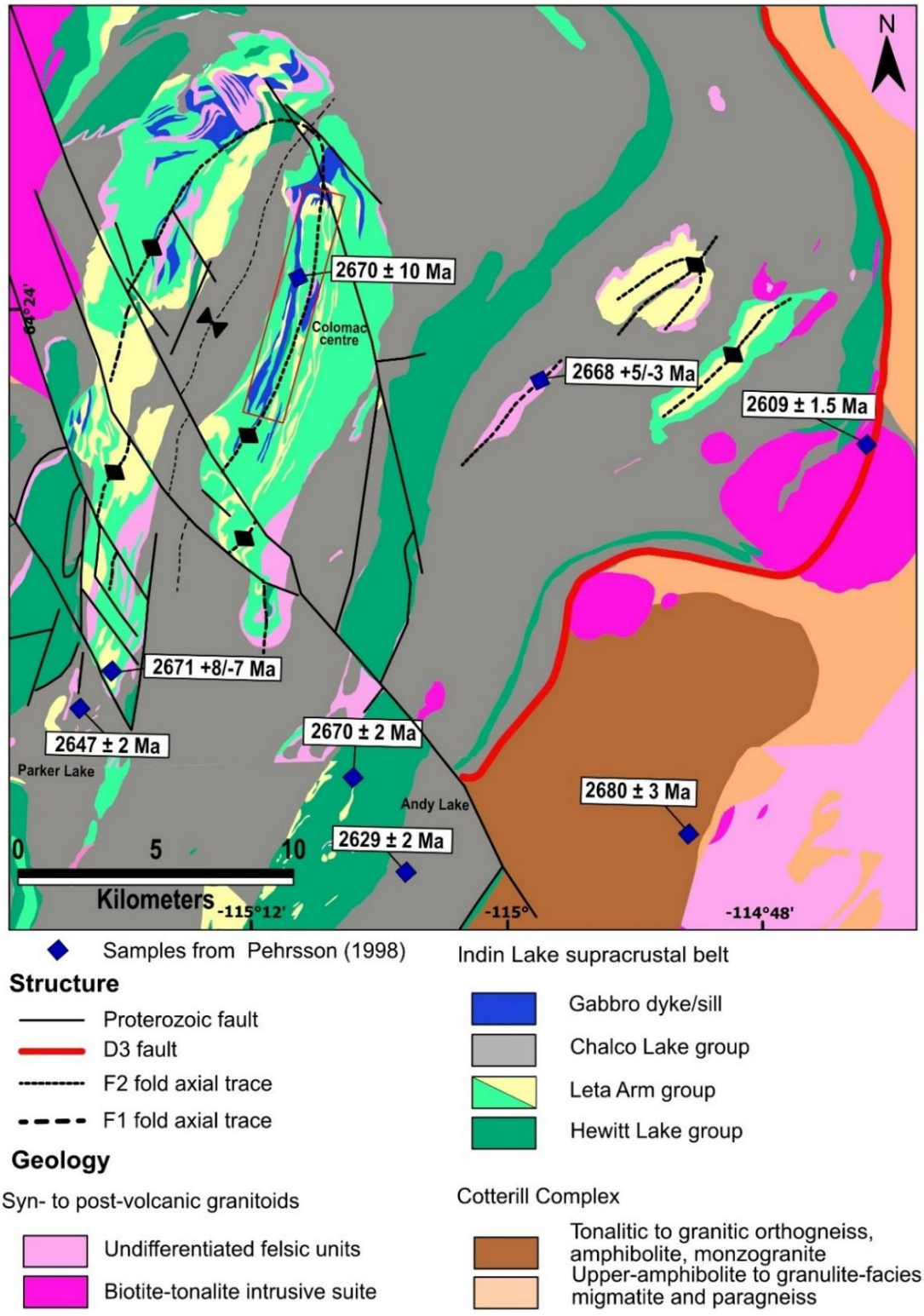

Figure 2.2. Geological map of the ILSB showing deformation structures, ages from previous studies and the Colomac centre area (modified after Pehrsson, 1998; Pehrsson & Villeneuve; 1999; STLLR Gold Incorporated, 2023).

The uppermost Chalco Lake group forms a large portion of the ILSB and consists of graded greywacke, mudstones, minor iron-formation, conglomerate, and felsic volcanic rocks. The rocks have been interpreted to have formed in depositional settings representative of submarine

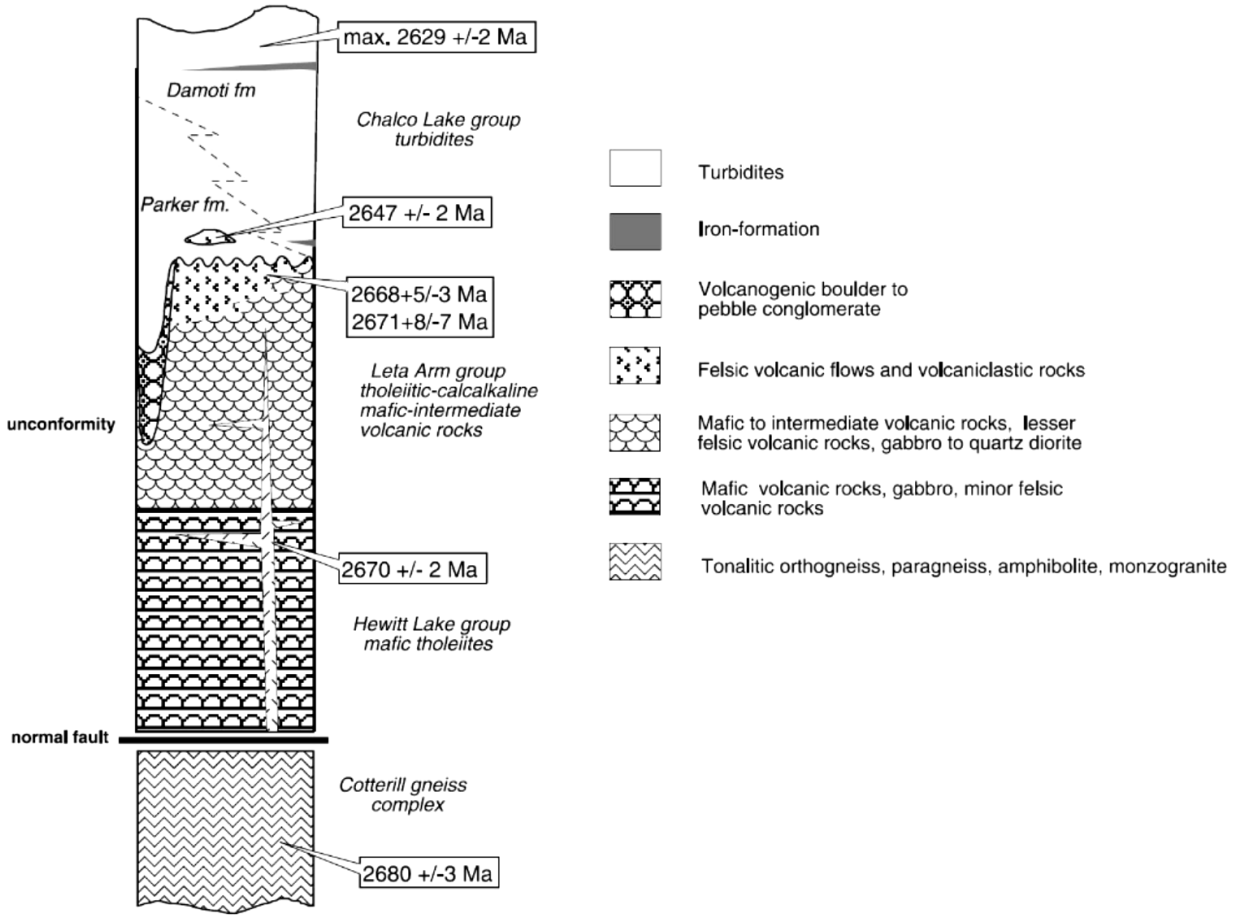

Figure 2.3. Lithostratigraphic column of the ILSB showing ages, formations and boundaries between the ILSB groups (Pehrsson, 1998; Pehrsson & Villeneuve, 1999; STLLR Gold Incorporated, 2023).

turbidites that have been subdivided into the central Parker Formation and marginal Damoti Formation (Fig. 2.3; Pehrsson, 1998; Pehrsson & Villeneuve, 1999). Thick beds of the Parker Formation (2647 ± 2 Ma; rhyolite) underlie the center of the ILSB where rocks comprise silty to sandy turbidites interbedded with felsic volcanic flows, volcanic conglomerate, hypabyssal intrusions and breccias (Figs. 2.2 & 2.3; Pehrsson, 1998). The contact between the Parker

Formation and the Leta Arm is marked by a narrow polymictic volcanic conglomerate. Rocks of the Damoti Formation (2629 ± 2 Ma; greywacke) are thinly bedded, directly deposited on the Parker Formation and mark the margins of the ILSB (Fig. 2.3). The formation includes pelite-dominated turbidites interlayered with iron formation and sulfidic and graphitic argillite (Brophy, 1995; Pehrsson & Kerswill, 1996).

The ILSB is interpreted to have formed from fractionated mantle melts that had little interaction with significantly older crust (positive ε_{Nd} signatures; Chacko at el., 1995; Pehrsson, 1998). Despite minor geochemical differences between the Hewitt Lake and Leta Arm groups (e.g., abundant calc-alkaline rocks in the Leta Arm group), they could be genetically associated (Pehrsson, 1998). Mafic tholeiites of both groups have similar Ni (32-186 ppm) values, flat REE patterns characteristic of Archean mafic volcanics, low to moderate TiO_2 (0.88-1.75 wt%) and $(La/Yb)_{ch}$ >1, suggesting they are geochemically similar. Pehrsson (1998) proposed that the tholeiites of the two groups formed in a juvenile arc setting. The arc then evolved to form minor and more abundant calc-alkaline suites of the Hewitt Lake and Leta Arm groups respectively. The Hewitt Lake group formed a submarine substrate on which rocks of the Leta Arm group were deposited in a subaerial environment during uplift as a result of an emergent modern-day-type arc at the time that the Leta Arm group was forming.

The Chalco Lake group calc-alkaline felsic rocks are interpreted as a geochemically distinct suite with no link to the Hewitt Lake and Leta Arm groups. They are interpreted to have formed in a submarine setting to deep marine basin by injection into and on top of the Leta Arm group by 2647 Ma (Fig. 2.3; Henderson, 1998; Pehrsson, 1998). Their tectonic setting is characterised as either forearc or back-arc basin that transitioned to a remnant ocean basin environment (Pehrsson, 1998).

2.2.2. Deformation and metamorphism

Five deformation events (D_1-D_5) have been identified in the ILSB, three Archean (D_1-D_3) and two Proterozoic (D_4 and D_5; Pehrsson, 1998). D_1 is associated with low to middle greenschist facies metamorphism at 4-5 kbar between 2629 and 2609 Ma (crystallization age of the Strachan pluton), causing folding of bedding planes into moderately to steeply doubly-plunging isoclinal folds (Pehrsson, 1998). Dip-slip faults and planar fabrics observable as bedding-parallel slatey cleavage and foliation also occur and likely formed in an originally east- northeast-trending fold-fault belt (Pehrsson & Villeneuve, 1999). Pehrsson and Villeneuve (1999) interpret D_1 as an imbrication event of the ILSB to a structural stack. D_2 occurred between 2609 Ma and 2590 Ma (age of monzogranite intrusions that crosscut D2 structures) and overprints bedding planes by S_2 cleavage, faults, and upright to open isoclinal folds. Coeval with D_1 and D_2 are regional metamorphic events that range in grade from greenschist to amphibolite (M_2) facies respectively (Fig. 2.2, Pehrsson, 1998). M_1 was low to middle greenschist facies metamorphism at 4-5 kbar (Pehrsson & Chacko, 1997). M_2 resulted in regional upper-amphibolite low-pressure (LP) high-temperature (HT) conditions at 350-600°C and 3.3-4 kbar (Pehrsson and Villeneuve, 1999). D_1 and D_2 formed the present-day architecture of the rocks in the belt (Pehrsson, 1998; Pehrsson & Villeneuve, 1999). D_3 juxtaposed the ILSB with the Cotterill Complex along the Daran Lake normal fault at ~2590 Ma (Pehrsson, 1998; Pehrsson & Villeneuve, 1999). This event is associated with high-grade metamorphism at retrograde amphibolite-facies and is the consequence of melt-assisted exhumation of the Cotterill complex gneisses (Pehrsson & Chacko, 1997; Pehrsson, 1998). The Proterozoic D_4 and D_5 events occurred between 2035 and 1830 Ma and were of relatively low temperature conditions than the above events. D_4 formed local open cross-folds, cleavage planes, kink bands and extensive NW-trending sinistral strike-slip faults while D_5 formed exhibits

cleavage, kink bands and minor gently W to SW dipping reverse faults (Fig. 2.2; Pehrsson, 1998; Pehrsson & Villeneuve, 1999).

2.2.3. Mineralisation in the ILSB

A large fraction of the mineralisation in the ILSB is hosted in pre-deformation intrusive suites of the Leta Arm and Hewitt Lake groups. The belt hosts about 131 gold occurrences which have been discovered since the 1930s including the Colomac, Goldcrest, Grizzly Bear, 24 zone, and 27 zone deposits of the Leta Arm group. Minor mineral occurrences of the Cass, Kim and Snowden gold deposits are found in the Hewitt Lake group (Morgan, 1991; STLLR Gold Incorporated, 2023). This project is associated with the previously mined Colomac Main deposit (Figs. 2.2 & 2.4; Morgan, 1991; Pehrsson and Villeneuve, 1999). The deposit is hosted within the 2671±10 Ma medium-grained doleritic to gabbroic Colomac sill complex on the eastern Leta Arm group andesites (Morgan, 1991). The sill is interpreted to be synvolcanic and subparallel to volcanic rocks of the Leta Arm group and has a NNE strike and subvertical east-dipping foliation as a result of rotation during deformation (Morgan, 1991). The diorite dominantly consists of blue quartz-eye features and magnetite contents up to 15%. Incorporated within the sill are 10s to 100s of meter-thick andesitic enclaves (15%) possibly acquired from neighbouring andesites (NWT Geoscience Office, 2012). Accessory mineral phases include amphibole, biotite, chlorite, carbonate, epidote, pyrite (≤2%), pyrrhotite, and magnetite (NWT Geoscience Office, 2012).

Trace element data from the sill supports crystal fractionation of the magma to form a large package of tonalite-trondhjemite lithologies with basal coarse-grained mafic rocks (now the western part of the Colomac sill) and upper fine to medium-grained intermediate to felsic rocks (now the eastern part of the sill; Figs. 2.2 & 2.4; NWT Geoscience Office, 2012). The upper

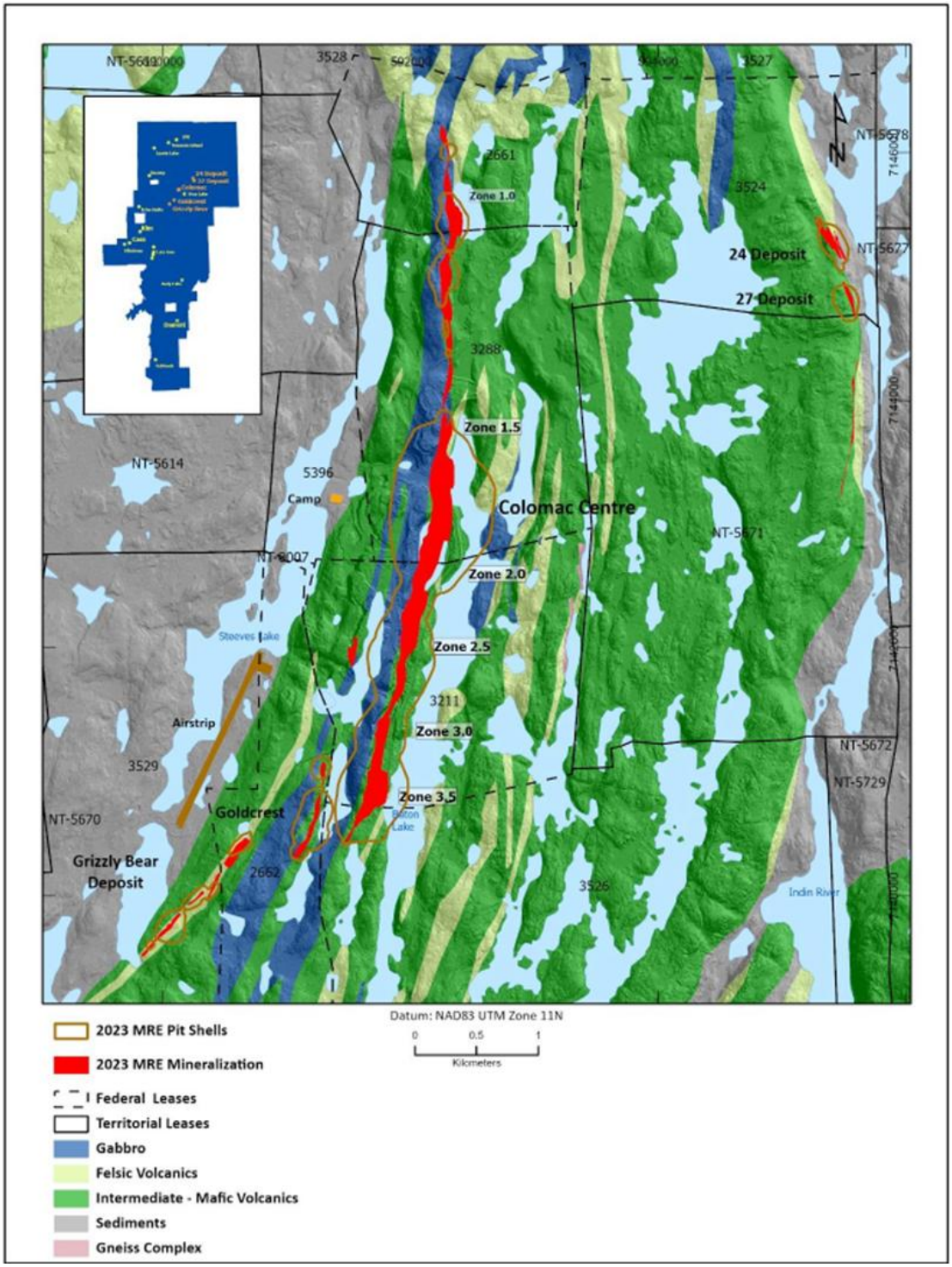

Figure 2.4. Geological map of the Colomac sill in the eastern Leta Arm group showing sites of mineralisation (STLLR Gold Incorporated, 2023).

(eastern) diorite portion of the sill hosts a large proportion of the gold mineralisation due to its competency and brittle behaviour during deformation, which maximized fluid flow and precipitation in quartz stockworks and 0.5-10 cm-thick tensional quartz veins (STLLR Gold Incorporated, 2023). Gold grades in the deposit for open pit resource estimates range between 1.45 g/t Au and 1.97 g/t Au for inferred tonnages of 54.404 million tonnes and 2.625 million tonnes respectively. Underground resource estimates show a grade range of 1.77-1.97 g/t Au at an inferred tonnage ranging between 8.750-10.017 million tonnes (Lund et al., 2023; STLLR Gold Incorporated, 2023).

3. Methods

3.1. Field sampling

Field sampling was conducted in the summer of 2023 by walking traverses across representative lithologies based on previous mapping in the eastern, western, southern Leta Arm group and southern Hewitt Lake group. This was done to maximize coverage of the belt in the property, mostly on sub-crop due to low rock exposure and high vegetation cover in the area. Sampling focused mainly on rock-type distribution and field features where observable. The ILSB was mapped through a series of geological traverses along riverbed channels and perpendicular to dominant lithological contacts. Geological traverses and other observations led to the development of a revised geological map. As some areas between traverses were not mapped in this study, the development of this new map also used information from previous mapping and drilling by company geologists in conjunction with inferences from previous mapping by Pehrsson (1998).

In the Leta Arm group (on previous maps), one NW-SE trending transverse was taken in the east (Grizzly bear-24/27 zones), two NE-SW trending transverses were made in the south (Kim-Cass) and four east trending transverses were taken in the western (Swamp) area (Fig. 3.1). Only the southwest part of the Hewitt Lake group was examined and sampled for this study. The Leta Arm group is preserved in the central part of the mapped area (light green to yellow units) and is surrounded by the Hewitt Lake group (dark green units; Fig. 3.1). A thin section and geochemistry sample were simultaneously collected from each locality. Samples for geochronology were acquired only from felsic units in all parts of the belt as these units have shown to have visible zircon in previous studies. A total of 210 samples were collected from both groups. (Fig. 3.1; Appendix II) An additional four geochronology samples were acquired from drill core in the

summer of 2024 from felsic units of the eastern Leta Arm Group as previous lithologies from this section yielded little to no zircon.

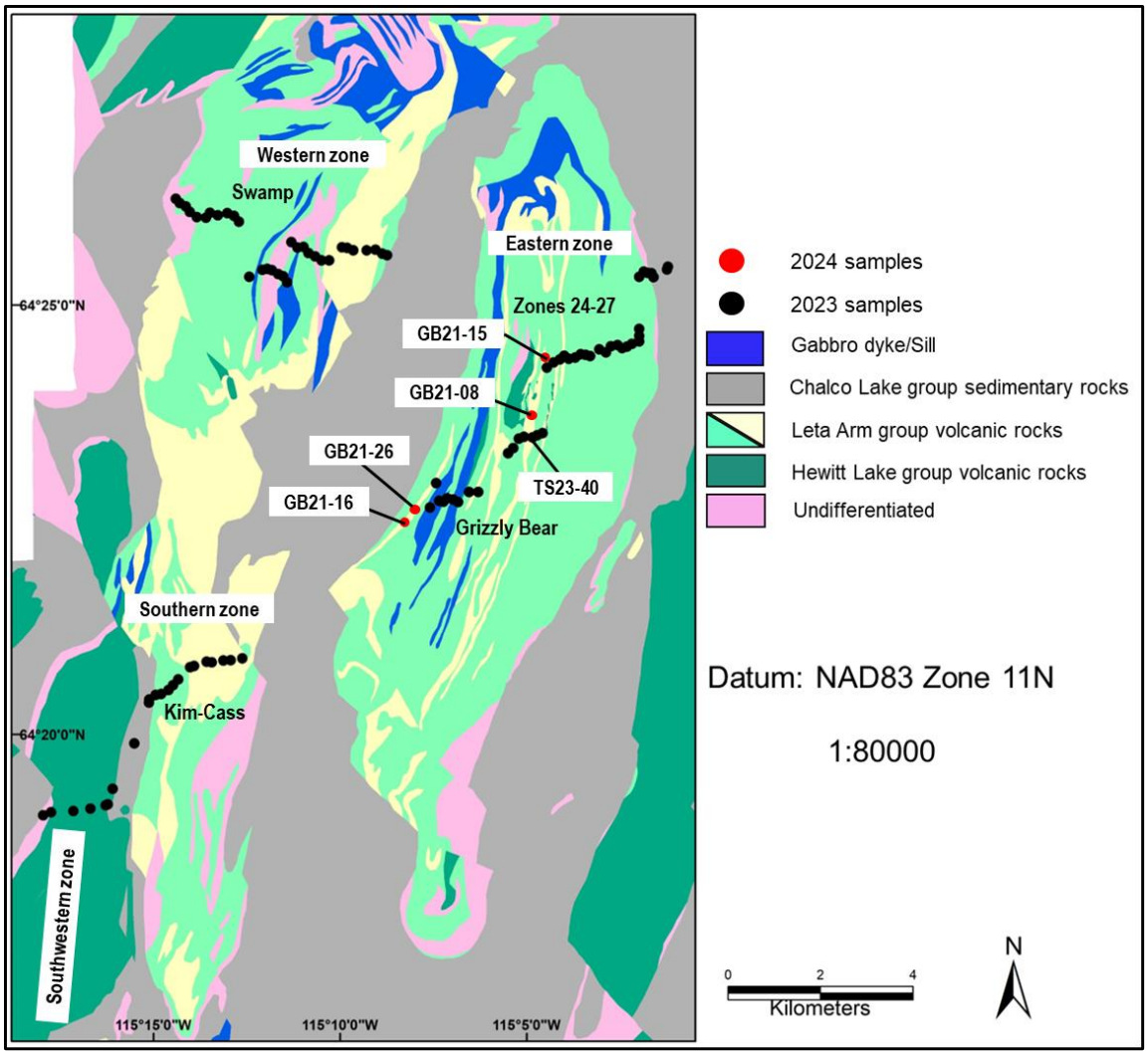

Figure 3.1. Geological map of the study area showing sample locations and spatial zones (Pehrsson, 1998; STLLR Gold Incorporated, 2023).

3.2. Petrography

Polished thin samples from 40 samples from representative lithologies of both groups were prepared at Lakehead University's lapidary facility by the technicians at the university. The polished thin sections were then imaged using a combination of the Zeiss axioscope and Olympus

SC180 camera attached to the Olympus BX 51 microscope at Lakehead University. Petrographic analysis was conducted to determine modal abundances, classify rock types, establish textural relations, identify alteration minerals and characterize deformation. The petrography was carried out using PPL plain polarized light (PPL) and XPL crossed polarized light (XPL) photomicrographs (Appendix I). Volcanic rock types were classified as basalt, andesite, dacite and rhyolite using the IUGS subcommision on the Systematics of Igneous Rocks (Le Bas, & Streckeisen, 1991). Silica content as well as major and trace element abundances from whole-rock geochemistry were used in combination with petrography to determine rock types. This was done by plotting the elements against silica for rock classification on discrimination diagrams (Chapter 4.4).

3.3. Whole-rock geochemistry

The 96 samples collected for geochemistry were submitted to ALS in Yellowknife Bay for complete characterization package (CCP-PKG01) which includes major, trace, and volatile trace elements together with base metals, C and S. The analysis was completed by ALS and the method involved crushing the sample into powder material (<75 μm) followed by fusion within lithium borate ($LiBO_2/Li_2B_4O_7$). This maximized the liberation of major and trace elements for analysis with ICP-ES (inductively coupled plasma-optical emission spectroscopy) and ICP-MS (inductively coupled plasma mass spectrometry) respectively. During this process fluids retained in the rock are also expelled and recorded as LOI (Loss on Ignition). Details on representative elemental abundances used in the thesis and LOI are found in Appendix II.

3.4. Electron Probe Microanalysis (EPMA)

Three polished thin sections of basalts and an andesite were sent to the Department of Earth Sciences at the University of Manitoba for EPMA of amphibole grains. The analysis was done by the University of Manitoba and utilized the SX-100 Electron Probe Microanalyzer by Cameca (Gennevilliers Cedex, France) for major element and halogen contents. The model uses mass absorption coefficient (MAC) values from Chantler et al. (2005). The standards used for the analysis include pyrope (Ca, Si), ribeckite (F), pyrope (Al), rutile (Ti), orthoclase (K), tugtuphite (Cl), olivine (Mg), fayalite (Fe), albite (Na), and spessartite (Mn). Operating conditions were: accelerating voltage of 15 kV, beam current of 20 nA with a beam size of 5μm and raster length of 66 μm. Peak counting times were 60 seconds for Ca, 30 seconds for Fe and Mn and 20 seconds for Si, Mg, Al, Ti, K, Na, Cl and F (See appendix III for EPMA analysis report).

3.5. U-Pb zircon Isotope Dissolution Thermal Ionization Mass Spectrometry (ID-TIMS)

ID-TIMS was used in this study to measure parent-daughter isotopic ratios of uranium (U) and lead (Pb) in zircon, which are required for geochronology. This method was used due to its ability to produce dates with accuracy and precision 10-100 times higher than in situ techniques such as LA-ICP-MS (laser ablation inductively-coupled plasma mass spectrometry). It can also measure isotopic ratios from small-size or zoned crystals. Initially, seven samples were submitted for geochronology in 2023 to the Pacific Center for Isotopic and Geochemical Research of the University of British Columbia (PCIGR) and of these, only one (TS23-40; Appendix IV) yielded zircons. An additional four samples were sent to the University of Toronto in 2024 and three samples (TS23-01, TS23-05 and TS23-07 from drillholes GB21-16, NL21-08 and GB21-26 respectively) yielded zircons (Fig. 3.1; Appendix IV). Both labs followed the procedure of Mattinson (2005) for crushing, acid dissolution and separation of zircons. The samples were

crushed using a jaw crusher, ground to powder (<200 μm) from which heavy minerals were separated through a shaking riffled water (Wilfley) table, and processed further by density separations with methylene iodide, and magnetic separations with a Frantz isodynamic separator. The highest quality, least magnetic, freshest, least cracked, core-and inclusion-free grains of zircon were hand-picked in alcohol under a binocular microscope.

At the University of Toronto, the zircon grains were chemically abraded first via annealing in quartz crucibles at 900°C for 2 days (procedure modified after Mattinson, 2005). This removed much of the radiation damage induced by Pb-loss through decay of U and Th contained in the mineral, rendering least altered zircon more inert to chemical attack. The annealed grains were subsequently etched in approximately 0.10 ml of concentrated hydrofluoric (HF) acid for several hours in Teflon vessels at 205°C. Chemically abraded zircon fractions were washed and sonicated in 7N HNO_3 for approximately 30 minutes prior to dissolution. A mixed ^{205}Pb-^{235}U isotopic spike was added to the dissolution capsules during sample loading. Zircon was dissolved using concentrated HF in Teflon bombs at 205°C for 3-4 days, then dried and re-dissolved in 3N HCl overnight (Krogh, 1973). U and Pb were isolated using 50 μLanion exchange columns using HCl elutions, dried down, and then loaded onto outgassed zone-refined rhenium filaments with silica gel (Gerstenberger & Haase, 1997). The PCIGR facility in British Columbia also mixed zircon grains in HF and nitric (HNO_3) acids at ratios of 10:1, sealed and left for complete dissolution for a duration of 40 hours following the method of Scoates and Scoates (2013). The solution was subsequently evaporated at 130°C on a hot plate followed by mixing of the remains with a 3.1N hydrochloric acid (HCl) using a high-pressure device at 210°C and left for 12 hours (Scoates and Scoates, 2013).

Lead (Pb) and UO_2 were analyzed on a VG354 mass spectrometer using a Daly collector in pulse counting mode. The mass discrimination correction for this detector was constant at 0.07%/AMU. Thermal mass discrimination corrections were 0.10%/AMU for Pb and U. Deadtime of the Daly system was 18 ns for Pb during the analytical period, monitored using the SRM982 Pb standard. Mass spectrometer data was reduced using in-house software (UtilAge program) coded by D. Davis. Corrections for initial ^{230}Th disequilibrium in zircon have been applied to the $^{206}Pb/^{238}U$ ages, assuming a Th/U ratio in the magma of 4.2. All common Pb was assigned to procedural blank. Initial Pb from geological sources above 1 picogram was corrected using the Pb evolution model of Stacey and Kramers (1975). Lead (Pb) and uranium (U) separation and purification at the PCIGR facility was by ion exchange using the methodology of Parrish et al. (1987) then removed and put into containers employing methods of Scoates and Scoates (2013). The facility took BSE (back-scattered electron) images of the zircons and analyzed them with a VG354S mass spectrometer or VG54R TIMS instrument linked to a UBC ^{205}Pb-$^{233-235}U$ isotope tracer or an EARTHTIME ET535 tracer.

Plotting of Concordia curves and averaging of age results from the University of Toronto were carried out using Isoplot 3.71 Add-In for MS Excel, of Ludwig (2009). The curve for Concordia in these plots is shown as a 'band', incorporating uncertainties in the ^{235}U and ^{238}U decay constants. Final ages for the samples do not incorporate uncertainties in the U decay constants. Age errors and error ellipses are shown at the 2 sigma or 95% level of confidence. In the Concordia diagrams presented, each show a dashed chord through the data, the calculated weighted average age (on Concordia) for the data, and the origin (this is shown for reference only and is not involved in a regression of the data). For weighted average calculations, data points are weighted according to

the inverse-square of their assigned errors. Concordia diagrams from the PCIGR facility were plotted using the Ludwig (2003) procedure on IsoplotR software.

3.6. Samarium-Neodymium (Sm-Nd) isotope analysis by TIMS

Samarium and Nd isotopes are used to characterize the source of magma from which igneous rocks originate. This is commonly achieved by comparing initial mantle Nd ratios during the formation of crustal material and product ratios of Sm and Nd in crustal rocks formed from evolved melts that segregated from the mantle. The increase of $^{143}Nd/^{144}Nd$ ratios is influenced by the incorporation of radiogenic ^{143}Nd in felsic minerals during fractional crystallisation and this permits constraints on the timing of crustal material formation. Whole-rock geochemistry was used to select the 13 least altered samples for Sm-Nd analysis. The samples were then sent to the University of Newfoundland Memorial. Sample preparation began by weighing samples into Savilex Teflon capsules which were then spiked with a mixed $^{150}Nd/^{149}Sm$ spike before being dissolved using a 6 ml (2:1) mixture of 29 M HF-15 M HNO_3. The solution was evaporated to dryness after a week of acid digestion on a hotplate and taken back up in 8M HNO_3 for a week followed by 6M HCl for another week. The dried sample was then re-dissolved in 2.5 M HCL. Samples were then loaded into a column containing cation exchange resin AG-50W-X8, H^+ form, 200-400 mesh where a Sr fraction could be isolated followed by collection of bulk rare earth elements (REE_S). This bulk solution was dried and taken up in 0.18 M HCl and loaded on a second column containing Eichrom Ln resin (50-100 mesh) to isolate Sm and Nd separately from the other REES. All reagents were purified to ensure a low contamination level. Samarium and Nd concentrations and isotopic compositions were determined using a multi-collector Finnigan Mat 262 mass spectrometer in static mode for concentration determination, and dynamic mode for isotopic composition determination. Instrumental mass fractionation of Sm and Nd isotopes were

corrected using a Rayleigh law relative to $^{146}Nd/^{144}Nd = 0.7219$ and $^{152}Sm/^{147}Sm = 1.783$. The reported $^{143}Nd/^{144}Nd$ ratios were corrected for the deviation of repeated duplicates of the JNdi-1 standard from the accepted value of $^{143}Nd/^{144}Nd = 0.512115$ (Tanaka et al., 2000). The mean value of Jndi-1 for these analyses was $^{143}Nd/^{144}Nd = 0.512104 \pm 5$ (1SD, n=4) while the long-term mean was 0.512099 ± 8 (1SD, n=349). The received from the lab were used to calculate the ε_{Nd} values presented in this study. The values were calculated using CHUR (Chondritic Uniform Reservoir) and depleted mantle normalizing values of DePaolo and Wasserburg (1976).

4. Results

4.1. Overview of rock distribution in the study area

The majority of the rock samples were collected along the traverses and the zones established in Chapter 3 will be used to characterize the Leta Arm and Hewitt Lake group assemblages previously distinguished based on geochemistry and geochronology (Pehrsson, 1998). The different lithologies identified from field observations were supported by both petrography and whole-rock geochemistry (see details in Chapter 5). Field, petrographic and geochemical data were not consistent with the lithologies on previous maps and this study addresses this knowledge gap. Using previous field observations in conjunction with previous maps, the Leta Arm group on the eastern part of the mapped area is dominantly characterized by a large proportion of mafic rocks (75%, light green colour) intruded by and interlayered with <0.5 km-wide NE-trending felsic lenses (~10%) as well as quartz diorite to gabbroic units of the Colomac sill complex (~15%, blue) known to host mineralization (Figs. 3.1 & 4.1). Intermediate rocks make up <5% of the eastern zone and were observed mostly near the Grizzly Bear zone. The proportion of mafic and felsic rocks is 60% and 5%, respectively, in the western Leta Arm group zone whereas intermediate rocks increase to up to 30% and dominantly span the central and eastern part of the western zone. The western zone occasionally contains sub-concordant lenses of gabbro similar to those of the Colomac sill complex in the eastern zone. In contrast, the southern Leta Arm group area (Kim-Cass) does not contain significant volumes of mafic rocks or gabbroic lenses. It is made up of felsic rocks (60%) and lenses of mafic-intermediate rocks (40%). The southwestern Hewitt Lake group consists largely of mafic (90%) and intermediate rocks (~10%) which propagate towards the southern Leta Arm group zone and are separated from it by a thin unit of sedimentary rocks.

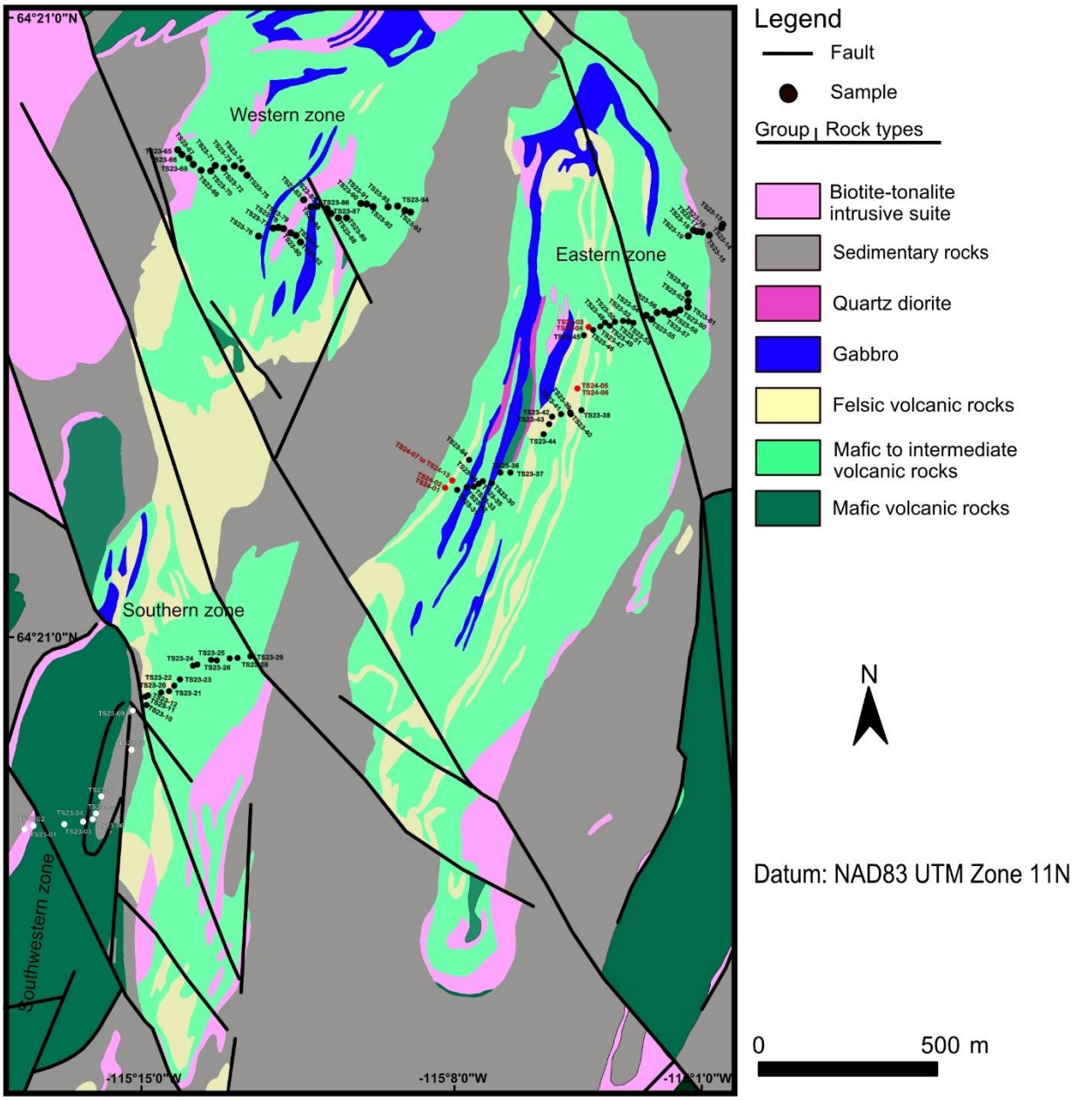

Figure 4.1. Map of the ILSB *showing locations of samples from 2023 (black and white) and 2024 (red) from the different spatial zones assigned to mapped area (modified after Pehrsson, 1998; STLLR Gold Incorporated, 2023).*

4.1.1. Field observations and cross-cutting relationships

The Andy Lake area and Kim area in the southwestern Hewitt Lake group were well exposed in outcrop and provided an opportunity to observe the limited cross-cutting relationships among rock types in the field (Fig. 4.2A). In the Andy Lake area, the Leta Arm group basalts are characterised

by pillow structures and banding. Pillows occur as light-coloured undeformed spherical-shaped to structures with dark grey rims (Fig. 4.2B). Other basalts in this area have elongated stringer-like features that are cut-off along thin chilled margins and display elongated clasts with long axes deflecting away from contacts (Fig. 4.2C). The directional flow of the stringer-like material around clasts results in a feature that mimics pillows. Contacts are sharp to gradational and in some cases may mark the termination of banding or pillows along contacts with crosscutting units (Fig. 4.2D). Some volcanic flows entrained 2.2-0.5 cm grey-to-brown xenolithic clasts which are lighter-coloured than the host flow units. The clasts are similar to rocks in contact with the volcanic flows and may be evidence for rip ups (Fig. 4.2E). Surface weathering is manifested by bleaching in

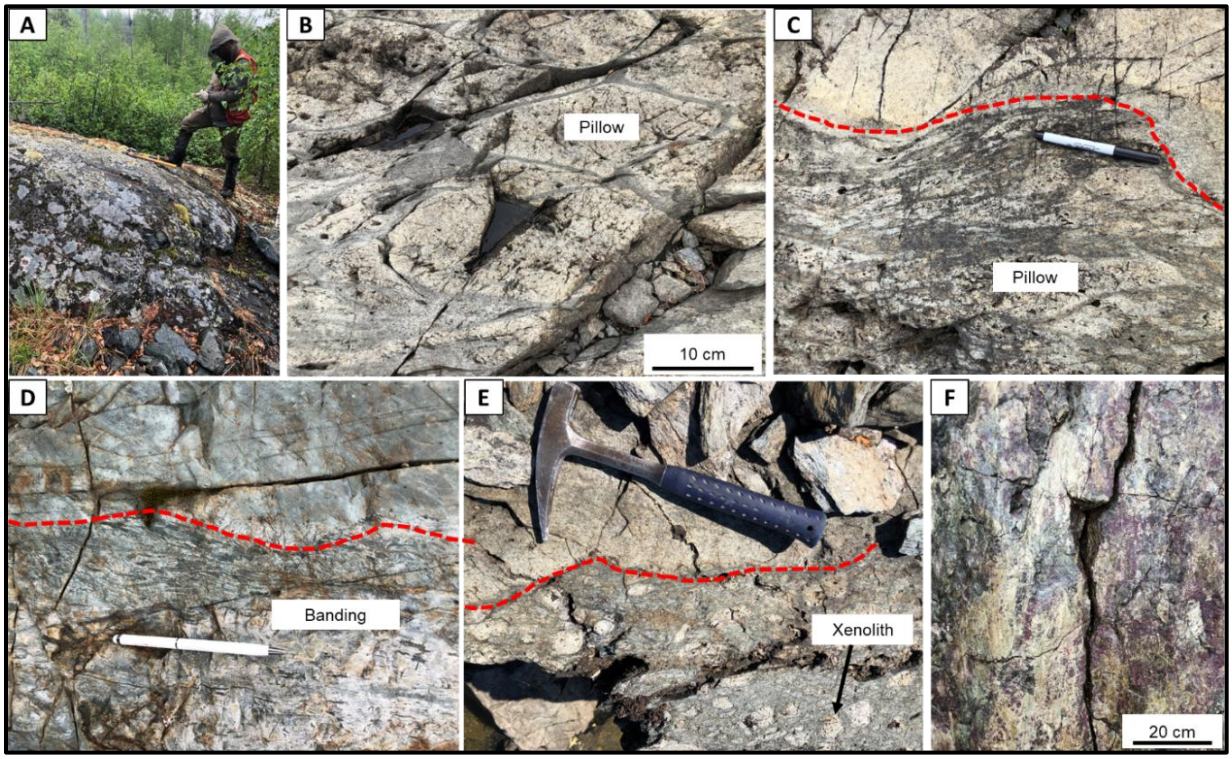

Figure 4.2. A) A basaltic outcrop from the Kim area in the southern Leta Arm group. B) Bleached pillows. C) Deformed pillows deflected along chilled margin. D) Flow banding with gradational grain size near a chilled margin. E) Rip-ups in a lava flow. F) Surface oxidation and bleaching on a basalt. Figures A&F are from the Kim area 7km north of Parker Lake whereas Figures B-E are from the Andy Lake area.

both sections and a red colouration (possibly oxidation) south of Kim (Fig. 4.2F). Due to low relief and obscurity of outcrop by vegetation in the sampled parts of the belt, field observations of contacts were limited. Although no samples were collected from the above sections, we used field observations from there as a proxy for the sampled study area to make inferences on contact relations. The contact between flows are primary as shown by magmatic structures. However, no younger directions were established due to limited surface exposure between volcanic flows and lithostratigraphic units.

4.2. Petrography

4.2.1. Basalts

Basalts of the Leta Arm group show variations in mineralogical modal composition and degree of alteration between domains. Textures were determined by the number of phenocrysts present compared to groundmass. Intergranular textures are common in basalts and are defined by euhedral to subhedral ferromagnesian minerals and plagioclase with small interstitial grains of the same minerals. Grain size in the basalts ranges from 300 μm to 800 μm and all the basalts are chloritized. In the eastern zone, the basalts are comprised of plagioclase (40-50%), euhedral to subhedral clinopyroxene (25-30%), hornblende (~10%), orthopyroxene (5%) and Fe-Ti oxides (~3%) as shown in Figure 4.3A. These basalts are weakly altered as over 50% of their primary textures are visible and alteration minerals observed include partial replacement of clinopyroxene by secondary hornblende and actinolite, Fe-Ti oxides by rutile, and plagioclase to sericite (e.g., Fig. 4.3A). Actinolite occurs as pseudomorphs of pyroxene while secondary hornblende forms an irregular brown groundmass patch enclosing actinolite within the altered grains (Fig. 4.3A). Although minor and not pervasive, chlorite usually overprints the basalts in this eastern zone. Primary Fe-Ti oxides

are either net-textured or occur as subhedral grains within rutile. Secondary Fe-Ti oxides form along grain boundaries of altered ferromagnesian grains.

In the western zone, basalts are made up of relict clinopyroxene (~60%), orthopyroxene (20%), and plagioclase (10%). Primary quartz was rarely observed (<5%) and basalts in this domain are distinguished by their strongly altered nature (Fig. 4.3B). The alteration of pyroxenes formed yellowish brown to grey secondary amphiboles occasionally associated with ~5% modal abundances of rounded to subrounded opaque Fe-Ti oxides grains. Many of the Fe-Ti oxides are mostly concentrated on the grain boundaries of highly altered grains (Fig. 4.3B).

Hewitt Lake group basalts contain hornblende (~50%), plagioclase (20%), clinopyroxene (15%), minor orthopyroxene (5-10%), quartz (10%), biotite (~5%) and Fe-Ti oxides (1-3%; Figs. 4.3C&D). Most hornblende grains in the Hewitt Lake group basalts are characterized by a light brown to dark brown colour and have well-developed euhedral grains (150 μm to 500 μm) with a prismatic to subrounded habit. The hornblende is generally unaltered and displays clear grain boundaries with other polymineral relict grains. Although the morphology and textural relations with other mineral phases is characteristic of magmatic origin, their co-existence with actinolite and quartz-carbonate phases suggest they were possibly overprinted by metamorphism (Figs. 4.3C&D). Plagioclase and pyroxenes are less abundant than hornblende and have euhedral habits. Fe-Ti oxides show a preferred orientation and occur as anhedral grains or patches within and along the boundaries of hornblende and pyroxenes, possibly suggesting that they grew along some weak cleavage or foliation plane (Fig. 4.3C). This is suggestive of a localized deformation event that partially affected some of the minerals in the basalts. It is unclear whether this apparent weak cleavage is related to the recrystallization of quartz. The basalts are chloritized and contain

anhedral quartz and fine-grained carbonates surrounding undeformed primary grains (Fig. 4.3D). Chlorite together with the quartz and carbonates likely formed by alteration processes.

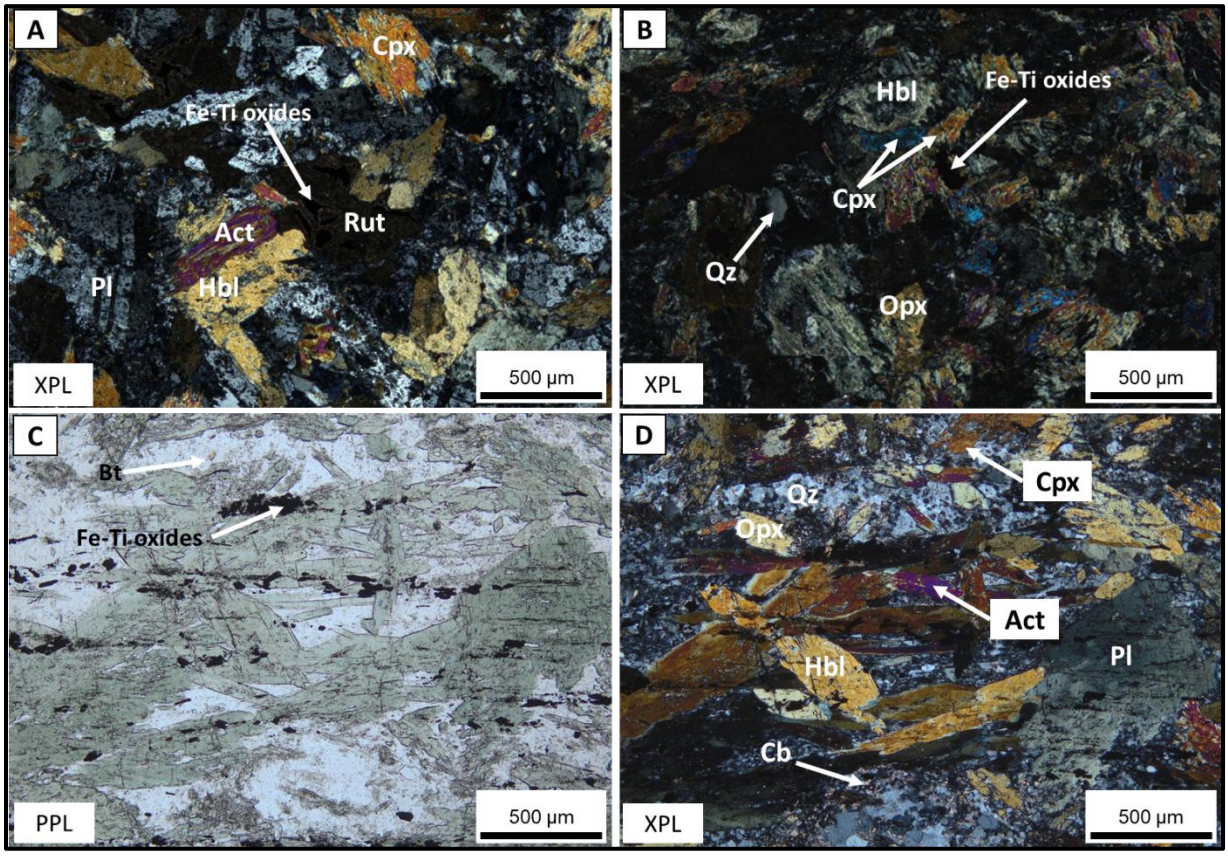

Figure 4.3. A) Sample TS23-31 of the eastern Leta Arm group zone basalt showing alteration of rutile to Fe-Ti oxides and replacement of pyroxenes by amphiboles and secondary plagioclase. B) Sample TS23-81 of the western Leta Arm group zone basalt exhibiting partial replacement of pyroxenes by amphiboles. C) and D) are photomicrographs of the southwestern Hewitt Lake group basalt showing primary amphibole and secondary quartz associated with carbonates (TS23-08). XPL=cross-polarized light, PPL=plain polarized light, Pl=plagioclase, Hbl=hornblende, Cpx= clinopyroxene, Opx=orthopyroxene, Bt=biotite, Rut= rutile, Act=actinolite, Qz=quartz.

4.2.2. Andesites

Andesites were mapped in the Hewitt Lake group and the Leta Arm group eastern and western zones of the mapped area. Petrographic analysis and interpretation of the southern Leta Arm group andesites was challenging due to their highly deformed, fine-grained and altered nature. Their composition was confirmed using whole-rock geochemistry. The petrography of analysed

andesites show variable abundances between amphibole and biotite (Fig. 4.4). The andesites in the east comprise euhedral hornblende (~40-45%), plagioclase (~25%), clinopyroxene (10%), biotite (5%), and minor orthopyroxene (~5%). The andesites are hornblende-rich and show widespread calcite, chlorite and epidote alteration (Fig. 4.4A). Patches of epidote and calcite were observed mainly within plagioclase and less in ferromagnesian minerals. This process is likely associated with the breakdown of plagioclase during metamorphism by alteration processes such as epidotization. Hornblende grains (500-850 μm) together with actinolite, occur as pseudomorphs of pyroxenes that are often twinned with prismatic habits and are distinguished from magmatic hornblende in basalts by their green to light grey colour with strong brownish-yellow to purple interference colours (Fig. 4.4A). The pervasive alteration and formation of hornblende and actinolite after pyroxene indicate metamorphism that likely resulted in these colours uncommon for primary hornblende.

Andesites on the western part have up to 70% plagioclase, are biotite-rich (~20%) but devoid of hornblende and show a well-developed foliation. Biotite occurs as euhedral grains formed at the edge of plagioclase microlithons which are interpreted to be primary and likely formed during crystallization (Fig. 4.4B). Clinopyroxene is minor (<5%) and occurs in biotite-rich sections along the edges of microlithons. Andesites in this domain are less altered than eastern andesites, have primary textures and show minor recrystallisation of plagioclase defined by <100 μm grains surrounding ~50 μm primary plagioclase that are closely associated with quartz grains of a similar size (Fig. 4.4B). Biotite and pyroxene are partially altered to chlorite whereas plagioclase is altered to sericite (Fig. 4.4B).

The Hewitt Lake group andesites have similar compositions to andesites on the western Leta Arm group zone except they are more biotite-rich (~35%), contain hornblende (~20%), quartz (10%),

actinolite (~5%), have less plagioclase phenocrysts (<10%) and do not contain pyroxene. The biotite grains are oriented subparallel to a weak fabric in the rock. They are likely primary as they do not appear to overprint deformation or primary phases (Fig. 4.4C&D). Although relatively fine-grained compared to amphibole and biotite, plagioclase feldspar forms phenocrysts in places (Fig. 4.4D). The matrix is composed predominantly of quartz and smaller grains of biotite, plagioclase and hornblende. Evidence of alteration is minimal and alteration assemblages are similar to those of the western andesites (e.g., chlorite after biotite).

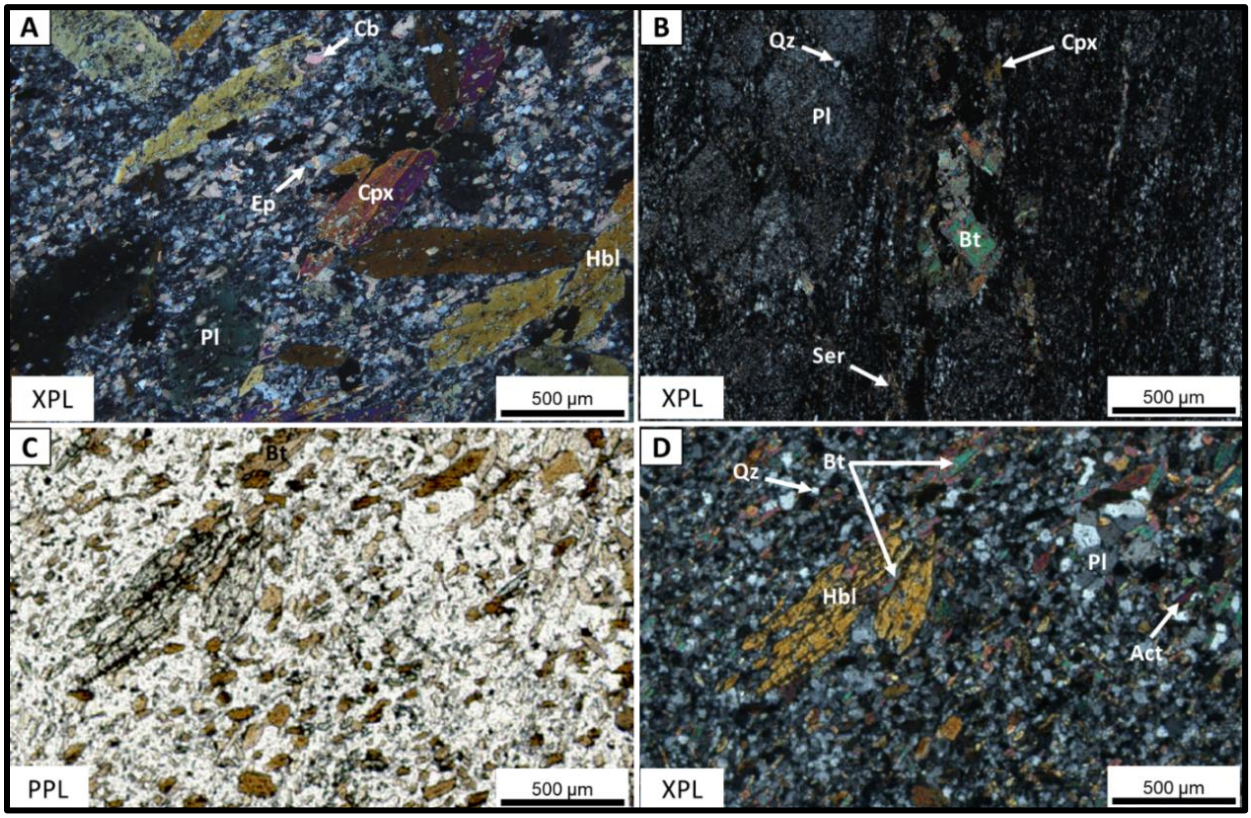

Figure 4.4. A) Sample TS23-61 of the eastern Leta Arm group zone andesite porphyry showing pseudomorphic hornblende after pyroxene and pervasive carbonatization and epidotization. B) Sample TS23-95 is the western Leta Arm group zone andesite showing plagioclase microlithons surrounded by euhedral biotite suggesting that these are primary. C) and D) are photomicrographs of sample TS23-01 in the Hewitt Lake group andesite with biotite along a weak foliation suggesting it formed during a metamorphic process. The porphyritic nature of the andesites implies they formed in hypabyssal associated environment sometime during the volcanic event. XPL=cross-polarized light, PPL=plain polarized light, Pl=plagioclase, Hbl=hornblende, Bt=biotite, Cpx=clinopyroxene, Act=actinolite, Ep=epidote, Cb=carbonates, Qz=quartz, Ser=sericite.

4.2.3. Dacites

Rocks of dacitic composition are found in all zones of the Leta Arm Group but not in the sampled parts of the Hewitt Lake Group. The dacites are porphyritic with phenocrysts of quartz and albite in a very fine-grained sericitized quartz-feldspar matrix that occurs as brown to grey patchy material. The dacites are variably altered and slightly deformed. Both the eastern and western dacites have a weak foliation marked by sericite-quartz matrix and opaques, along which biotite and carbonate phenocrysts are preferentially oriented (Fig. 4.5 A&B). The southern dacites have moderate to strongly deformed varieties. Moderately deformed dacites show carbonates and epidote pressure shadows around feldspar phenocrysts whereas sericite and quartz mainly form

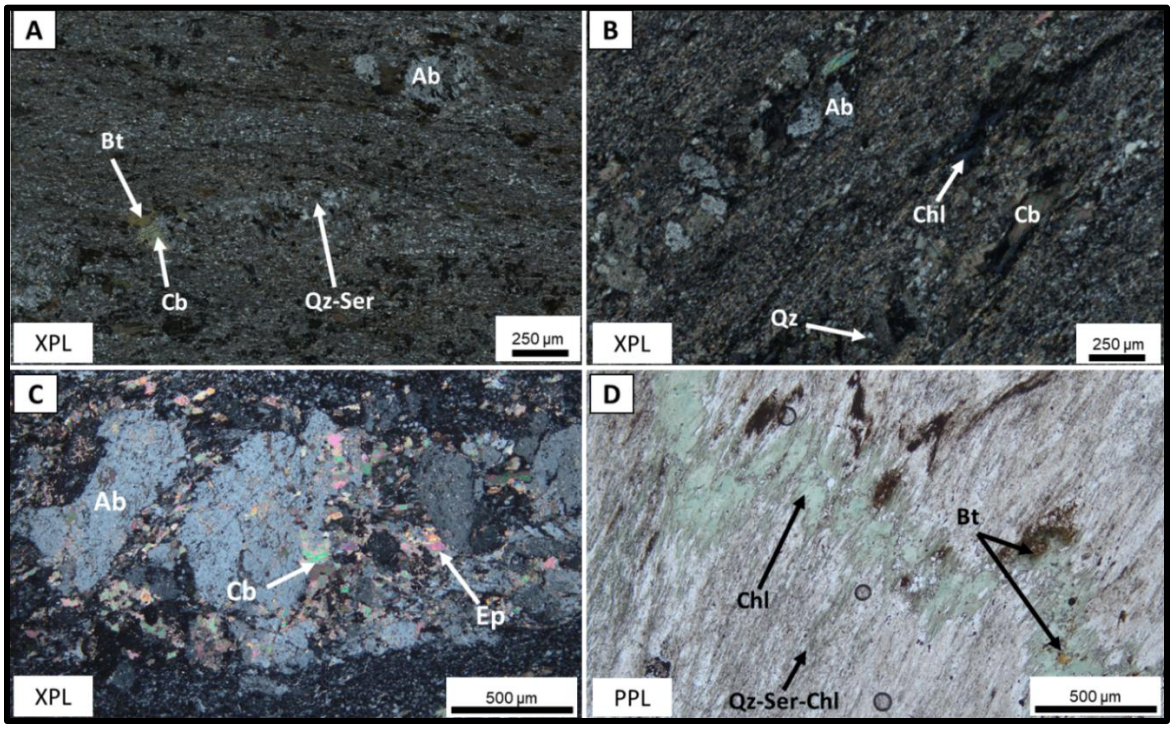

Figure 4.5. Dacites of the Leta Arm group. A) Biotite-bearing dacite of the eastern zone (TS23-55). B) Chlorite alteration along weak foliation in the western zone dacite (TS23-87). C) Carbonate-epidote-sericite alteration in a non-foliated southern zone dacite porphyry (TS23-25). D) Folded primary biotite and euhedral metamorphic biotite in a chloritized and sericitized foliated fine-grained dacite from the southern zone (TS23-20). XPL=cross-polarized light, PPL=plain polarized light, Ab=albite, Bt=biotite, Qz=quartz, Chl=chlorite, Ser=sericite.

the matrix (Fig. 4.5C). Deformation fabric in the southern dacites occurs as a strong foliation defined by quartz and sericite and crenulation cleavage formed on quartz veins (Fig. 4.5D). Biotite is only observed in the eastern and southern dacites (Fig. 4.5A&D) whereas chlorite is only observed in the western and southern dacites (Fig. 4.5B&D). Metamorphic biotite grew on chloritized and crenulated veins whereas pre-existing biotite is deformed together with the dacites to mimic the crenulation (Fig. 4.5D).

4.2.4. Rhyolites

Rhyolites were only found in the eastern Leta Arm group zone to the east of the Colomac sill (Fig. 4.1). The rocks are aphanitic to slightly porphyritic with grain sizes ranging from 2mm in the

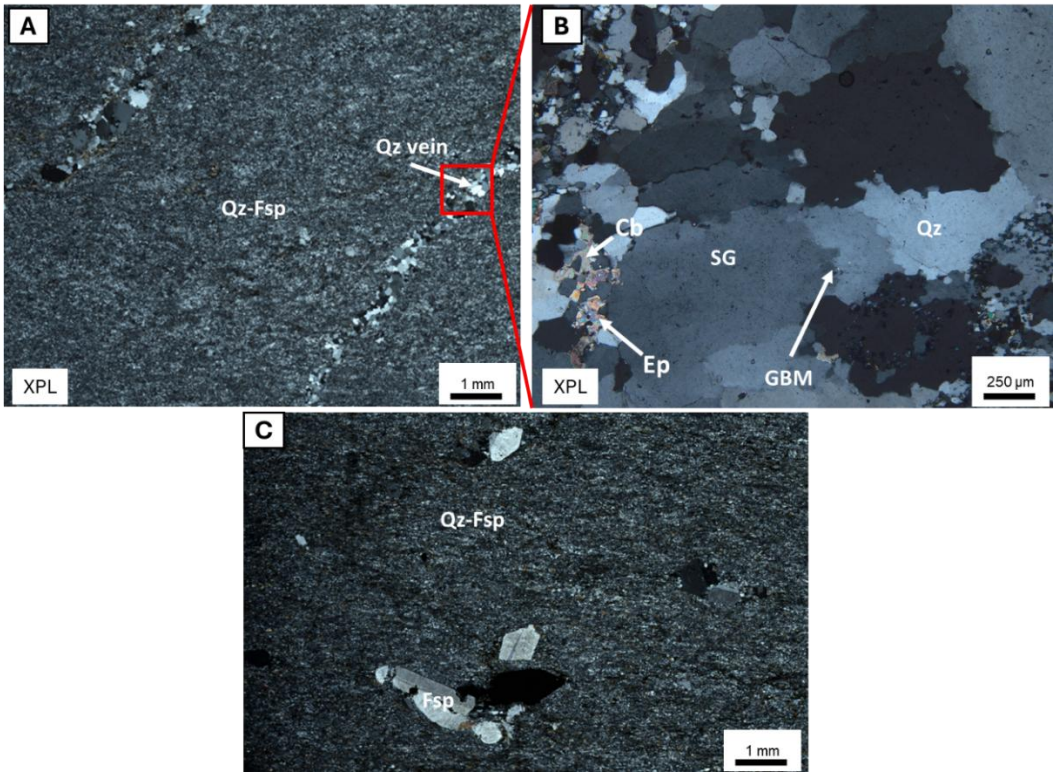

Figure 4.6. A) Microscale quartz veins crosscutting of a rhyolite sample (TS23-43). B) A zoomed-in section of a quartz vein in XPL that shows a quartz-epidote assemblage with plastic deformation in quartz. C) Rhyolitic feldspar porphyry (TS23-40). Recrystallization is by plastic deformation represented by grain boundary migration (GBM) microstructures and subgrains (SG). XPL=cross-polarized light, PPL=plain polarized light, Qz=quartz, Fsp=albite, Cb=carbonate, Ep=epidote.

phenocrysts to <200 μm in the matrix (Figs. 4.6A&C). The composition of aphanitic rhyolites was determined using whole-rock geochemistry as modal abundances were difficult to determine due to small grain sizes. The rhyolites consist of fine-grained quartz and sericite grains crosscut by millimeter to micrometer quartz-carbonate-epidote veins (Fig 4.6A). The veins are plastically deformed by dynamic recrystallization of quartz (Fig. 4.6B). Microstructures include grain boundary migration (GBM) and subgrains (SG) of quartz in which interfingering lobate grain boundaries represent grain boundary migration and obscure pre-existing grain morphology (Fig. 4.6B).

4.3. Amphibole compositions and textures from electron microprobe analysis (EPMA)

Petrographic analysis revealed different amphibole textural relationships and morphologies so EPMA was used to determine whether they are magmatic or metamorphic (Figs. 4.7 & 4.8). The amphiboles are from a basalt (TS23-31) and andesite (TS23-61) of the eastern Leta Arm (LA) group and a basaltic sample from the southwestern Hewitt Lake (HL) group (TS23-08). The EPMA data show a spread of calcic amphibole compositions between actinolite and hornblende (Figs. 4.7 & 4.8). Based on textural relationships and EPMA data, amphibole grains in the eastern LA group basalt are actinolitic to ferro-hornblende in composition and show a complex core-margin association between these compositions. Some grains in the basalt showed replacement textures identified using petrography whereas some did not and were characterised with back-scattered electron (BSE) images and EPMA data. Grains which were identified using EPMA typically had replacement actinolite rims around ferro-hornblende relics (Fig. 4.8A&B). Those that were identified using petrography contain ferro-hornblende rims around pseudomorphic actinolite grains that occur as relics of what was initially clinopyroxene (Fig. 4.8C&D).

The eastern LA group andesite and HL group basalt data all plot in the hornblende field which consists of both ferro-hornblende and magnesio-hornblende (Fig. 4.7). Amphiboles from the eastern LA group andesite are all ferro-hornblende in composition and coexist with altered pyroxene (possibly pseudomorphic actinolite; Fig. 4.8E&F). The HL group amphiboles have a euhedral morphology and clear grain boundaries with neighboring pyroxenes and plagioclase suggesting that they retained their primary texture (Fig. 4.8E&F). In the basalt, magnesio-hornblende forms the grain boundaries of amphiboles whereas ferro-hornblende forms the core (Fig. 4.8G&H).

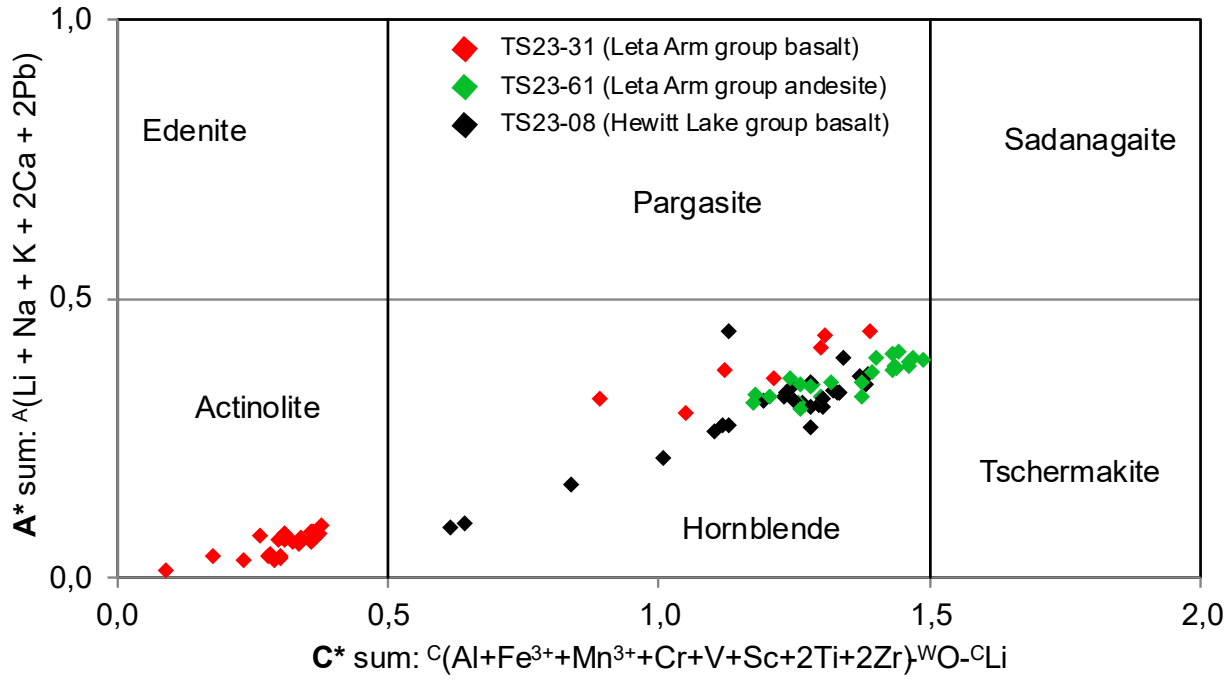

Figure 4.7. Calcic-amphibole compositions of the LA group andesite (green) and HL group basalt (black) plotting in the hornblende field and LA group basalt (red) plotting between tremolite-actinolite to hornblende fields (adapted from Locock, 2014 and references therein).

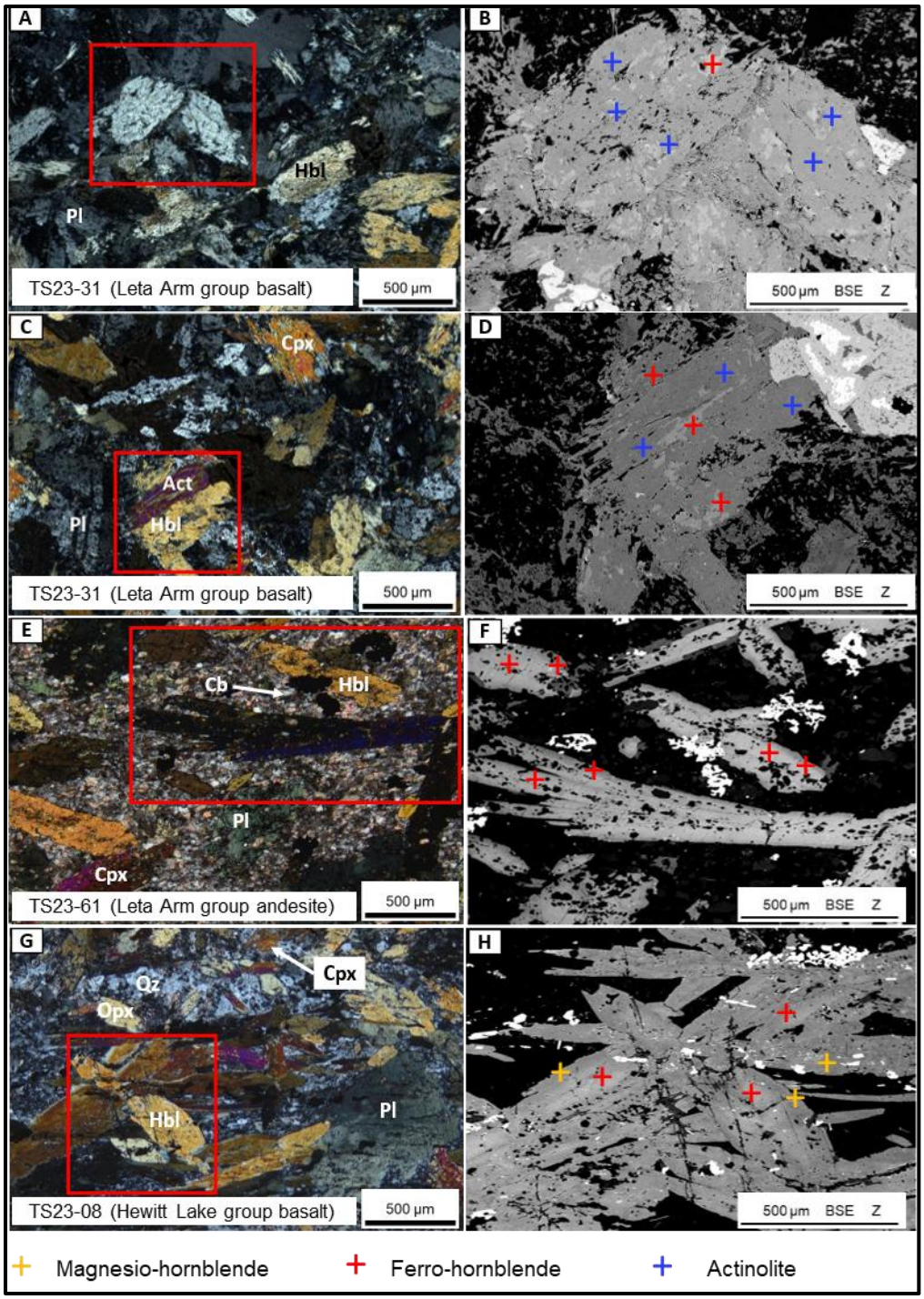

Figure 4.8. A) Hornblende corona around pyroxene grain in an eastern Leta Arm group basalt. B) Pseudomorphic amphibole, in places with purple interference colours on what was primarily pyroxene. C) Euhedral amphibole in the Hewitt Lake group interpreted as primary hornblende based on morphology and textural relationship with other phases. B), D), F) and H) are back-scattered electron (BSE; in Z field of view) images of A), C) E) and G) respectively. XPL= cross-polarized light, HL=hornblende, Cpx=clinopyroxene, Opx=orthopyroxene, Pl=plagioclase, Rut=rutile, Cb=carbonates.

4.4.Whole-rock geochemistry

Ninety-six samples from the different zones were analyzed for whole-rock geochemistry (Fig. 4.1 & appendix I). The major element data was divided into compositional groups based on silica content hereby referred to as mafic (35-52 wt%), intermediate (53-63 wt%), and felsic (>63 wt%) rocks. Trace elements were plotted on bivariate diagrams and primitive mantle-normalized spider plots using normalization values of Sun and McDonough (1989). Detailed classifications and geochemical characterization between zones and rock types are described below.

4.4.1. Major elements

The LA and HL group volcanic rocks show a wide range of subalkaline compositions with the loss on ignition (LOI) ranging from 0.37 to 11.7 wt%. Over 70% of the samples have LOI values below 6.0 wt%. Magnesium number ranges between 0.12 to 0.58 for all rocks with no systematic link between groups of lithologies. On the TAS diagram (Total alkali (Na_2O+K_2O) plotted against silica (SiO_2)), mafic rock types include picrobasalt, basalt, minor trachybasalt with one sample plotting on the low-alkali end of the foidite field (Fig. 4.9A). Intermediate rocks consist mainly of basaltic andesite, andesite and minor basaltic trachyandesite to trachyandesite whereas felsic compositions include rhyolite and dacite. Rhyolite and dacite were only observed in the LA group and therefore geochemical comparisons between the LA and HL groups will be based mainly on basaltic and andesitic rock types. The AFM diagram (Na_2O+K_2O, FeO and MgO) reveals tholeiitic and calc-alkaline end members for both groups, with nearly all basaltic rocks plotting in the tholeiitic field (Fig. 4.9B).

Bivariate plots of major elements versus SiO_2 (Figs. 4.10A-F) show values that range between 10.2-20.7 wt% Fe_2O_3, 12.05-18.10 wt% Al_2O_3, 2.92-8.49 wt% MgO, 2.27-12.45 wt% CaO, 0.75-

5.06 wt% Na_2O and 0.01-2.58 wt% K_2O in basaltic rocks. In andesites, concentrations range between 4.62-12.55 wt% Fe_2O_3, 11.75-21.10 wt% Al_2O_3, 1.66-5.99 wt% MgO, 0.39-9.26 wt% CaO, 1.61-6.54 wt% Na_2O, and 0.07-3.48 wt% K_2O. Dacitic to rhyolitic rocks have high K_2O contents up to 4.21 wt%. The felsic rocks also exhibit variable Fe_2O_3 (2.32-7.26 wt%), CaO (0.27-6.21 wt%), Al_2O_3 (10.90-19.0 wt%), Na_2O (0.41-5.81 wt%), and the lowest MgO (0.33-2.39 wt%).

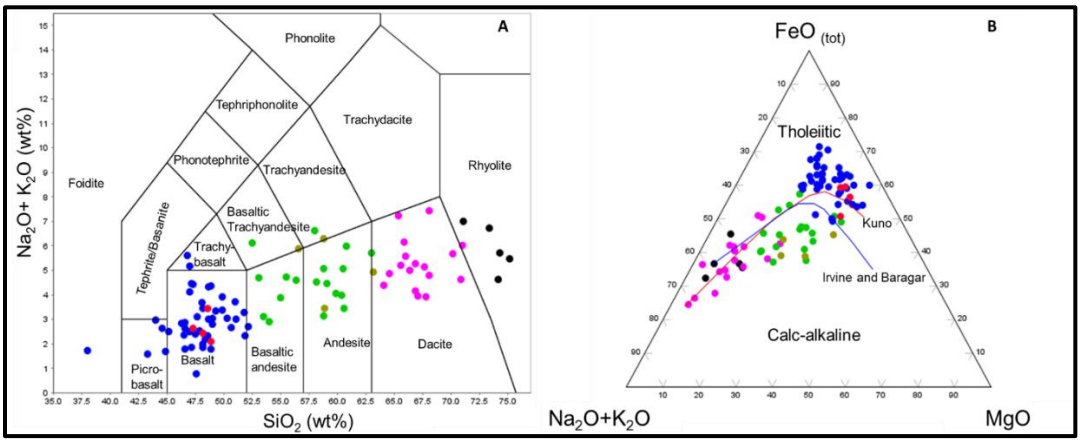

Figure 4.9. A) Total alkali and silica (TAS) diagram. B) AFM (Na_2O+K_2O against FeO against MgO) diagram. Both diagrams show the various rock classifications of the Leta Arm group and Hewitt Lake group rocks (After Le Maitre et al., 1989; Jensen, 1976).

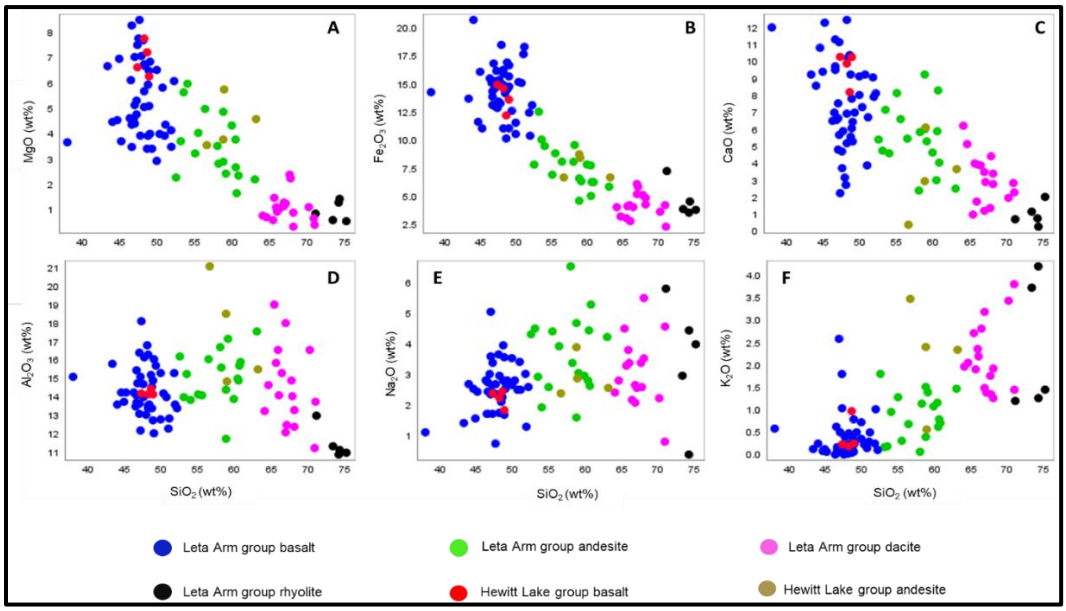

Figure 4.10. Harker diagrams of silica versus major element oxides of the Leta Arm and Hewitt Lake groups.

4.4.2. Trace elements

The trace element data plotted against SiO_2 supports compositional grouping of the rocks (Figs 4.11A-F). The plots also highlight overlaps between compositional groups. Basalts of both groups plot between ranges of 34-63 ppm Co, 23-51 ppm Sc, 5275-13608 ppm Ti, 47-199 ppm Zr, 1.91-11.55 ppm Nb and 1.38-5.26 ppm Hf. Concentrations in andesites range between 15-32 ppm Co, 7-27 ppm Sc, 2038-8273 ppm Ti, 119-214 ppm Zr, 6.26-23.5 ppm Nb and 2.74-5.15 ppm Hf. A large proportion of the dacites have low Co (1-14 ppm), Sc (4-14 ppm) and Ti (1199-4436 ppm) values, which is in the same range as the rhyolites (Figs. 4.11A-C). The dacites are also characterised by Zr (151-301 ppm), Nb (6.26-11.8 ppm) and Hf (3.7-7.41 ppm) values that overlap with those of andesites, except for two eastern zone dacite samples (TS23-44 and TS23-45, Figs. 4.11D-F). These two dacite samples have Zr (456-568 ppm), Nb (22-29 ppm) and Hf (11.50-14.15 ppm) concentrations that are similar to the rhyolites (Figs. 4.11D-F).

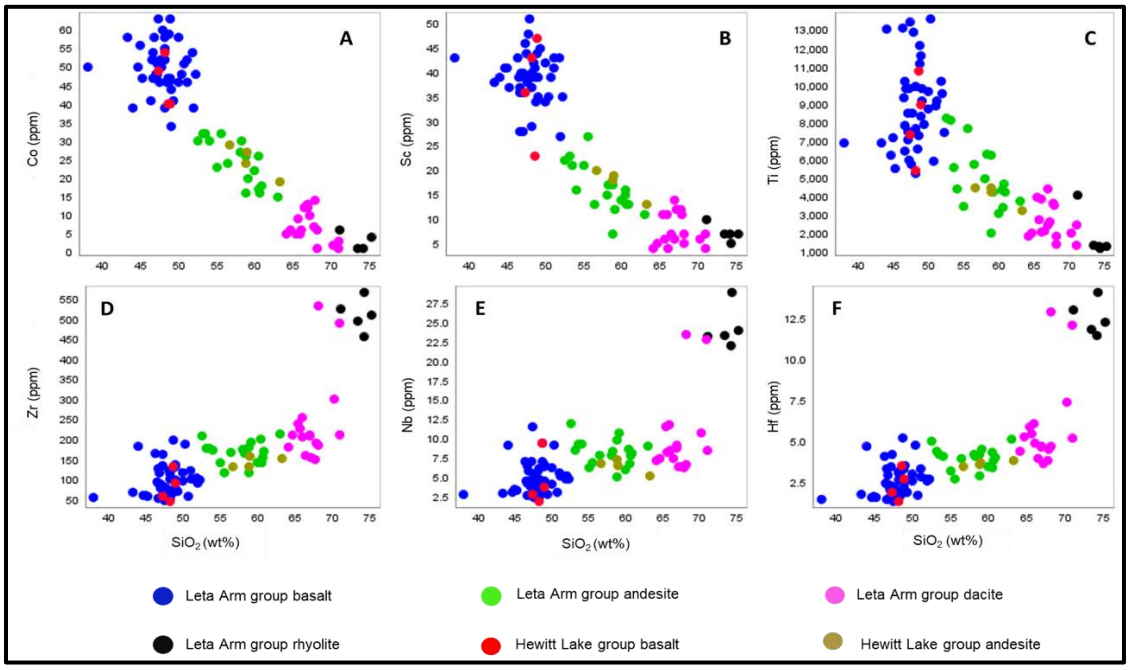

Figure 4.11. Diagrams of compatible (Co, Sc, and Ti) and incompatible high field strength elements (HFSE; Zr, Nb and Hf) versus SiO_2.

Primitive mantle-normalized spider diagrams were plotted by lithology from each zone to examine similarities between overlapping geochemical groupings and determine internal differences between the zones. Basalts are characterized by slightly LREE-enriched patterns (La/Sm_N= 0.67-2.69), minor to no Ti anomalies, and low and Gd/Yb_N (0.71-2.17) ratios (Figs. 4.12A-D). The eastern basalts have a negative Nb anomaly, a positive Th anomaly and La/Sm_N values up to 2.69 (Fig. 4.12A). The opposite is observed for basalts of the western LA group zone and southwestern HL group zones which exhibit minor to slightly positive Nb anomalies, have La/Sm_N <2 and lack a Th anomaly (Figs. 4.12B-D). Only one basaltic sample in the southwestern HL group zone has a steep REE profile represented by minor LREE enrichment (La/Sm_N= 1.99) and HREE fractionation (Gd/Yb_N= 2.17; Fig. 4.12D). Although 98% of the basalts have Nb/Nb* values <1, two basaltic samples from the eastern and western LA group have maximum Nb/Nb* values >1 (1.17 at T23-30 and 1.43 at TS23-75 respectively).

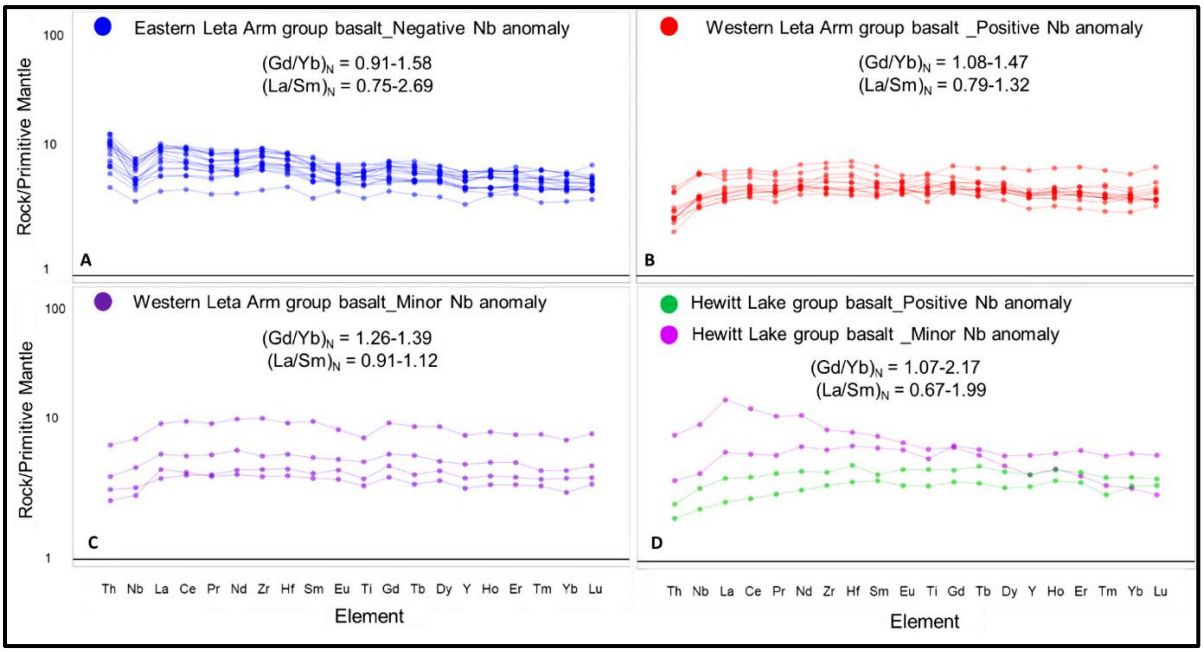

Figure 4.12. Primitive mantle-normalized spider diagram of basalts. A) Leta Arm group positive Nb anomaly basalt. B) Leta Arm group minor Nb anomaly basalt. C) Leta Arm group negative Nb anomaly basalt. D) Hewitt Lake group positive Nb (green) and minor Nb (pink) anomaly basalts. Normalizing values from Sun and McDonough (1989).

Basaltic andesites and andesites from all zones have steeper profiles than basalts and are characterised by a positive Th anomaly, negative Nb and Ti anomalies, Gd/Yb_N ratios <2.80 and Nb/Nb* values <0.33 (Figs. 4.13A-D). The eastern zone basaltic andesites have low La/Sm_N values (1.33-2.50) and are distinguished by weak negative Ti anomalies compared to andesites of other zones which are more LREE-enriched with La/Sm_N values reaching up to 4.33 (Fig. 4.13A versus Figs. 4.13B-D). All andesites show positive Zr-Hf anomalies except the western LA group and southwestern HL group zones which have both positive and negative Zr-Hf anomalies (Figs. 4.13B&D).

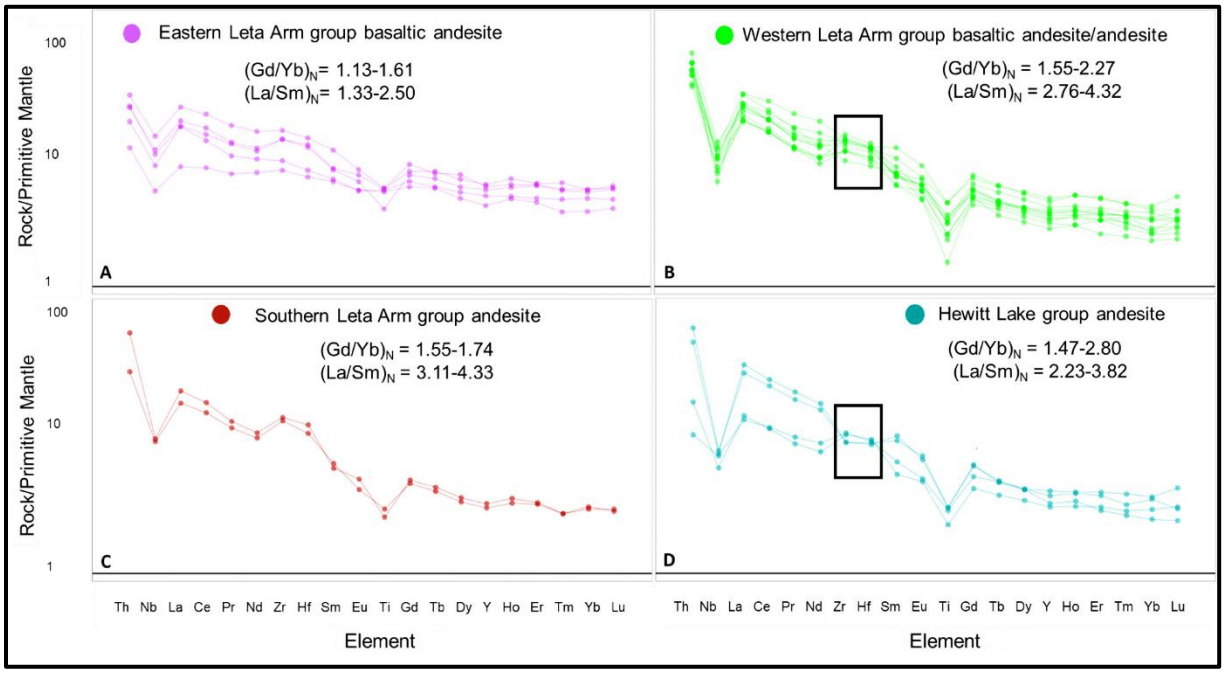

Figure 4.13. Primitive mantle-normalized spider diagrams of intermediate rocks. A) Basaltic andesite of the eastern Leta Arm group zone with minor to negative Ti anomalies and variable positive Zr-Hf anomalies. B) Western Leta Arm group zone andesite with negative Ti anomalies and minor positive and negative Zr-Hf anomalies. C) The southern Leta Arm group zone andesite with pronounced positive Zr-Hf anomalies. (D) The Hewitt Lake group andesite with Ti and Zr-Hf anomalies are similar to the western Leta Arm group zone andesite. Black boxes in B) and D) mark positive and negative Zr-Hf anomalies. Normalizing values from Sun and McDonough (1989).

Dacites from all zones are characterised by positive Th anomalies, negative Nb and Ti anomalies, Gd/Yb_N ratios <1.89, positive Zr-Hf anomalies, Nb/Nb* values <0.33 and La/Sm_N values up to

5.47 (Figs. 4.14A-D). Rhyolites have similar REE profiles to dacites but show moderate La/Sm_N (1.98-3.09) values and weak HREE fractionation (Gd/Yb_N= 0.93-1.38) than dacites. Overlapping geochemical characteristics between rhyolites and the two eastern LA group zone dacite samples mentioned above are also present and show very strong negative Ti anomalies (Fig. 4.14C). Dacite samples that do not overlap with rhyolites exhibit a slightly stronger HREE fractionation than those which overlap. Although some overlaps exist, average REE profiles of felsic rocks show an increase in elemental concentrations from the western to southern to eastern LA group dacites, with rhyolites plotting at the highest concentrations (Fig. 4.14D).

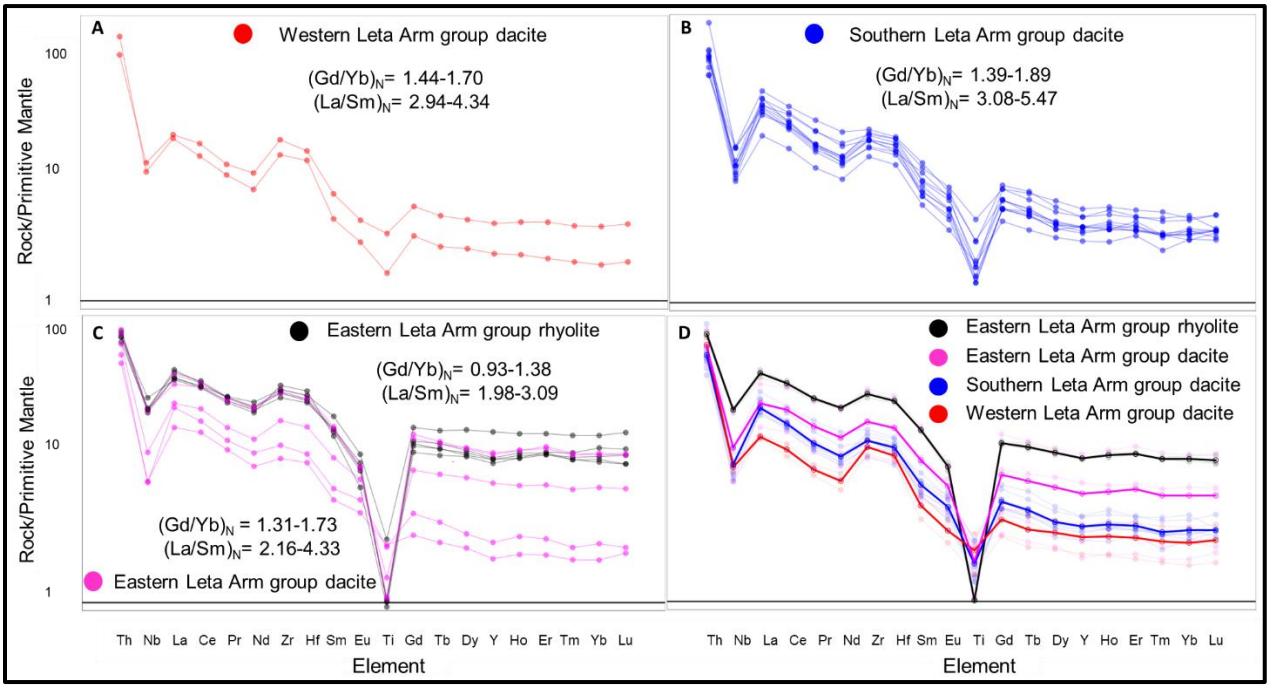

Figure 4.14. A) Eastern Leta Arm group dacite and rhyolite spider plots showing overlapping concentrations between two dacitic samples and rhyolites at the highest REE profiles with strong negative Ti anomalies. B) Western Leta Arm group dacite. C) Southern Leta Arm group dacite. D) Average profiles of Leta Arm group dacites through rhyolites by spatial zones. Normalizing values from Sun and McDonough (1989).

The felsic lenses from drillholes (TS24 samples) have REE patterns and anomalies similar to other rhyolites in the eastern LA group (Fig. 4.15). They are characterized by negative Nb and Ti anomalies, positive Zr and Hf anomalies, are LREE enriched (La/Sm_N= 1.43-2.60), show weak

HREE fractionation (Gd/Yb_N= 1.05-1.47) and with similar high absolute abundances except two samples (TS24-02 and TS24-06) which show pronounced positive Zr and Hf anomalies and slightly erratic REE profiles in places.

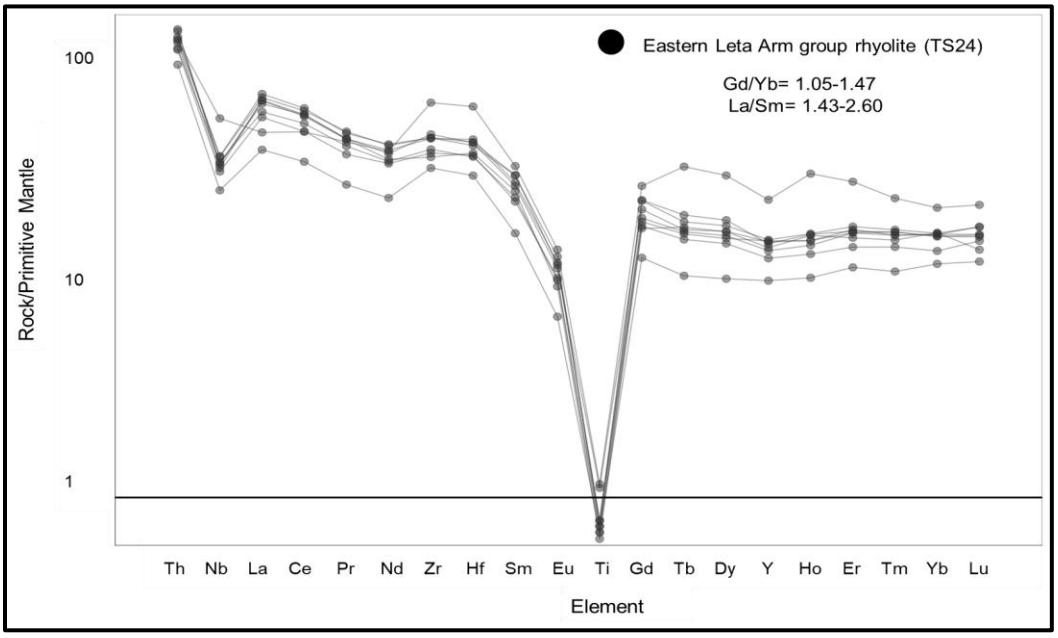

Figure 4.15. Primitive mantle-normalized plot of felsic samples (TS24) from drillholes in the eastern Leta Arm Group.

4.5.U-Pb TIMS geochronology

Surface and drillhole samples from felsic units of the eastern LA group were analyzed for geochronology to constrain the timing of magmatism in the study area. Only one surface sample, TS23-40, yielded zircons (Figs. 3.1 & 4.16) Drillhole samples were taken from intervals marked by red boxes and include samples TS24-01, TS24-05, and TS24-07 from drillholes GB21-16, NL21-08 and GB21-26 respectively (Figs 3.1 & 4.17A-C; Appendix IV). Schematic sections of drillholes GB21-16 and NL21-08. There was no schematic section provided by STLLR Gold Inc for drillhole GB21-26. Sample TS24-01 is a bleached, fine-grained felsic volcanic lapilli unit with pervasive sericite alteration and moderate foliation. Sample TS24-05 was taken from a very dark grey volcanic fragmental unit with little to no sericite alteration. Sample TS24-07 is a light grey

volcanic quartz porphyritic flow, with 5-10% anhedral 1-2mm quartz phenocrysts and 1-5% 2-5mm oval-shaped amygdules infilled with carbonates, in a very fine groundmass of anhedral plagioclase and quartz. There is also very dense quartz veining in the porphyritic flow. Sample TS23-40 is an aphanitic to slightly porphyritic rhyolite with <5% feldspar phenocrysts and occurs along the same lens as TS24-05 of drillhole NL21-08 (Fig. 3.1). Of the zircons recovered from the samples, only three grains from each TS24 sample and six grains from TS23-40 sample zircon population were used for analysis as they are the least broken to cracked and their habits range from euhedral homogenous to prismatic elongate (Figs 4.16B & 4.17D-F). Simple forms are common with low-order faces and square to slightly flattened cross-sections. The zircons in all four samples are clear, colourless to pale yellow with a grain size range between ~50-300 µm and Th/U values ≥ 0.5 (Appendix IV).

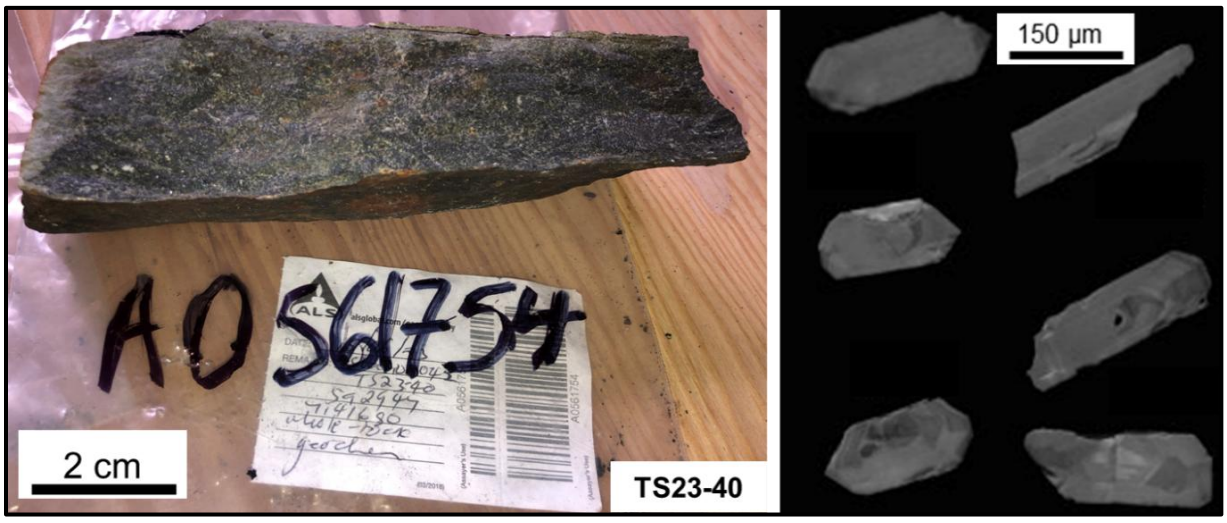

Figure 4.16. Hand specimen of sample TS23-40 and BSE (back-scattered electron) images of zircons analyzed from the sample.

Zircon grains in sample TS24-01 had moderate U concentrations of ~100-200 ppm with calculated Th/U ratios of 0.51-0.54, typical of igneous compositions. All three fractions revealed calculated model $^{207}Pb/^{206}Pb$ concordant ages ranging between 2673.3-2673.8 Ma (2σ= 2.0 to 1.3) with 0.1-

0.2% discordance (Fig. 4.15A; Appendix IV). A weighted average $^{207}Pb/^{206}Pb$ age calculated for the three overlapping and concordant analyses is 2673.6 ± 0.9 Ma, with a 90% probability of fit.

Sample TS24-05 showed lower overall total radiogenic Pb content and U abundances of ~50-70 ppm compared to TS24-01. There is also a concordant but slight dispersion of isotopic results for the three analyses with a discordance of 0.0-0.7% and $^{207}Pb/^{206}Pb$ ages between 2671.5-2673.3 Ma (2σ= 3.1 to 1.6), averaging to a calculated weighted $^{207}Pb/^{206}Pb$ age of 2672.5 ± 1.1 Ma (Fig. 4.18B; Appendix IV). An MSWD of 1.1 and a probability of fit of 35% (a minimum of 15% is generally considered acceptable; Ludwig, 2003) were also determined.

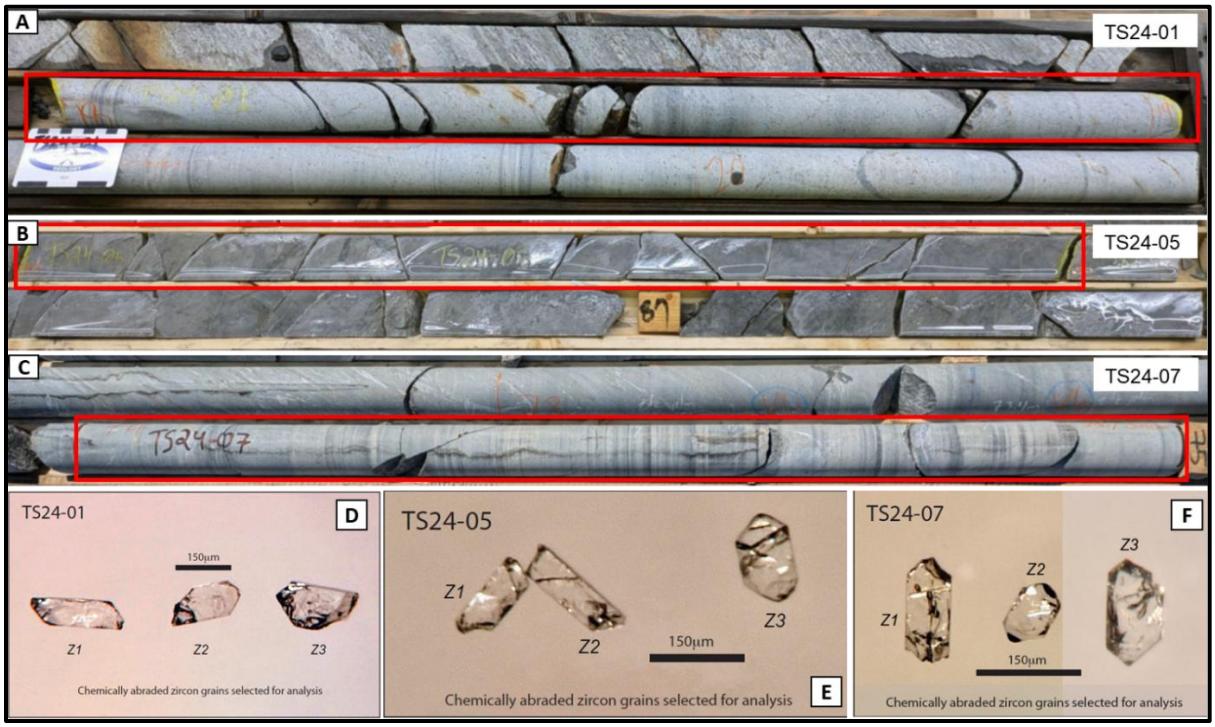

Figure 4.17. Drillhole samples selected for U-Pb geochronological analysis (A-C) and chemically abraded zircon grains from the samples after crushing and separation (D-F). U= Uranium, Pb= Lead.

The range of $^{207}Pb/^{206}Pb$ zircons ages from sample TS24-07 are between 2669.2-2671.1 Ma with concordance of -0.1 to 0.4% and a weighted average $^{207}Pb/^{206}Pb$ age of 2669.8 ± 2.5 Ma. This error was based on the 95% confidence error of the weighted average. The 2σ internal error reduces to

± 1.1 Myr if the error propagated from the assigned datapoint errors is used. This is analogous to extending a regression anchored at 0 Ma through the data and would yield an MSWD of 1.3 and a probability of fit of 28% which is also acceptable (Ludwig, 2003). An analyses of the concordant zircons (Z1 and Z3) which have -0.1% discordance, yielded a weighted average $^{207}Pb/^{206}Pb$ age of 2669.3 ± 1.2 Ma at a probability of fit of 93%.

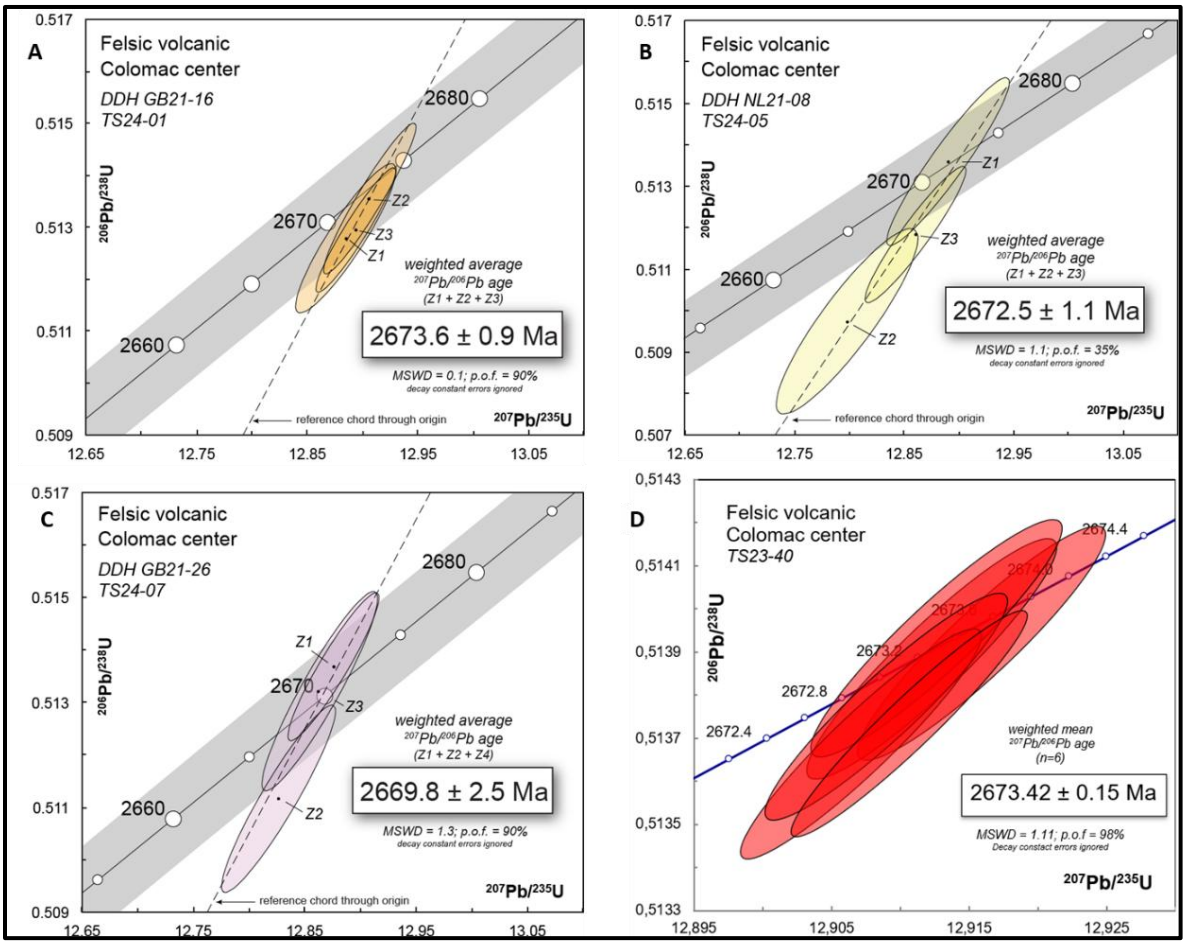

Figure 4.18. Concordia diagrams for samples A) TS24-01, B) TS24-05, C) TS24-07 and D) TS23-40.

Sample TS23-40 had zircons with Th/U ratios between 0.52-0.63 and yielded a weighted mean $^{207}Pb/^{206}Pb$ age = 2673.42 ± 0.15 Ma with a 2s of 2.33, MSWD = 1.11 and probability of fit of 98% (Fig. 4.18D). Correlating coeficients range between 0.93-0.96 and ellipses show good overlaps. The ages are similar to those of TS24-01 and TS24-05.

4.6. Sm/Nd Isotopes

The selection of samples for Sm/Nd isotope analysis in Figure 4.19 was based on trace element data from whole-rock geochemistry of both the HL (TS23-02 and TS23-04) and LA (TS23-11, TS23-35, TS23-37, TS23-40, TS23-45, TS23-49, TS23-56, TS23-73, TS23-81, TS23-82 and TS23-90) groups. Primitive mantle-normalized REE plots of analyzed samples have variable Nb anomalies and are of basaltic to rhyolitic composition. Samples with strong negative Nb and Ti anomalies and positive Zr-Hf anomalies generally have steeper patterns with negative Ti anomalies (Fig. 4.19A&B). Those with moderate slopes have strong to moderate negative Ti and Nb anomalies and minor Zr-Hf anomalies (Fig. 4.19C&D). Samples with minor to positive Nb anomalies are nearly flat (Fig. 4.19E). Samples of the Hewitt Lake group have both flat REE and steep REE patterns (Fig. 4.19F).

The Sm/Nd isotopic data of analyzed samples is shown in Table 4.1. The samples have $^{147}Sm/^{144}Nd$ ratios ranging between 0.1159 and 0.2102 whereas $^{143}Nd/^{144}Nd$ ratios range from 0.5113 to 0.5130. Initial $^{143}Nd/^{144}Nd$ ratios range from 0.5090 to 0.5094. Epsilon Nd (ε_{Nd}) values for most of the samples range from 1.12 to 2.22 and are within error of each other (2σ= 0.1 to 0.3) except sample TS23-40 which has ε_{Nd} of 0.37 and 2σ of 0.9.

Table 4.1. Sm-Nd isotope data for the Leta Arm group and Hewitt Lake group samples.

Sample	Group	Zone	Lithology	Age (Ma)	$Nd_{(ppm)}$	$Sm_{(ppm)}$	$^{143}Nd/^{144}Nd$	$^{147}Sm/^{144}Nd$	$^{143}Nd/^{144}Nd_{init}$	$\varepsilon_{Nd \pm 2\sigma}$
TS23-40	Leta Arm	East	Rhyolite	2672	39,68	8,80	0,5116	0,1341	0,5090	0,37 ± 0,93
TS23-49	Leta Arm	East	Rhyolite	2672	49,21	12,50	0,5120	0,1536	0,5092	1,93 ± 0,30
TS23-45	Leta Arm	East	Dacite	2672	45,65	10,32	0,5116	0,1367	0,5091	1,12 ± 0,20
TS23-11	Leta Arm	South	Andesite	2672	23,88	4,86	0,5114	0,1230	0,5092	1,33 ± 0,17
TS23-82	Leta Arm	West	Andesite	2672	18,54	3,72	0,5114	0,1213	0,5092	1,81 ± 0,32
TS23-90	Leta Arm	West	Andesite	2672	27,22	5,22	0,5113	0,1159	0,5092	1,49 ± 0,12
TS23-37	Leta Arm	East	Basaltic andesite	2672	12,98	3,17	0,5118	0,1477	0,5091	1,70 ± 0,18
TS23-35	Leta Arm	East	Basalt	2672	17,88	5,38	0,5125	0,1820	0,5094	1,26 ± 0,31
TS23-56	Leta Arm	East	Basalt	2672	10,43	3,12	0,5125	0,1809	0,5093	2,19 ± 0,27
TS23-73	Leta Arm	West	Basalt	2672	6,55	2,15	0,5128	0,1985	0,5093	2,11 ± 0,22
TS23-81	Leta Arm	West	Basalt	2672	7,60	2,52	0,5128	0,2005	0,5093	1,68 ± 0,28
TS23-02	Hewitt Lake	Southwest	Andesite	2671	16,05	3,67	0,5117	0,1382	0,5093	2,22 ± 0,31
TS23-04	Hewitt Lake	Southwest	Basalt	2671	5,38	1,87	0,5130	0,2102	0,5093	1,63 ± 0,26

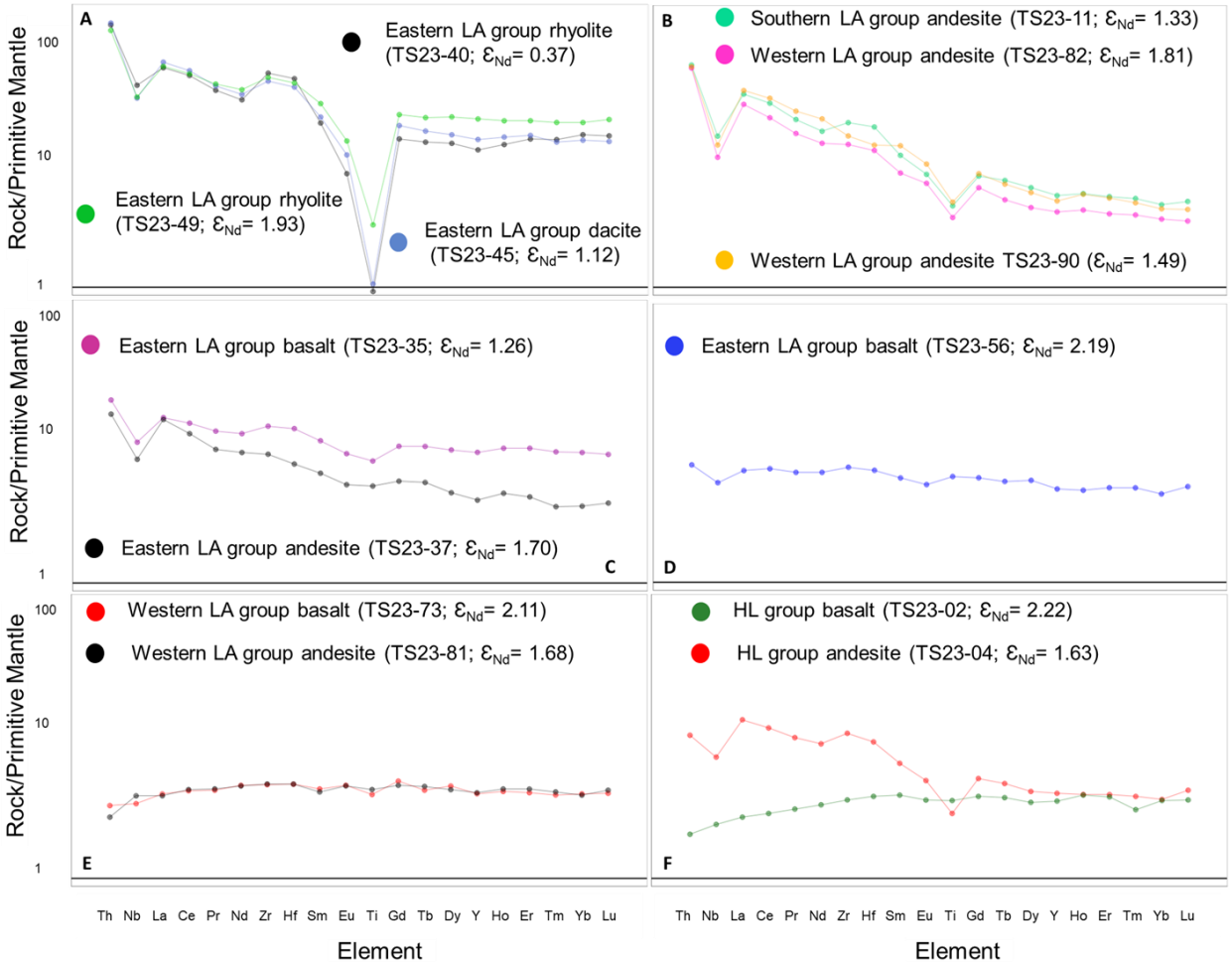

Figure 4.19. Primitive mantle-normalized patterns of selected samples for Sm-Nd isotope analysis. A) Steep LREE-enriched patterns with strong negative Ti and Nb anomalies. B) Moderately steep REE patterns with less pronounced negative Ti anomaly. C) Moderately steep REE patterns with minor negative to no Ti anomalies. D) Weakly LREE-enriched patterns with minor negative Nb anomaly. E) Nearly flat REE patterns minor to positive Nb anomalies. F) Steep REE pattern in andesite and flat REE pattern in basalt of the Hewitt Lake group. Normalizing values from Sun and McDonough (1989).

5. Discussion

5.1. Rock types in the Leta Arm group and Hewitt Lake group

A revised geological map, improved with petrographic results from this study, is presented in Figure 5.1. Some of the lithologies were inadequately classified from previous studies and the new map shows actual rock distribution confirmed using petrography, geochemistry, geochronology and isotope data. New data showed a wide range of compositions from basalt to rhyolite in the LA group. The HL group only consists of basalts and andesites. Basalts of both groups contain plagioclase, clinopyroxene, and minor orthopyroxene with amphibole and minor biotite only observed in basalts of the HL group (Fig. 4.3A-D and Fig. 4.3C&D respectively). Andesites show a significant decrease in pyroxene content and more widespread hornblende and biotite, particularly in the HL group (Fig. 4.4). Minor quartz, actinolite, rutile and Fe-Ti oxides form part of the matrix and/or occur along grain boundaries of plagioclase, hornblende and pyroxenes. Smaller grains of hornblende, plagioclase, biotite and pyroxenes were also observed in the matrix. Dacite and rhyolite were only observed in the LA group (Figs. 4.5 & 4.6). Feldspar and quartz form phenocrysts in all dacites and are associated with a very fine-grained quartzo-feldspathic matrix (Fig. 4.5). Biotite was only observed in the eastern and southern dacites (Fig. 4.5A&C). Differences in modal abundances are consistent with crystal fractionation supported by trends on Harker diagrams as there is a progressive decrease in mafic minerals in the intermediate to felsic rocks. This trend is more obvious in the LA group due to its variable rock types compared to the southwestern HL group which only consists of basalt and andesite. The change in modal abundances is, however, more systematic in the HL group as there is no significant decrease in mafic minerals from basalt to andesite compared to the LA group which shows drastic changes

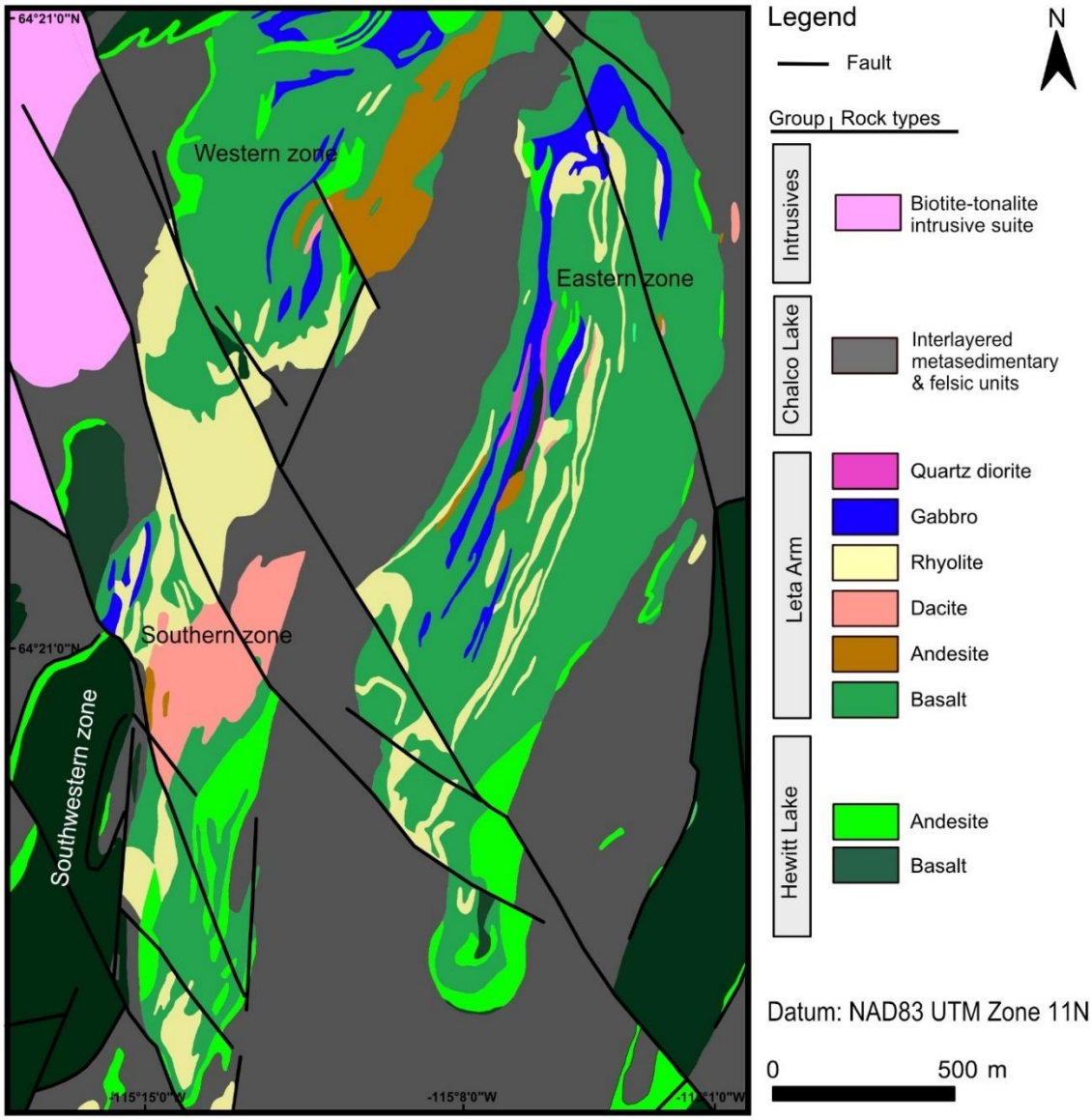

Figure 5.1. Updated geological map of the Indin Lake supracrustal belt based on new mapping and extrapolations based on Pehrsson (1998).

between rock types. Given the high pyroxene content in the LA group basalt as opposed to high amphibole and biotite content in the HL group basalt, it is likely that the HL and LA group evolved from magma bodies of different compositions. The petrology of the HL group rocks suggests they formed from a hydrous magma which stabilized and fractionated amphibole and biotite, followed

by the formation of the LA group rocks in less hydrous conditions resulting in increased pyroxene content.

Relic and pseudomorphic grains in basalts and andesites are euhedral to subhedral and have defined grain boundaries, with some overprinting in altered sections. Grain sizes are variable from fine- to medium-grained in both basalt and andesite with intergranular textures in basalts to slightly porphyritic in andesites (Fig. 5.2A&B). Dacites show more obvious porphyritic textures compared to andesites (Fig. 5.2C). Porphyritic textures in the rocks are suggestive of two-stage cooling initiated by the emplacement of magma in a hypabyssal environment to form phenocrysts followed by rapid cooling or extrusion to form smaller grains of the same compositions together with

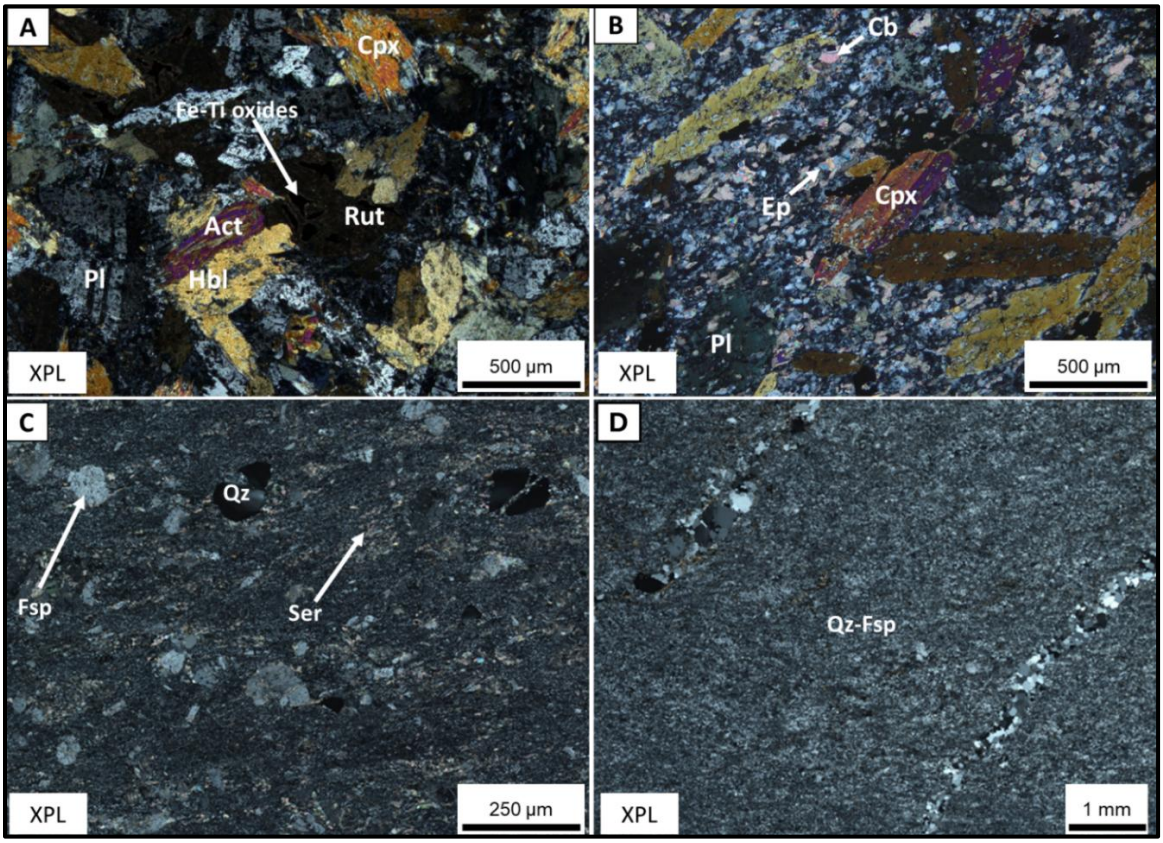

Figure 5.2. Variable textures in the ILSB rocks. A) basalt, B) andesite, C) dacite, D) rhyolite. XPL=cross-polarized light, Pl=plagioclase, Hbl=hornblende, Cpx=clinopyroxene, Rut=rutile, Act=actinolite, Ep=epidote, Cb=carbonates, Qz=quartz, Ser=sericite.

accessory phases in the groundmass (Le Maitre et al., 2002; Vernon & Clarke, 2008). The predominance of aphanitic texture in rhyolites suggests rapid surface cooling (Fig. 5.2D). The different textures in the volcanic rocks control the degree to which they are deformed. Aphanitic rocks show a moderate to strong foliation fabric and are associated with penetrative chlorite whereas intergranular to porphyritic rocks show microstructures in euhedral phenocrysts or crosscutting quartz veins and exhibit a weak foliation in the groundmass (Figs. 4.4 & 4.5).

5.2. Alteration, metamorphism and deformation in the Leta Arm and Hewitt Lake groups

The replacement of primary phases in the volcanic rocks is variable in each zone with over 50% of the mineral phases showing intense to moderate alteration. Secondary phases in the rocks include actinolite, ferro-hornblende, biotite, chlorite, carbonates, epidote, sericite, quartz and Fe-Ti oxides. The formation of secondary phases in the ILSB would require some type of metasomatic or metamorphic process. This occurs when fluids expelled from the crystallizing magma modify the chemistry of prevailing crystals to form assemblages of hornblende-actinolite-chlorite-carbonates and other silicates at 150-400°C (Le Maitre et al., 2002). This mechanism would explain the rims of secondary phases around euhedral to subhedral primary phases (Fig. 4.8). In rocks where ferro-hornblende replaces pseudomorphic actinolite and magnesio-hornblende, it occurs as coronas around relic phases suggesting it formed later than the phases it encloses whereas in some parts it is enclosed by actinolite rims along grain boundaries which suggests it formed earlier than actinolite (Fig. 4.8). In some rocks of the eastern LA group euhedral ferro-hornblende is predominant and does not form cores or coronas around other phases, suggesting it has either completely replaced pre-existing phases or is primary (Fig. 4.8). The possibility of ferro-hornblende being entirely primary is questionable as it coexists with altered pyroxenes and occurs in highly carbonatized and chloritized rocks in which all the groundmass is overprinted by

alteration (Fig. 4.4A). The occurrence of ferro-hornblende as an enclosing phase around pseudomorphic actinolite in other rocks, which formed by the alteration of pyroxenes, also supports this statement. It is therefore likely that ferro-hornblende formation in the ILSB is related to hydrothermal fluids and was on a regional scale regardless of its timing relative to actinolite formation.

Widespread carbonates, sericite and epidote alteration in intermediate to felsic rocks highlight that plagioclase was the main phase being altered (Fig. 5.3). This alteration assemblage is associated with secondary quartz formed by silicification. Carbonates and epidote are often found incorporated within and surrounding ferro-hornblende grains in the eastern LA group. Chlorite is found overprinting plagioclase and ferromagnesian minerals in basalts and the eastern LA group andesite (Figs. 4.3 & 4.4A). Metamorphic biotite postdates foliation and occurs as undeformed euhedral grains which formed overgrowths along pre-existing chlorite in contrast to primary phases which occur either as euhedral phenocrysts in weakly deformed rocks or is deformed with the rock to form a foliation (Fig. 4.5D). Secondary Fe-Ti oxides were observable along grain boundaries and cleavage planes of ferro-magnesian minerals whereas the primary Fe-Ti oxides of the eastern LA group basalts are partially replaced by accessory rutile to form a core-rim relationship (Fig. 5.2A).

The formation of biotite after chlorite, epidote and carbonates after plagioclase, actinolite after pyroxenes, and subsequent ferro-hornblende after actinolite and magnesio-hornblende would require temperature conditions higher than metasomatism (>350 °C; Pearce, 1996; Polat & Kerrich, 2001; Pirnia et al., 2014). Consistently, the replacement of actinolite (and magnesio-hornblende) by ferro-hornblende is compatible with a change from greenschist to amphibolite facies, demonstrating an increase in metamorphic grade (Hashimoto, 1972; Frey et al. 1991;

Vernon & Clarke, 2008; Lagat, 2009). Deformation microstructures such as grain boundary migration and subgrain rotation in quartz and feldspar grains in the ILSB support exposure of the rocks to high temperatures spanning 450-700 °C (Stipp et al., 2002). This is consistent with observations from previous studies stating that the ILSB was subjected to greenschist (M1) to amphibolite (M2) facies metamorphism at 3.8-4 kbar and 350-625°C pressure-temperature conditions, both associated with D1 and D2 in the ILSB (Pehrsson, 1998; Pehrsson & Villeneuve, 1999). The replacement of ferro-hornblende by actinolite can be explained by retrograde metamorphism. However, this is restricted to the eastern LA group and no other mineral assemblages representative of retrogression were observed elsewhere.

Carbonate-sericite-epidote formation was not ubiquitous and likely resulted from pervasive alteration associated with the injection of hydrothermal fluids along faults. This has been suggested to be related to the formation of the Colomac deposit by fluid-rock interaction during later brittle deformation, precipitating gold and associated sulphides (Morgan, 1991). Based on the above interpretations, it is clear that lithological and textural modifications in the ILSB occurred mainly by a combination of processes during metamorphism, and interaction with hydrothermal fluids.

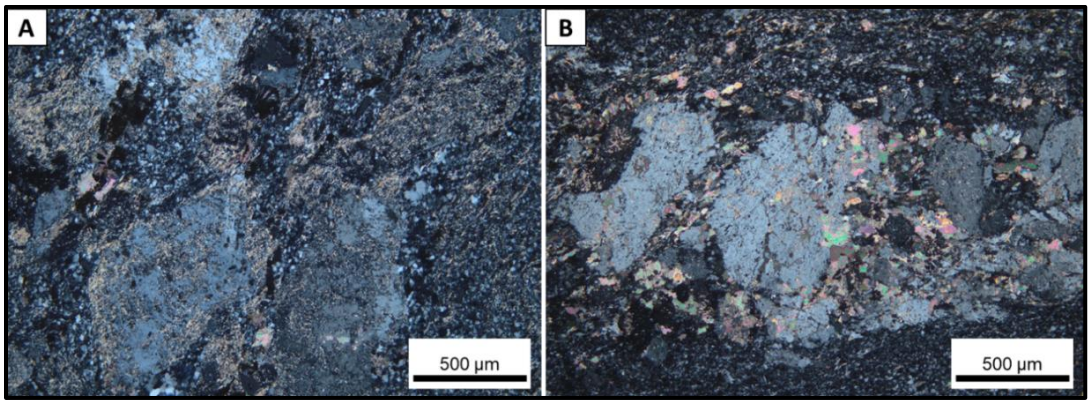

Figure 5.3. A) Sericite and minor carbonate alteration in a dacite porphyry that shows recrystallized quartz around felspar phenocrysts. B) Epidote, carbonates and minor sericite around feldspar phenocrysts in a dacite porphyry.

5.3. Petrogenetic and contamination processes in the ILSB volcanic rocks

Major and trace element geochemistry of the ILSB indicates a variety of subalkaline compositions that are consistent with tholeiitic to calc-alkaline trends (Figs. 4.9B & 5.4). Strong positive correlations between SiO_2 and K_2O and negative correlations between SiO_2 and MgO, Fe_2O_3 and CaO are often associated with crystal fractionation whereby magma evolves from mafic to felsic rocks along the same trend (Fig. 4.10; Abdel-Halim, 2023). Fractionation in the LA group rocks occurred by the concentration of clinopyroxene, orthopyroxene and Fe-Ti oxides in basalts,

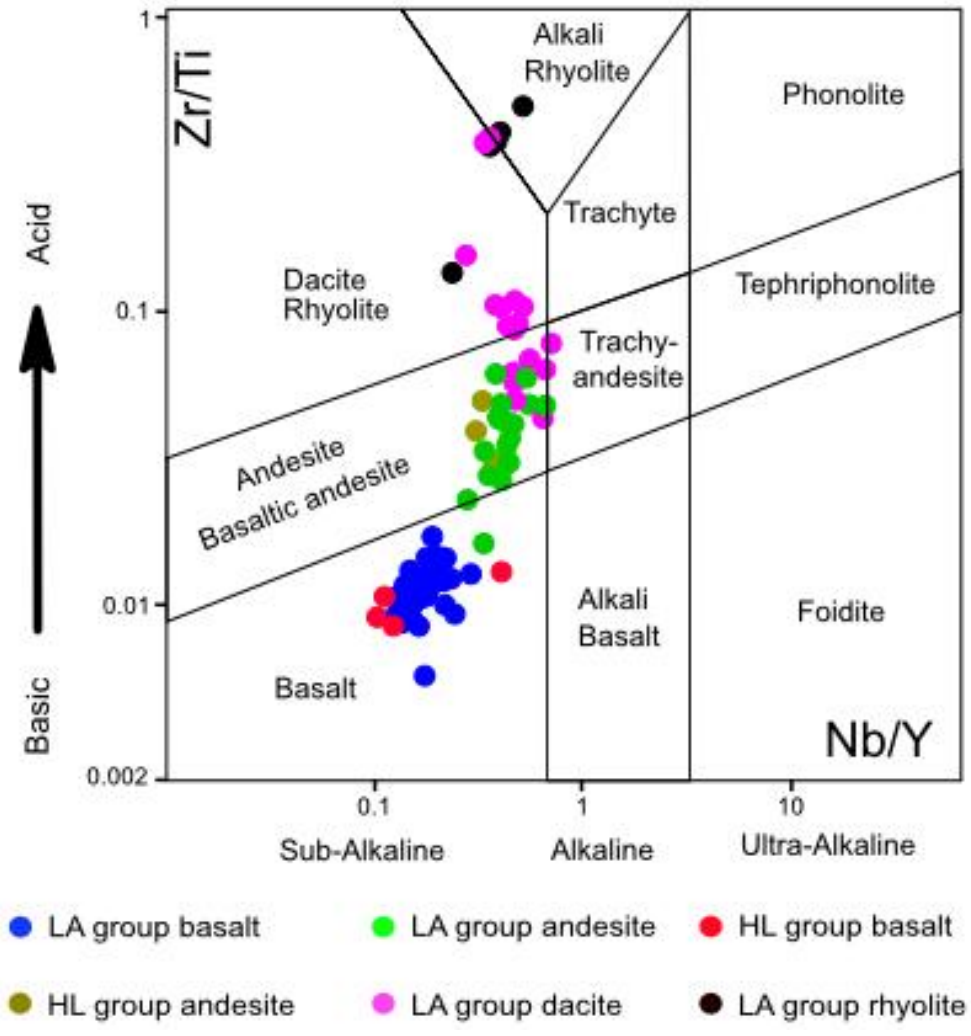

Figure 5.4. Immobile element–based TAS proxy diagram (modified after Pearce, 1996 and Pearce, 2014).

accompanied by a slight increase in biotite and minor quartz in andesites and ultimately the concentration of more felspar and quartz in dacites and rhyolites. In the HL group, fractionation resulted in the concentration of amphibole, pyroxenes, minor plagioclase and biotite in basalts to increased biotite, plagioclase, quartz and phenocrystic hornblende in andesites. These fractionation trends are consistent with a decline in Co, Sc, Ti and increasing Zr, Nb, and Hf with increasing silica as the composition shifts from basalt to rhyolite (Figs. 4.11 & 5.5). Latypov (2009) attributes such trends to rocks that formed from the same magma. However, this is not consistent with petrographic analysis as it has shown that the HL group is amphibole-rich whereas the LA group is clinopyroxene-rich. Plots of mobile and immobile elements against Zr show scattering of mobile elements (K) whereas immobile elements (Ti) show clear linear trends, clear rock type groupings and minimal scattering (Fig. 5.5). The scattering observed could be a result of remobilization during metamorphism as these elements are known to be variably mobile under such conditions (Rollinson, 1993; Murphy, 2007).

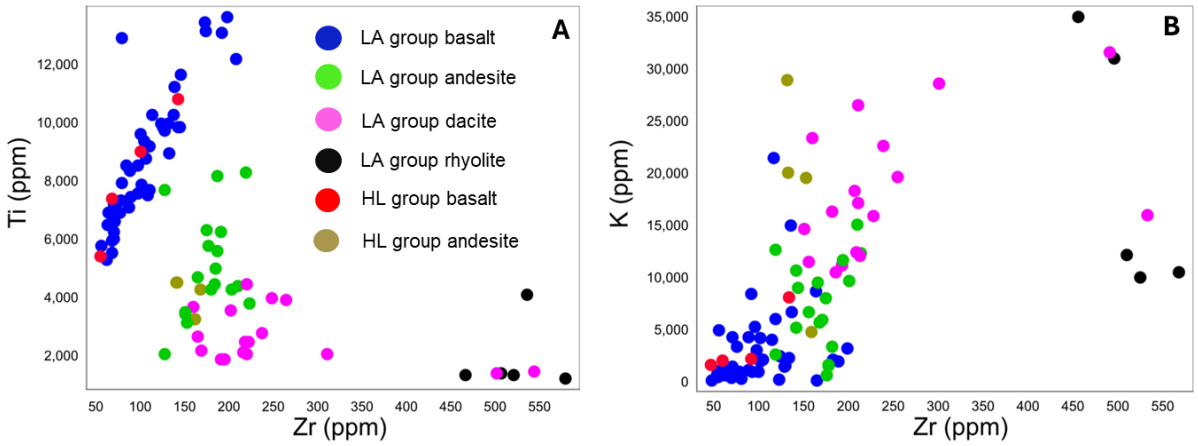

Figure 5.5. Discrimination plots of mobile (K) and immobile elements (Ti) against Zr.

Primitive mantle-normalized spider plots of basalts show variable REE patterns (Fig. 4.12). Basalts of the HL and western LA group consist of nearly flat REE with minor to positive Nb anomalies,

low La/Sm_N (<2.0) and low Th contents, except one basaltic sample (TS23-03) in the HL that shows a steep REE profile. This anomalous sample shows LREE enrichment from La to Nd and HREE fractionation. The eastern LA group basalts have a negative Nb anomaly, a positive Th anomaly and LREE enrichment with La/Sm_N values up to 2.69. All basalts in the HL and LA groups are characterized by minor to no Ti anomalies, no Zr-Hf anomalies, Nb/Nb* <1.43, and Gd/Yb_N ratios of <1.7 except in the anomalous HL basalt which has a Gd/Yb_N of 2.17.

The flat REE patterns in the ILSB basalts are broadly similar to MORB. However, the lack of LREE depletion characteristic of modern MORB suggests they are not MORB (Kerrich & Wyman, 1997; Pearce et al., 2005; Zheng, 2019). True MORB-like signatures are rare in the Archean and the signatures observed in the basalts likely represent oceanic plateaus or primitive arc tholeiites formed in a subduction zone setting (Kerrich & Polat, 2006; Murphy, 2007; Polat, 2013). Oceanic plateaus are mantle-derived, flat-topped features of thick oceanic crust associated with large volume plume eruptions (Coffin & Cahagan 1995; Kerrich & Wyman, 1997). They are characterized by flat to weakly LREE-enriched patterns, positive Nb anomalies, and HREE depletion as they originate from deep mantle sources in the garnet stability field (Mahoney et al., 1993; Kerrich & Wyman, 1997; Pearce et al. 2005). Western basalts of the ILSB are representative of this signature due to their near flat REE patterns, minor depletion to weak LREE enrichment and lack of negative Nb anomalies. The basalts are weakly HREE-depleted (Gd/Yb_N ratios of <1.7), which suggests shallow melting above the garnet stability field (Murphy, 2007; Qin et al., 2024). The anomalous Gd/Yb_N (2.17) in sample TS23-03 of the HL group basalts possibly indicates slightly deeper melting and if so, the western basalts likely represent either melting at variable depths or heterogeneities in the magma source region. On the other hand, the eastern LA group basalts are consistent with geochemical signatures of primitive arc tholeiites which form in

the early stages of arc development by metasomatism of a mantle wedge by fluids derived from the subducting slab (Stern and Hanson, 1991; Barrett & MacLean, 1999; Cousens, 2000; Hawkesworth et al., 1993). This mechanism initiated LREE enrichment which resulted in a slightly steeper REE slope than that of the western basalts, representing the onset of an arc system. The arc signature is more prominent in intermediate to felsic rocks and is accompanied by a positive Th anomaly and negative Nb and Ti anomalies. The majority of intermediate to felsic rocks in the ILSB show only positive Zr-Hf anomalies except the western andesites which show both positive and negative Zr-Hf anomalies.

Negative Nb, Ti, Zr and Hf anomalies are typical of arc rocks due to their low solubility in fluids meaning they are retained in the subducting slab during metasomatism of the subarc mantle (Hawkesworth et al., 1993; Sisson & Grove, 1993; Pearce & Peate, 1995; Grove et al. 2003; Smithies et al., 2004; Murphy, 2007). As positive Zr-Hf anomalies are not representative of arc rocks they can be attributed to fractionation in conjunction with pronounced negative anomalies of other elements in intermediate to felsic rocks. Murphy (2007) implied fractionation in arc magmas from observations of parallel REE profiles, as also seen in the ILSB data. Although fractionation may be a contributing factor, it is not a requirement for arc magmas as they are inherently depleted in HFSE and fractionation would not yield positive Zr-Hf anomalies (Kerrich & Wyman, 1997; Polat & Kerrich, 2001). Another cause for the positive Zr-Hf anomalies could be the loss of LREE relative to HFSE by alteration/metamorphism as LREE are mobile during such processes, resulting in the preservation of positive anomalies of HFSE, including Th (Rollinson, 1993; Polat and Hofmann, 2003). To test this, zirconium was compared with LREEs in Figure 5.6 to determine the degree of element mobility due to its low mobility during metamorphism (Pearce, 1996; Le Maitre et al., 2002; Ague, 2017). Diagrams of Zr plotted against LREEs of samples

(intermediate to felsic rocks) that have positive Zr-Hf anomalies show a positive correlation with minor scattering, indicating minimal effects of post-magmatic processes on LREE absolute abundances (Fig. 5.6). This rules out fractionation and metamorphism as possible causes for positive Zr-Hf anomalies in the ILSB.

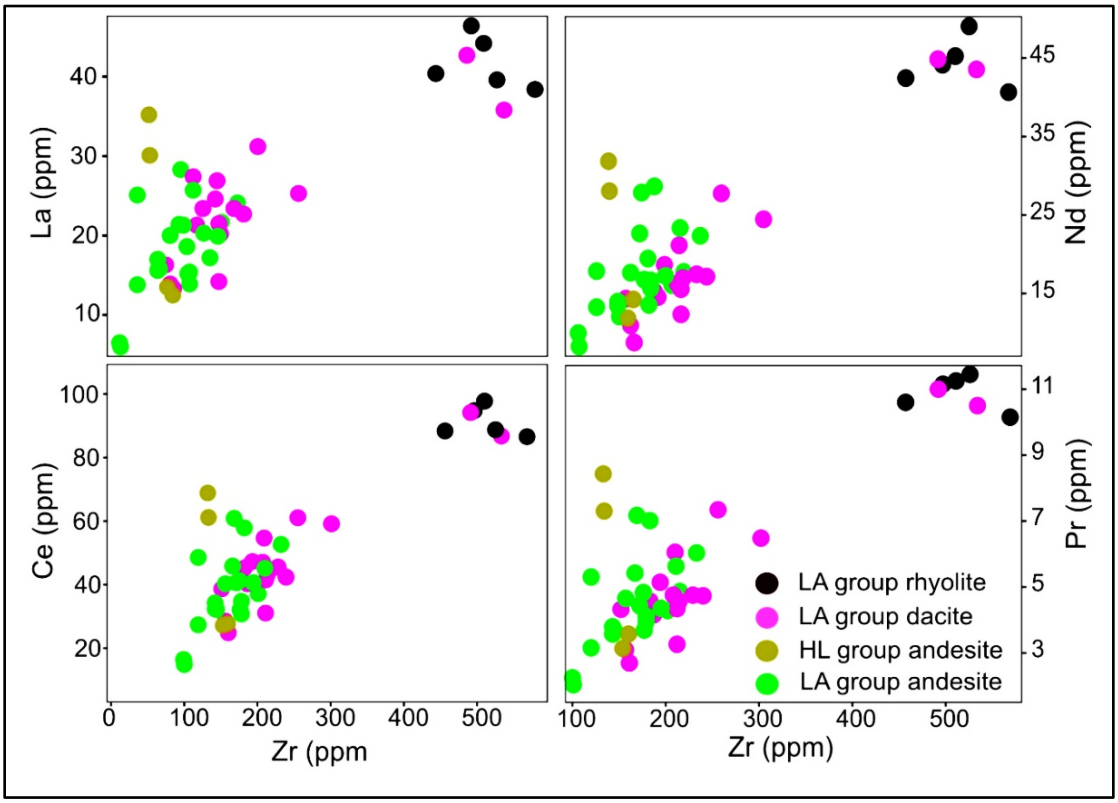

Figure 5.6. Diagrams of zirconium plotted against light rare earth elements to determine the effects of metamorphism on LREE (light rare-earth element) mobility.

Given that the above interpretations do not exclusively account for some of the geochemical trends in the ILSB, contamination by continental crust might explain some of the geochemical characteristics. Contamination can be either by assimilation of crustal rocks or direct input of ocean floor sediments into the subarc mantle during subduction in the case of arc magmas (Hawkesworth et al., 1993). Radiogenic isotope data were used to investigate the role of contamination in forming

the characteristics observed in the ILSB. Neodymium (Nd) is slightly more incompatible than samarium (Sm) and concentrates in the mantle rather than in the crust. This drives the evolution of the mantle towards high $^{143}Nd/^{144}Nd$ ratios and that of the crust towards low $^{143}Nd/^{144}Nd$ (DePaolo, 1981; Rasskazov et al., 2005; Murphy, 2007). Over time, depleted mantle sources evolve towards positive ε_{Nd} values whereas the crust evolves towards negative ε_{Nd} values (Murphy, 2007). Volcanic rocks analyzed for Sm/Nd isotopes in this study have ε_{Nd} values ranging between 0.37 and 2.22, which are similar to those of Pehrsson (1998) which range from 0.22 to 1.87.

Positive ε_{Nd} values have been interpreted in other studies, such as in the Abitibi greenstone belt, to be associated with Archean rocks derived from a depleted mantle estimated at 2.7 Ga to have an ε_{Nd} of +3 (DePaolo, 1981; Blichert-Toft & Albarede, 1994; Hollings & Wyman, 1998; Hollings et al., 1999; Tomlinson et al., 2004; Rasskazov et al., 2005; Murphy, 2007). The juvenile positive ε_{Nd} values in the ILSB suggest they are derived from an Archean depleted mantle and had no interaction with significantly older crust as it would require basement that is at least 50 Myr older to modify the ε_{Nd} values of the rocks (DePaolo & Wasseburg, 1976). No significantly older basement has been identified in the ILSB but the location of the Cotterill tonalite near metavolcanic rocks in the belt makes it a possible contaminant even though it does not form an in-situ basement to the rocks (Pehrsson, 1998; Pehrsson & Villeneuve, 1999). The ~9 Myr age gap between the tonalite and volcanic rocks indicates that it would not have significantly changed the isotopic composition of the volcanic rocks, so any contamination would not have modified the ε_{Nd} values. This is also supported by the euhedral zircon morphologies and high Th/U values ($\geq$0.5; appendix IV) often associated with primary zircons formed during crystallization and indicate no inheritance from older crust (Kirkland et al., 2015; Lopez-Sanchez et al., 2016).

Contamination by continental crust is often associated with negative Nb anomalies, LREE enrichments, positive Zr-Hf and low $^{143}Nd/^{144}Nd$ values (Pearce, 1982; Crawford et al., 1989; Lightfoot et al., 1991; Storey et al., 1992; Rollinson, 1993; Kerrich & Wyman, 1997). This signature is observed in the ILSB and explains the positive Zr-Hf anomalies which are inconsistent with simple fractionation or metamorphism of arc rocks. Some studies use the correlation of Nb anomalies with increasing SiO_2 and LREE and Th enrichment as a measure of contamination (Hollings & Wyman, 1998; Hollings et al., 1999). When Nb/Nb* is plotted against these elements, the ILSB shows evolution towards higher La/Sm_N, SiO_2 and Th; all consistent with contamination (Fig. 5.7). An example of contaminated mantle-derived rocks from other studies are tholeiites of

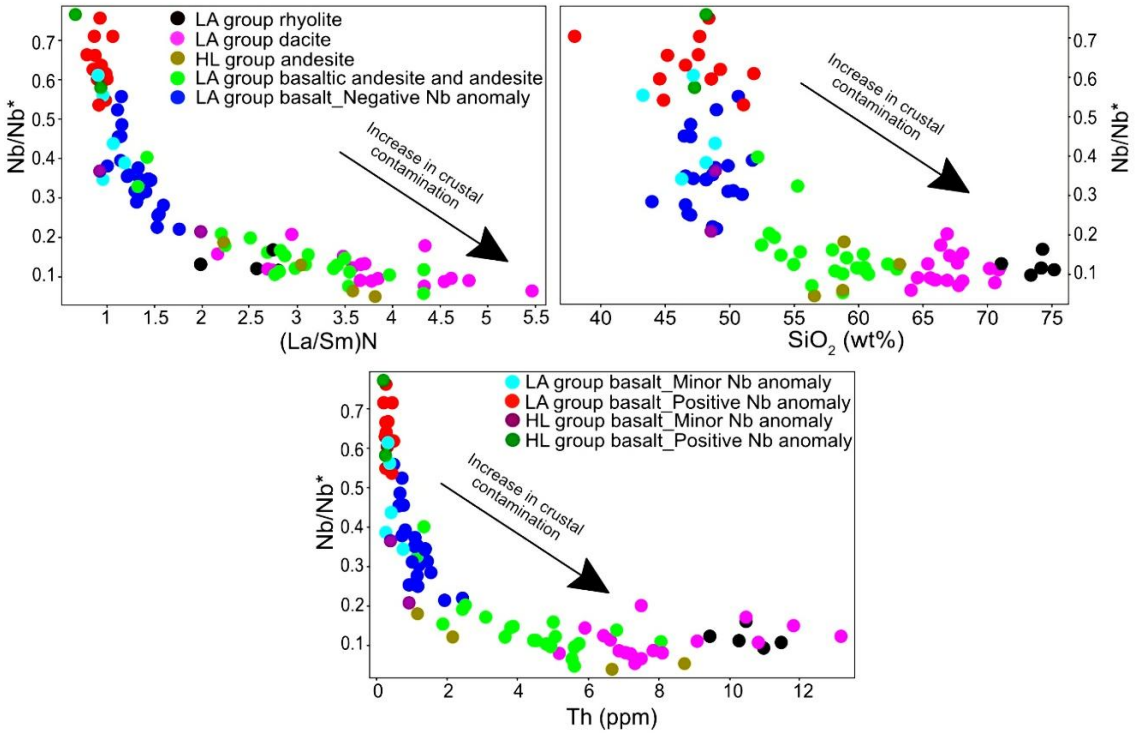

Figure 5.7. Discrimination diagrams for element behaviour during contamination.

the Kerguelen Plateau which have $^{143}Nd/^{144}Nd$ of <0.5127, suggesting the rocks have interacted with continental crust as it is associated with low $^{143}Nd/^{144}Nd$ (DePaolo, 1981; Storey et al.,

1992). A majority of the ILSB have lower $^{143}Nd/^{144}Nd$ (<0.5125) and negative Nb anomalies except the western basalts which slightly higher $^{143}Nd/^{144}Nd$ between 0.5128-5130 and lack a negative Nb anomaly, suggesting that they are less contaminated than other rocks in the belt.

5.4. Timing of magmatism in the ILSB

New high-precision zircon geochronology of felsic lenses from the eastern zone of the LA group yielded ages of 2673.6 ± 0.9 Ma, 2672.5 ± 1.1 Ma, 2669.8 ± 2.5 Ma and 2673.42 ± 0.15 Ma from TS24-01, TS24-05, TS24-07 and TS23-40 respectively (Figs. 3.1 & 4.18). The similar weighted mean ages for felsic volcanic samples TS24-01, TS24-05 and TS23-40 suggest that these three units could be correlative and may point to a repetition of the volcanic stratigraphy along strike even though they are not proximal to one another. Structural modifications possibly played a part in transposing some of the felsic lenses as ages for samples TS24-07 and TS24-01, which are correlated between drillholes GB21-26 and GB21-16 respectively, do not overlap in age at the 95% confidence level (Figs. 3.1 & 4.18). This is likely associated with the large number of faults observed in the study area and the multiple tectonic events that had the potential to form structural breaks as documented in previous studies (Pehrsson, 1998; Pehrsson & Villeneuve, 1999). The tight spread of ages suggests broadly coeval magmatism and are indicative of an event at ca. 2673 Ma and one at 2670 Ma.

Ages of Pehrsson (1998) and Pehrsson & Villeneuve (1999) are broadly coeval with those from this study (Figs. 5.8 & 5.9). In their study, a 2670 ± 2 Ma age from a crosscutting felsic sill that contained inherited zircons with an age of 2687 ± 6 Ma in the Hewitt Lake group was used to infer the deposition of the group to be between 2700-2680 Ma (Pehrsson, 1998). The age of the sill was interpreted to be the minimum depositional age of the Hewitt Lake group whereas the 2671+8/-7 Ma and 2668 +5/-3 Ma ages of the Leta Arm group were interpreted to represent its true eruption

age (Figs. 5.8 & 5.9;). Similar ages of felsic rocks to the ILSB were acquired in other parts of the western Slave Province (Isachsen & Bowring, 1994 and references therein).

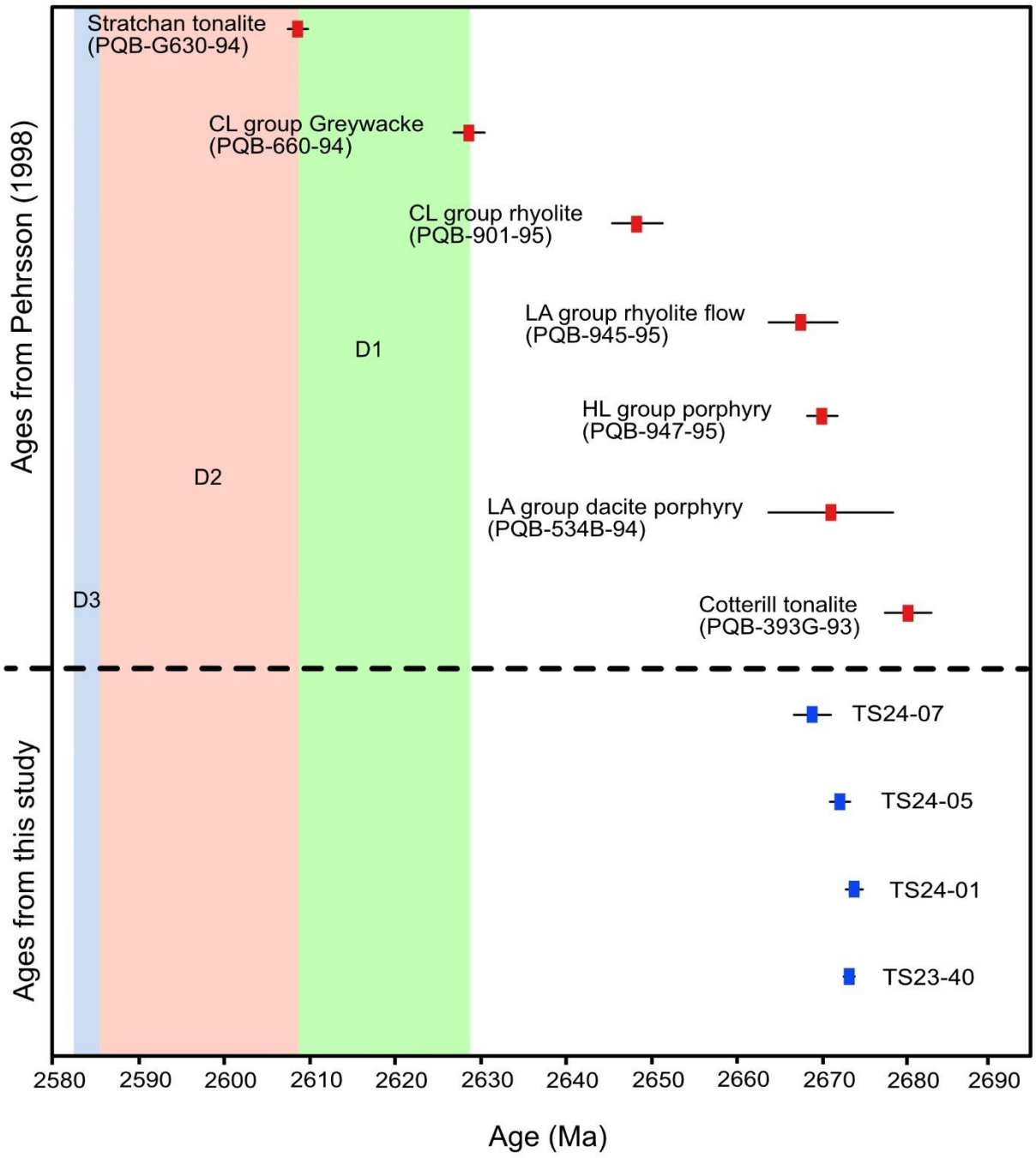

Figure 5.8. Summary of new and previous geochronological data. Data from previous studies includes time intervals of deformation events (Pehrsson, 1998).

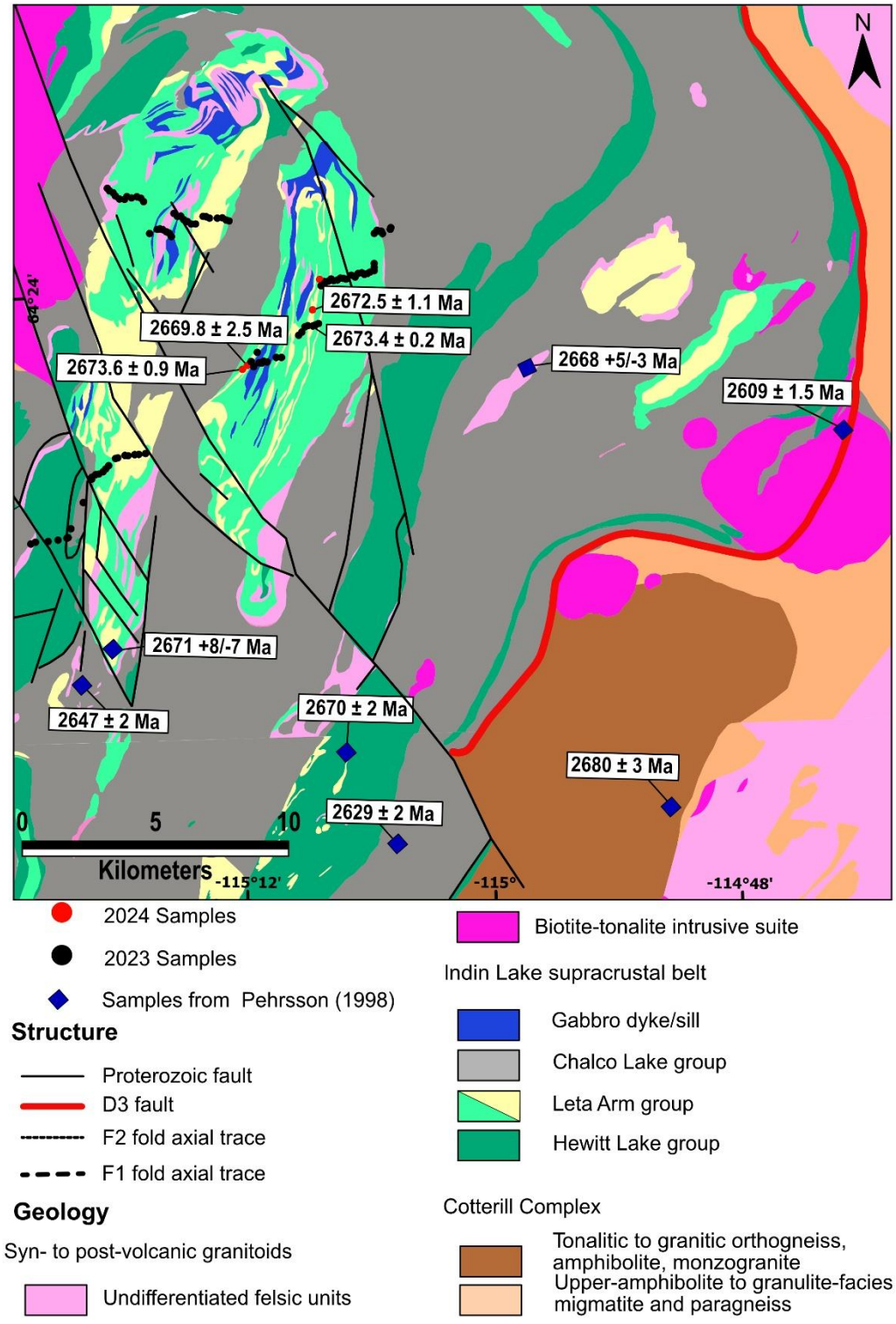

Figure 5.9. Ages of the Indin Lake Supracrustal Belt from this study and previous study of Pehrsson (1998).

Integrated previously published dates and those from this study constrain the timing of magmatism in the Leta Arm group to be between 2673-2668 Ma. Differences in age between the minimum age

of deposition between rocks of the Hewitt Lake and Leta Am groups maintain interpretations of Pehrsson (1998) that the groups were not deposited concurrently and that the LA group is younger than the HL group. However, this comparison introduces some bias as it is based on data from the eastern and southern LA group and one crosscutting sill from the eastern HL group only. The comparison in age between the groups could be optimized by comparing ages from all zones of both assemblages and this study cannot confirm with certainty that the assemblages are geochronologically distinct. The bounding Cotterill tonalite in the eastern ILSB was also dated by Pehrsson (1998) and yielded an age of 2680 ± 3 Ma, suggesting it does not represent basement to the ILSB as it is broadly coeval with volcanic rocks in the belt (Figs. 5.8 & 5.9; Pehrsson & Villeneuve, 1999). The slightly coeval nature of the bounding Cotterill tonalite suggests that magmatism in both the tonalite and ILSB volcanic rocks collectively occurred over short periods, indicating a complex geodynamic history.

5.5. Tectonic setting

New data from the ILSB volcanic rocks show a range of geochemical trends compatible with oceanic plateaus and subduction zones. Both the LA and HL groups have rocks of tholeiitic and calc-alkaline compositions but there is variability in geochemical signatures, particularly between the western basalts (positive and minor Nb anomalies) and other rocks in the belt (negative Nb anomaly basalts and intermediate to felsic rocks; Figs. 5.10, 5.11 & 5.12). The western basalts from both the LA and HL groups show plateau signatures (within-plate basalts, WPB) characterized by flat REE patterns and a lack of negative Nb anomaly while the eastern basalts and intermediate to felsic rocks from all zones have an arc-type signature (subduction zone, SZ) characterized by LREE enrichment and negative Ti and Nb anomalies (Figs. 5.10, 5.11 & 5.12). Although the western basalts of both assemblages are mineralogically distinct (LA group basalts

are pyroxene-rich, HL group basalts are amphibole-rich), they are geochemically and isotopically similar. Low Gd/Yb_N values (≤2.80) suggest melting in an oceanic setting at shallow crustal levels above the garnet stability zone for all ILSB rocks (Tarney & Jones, 1994; Murphy, 2007; Rollinson, 1993). Additionally, positive ε_{Nd} in conjunction with the lack of inherited zircons from new isotopic and geochronological data suggest any contamination would have been by crust of similar age. Minor age gaps between the ILSB rocks imply magmatism occurred over short intervals.

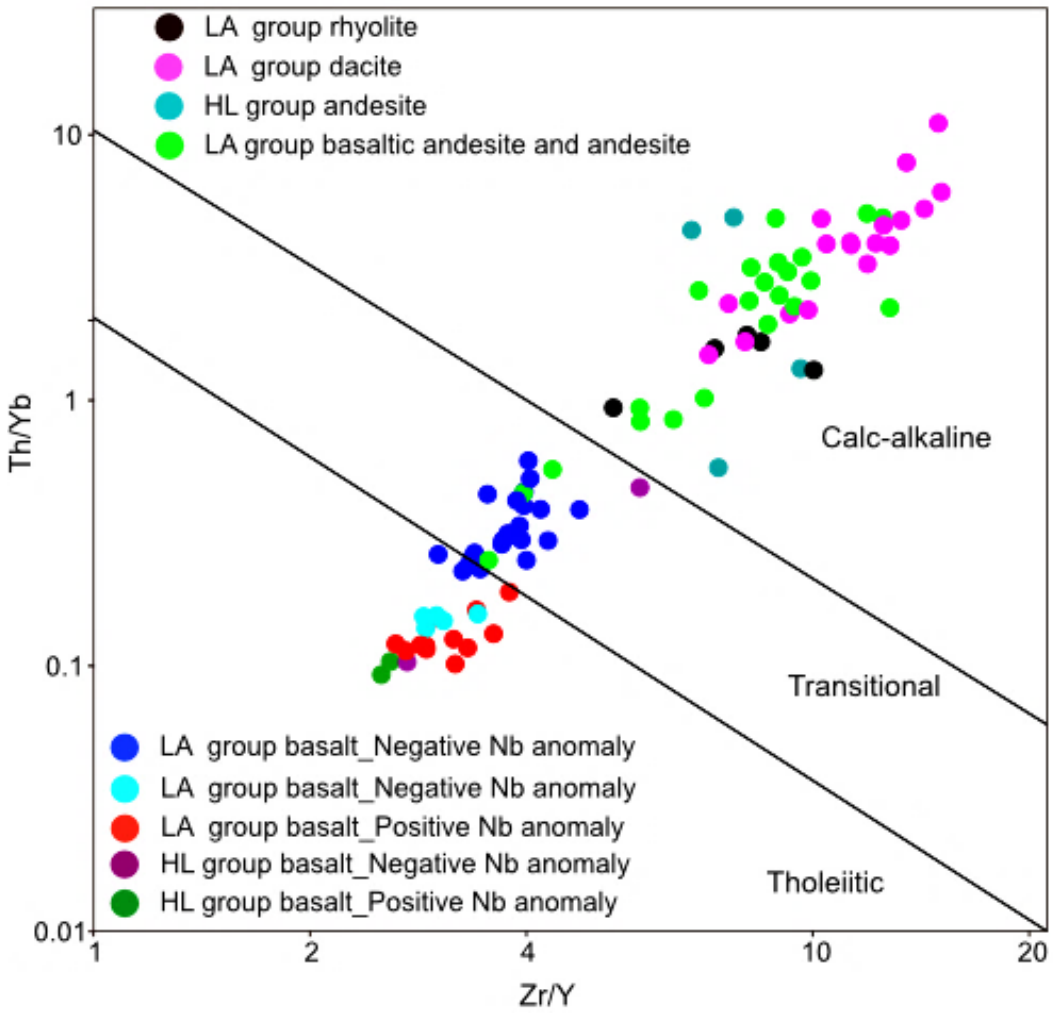

Figure 5.10. Magmatic Affinity diagram for the Leta Arm and Hewitt Lake group rocks (modified after Ross and Bedard, 2009).

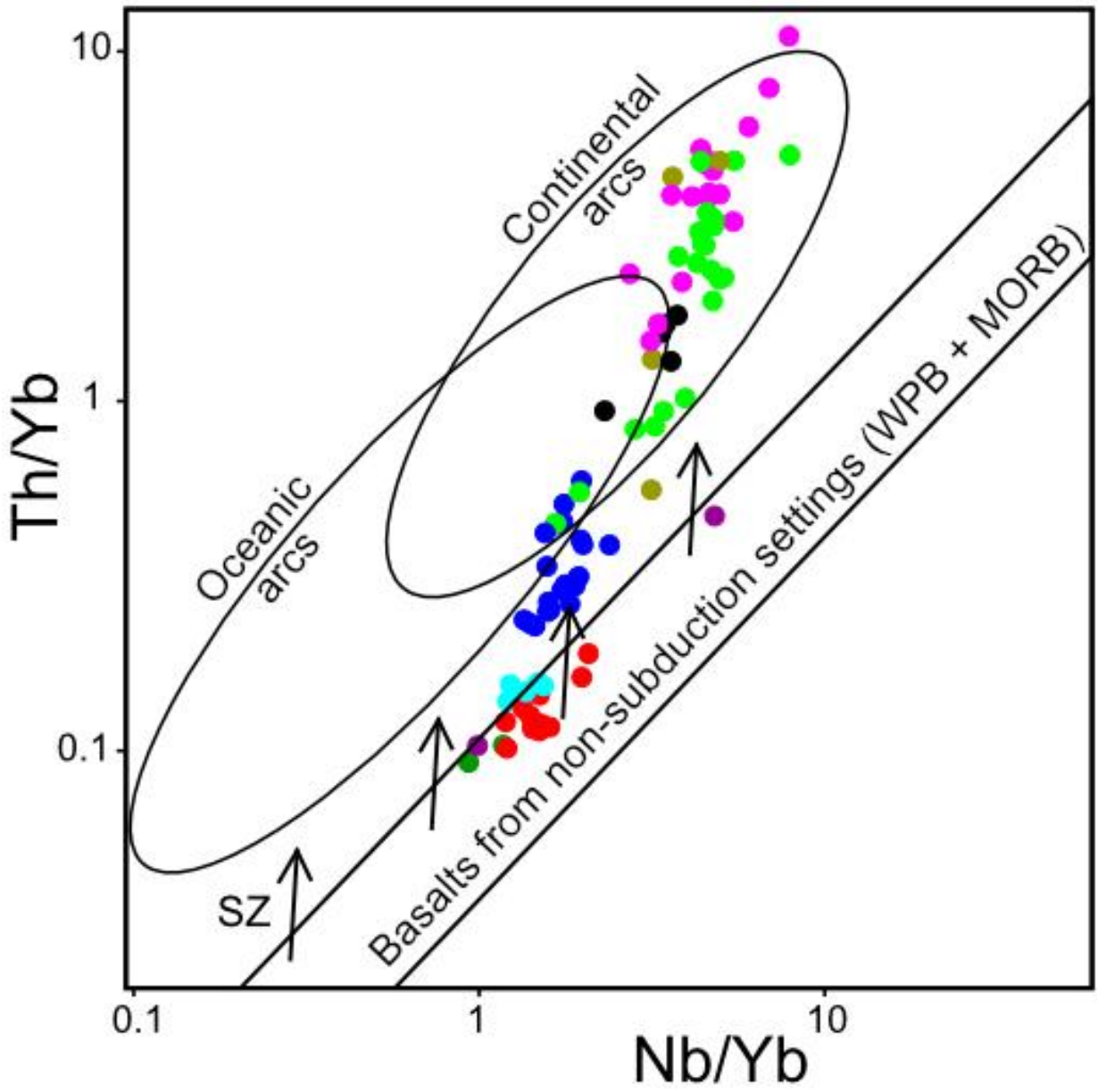

Figure 5.11. The Th/Nb proxy of Pearce (2014) is used to distinguish subduction zone (SZ) from within-plate basalts (WPB) and mid-ocean ridge basalts (MORB).

Based on the evidence provided we propose an interplay of oceanic plateau and subduction zone settings. The formation of the western basalts in an oceanic plateau likely took place first and underwent minor crustal contamination which resulted in positive-Nb anomaly tholeiites with high $^{143}Nd/^{144}Nd$ ratios. Plateaus are thick and buoyant oceanic crustal blocks and their buoyancy renders them resistant to subduction upon collision with other crustal blocks (Cloos, 1993). This

collision leads to a subduction back-stepping and the formation of a new subduction zone behind the plateau, particularly in plateaus that clog subduction zones within a few million years of formation (e.g., Ontong Java Plateau; Cloos, 1993; Kerr & Mahoney, 2007). Because of this

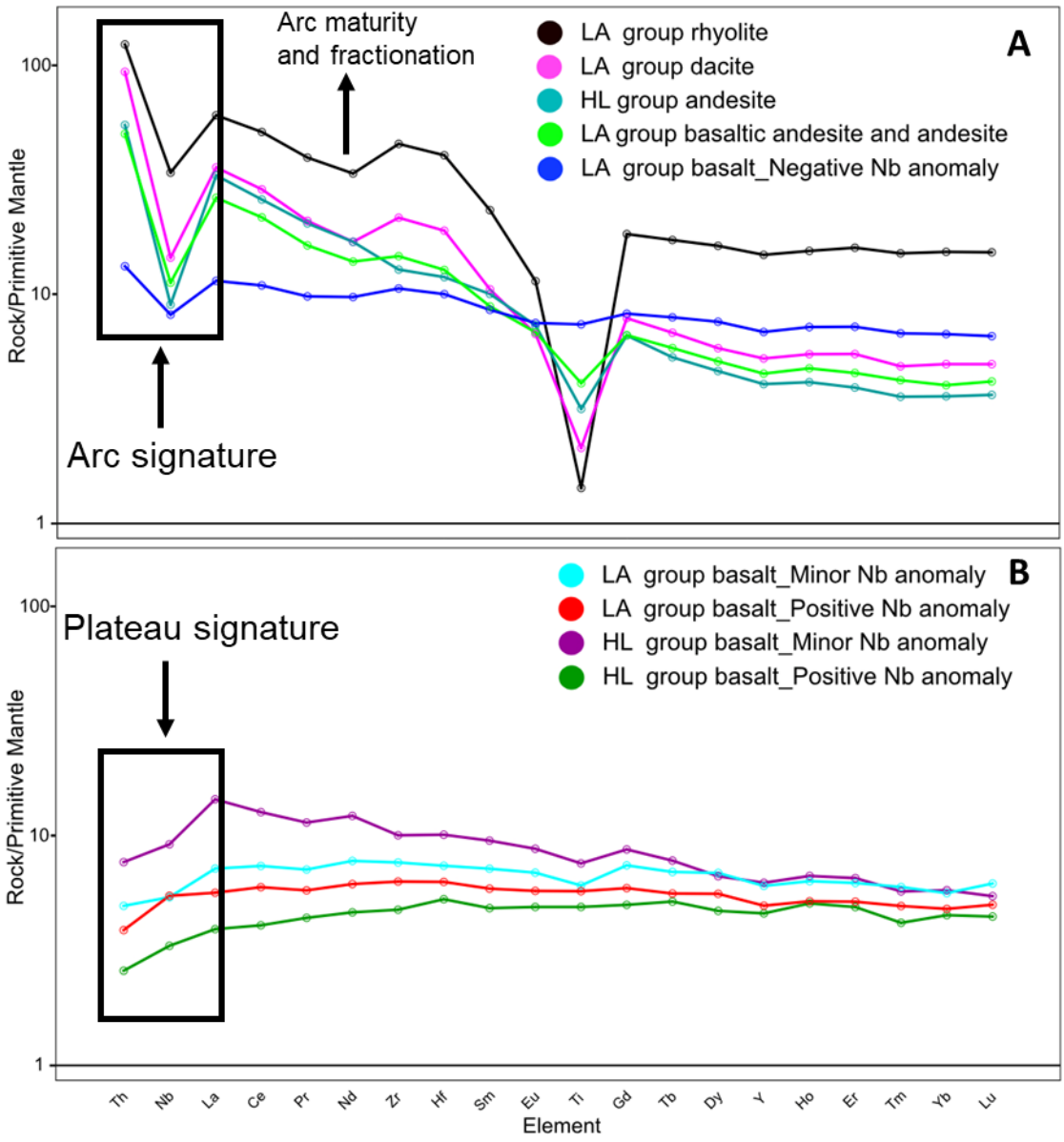

Figure 5.12. Median primitive mantle-normalized spider plots of the Leta Arm group and Hewitt Lake group rocks showing an evolving juvenile arc system from flat plateau patterns to LREE-enriched arc patterns with strong negative Ti and Nb anomalies and negative to positive Zr-Hf anomalies. Normalizing values from Sun and McDonough (1989).

association oceanic plateaus are sometimes spatially and temporally related to subduction zones in accretionary settings (Abbott & Mooney, 1995; Kerr, 2003; Kerr & Mahoney, 2007). The collision would then be followed by arc magmatism and eruption of arc magmas into the pre-existing plateau. In the case of the ILSB, this change in tectonic setting from plateau to arc signature is marked by a change from tholeiitic basalts with flat REE patterns to LREE-enriched transitional basalts (primitive arc tholeiites) and calc-alkaline rocks in Figures 5.10, 5.11 and 5.12. Arc magmatism in the belt is represented by the eastern LA group basalts and intermediate to felsic rocks which have negative Nb anomalies.

To infer the position of the plateau and direction of the subducting slab, previous models should be considered. Pehrsson (1998) inferred the formation of the LA and HL groups in a northeastern juvenile arc that was separated some distance from a southwestern continental arc where the Coterill tonalites formed (2680-2670 Ma; Fig. 5.13). However, this model characterised all geochemical trends in the ILSB as a juvenile arc signature and that the HL group formed a substrate on which the LA group erupted (Pehrsson, 1998). This interpretation does not align with the new data as the western basalts of both groups have similar geochemistry and isotopic signatures compatible with oceanic plateaus rather than subduction zones. There is also no conclusive evidence from age data for significant differences in timing of magmatism in the volcanic rocks and these groups cannot be interpreted to represent different assemblages based on petrography alone. The model of Pehrsson (1998) further implied the deposition of the Chalco Lake group on the juvenile arc in a back-arc basin (ca. 2647-2629 Ma) and imbrication of the ILSB volcanic and sedimentary rocks onto the southwestern continental arc (2629-2609 Ma, D1) to form southwest-vergent F1 folds. This was followed by folding of the ILSB rocks together with associated

granitoids by NW-directed shortening (ca. 2609-2590 Ma) to form the D2 fold geometry of the belt seen presently (Fig. 5.13; Pehrsson, 1998; Pehrsson & Villeneuve, 1999). No correlation

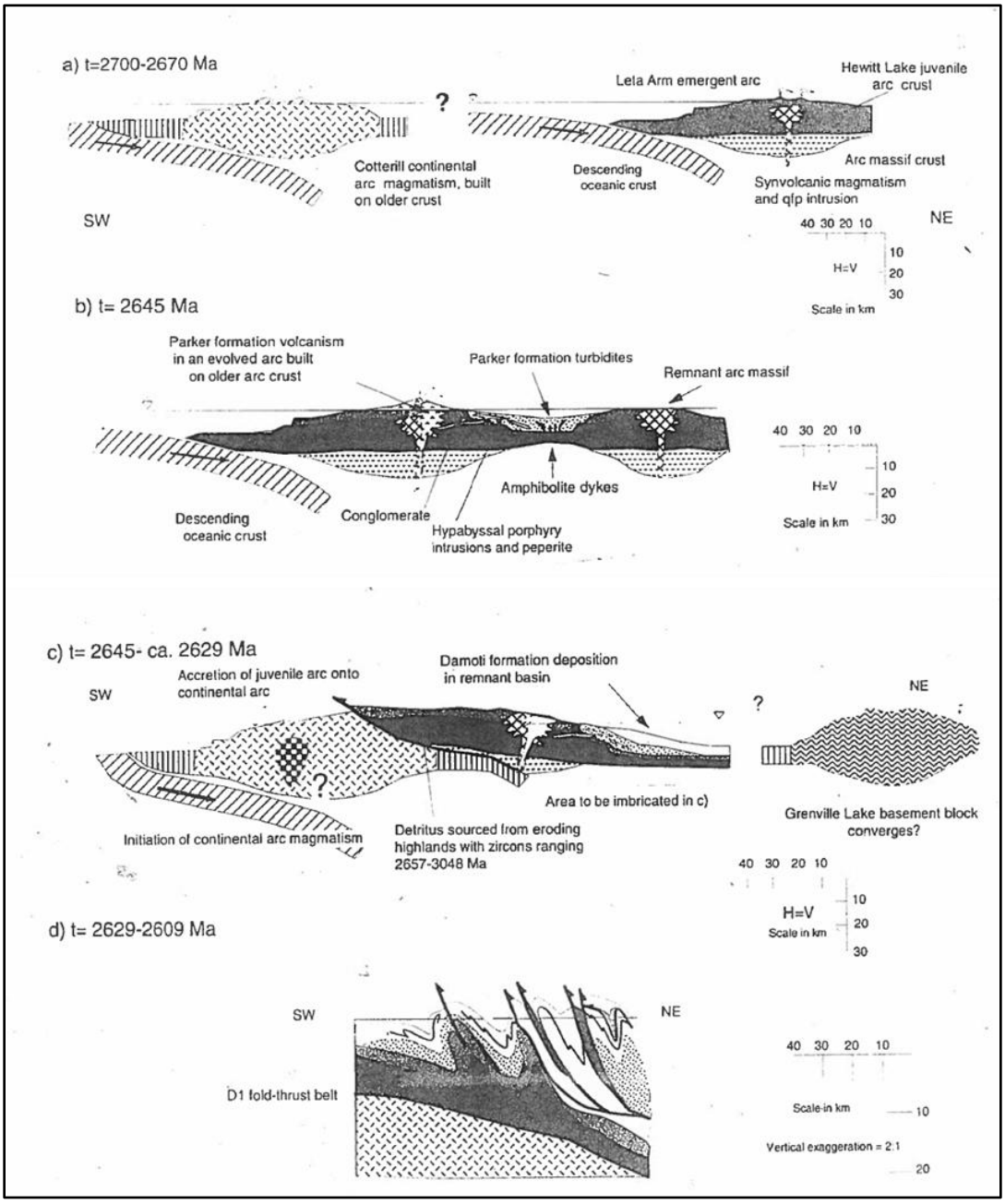

Figure 5.13. Tectonic model of the Indin Lake supracrustal belt. a) The formation of the Coterill Complex and distal deposition of the Leta Arm group on the Hewitt Lak group. b) Deposition of the Parker Formation sediments in a back-arc basin and felsic volcanism onto the Leta Arm group. c) Accretion of the continental and juvenile arcs and concurrent deposition of the Damoti Formation. d) The imbrication of the ILSB rocks along a southwest-vergent fold-thrust belt (Pehrsson, 1998).

between the Chalco Lake group and the other assemblages was made in this study, as sampling focused on the LA and HL groups (Fig. 4.1). There were also no tectonic contacts observed between LA and HL groups to support imbrication. It is, however, possible that D1 imbrication is only observable at a larger scale as evidenced by different ages correlated along the strike of juxtaposed felsic lenses.

If the ILSB is folded and all rocks were formed in an arc environment as interpreted by Pehrsson (1998), there should typically be symmetric geochemical signatures between the limbs of the D2 regional fold along the fold axis. A slight inward transition from mafic to felsic rocks is evident and even though intermediate to felsic units predominantly occur as lenses or lobes within basalts, they generally form the core of the ILSB while basalts form the outer parts (Fig. 5.14). Consequently, estimations of transitions in tectonic setting and direction of the subducting slab can be attempted. Assuming a pre-deformation (pre-D1) location of tectonic settings, the plateau signature with positive and minor Nb anomaly basalts would be in the northeastern ILSB whereas the arc signature with negative Nb anomaly basalts would be in the southwest along a NE-strike orientation (Fig. 5.14). This would require a northeastern crustal block that propagates towards the southwest to collide with the plateau resulting in arc magmatism and a new subduction zone with a northeast-directed subducting oceanic slab behind the plateau of the ILSB. There is currently no evidence for an eastern crustal block during the formation of volcanic rocks in the ILSB. However, the northeastern Grenville Lake basement block was speculated by Pehrsson (1998) to have existed during D1 and this possibly suggests a southwest-directed crustal blocks near the ILSB and that tectonic processes likely existed in the northeast even before D1 (Fig. 5.13). This collision and associated arc magmatism would have led to the initial eruption of primitive arc tholeiites along

the edge of the plateau followed by increased eruptions of intermediate to felsic rocks into the plateau as the arc matured and subduction progressed.

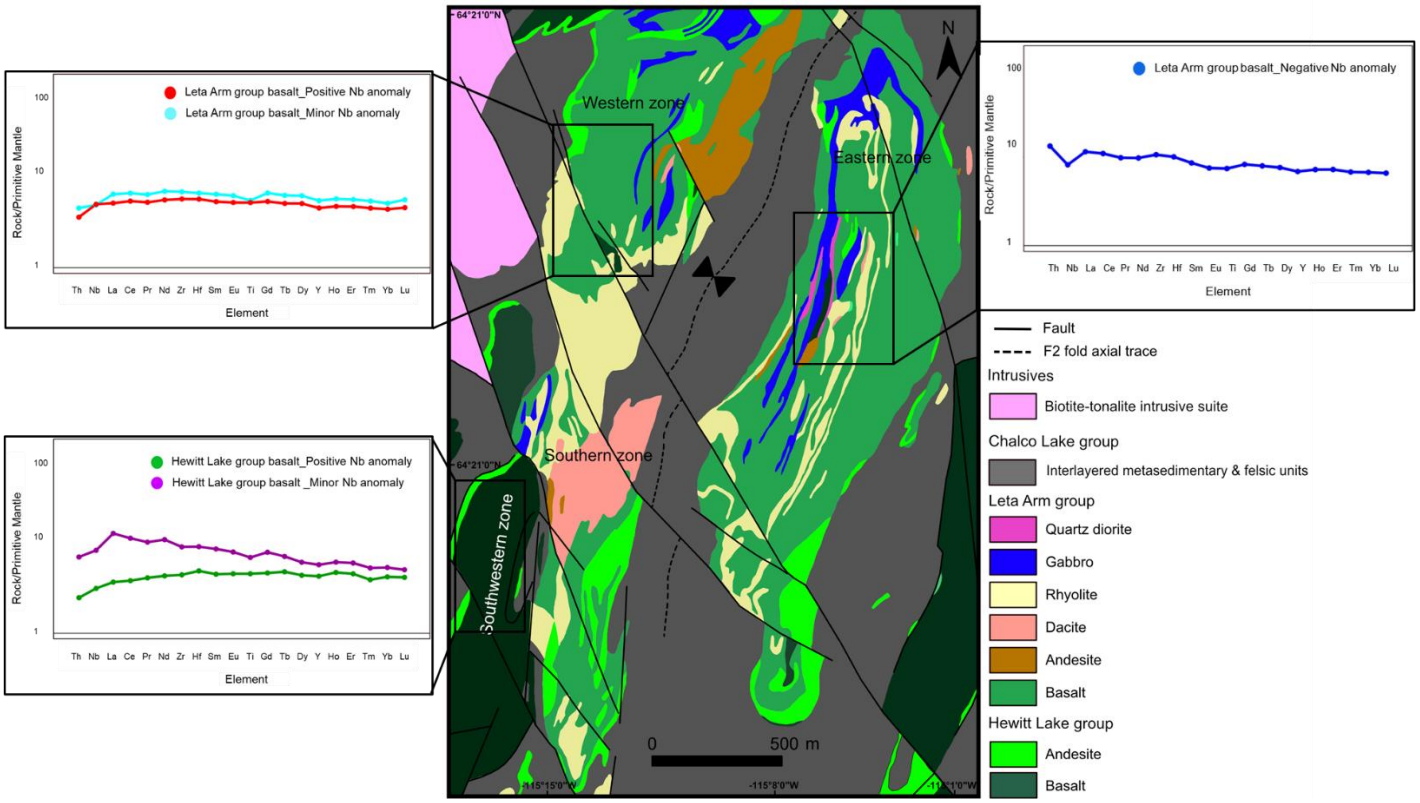

Figure 5.14. Geochemical trends of basalts from different zones along the limbs of D2 regional fold in the ILSB (modified after Pehrsson, 1998).

We adopted schematic examples from Kerr & Mahoney (2007), as shown in Figure 5.15a, to illustrate the stages involved in plateau-arc interaction in context of the ILSB. This was then used in combination with modifications of the tectonic model of Pehrsson (1998) in Figure 5.15a to demonstrate the transition from plateau to arc rocks in the ILSB in Figure 5.15b. Figure 5.15a shows the westward migration and collision of the inferred crustal block into the plateau. As the plateau resisted subduction, it clogged the subduction zone and this resulted in the formation of a new subduction zone west of the plateau. The subduction zone modified after Pehrsson (1998) in

Figure 5.15b shows the emplacement of primitive arc tholeiites and intermediate to felsic rocks into the already-existing plateau basalts of the ILSB.

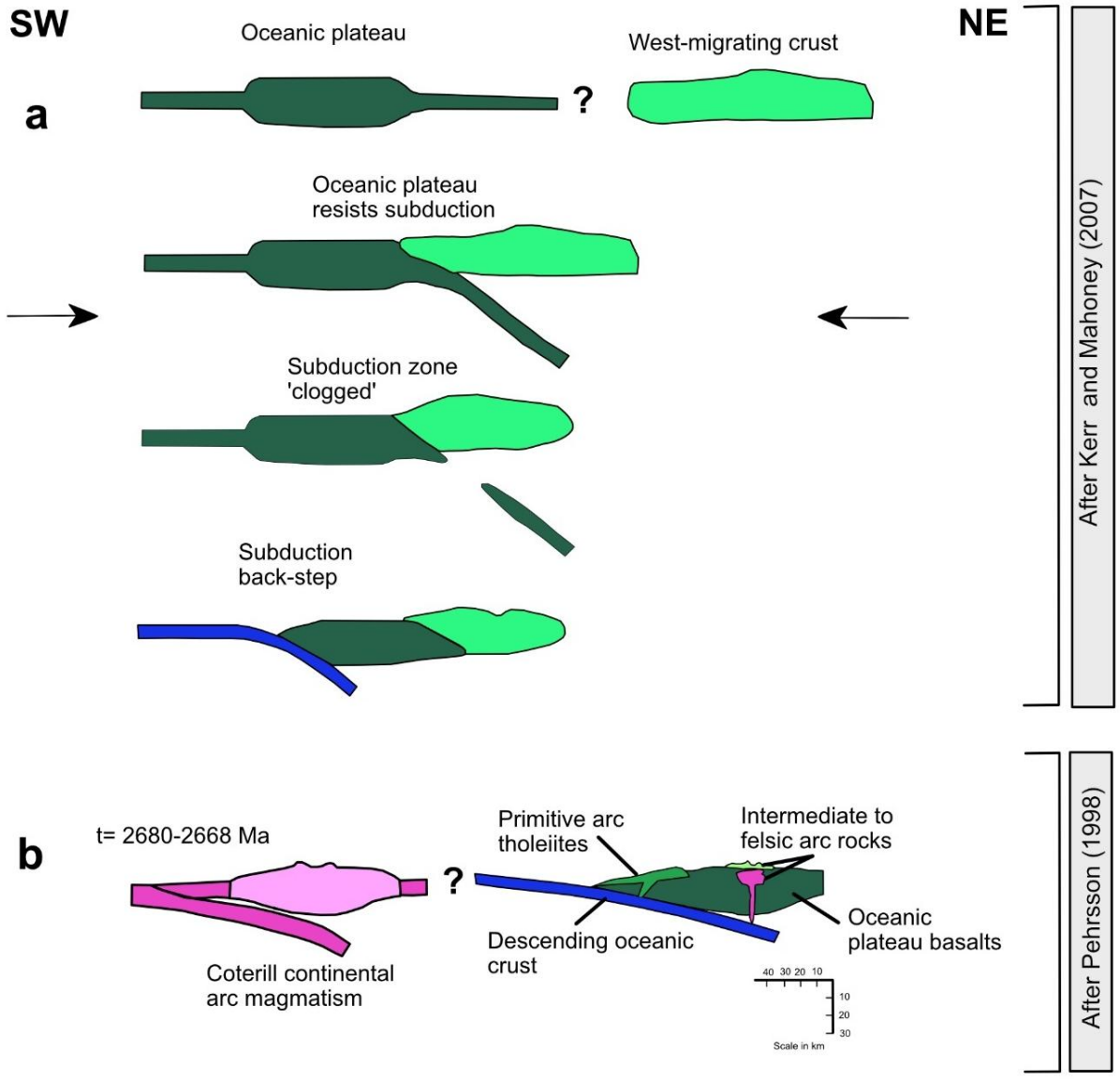

Figure 5.15. a) Schematic representation an example of plateau-crust collision to form a subduction zone (adapted from Kerr & Mahoney, 2007). b) Tectonic model of the ILSB showing the emplacement of arc magmas into plateau basalts (modified after Pehrsson, 1998).

6. Conclusions

Petrography, whole-rock geochemistry, mineral chemistry, U-Pb TIMS geochronology, and radiogenic Sm/Nd isotopes were used to understand the petrogenesis and tectonic setting of volcanic rocks of the Leta Arm (LA) and southwestern Hewitt Lake (HL) groups in the Indin Lake Supracrustal Belt (ILSB). The LA group contains basalt, andesite, dacite and rhyolite whereas the HL group comprises only basalt and andesite. Primary mineralogy in basalts from both groups include plagioclase, clinopyroxene, and minor orthopyroxene. However, basalts of the LA group are pyroxene-rich whereas those in the HL group are amphibole-rich and biotite-bearing. Andesites of both groups contain plagioclase, amphibole, pyroxene minor biotite and quartz. Magnesio-hornblende is the main amphibole in the HL group and is primary with euhedral morphology whereas ferro-hornblende and actinolite dominate in the LA group and are secondary. In both groups, ferro-hornblende replaces primary phases and its timing relative to actinolite formation suggests that the ILSB rocks have been subjected to prograde and retrograde metamorphism at greenschist to amphibolite facies. Dacites and rhyolites contain mainly plagioclase and quartz and show evidence of deformation. Textures in the groups range from intergranular in basalts, porphyritic in andesites and dacites, and ultimately aphanitic in rhyolites.

Petrography and geochemistry show evidence of evolution by crystal fractionation supported by increasing felsic compositions with decreasing ferromagnesium as well as negative correlations between silica and compatible elements. Both the LA and HL groups consist of tholeiitic to calc-alkaline rocks but new data cannot distinguish the groups by geochemistry and isotopic signatures. However, this study assigned zones to the groups to show spatio-chemical associations and establish the tectonic setting. The western basalts from both groups are consistent with rocks formed at an oceanic plateau characterized by flat REE profiles on primitive-mantle normalized

diagrams and a lack of negative Nb anomalies. Conversely, basalts of the eastern LA group and intermediate to felsic rocks from all zones in the ILSB have an arc-type signature shown by negative Nb and Ti anomalies, a positive Th anomaly, moderate to steep REE profiles as a result of LREE enrichment. Plateau signatures were not identified in previous studies. New data was used to modify the tectonic model of Pehrsson (1998). The juxtaposition of oceanic plateau basalts and arc rocks occurred by the collision of the plateau with a west-migrating crustal block in the eastern ILSB, clogging the subduction between the colliding blocks and forming a subduction zone behind the plateau where the eruption of arc magmas took place. The arc magmas were injected into and onto the plateau.

Similar ages between felsic rocks of both groups suggest that magmatism in the volcanic rocks occurred over short periods. This magmatism is slightly coeval with the crystallization age of the bounding Coterill tonalites and implies contemporaneous magmatism in the ILSB rocks. Isotope data showed no contamination by significantly older crust in the ILSB as all rocks have positive ε_{Nd} values and the Coterill tonalites are inferred as the possible contaminant to the volcanic rocks. However, the western plateau basalts showed slightly higher $^{143}Nd/^{144}Nd$ values (0.5128-5130) than arc rocks (<0.5125) which indicates lower contamination in the plateau rocks. Slightly higher contamination in the arc rocks could a result of sediment input or interaction with the metasomatized mantle. Low Gd/Yb_N ratios and positive ε_{Nd} values suggest shallow melting of a depleted mantle in an oceanic setting.

Only the mineralogical differences between the HL and LA groups (amphibole-rich and pyroxene-rich) indicate that they likely formed from different magma compositions. It is probable that the limited number of petrographic samples and the regional metamorphism in the belt introduced some bias on the characterization of the groups and that they could be genetically linked. However,

it is not possible to conclude at this stage why their petrography does not align with other data. Generally, the LA and HL group are similar in many aspects and show to have evolved similarly despite their different mineralogy. This attests to a complex petrogenetic and tectono-metamorphic history in the ILSB, which can be resolved by further studies. Future studies should focus on detailed mapping of the HL group to better characterize its composition and its relation to the LA group. Previous data shows larger age errors and raises questions on the constraints made in previous work. Detailed geochronology on the two groups is required to establish clear temporal relations as new data acquired by more precise analytical methods shows more similarities in their timing and petrogenesis. Extensive isotope analysis and amphibole chemistry should be considered for better characterization of magma sources and degree of metamorphism across the belt. Reinterpretation of the stratigraphy and structural relationships are required as new data shows that the plateau basalts from both the HL and LA group formed earlier than arc rocks and it is possible that the two assemblages represent the same lithostratigraphic unit.

References

Abdel-Halim, A.H., 2023. Hydrothermal alteration of Ni-rich sulfides in peridotites of Abu Dahr, Eastern Desert, Egypt: Relationships among minerals in the Fe-Ni-Co-OS system, fO_2 and f S2. *American Mineralogist*, *108*(3), pp.614-633.

Abbott, D. and Mooney, W., 1995. The structural and geochemical evolution of the continental crust: support for the oceanic plateau model of continental growth. *Reviews of Geophysics*, *33*(S1), pp.231-242.

Ague, J.J., 2017. Element mobility during regional metamorphism in crustal and subduction zone environments with a focus on the rare earth elements (REE). *American Mineralogist*, *102*(9), pp.1796-1821.

Anglin, C.D. and Wright, D.F, 2006. The Yellowknife EXTECH III Project: Overview and highlights: Chapter 1 in Gold in Yellowknife Greenstone belt, Northwest Territories: Results of the EXTECH III Multidisciplinary Research Project (ed.) Anglin, C.D., Falck, H., Wright, D.F, and Ambrose E.J; Geological Association of Canada, Mineral Deposits Division, Special Publication No.3, p.1-10.

Anhaeusser, C.R., 2014. Archaean greenstone belts and associated granitic rocks–a review. *Journal of African Earth Sciences*, *100*, pp.684-732.

Barrett, T.J. and MacLean, W.H., 1997. Volcanic sequences, litho-geochemistry, and hydrothermal alteration in some bimodal volcanic-associated massive sulfide systems.

Bleeker, W., Ketchum, J.W. and Davis, W.J., 1999. The Central Slave Basement Complex, Part II: age and tectonic significance of high-strain zones along the basement-cover contact. *Canadian Journal of Earth Sciences*, 36(7), pp.1111-1130.

Blichert-Toft, J. and Albarede, F., 1994. Short-lived chemical heterogeneities in the Archean mantle with implications for mantle convection. *Science*, *263*(5153), pp.1593-1596.

Brophy, J.A., 1995. Additional evidence for syngenetic gold enrichment in amphibolitic banded iron-formation, Slave Province. *Exploration Overview*, p.3.

Chacko, T., Creaser, R.A, Farquhar, J. and Muehlenbachs, K., 1995. The deep crust of the western Slave Province-initial petrologic and isotopic data from the high-grade rocks of the Ghost Domain. Slave-Northern Cordillera Lithospheric Experiment (SNORCLE), Transect Meeting 1995 (April 8-9, 1995), University of Calgary, Alberta. 44: p.4.6.

Cloos, M., 1993. Lithospheric buoyancy and collisional orogenesis: subduction of oceanic plateaus, continental margins, island arcs, spreading ridges, and seamounts. Geological Society of America Bulletin 105, 715–737.

Coffin, M.F. and Gahagan, L.M., 1995. Ontong Java and Kerguelen Plateaux: Cretaceous Icelands?. *Journal of the Geological Society*, *152*(6), pp.1047-1052.

Crawford, A.J., Beccaluva, L. and Serri, G., 1981. Tectono-magmatic evolution of the West Philippine-Mariana region and the origin of boninites. *Earth and Planetary Science Letters*, *54*(2), pp.346-356.

Cousens, B.L., 2000. Geochemistry of the archean Kam group, Yellowknife greenstone belt, slave province, Canada. *The Journal of geology*, *108*(2), pp.181-197.

DePaolo, D.J., 1981. Neodymium isotopes in the Colorado Front Range and crust–mantle evolution in the Proterozoic. *Nature*, *291*(5812), pp.193-196.

DePaolo, D.J. and Wasserburg, G.J., 1976. Inferences about magma sources and mantle structure from variations of $^{143}Nd/^{144}Nd$. *Geophysical Research Letters*, *3*(12), pp.743-746.

DePaolo, D.J. and Wasserburg, G.J., 1976. Nd isotopic variations and petrogenetic models. *Geophysical research letters*, *3*(5), pp.249-252.

Frey, F.A., Garcia, M.O., Wise, W.S., Kennedy, A., Gurriet, P. and Albarede, F., 1991. The evolution of Mauna Kea volcano, Hawaii: petrogenesis of tholeiitic and alkalic basalts. Journal of Geophysical Research: Solid Earth, 96(B9), pp.14347-14375

Frith, R.A., 1993. Precambrian geology of the Indin Lake map area, District of Mackenzie, Northwest Territories (Vol. 424). Geological Survey of Canada.

Gerstenberger, H. and Haase, G., 1997. A highly effective emitter substance for mass spectrometric Pb isotope ratio determinations. *Chemical Geology*, *136*(3-4), pp.309-312.

Grove, T.L., Elkins-Tanton, L.T., Parman, S.W., Chatterjee, N., Müntener, O. and Gaetani, G.A., 2003. Fractional crystallization and mantle-melting controls on calc-alkaline differentiation trends. *Contributions to Mineralogy and Petrology*, *145*, pp.515-533.

Hashimoto, M., 1972. Reactions producing actinolite in basic metamorphic rocks. *Lithos*, *5*(1), pp.19-31.

Hawkesworth, C.J., Gallagher, K., Hergt, J.M. and McDermott, F., 1993. Mantle and slab contribution in arc magmas. *Annual Review of Earth and Planetary Sciences, Volume 21, pp. 175-204.*, *21*, pp.175-204.

Henderson, J.B., 1998. Geology of the Keskarrah Bay Area, District of Mackenzie, Northwest Territories (Vol. 527). *Geological Survey of Canada*.

Henderson, J.B., 1972. Sedimentology of Archean turbidites at Yellowknife, Northwest Territories. *Canadian Journal of Earth Sciences*, 9(7), pp.882-902.

Hollings, P. and Wyman, D., 1998. Trace element and Sm–Nd systematics of volcanic and intrusive rocks from the 3 Ga Lumby Lake Greenstone belt, Superior Province: evidence for Archean plume–arc interaction. *Lithos*, 46(2), pp.189-213.

Hollings, P., Wyman, D. and Kerrich, R., 1999. Komatiite-basalt-rhyolite volcanic associations in Northern Superior Province greenstone belts: significance of plume-arc interaction in the generation of the proto continental Superior Province, *Lithos*, vol. 46, p.137-161.

Isachsen, C.E. and Bowring, S.A., 1994. Evolution of the Slave craton. *Geology*, *22*(10), pp.917-920

Kerr, A.C., 2003. Oceanic plateaus, In: The Crust, pp 537–566 (Ed R.L. Rudinck) Vol. 3 Treatise on Geochemistry (eds. Holland, Holland, H.G., Turekian, K.K.) Elsevier-Pergamon, Oxford.

Kerr, A.C. and Mahoney, J.J., 2007. Oceanic plateaus: Problematic plumes, potential paradigms. *Chemical Geology*, *241*(3-4), pp.332-353

Kerrich, R. and Polat, A., 2006. Archean greenstone-tonalite duality: Thermochemical mantle convection models or plate tectonics in the early Earth global dynamics?. *Tectonophysics*, pp.141-165.

Kerrich, R. and Wyman, D.A., 1997. Review of developments in trace-element fingerprinting of geodynamic settings and their implications for mineral exploration. *Australian Journal of Earth Sciences*, *44*(4), pp.465-487

Krogh, T., 1973. A low-contamination method for hydrothermal decomposition of zircon and extraction of U and Pb for isotopic age determinations. *Geochimica et Cosmochimica Acta*, *37*(3), pp.485-494.

Lagat, J., 2009. Hydrothermal alteration mineralogy in geothermal fields with case examples from Olkaria domes geothermal field, Kenya. *Dipresentasikan dalam short course IV on exploration for geothermal resources*.

Latypov, R., 2009. Testing the validity of the petrological hypothesis 'no phenocrysts, no post-emplacement differentiation'. *Journal of Petrology*, 50(6), pp.1047-1069.

Le Bas, M. and Streckeisen, A., 1991. The IUGS systematics of igneous rocks. J*ournal of the Geological Society* 148. 825-833. 10.1144/gsjgs.148.5.0825.

Le Maitre, R. W., Streckeisen, A., Zanettin, B., Le Bas, M. J., Bonin, B., Bateman, P. and Lameyre, J., 2002. Igneous rocks. A classification and glossary of terms, 2. Cambridge University Press.

Lightfoot, P.C., Sutcliffe, R.H. and Doherty, W., 1991. Crustal contamination identified in Keweenawan Osler Group Tholeiites, Ontario: A Trace Element Perspective. *The Journal of Geology*, vol. 99, p. 739-760.

Ludwig, K.R., 2009. User's manual for Isoplot 3.71 a geochronological toolkit for Excel. Berkeley Geochronological Center Special Publication 4, 72p.

Ludwig, K.R., 2003. Isoplot 3.09: A geochronological toolkit for Microsoft Excel. Berkeley Geochronology Center, Special Publication 4, Berkeley

Lund, M., Boudreau, S., Durieux, G. and Pelletier, C. 2022. NI 43 101 Technical Report and Update of the Mineral Resource Estimate for the Indin Lake Gold Property, Northwest Territories, Canada., 286 pages.

Mahoney, J.J., Storey, M., Duncan, R.A., Spencer, K.J. and Pringle, M., 1993. Geochemistry and geochronology of the Ontong Java Plateau. In: Pringle, M., Sager, W., Sliter, W., Stein, S. (Eds.), The Mesozoic Pacific: Geology, Tectonics, and Volcanism. American Geophysical Union Monograph, vol. 77, pp. 233–261.

Mattinson, J.M., 2005. Zircon U–Pb chemical abrasion ("CA-TIMS") method: combined annealing and multi-step partial dissolution analysis for improved precision and accuracy of zircon ages. *Chemical Geology*, *220*(1-2), pp.47-66.

Morgan. J., 1991. Gold deposits in the Indin Lake supracrustal belt. In Mineral deposits of the Slave Province, Northwest Territories. Field Trip Guidebook, 8th IAGOD Symposium. Edited by W.A. Padgham and D. Atkinson. Geological Survey of Canada, Open File 2168, pp. 67-83.

Murphy, J.B., 2007. Arc magmatism II: Geochemical and isotopic constraints on petrogenesis. Geoscience Canada, v. 34, in press.

Murphy, J.B., 2006. Igneous rock associations 7. Arc magmatism I: relationship between subduction and magma genesis. Geoscience Canada, 33(4), pp.145-168.

NWT Geoscience Office., 2012a. Detailed Showing Report-Showing ID086BSW0004–Colomac.

Parrish, R., Roddick, J.C., Loveridge, W.D. and Sullivan, R.W., 1987. Uranium-lead analytical techniques at the geochronology laboratory, Geological Survey of Canada: Geological Survey of Canada Paper 87-2, p. 3–7.

Pearce, J.A., 2014. Immobile element fingerprinting of ophiolites. *Elements*, 10 (2), pp.101-108.

Pearce, J.A., 1996. Sources and settings of granitic rocks. *Episodes*, 19, pp.120-125.

Pearce, J.A., 1982. Trace element characteristics of lavas from destructive plate boundaries, in Thorpe, R.S., eds., Andesite: Chichester, Wiley, p.525-548.

Pearce, J.A. and Peate, D.W., 1995. Tectonic implications of the composition of volcanic arc magmas. *Annual Review of Earth and Planetary Sciences, Volume 23,* pp.251-286.

Pearce, J.A., Stern, R.J., Bloomer, S.H. and Fryer, P., 2005. Geochemical mapping of the Mariana arc-basin system: implications for the nature and distribution of subduction components. *Geochemistry, Geophysics, Geosystems 6*, Q07006. https://doi.org/10.1029/2004GC000895.

Pehrsson, S.J., 2002. The 2.7–2.63 Ga Indin Lake supracrustal belt: an Archaean marginal basin–foredeep succession preserved in the western Slave Province, Canada. *Precambrian sedimentary environments: a modern approach to ancient depositional systems*. *Blackwell Publishing Ltd., Oxford, UK,* pp. 121–152. https://doi.org/10.1002/9781444304312.ch6

Pehrsson, S.J., 1998. Deposition, deformation and preservation of the Indin Lake supracrustal belt, Slave Province, Northwest Territories. Ph.D. thesis, Queen's University, Kingston, Ontario.

Pehrsson. S.J., and Chacko. T., 1997. Contrasting styles of deformation and metamorphism between mid- and upper-crustal rocks of the western Slave Province, Northwest Territories. In Current research, part C. Geological Survey of Canada, Paper 97-IC. pp. 15-25.

Pehrsson, S.J., Grant, J.A., Dorval, A.C. and Lewis, M., 1995. Stratigraphy and structure of the Indin Lake area. western Slave Province, Northwest Territories. In Current research, part E. Geological Survey of Canada, Paper 95-IE, pp. 149-159.

Pehrsson, S.J. and Kerswill, J.A., 1996. Geology of the Indin Lake area, implications for mineral exploration in the western Slave Province. In Exploration Overview 1996. Edited by S. Goff, P. Beales, and I. Igboji. NWT Geological Mapping Division. Indian Affairs and Northern Development, Yellowknife, pp. 3-28.

Pehrsson, PS.J. and Villeneuve, M.E., 1999. Deposition and imbrication of a 2670-2629 Ma supracrustal sequence in the Indin Lake area, southwestern Slave Province, Canada. *Canadian Journal of Earth Sciences*, *36*(7), pp.1149-1168.

Pirnia, T., Arai, S., Tamura, A., Ishimaru, S. and Torabi, G., 2014. Sr enrichment in mantle pyroxenes as a result of plagioclase alteration in lherzolite. *Lithos*, *196*, pp.198-212.

Polat, A., 2013. Geochemical variations in Archean volcanic rocks, southwestern Greenland: Traces of diverse tectonic settings in the early Earth. *Geology*, *41*(3), pp.379-380.

Polat, A. and Hofmann, A.W., 2003. Alteration and geochemical patterns in the 3.7–3.8 Ga Isua greenstone belt, West Greenland. *Precambrian Research*, *126*(3-4), pp.197-218.

Polat, A and Kerrich, R., 2001. Magnesian andesites, Nb-enriched basalts, andesites, and adakites from late-Archean 2.7 Ga Wawa greenstone belts, Superior Province, Canada: implications for late Archean subduction zone petrogenetic processes, *Contrib. Mineral Petrol*., vol. 141, p.36-52.

Poulsen, K.H., Robert, F. and Dubé, B., 2000. Geological classification of Canadian gold deposits; Geological Survey of Canada, Bulletin 540, pp. 106.

Qin, T., Fang, J., Zhang, Y., Ding, X., Yu, G. and Yang, H., 2024. Geochronology and geochemistry of Daerlong granitic complex in Linkou area, eastern Heilongjiang: petrogenesis and tectonic implications. *Global Geology*, *27*(4), pp.177-195.

Rasskazov, S., Taniguchi, H., Goto, A. and Litasov, K., 2005. Magmatic expression of plate subduction beneath East Asia in the Mesozoic through Cenozoic (Doctoral dissertation, Tohoku University).

Robb, M.E., 1997. Colomac Mine - Indin Lake Belt Area 1997 Report, Royal Oak Mines Inc. Western Canada – Exploration.

Rollinson, H.R., 1993. Using Geochemical Data: Evaluation, Presentation, Interpretation: Longman/Wyllie, Harlow/New York.

Scoates, J. S. and Jon Scoates, R. F., 2013. Age of the Bird River Sill, Southeastern Manitoba, Canada, with implications for the secular variation of layered intrusion-hosted stratiform chromite mineralization. Economic Geology, 108(4), 895-907.

Sisson, T.W. and Grove, T.L., 1993. Experimental investigations of the role of H_2O in calc-alkaline differentiation and subduction zone magmatism. *Contributions to Mineralogy and Petrology*, *113*, pp.143-166.

Smithies, R.H., Champion, D.C. and Sun, S.S., 2004. Evidence for early LREE-enriched mantle source regions: diverse magmas from the c. 3· 0 Ga Mallina Basin, Pilbara Craton, NW Australia. *Journal of Petrology*, *45*(8), pp.1515-1537.

Stacey, J.S. and Kramers, J.D., 1975. Approximation of terrestrial lead isotope evolution by a two-stage model. *Earth and Planetary Science Letters* 26: 207-221.

Stern, R.A. and Hanson, G.N., 1991. Archean high-Mg granodiorite: a derivative of light rare earth element-enriched monzodiorite of mantle origin. *Journal of Petrology*, *32*(1), pp.201-238.

Stipp, M., Stünitz, H., Heilbronner, R. and Schmid, S., 2002. The eastern Tonale fault zone: A 'natural laboratory' for crystal plastic deformation of quartz over a temperature range from 250 to 700 °C. *Journal of Structural Geology*, 24, 1861-1884. 10.1016/S0191-8141(02)00035-4.

STLLR Gold Inc., 2023. NI 43-101 Technical Report and Update of the Mineral Resource Estimate for the Indin Lake Gold Property, Northwest Territories, Canada.

Storey, M., Kent, R. W., Saunders, A. D., Salters, V. J., Hergt, J., Whitechurch, H., Sevigny, J. H., Thirlwall, M. F., Leat, P., Ghose, N. C. and Gifford, M., 1992. Lower Cretaceous Volcanic Rocks on Continental Margins and their Relationship to the Kerguelen Plateau. In: Wise, S.W., Schlich, R., et al. (Eds.), Proceedings of the Ocean Drilling rogram Scientific Results 120, p. 33-53. Sun, S.S., McDonough, W.F., 1989. Chemical and isotopic systematics of oceanic basalts: implications for mantle composition and processes. Geological Society, London, Special Publications, vol. 42, p. 313-345.

Sun, S.S. and McDonough, W. F., 1989. Chemical and isotopic systematics of oceanic basalts: implications for mantle composition and processes. Geological Society, London, Special Publications, vol. 42, p. 313-345.

Tarney, J. and Jones, C.E., 1994. Trace element geochemistry of orogenic igneous rocks and crustal growth models. *Journal of the Geological Society*, *151*(5), pp.855-868.

Tomlinson, K. Y., Stott, G.M., Percival, J.A. and Stone, D., 2004. Basement terrane correlations and crustal recycling in the wester Superior Province: Nd isotopic character of granitoid and felsic volcanic rocks in the Wabigoon subprovince, N. Ontario, Canada. *Precambrian Research*, vol. 132, p. 245-274.

Van Breemen, O, Davis, W.J. and King, J.E., 1992. Temporal distribution of granitoid plutonic rocks in the Archean Slave Province, northwest Canadian Shield. *Canadian Journal of Earth Sciences*, *29*(10), pp.2186-2199.

Vernon, R. H. & Clarke, G. L., 2008. Principles of Metamorphic Petrology. Cambridge University Press.

Villeneuve, M.E., Henderson. J.R., Hrabi, R.B., Jackson, V.A. and Relf, C., 1997. 2.70-2.58 Ga plutonism and volcanism in the Slave Province, District of Mackenzie, Northwest Territories. In Radiogenic age and isotopic studies: Report I 0. Geological Survey of Canada, Current Research 1997-F, pp. 37-60.

Zheng, Y.F., 2019. Subduction zone geochemistry. *Geoscience Frontiers*, *10*(4), pp.1223-1254.

Appendix I: Sample lists and descriptions

List of methods used per sample ID

A list of analytical methods used for each sample ID.

2024 Samples						
Sample name	**Group**	**Thin section**	**Whole-rock Geochemistry**	**Geochronology**	**EPMA**	**Sm/Nd isotopes**
TS24-01	Leta Arm			●		
TS24-02	Leta Arm		●			
TS24-03	Leta Arm		●			
TS24-04	Leta Arm			●		
TS24-05	Leta Arm			●		
TS24-06	Leta Arm		●			
TS24-07	Leta Arm			●		
TS24-08	Leta Arm		●			
TS24-09	Leta Arm		●			
TS24-10	Leta Arm		●			
TS24-11	Leta Arm		●			
TS24-12	Leta Arm		●			
TS24-13	Leta Arm		●			
2023 Samples						
Sample name	**Group**	**Thin section**	**Whole-rock Geochemistry**	**Geochronology**	**EPMA**	**Sm/Nd isotopes**
TS23-01	Hewitt Lake	●	●			
TS23-02	Hewitt Lake		●			●
TS23-03	Hewitt Lake	●	●			
TS23-04	Hewitt Lake	●	●			●
TS23-05	Hewitt Lake		●			
TS23-06	Hewitt Lake		●			
TS23-07	Hewitt Lake		●			
TS23-08	Hewitt Lake	●	●		●	
TS23-09	Hewitt Lake		●			
TS23-10	Leta Arm		●			
TS23-11	Leta Arm	●	●			●
TS23-12	Leta Arm		●			
TS23-13	Leta Arm	●	●			

2023 Samples						
Sample name	**Group**	**Thin section**	**Whole-rock geochemistry**	**Sample name**	**Group**	**Thin section**
TS23-14	Leta Arm		●			
TS23-15	Leta Arm		●			
TS23-16	Leta Arm	●	●			
TS23-17	Leta Arm		●			
TS23-18	Leta Arm	●	●			
TS23-19	Leta Arm		●			
TS23-20	Leta Arm	●	●			
TS23-21	Leta Arm		●			
TS23-22	Leta Arm	●	●			
TS23-23	Leta Arm		●			
TS23-24	Leta Arm		●			
TS23-25	Leta Arm	●	●			
TS23-26	Leta Arm		●			
TS23-27	Leta Arm		●			
TS23-28	Leta Arm		●			
TS23-29	Leta Arm	●	●			
TS23-30	Leta Arm		●			
TS23-31	Leta Arm	●	●		●	
TS23-32	Leta Arm		●			
TS23-33	Leta Arm		●			
TS23-34	Leta Arm		●			
TS23-35	Leta Arm	●	●			●
TS23-36	Leta Arm		●			
TS23-37	Leta Arm		●			●
TS23-38	Leta Arm	●	●			
TS23-39	Leta Arm	●	●			
TS23-40	Leta Arm	●	●	●		●
TS23-41	Hewitt Lake		●			
TS23-42	Hewitt Lake		●			
TS23-43	Hewitt Lake	●	●			
TS23-44	Hewitt Lake		●			
TS23-45	Hewitt Lake	●	●			●

2023 Samples						
Sample name	**Group**	**Thin section**	**Whole-rock geochemistry**	**Sample name**	**Group**	**Thin section**
TS23-46	Hewitt Lake		●			
TS23-47	Hewitt Lake		●			
TS23-48	Hewitt Lake		●			
TS23-49	Hewitt Lake	●	●			●
TS23-50	Leta Arm	●	●			
TS23-51	Leta Arm	●	●			
TS23-52	Leta Arm		●			
TS23-53	Leta Arm	●	●			
TS23-54	Leta Arm		●			
TS23-55	Leta Arm	●	●			
TS23-56	Leta Arm		●			●
TS23-57	Leta Arm		●			
TS23-58	Leta Arm	●	●			
TS23-59	Leta Arm		●			
TS23-60	Leta Arm	●	●			
TS23-61	Leta Arm	●	●		●	
TS23-62	Leta Arm		●			
TS23-63	Leta Arm		●			
TS23-64	Leta Arm		●			
TS23-65	Leta Arm		●			
TS23-66	Leta Arm		●			
TS23-67	Leta Arm		●			
TS23-68	Leta Arm		●			
TS23-69	Leta Arm	●	●			
TS23-70	Leta Arm		●			
TS23-71	Leta Arm		●			
TS23-72	Leta Arm		●			
TS23-73	Leta Arm		●			●
TS23-74	Leta Arm	●	●			
TS23-75	Leta Arm		●			

2023 Samples						
Sample name	**Group**	**Thin section**	**Whole-rock geochemistry**	**Sample name**	**Group**	**Thin section**
TS23-76	Leta Arm	●	●			
TS23-77	Leta Arm	●	●			
TS23-78	Leta Arm	●	●			
TS23-79	Leta Arm		●			
TS23-80	Leta Arm	●	●			
TS23-81	Hewitt Lake	●	●			●
TS23-82	Hewitt Lake	●	●			●
TS23-83	Hewitt Lake		●			
TS23-84	Hewitt Lake	●	●			
TS23-85	Hewitt Lake		●			
TS23-86	Hewitt Lake		●			
TS23-87	Hewitt Lake	●	●			
TS23-88	Hewitt Lake		●			
TS23-89	Hewitt Lake		●			
TS23-90	Leta Arm		●			●
TS23-91	Leta Arm	●	●			
TS23-92	Leta Arm		●			
TS23-93	Leta Arm		●			
TS23-94	Leta Arm		●			
TS23-95	Leta Arm	●	●			
TS23-96	Leta Arm		●			

Thin Section Descriptions

Sample: TS23-01

Rock type: Andesite

Spatial zone: Southwestern HL group

Description: Very fine-grained to slightly porphyritic. Consists of amphibole (~25%), biotite (20%), plagioclase (10%), and minor pyroxene (<10%). Alteration phases include actinolite

formed after pyroxenes, epidote and chlorite formed after biotite. Crosscut by high density quartz veins that are sub-parallel to weakly developed foliation marked by biotite and weakly by amphibole. Opaques appear secondary, have subrounded morphologies, and occur in very-fine grained sections.

Sample: TS23-03

Rock type: Basalt

Spatial zone: Southwestern HL group

Description: Consists of plagioclase laths in a fine-grained pyroxene-rich groundmass. Appears to be a trachybasalt. Lath sizes are <1mm and show no preferred orientation. Highly altered, with plagioclase (50%) altered to epidote. Pyroxenes have a brownish tint and are surrounded by secondary Fe-Ti oxides in places. Possible choritization is evident in plane polarized light photomicrograph.

Sample: TS23-04

Rock type: Basalt

Spatial zone: Southwestern HL group

Description: Highly altered. Actinolite is the main alteration phase and nearly all the primary mineralogy (over 80%) is overprinted. Cleavage planes of altered pyroxenes are observable in place but rarely. Chlorite is higher in this sample than nearby rocks. There is minor evidence of

shearing. Plagioclase is broken down and recrystallized and occurs at the boundary of altered pyroxenes together with nodules of Fe-Ti oxides.

Sample: TS23-08

Rock type: Basalt

Spatial zone: Southwestern HL group

Description: Consists of hornblende (~50%), plagioclase (20%), clinopyroxene (15%), minor orthopyroxene (5-10%) and biotite (~5%). Hornblende grains are euhedral grains, have a primary morphology and are less altered than other phases. Plagioclase and pyroxenes are subhedral and overprinted by chlorite and actinolite in most places. Quartz, carbonates and Fe-Ti oxides (1-3%) are secondary. Quartz and carbonates from the matrix whereas Fe-Ti oxides occur along cleavage planes and as patches along the boundaries of hornblende and pyroxenes. Weakly deformed and foliation is marked by the poor alignment of amphibole, pyroxenes and Fe-Ti oxides.

Sample: TS23-11

Rock type: Andesite

Spatial zone: Southern LA group

Description: Porphyritic with relict feldspar phenocrysts (0.5-1.5mm) in quartz-rich matrix. Foliated and show intense sericitization and minor carbonatization of feldspars. Iron-titanium oxides together with sericite define the foliation.

Sample: TS23-13

Rock type: Dacite

Spatial zone: Eastern LA group

Description: Consists of quartz (50%), plagioclase (20%), biotite (~15%) and minor pyroxene (10%). Quartz and plagioclase are euhedral whereas biotite is subhedral to lath-shaped and chloritized. Plagioclase is epidotized in places. Iron-titanium oxides are concentrated in the groundmass and are subhedral. Actinolite, chlorite and epidote form the alteration assemblage.

Sample: TS23-16

Rock type: Basalt

Spatial zone: Eastern LA group

Description: Comprised dominantly of highly altered pyroxene and plagioclase. Actinolite and chlorite are the main alteration phases and overprint nearly all the primary mineralogy. The rock is carbonatized and crosscut by quart-carbonate veins. Texture is intergranular and grain boundaries of altered pyroxenes Cleavage planes of altered pyroxenes are observable in place but rarely. Chlorite is higher in this sample than nearby rocks. There is minor evidence of shearing. Plagioclase is broken down and recrystallized and occurs at the boundary of altered pyroxenes together with nodules of Fe-Ti oxides.

Sample: TS23-18

Rock type: Andesite

Spatial zone: Eastern LA group

Description: Primary mineralogy is completely overprinted by alteration. Amphiboles form the main alteration phase and plagioclase is recrystallized. Amphiboles are yellowish brown to dark brown in slightly less altered sections and might be pyroxene.

Sample: TS23-20

Rock type: Andesite

Spatial zone: Southern LA group

Description: Highly sericitized, carbonatized and deformed andesite. Strong foliation is crosscut by and concordant with calcite veins. Chlorite forms the foliation in places together with Fe-Ti oxides. Quartz stylolite veins with peaks/axial planes parallel to foliation. Primary biotite is deformed with the rocks and secondary biotite occurs along chloritized zones.

Sample: TS23-22

Rock type: Andesite

Spatial zone: Southern LA group

Description: Strongly foliated (sheared) with foliation formed by sericite and preferentially oriented quartz-feldspar phenocrysts. Quartz eyes and recrystallized feldspar are observed in

places. Foliation anastomoses around the grains. Biotite and opaques also form the foliation but are very fine-grained. Carbonates occur in minor concentrations and replace feldspar phenocrysts.

Sample: TS23-25

Rock type: Dacite

Spatial zone: Southern LA group

Description:

Porphyritic and consists of feldspar (~10%) and quartz (20%) phenocrysts in a fine-grained quartz-sericite matrix which forms the foliation. Evidence of shearing by anastomosing matrix around phenocrysts. No kinematic indicators were observed but quartz-sericite shadow zones around feldspar grains are observed. Epidote/calcite dominates in fractured feldspar grains and along grain boundaries. Sericitization (>60%) and calcite/epidote (≤20%) are the alteration minerals observed.

Sample: TS23-29

Rock type: Dacite

Spatial zone: Southern LA group

Description: Similar to TS23-22 but feldspar and quartz-rich. There is minor biotite compared to TS23-22. This sample also shows high carbonatization.

Sample: TS23-31

Rock type: Basalt

Spatial zone: Eastern LA group

Description: Comprised dominantly of euhedral to subhedral plagioclase (40-50%), pyroxene. And minor primary phases of Fe-Ti oxides (~3%). Primary Fe-Ti oxides are either net-textured or occur as subhedral grains within rutile. Actinolite and hornblende make up 25-30%, and are secondary. These basalts are weakly altered as over 50% of their primary textures are visible. Fe-Ti oxides are replaced by rutile, and plagioclase is weakly altered to sericite Chlorite is minor but overprints the rock in places.

Sample: TS23-35

Rock type: Basalt

Spatial zone: Eastern LA group

Description: Similar to TS23-31 but more plagioclase -rich (60%). No evidence of hornblende but actinolite is observed. Fe-Ti oxides are euhedral and more widespread but not net-textured. Plagioclase is weakly altered by epidote.

Sample: TS23-38

Rock type: Basalt

Spatial zone: Eastern LA group

Description: Similar to TS23-35 but contains secondary quartz. Comprised dominantly of euhedral to subhedral lath-shaped pyroxene (40%) and anhedral plagioclase in the groundmass. Fe-Ti oxides (~3%) are form part of the foliation together with actinolite that formed after pyroxene.

Sample: TS23-39

Rock type: Rhyolite

Spatial zone: Eastern LA group

Description: Aphanitic and minor biotite-bearing. Minor nodules of recrystallized quartz. Very thin and dark veinlets or stringers. Composition of the rocks was confirmed with whole-rock geochemistry due its fine-grained nature.

Sample: TS23-40

Rock type: Rhyolite

Spatial zone: Eastern LA group

Description: Dominantly aphanitic with minor feldspar, quartz and traces of biotite. Crosscut by minor chloritic and quartz veins.

Sample: TS23-43

Rock type: Rhyolite

Spatial zone: Eastern LA group

Description: Similar to TS23-39 but crosscut by quartz-carbonate-epidote veins. Grain boundary migration and subgrains in the veins represent deformation. Some of the epidote is kinked.

Sample: TS23-45

Rock type: Dacite

Spatial zone: Eastern LA group

Description: Aphanitic, biotite-bearing and carbonatized. Contains specks of Fe-Ti oxides. The rocks is too fine-grained to determine modal abundances and grain sizes.

Sample: TS23-49

Rock type: Rhyolite

Spatial zone: Eastern LA group

Description: Aphanitic to slightly porphyritic and minor biotite-bearing. Minor recrystallized quartz. Very dark and strongly foliated. Biotite is chloritized. Composition of the rocks was confirmed with whole-rock geochemistry due its fine-grained nature.

Sample: TS23-50

Rock type: Basalt

Spatial zone: Eastern LA group

Description: Similar to TS23-35, however highly carbonatized. The carbonate from fine-grained to coarse-grained clusters. Epidote is minor occurs similar to carbonates. Chlorite overprints pyroxenes. Opaques are euhedral, cubic to hexagonal and form overgrowths on pyroxene domains.

Sample: TS23-51

Rock type: Andesite

Spatial zone: Eastern LA group

Description: Contains pyroxene, biotite and amphibole. However, amphibole is secondary and overprints other secondary phases. Crosscut by ~1μm chlorite veinlets. Opaques are euhedral, cubic to hexagonal and occur as patchy material or form overgrowths on pre-existing phases.

Sample: TS23-53

Rock type: Basalt

Spatial zone: Eastern LA group

Description: Highly carbonatized. Relict pyroxenes and biotite are pervasively overprinted. Amphibole forms part of the secondary phases including carbonate.

Sample: TS23-55

Rock type: Dacite

Spatial zone: Eastern LA group

Description: Porphyritic, consists of quartz, feldspar and minor biotite phenocrysts in a very fine-grained sericitized quartz-feldspar matrix that occurs as brown to grey patchy material. It is epidotized and carbonatized in places and is associated with Fe-Ti oxides. Foliation is weak and is marked by preferentially oriented Fe-Ti oxides and some of the phenocrysts.

Sample: TS23-58

Rock type: Basalt

Spatial zone: Eastern LA group

Description: Altered basalt with secondary amphibole nodules. Primary mineralogy is overprinted. Amphibole (70%) have a bladed habit and is clustered. Secondary Minor quartz in the matrix. Fe-Ti oxides occur as patches.

Sample: TS23-60

Rock type: Basalt

Spatial zone: Eastern LA group

Description: Highly carbonatized. Biotite-bearing. Relict biotite is pervasively chloritized.

Sample: TS23-61

Rock type: Andesite

Spatial zone: Eastern LA group

Description: Primary mineralogy includes pyroxenes and plagioclase which have been altered to hornblende and actinolite. The rocks are highly carbonatized, chloritized and epidotized.

Sample: TS23-69

Rock type: Basalt

Spatial zone: Western LA group

Description: Porphyritic, foliated and highly altered. Consists of euhedral quartz (20%) and plagioclase (10%) phenocrysts. The phenocrysts are often fractured and carbonatized. Iron-titanium oxides form part of the foliation and appear elongated.

Sample: TS23-74

Rock type: Basalt

Spatial zone: Western LA group

Description: Aphanitic and dark. Crosscut by thin calcite veinlets. Composition of the rocks was confirmed with whole-rock geochemistry due its fine-grained nature.

Sample: TS23-76

Rock type: Basalt

Spatial zone: Western LA group

Description: Fine-grained, foliated and highly altered. Appears to have high opaques and Fe-Ti oxides which form part of the foliation and appear elongated in places. Carbonatization is pervasive no primary mineralogy is preserved.

Sample: TS23-77

Rock type: Basalt

Spatial zone: Western LA group

Description: Comprised of subhedral primary pyroxene (70%), plagioclase (20%), minor quartz (5%) and Fe-Ti oxides (~3%). Actinolite partially replaced pyroxenes.

Sample: TS23-78

Rock type: Basalt

Spatial zone: Western LA group

Description: Slightly porphyritic and weakly. Carbonatized and sericitized and foliation is formed by sericite and Fe-Ti oxides.

Sample: TS23-80

Rock type: Dacite

Spatial zone: Western LA group

Description: Porphyritic. Phenocrysts include feldspar and minor quartz. Foliation is weak and chlorite and carbonate veinlets are sub-parallel to the foliation. Fe-Ti oxides are rare but occur as patches proximal to veins.

Sample: TS23-81

Rock type: Basalt

Spatial zone: Western LA group

Description: Comprised of subhedral primary pyroxene (70%), plagioclase (20%), minor quartz (5%) and Fe-Ti oxides (~5-7%) including rutile. There is increased Fe-Ti oxides content and form net-textured patterns. Actinolite partially replaced pyroxenes.

Sample: TS23-82

Rock type: Dacite

Spatial zone: Western LA group

Description: Strongly foliated and altered. Foliation is formed by sericite injected carbonate veins. Composition was determined using whole-rock geochemistry.

Sample: TS23-84

Rock type: Gabbro

Spatial zone: Western LA group

Description: Coarse-grained (0.5-4mm), weakly foliated and comprised of subhedral primary pyroxene (70%), plagioclase (20%), minor quartz (5%) and Fe-Ti oxides (~3%). Rutile replaces Fe-Ti oxides while actinolite replaces pyroxenes. The rock is crosscut by a quartz-carbonate vein which has been folded along the preferred orientation of pyroxene. Plagioclase is anhedral and forms the groundmass.

Sample: TS23-87

Rock type: Dacite

Spatial zone: Western LA group

Description: Aphanitic to slightly porphyritic and minor biotite-bearing. Foliated and highly altered. Alteration is by chloritization, carbonatization, and sericititazion all of which form the foliation. Biotite is chloritized. Determination of composition was achieved by using a combination of petrography with whole-rock geochemistry.

Sample: TS23-91

Rock type: Basalt

Spatial zone: Western LA group

Description: Comprised dominantly of euhedral to subhedral lath-shaped pyroxene (40%) and anhedral plagioclase in the groundmass. Fe-Ti oxides (~3%) are form part of the foliation together with actinolite that formed after pyroxene. The rock contains secondary quartz and overprints pre-existing phases, evidence of silicification.

Sample: TS23-95

Rock type: Andesite

Spatial zone: Western LA group

Description: Contain up to 70% plagioclase, is biotite-bearing (~20%) and show a well-developed foliation. Biotite occurs as euhedral grains formed at the edge of plagioclase microlithons Clinopyroxene is minor (<5%) and occurs in biotite-rich sections along the edges of microlithons. Primary textures are retained but the rock shows minor recrystallisation of plagioclase defined by <100 μm grains surrounding ~50 μm primary plagioclase that are closely associated with quartz grains of a similar size Biotite and pyroxene are partially altered to chlorite while plagioclase is altered to sericite.

Appendix II: Whole-rock geochemistry data (Fig. 4.1)

Representative major and trace element analyses for the ILSB samples. REE ratios (La/Sm_N, Gd/Yb_N and Nb/Nb*) are mantle-normalized using normalization values of Sun and McDonough (1989).

Hewitt Lake group (Southwestern zone)									
Sample name	TS23-01	TS23-02	TS23-03	TS23-04	TS23-05	TS23-06	TS23-07	TS23-08	TS23-09
Easting (UTM83-11N)	582363	582538	583016	583386	583765	583720	583868	584334	584654
Northing (UTM83-11N)	7133501	7133566	7133597	7133647	7133740	7133719	7134073	7135056	7135938
SiO_2 (wt%)	63.20	58.90	48.60	48.20	58.80	47.30	56.60	48.90	70.60
TiO_2 (wt%)	0.54	0.71	1.80	0.90	0.75	1.23	0.75	1.50	0.90
Al_2O_3 (wt%)	15.50	14.85	14.45	14.15	18.50	14.20	21.10	14.15	13.75
Fe_2O_3 (wt%)	6.73	8.46	12.20	14.65	8.75	14.95	6.72	13.65	3.24
MnO (wt%)	0.08	0.12	0.17	0.22	0.06	0.20	0.03	0.33	0.08
MgO (wt%)	4.59	5.74	7.22	7.75	3.78	6.62	3.54	6.27	0.43
CaO (wt%)	3.68	6.11	8.21	9.88	2.96	10.30	0.39	10.25	2.30
K_2O (wt%)	2.35	0.57	0.97	0.19	2.41	0.24	3.48	0.26	1.22
Na_2O (wt%)	2.57	2.89	2.46	2.25	3.89	2.39	2.40	1.84	4.35
P_2O_5 (wt%)	0.14	0.19	0.21	0.05	0.16	0.07	0.12	0.12	0.49
LOI	1.28	0.37	2.87	0.53	1.58	1.05	3.90	2.89	1.68
Mg#	0.57	0.57	0.54	0.51	0.46	0.47	0.51	0.48	0.21
Cr (ppm)	85.00	194.00	203.00	168.00	198.00	184.00	228.00	18.00	42.00
Co (ppm)	19.00	27.00	40.00	54.00	24.00	49.00	29.00	40.00	6.00
Ni (ppm)	68.00	115.00	115.00	82.00	89.00	92.00	52.00	31.00	8.00
Sc (ppm)	13.00	19.00	23.00	43.00	18.00	36.00	20.00	47.00	7.00
V (ppm)	97.00	131.00	219.00	295.00	155.00	355.00	183.00	433.00	73.00
Ta (ppm)	0.40	0.50	0.60	0.10	0.50	0.20	0.50	0.20	0.90
Nb (ppm)	5.20	6.55	9.41	1.91	7.26	2.83	6.80	3.73	14.80
Zr (ppm)	153.00	159.00	134.00	47.00	133.00	60.00	132.00	92.00	248.00
Hf (ppm)	3.86	3.74	3.54	1.38	3.64	1.90	3.51	2.73	5.74
Th (ppm)	2.16	1.16	0.92	0.19	8.75	0.25	6.69	0.39	4.93
U (ppm)	0.62	0.33	0.21	0.05	2.40	0.07	1.42	0.13	1.22
Y (ppm)	15.90	21.50	23.30	18.70	19.60	23.20	17.00	33.70	26.70
La (ppm)	13.50	12.50	14.50	2.10	30.10	3.30	35.20	5.40	41.10
Ce (ppm)	27.20	27.70	31.80	5.80	61.20	8.70	68.90	13.40	91.00
Pr (ppm)	3.18	3.62	4.29	0.98	7.35	1.45	8.48	2.04	11.85
Nd (ppm)	13.40	15.80	21.40	5.20	29.60	7.40	33.40	11.80	48.60
Sm (ppm)	2.87	3.63	4.72	2.03	5.43	2.28	5.96	3.77	9.26
Eu (ppm)	0.95	1.00	1.58	0.70	1.54	0.95	1.44	1.38	2.36
Gd (ppm)	2.95	3.70	5.13	2.66	4.52	3.32	4.64	5.30	7.41
Tb (ppm)	0.47	0.61	0.80	0.47	0.62	0.65	0.60	0.89	1.00
Dy (ppm)	2.92	3.60	4.47	2.96	3.59	4.00	3.56	5.39	5.63
Ho (ppm)	0.58	0.76	0.94	0.75	0.74	0.92	0.64	1.26	1.09
Er (ppm)	1.68	2.21	2.40	2.13	2.08	2.58	1.57	3.90	2.93
Tm (ppm)	0.24	0.33	0.31	0.26	0.27	0.36	0.22	0.54	0.35
Yb (ppm)	1.64	2.08	1.96	2.05	2.00	2.41	1.37	3.77	2.33
Lu (ppm)	0.26	0.37	0.26	0.31	0.25	0.35	0.20	0.55	0.34
$(La/Sm)_N$	3.04	2.23	1.99	0.67	3.58	0.94	3.82	0.93	2.87
$(Gd/Yb)_N$	1.49	1.47	2.17	1.07	1.87	1.14	2.80	1.16	2.63
Nb/Nb*	0.12	0.18	0.21	0.77	0.05	0.58	0.04	0.37	0.07

Leta Arm group (Southern zone)									
Sample name	TS23-10	TS23-11	TS23-12	TS23-20	TS23-21	TS23-22	TS23-23	TS23-24	TS23-25
Easting (UTM83-11N)	584658	584798	584915	585074	585175	585287	585543	585628	585899
Northing (UTM83-11N)	7136007	7136103	7136124	7136209	7136316	7136441	7136709	7136732	7136824
SiO_2 (wt%)	65.90	62.30	60.40	67.10	63.00	65.40	65.60	66.00	71.00
TiO_2 (wt%)	0.65	0.97	0.73	0.44	0.63	0.66	0.46	0.35	0.41
Al_2O_3 (wt%)	16.55	16.00	15.00	12.50	17.55	19.00	15.85	14.10	13.75
Fe_2O_3 (wt%)	4.27	5.15	7.78	5.87	5.89	3.11	4.14	2.80	2.32
MnO (wt%)	0.04	0.06	0.05	0.09	0.08	0.03	0.08	0.07	0.05
MgO (wt%)	1.09	1.54	3.77	1.25	2.19	0.59	1.48	0.93	0.41
CaO (wt%)	1.76	2.53	3.03	2.92	2.53	0.99	4.02	3.94	2.28
K_2O (wt%)	2.36	1.28	1.16	1.38	1.48	2.72	1.91	2.20	1.45
Na_2O (wt%)	3.80	4.53	2.81	2.57	4.22	4.50	3.29	3.38	4.58
P_2O_5 (wt%)	0.40	0.37	0.20	0.10	0.15	0.17	0.16	0.12	0.14
LOI	2.54	3.46	5.23	4.51	4.04	2.57	2.23	4.50	2.74
Mg#	0.34	0.37	0.49	0.30	0.42	0.27	0.41	0.40	0.26
Cr (ppm)	39.00	29.00	184.00	98.00	143.00	42.00	25.00	12.00	19.00
Co (ppm)	5.00	9.00	26.00	10.00	15.00	5.00	9.00	6.00	3.00
Ni (ppm)	6.00	13.00	82.00	35.00	51.00	13.00	20.00	10.00	6.00
Sc (ppm)	11.00	14.00	15.00	12.00	11.00	11.00	6.00	4.00	4.00
V (ppm)	66.00	120.00	126.00	74.00	96.00	89.00	51.00	38.00	33.00
Ta (ppm)	0.90	0.70	0.50	0.60	0.80	1.20	0.70	0.70	0.70
Nb (ppm)	11.80	11.50	8.63	6.36	9.09	11.60	8.30	8.46	8.45
Zr (ppm)	255.00	232.00	201.00	156.00	214.00	239.00	228.00	207.00	213.00
Hf (ppm)	6.12	5.91	4.37	3.70	5.15	5.91	5.51	4.91	5.21
Th (ppm)	7.08	5.08	3.88	5.92	8.08	13.20	6.89	8.12	6.64
U (ppm)	1.78	1.39	1.05	1.76	2.32	3.84	1.65	2.05	1.81
Y (ppm)	21.40	24.60	15.70	13.80	17.10	17.70	17.80	16.50	17.40
La (ppm)	31.20	24.10	17.20	13.90	21.70	22.70	23.40	24.60	20.20
Ce (ppm)	61.10	52.70	37.20	28.60	45.10	42.40	45.60	47.10	43.00
Pr (ppm)	7.39	6.08	4.33	3.14	4.91	4.78	4.80	4.80	4.60
Nd (ppm)	29.30	23.90	17.60	12.50	19.30	18.70	19.00	17.80	18.50
Sm (ppm)	5.51	5.05	3.57	2.58	3.24	4.00	3.93	3.31	3.65
Eu (ppm)	1.23	1.34	0.82	0.62	1.00	1.15	1.06	0.88	0.91
Gd (ppm)	4.96	4.62	3.26	2.59	3.49	3.82	3.82	3.18	3.74
Tb (ppm)	0.80	0.77	0.51	0.40	0.55	0.54	0.57	0.51	0.59
Dy (ppm)	4.13	4.61	2.86	2.37	3.09	3.19	3.11	2.97	3.05
Ho (ppm)	0.87	0.92	0.62	0.49	0.68	0.67	0.70	0.61	0.65
Er (ppm)	2.27	2.55	1.77	1.60	1.83	1.82	1.91	1.76	1.74
Tm (ppm)	0.32	0.38	0.23	0.19	0.23	0.25	0.24	0.26	0.25
Yb (ppm)	2.17	2.25	1.74	1.54	1.66	1.68	1.80	1.78	1.70
Lu (ppm)	0.36	0.36	0.24	0.23	0.25	0.27	0.24	0.27	0.27
$(La/Sm)_N$	3.66	3.08	3.11	3.48	4.33	3.67	3.85	4.80	3.58
$(Gd/Yb)_N$	1.89	1.70	1.55	1.39	1.74	1.88	1.76	1.48	1.82
Nb/Nb*	0.08	0.12	0.15	0.14	0.11	0.12	0.09	0.08	0.11

	Leta Arm group (Southern zone)				Leta Arm group (Eastern zone)				
Sample name	TS23-26	TS23-27	TS23-28	TS23-29	TS23-13	TS23-14	TS23-15	TS23-16	TS23-17
Easting (UTM83-11N)	586012	586264	586417	586670	595877	595854	595565	595523	595431
Northing (UTM83-11N)	7136814	7136853	7136861	7136895	7145371	7145308	7145147	7145233	7145242
SiO_2 (wt%)	64.60	66.90	68.10	64.10	67.70	67.80	56.40	50.30	47.30
TiO_2 (wt%)	0.34	0.41	0.31	0.31	0.61	0.59	0.96	2.27	2.24
Al_2O_3 (wt%)	14.65	12.10	13.30	13.25	14.90	14.05	16.05	14.20	18.10
Fe_2O_3 (wt%)	3.22	6.14	4.28	4.08	5.16	5.10	8.13	15.20	12.90
MnO (wt%)	0.07	0.09	0.09	0.18	0.06	0.11	0.22	0.50	0.34
MgO (wt%)	0.71	1.14	0.90	0.76	2.39	2.24	4.98	3.99	7.50
CaO (wt%)	5.15	3.48	3.42	6.21	1.38	4.41	5.46	7.30	2.27
K_2O (wt%)	2.06	1.49	1.26	1.96	1.76	1.34	0.68	0.23	1.04
Na_2O (wt%)	2.81	2.68	3.53	2.42	3.39	2.59	3.92	2.82	3.40
P_2O_5 (wt%)	0.12	0.19	0.11	0.10	0.13	0.12	0.26	0.25	0.20
LOI	4.67	4.57	4.19	6.64	1.91	1.11	1.77	2.28	4.12
Mg#	0.30	0.27	0.29	0.27	0.48	0.47	0.55	0.34	0.54
Cr (ppm)	16.00	14.00	15.00	11.00	151.00	167.00	175.00	68.00	213.00
Co (ppm)	6.00	13.00	6.00	5.00	7.00	14.00	24.00	48.00	63.00
Ni (ppm)	12.00	10.00	8.00	8.00	28.00	45.00	97.00	42.00	92.00
Sc (ppm)	5.00	6.00	5.00	4.00	12.00	11.00	13.00	35.00	46.00
V (ppm)	32.00	36.00	32.00	261.00	100.00	103.00	140.00	351.00	455.00
Ta (ppm)	0.70	0.70	0.70	0.60	0.50	0.50	0.40	0.60	0.40
Nb (ppm)	7.43	9.16	6.70	7.16	6.39	6.26	7.90	9.20	11.55
Zr (ppm)	211.00	209.00	186.00	182.00	151.00	193.00	168.00	189.00	164.00
Hf (ppm)	5.32	4.70	4.71	4.44	3.88	4.54	3.98	4.80	4.22
Th (ppm)	7.86	5.19	7.22	7.34	6.45	7.52	5.55	1.44	1.08
U (ppm)	2.04	1.35	1.39	1.87	1.88	2.14	1.41	0.50	0.36
Y (ppm)	15.90	21.20	17.80	17.70	10.00	13.50	18.20	44.10	40.10
La (ppm)	21.50	26.90	21.30	27.40	16.30	23.40	28.30	11.40	8.20
Ce (ppm)	41.50	54.70	40.30	45.30	38.70	47.30	60.90	29.20	22.80
Pr (ppm)	4.39	6.10	4.20	4.62	4.37	5.19	7.22	4.03	3.15
Nd (ppm)	17.10	22.70	16.10	16.80	15.90	20.20	29.40	20.10	16.50
Sm (ppm)	3.01	4.60	3.03	3.24	2.84	3.49	5.17	5.69	4.63
Eu (ppm)	0.80	1.12	0.75	0.91	0.85	1.08	1.74	1.68	1.32
Gd (ppm)	3.21	4.61	3.22	3.25	2.01	2.99	4.57	6.88	5.84
Tb (ppm)	0.51	0.69	0.56	0.53	0.32	0.46	0.65	1.21	1.14
Dy (ppm)	2.78	3.79	2.99	2.75	1.98	2.55	3.60	7.49	7.18
Ho (ppm)	0.61	0.80	0.62	0.61	0.39	0.54	0.71	1.76	1.70
Er (ppm)	2.07	2.23	1.92	1.78	1.13	1.52	1.96	5.05	4.81
Tm (ppm)	0.25	0.34	0.25	0.25	0.16	0.20	0.24	0.68	0.60
Yb (ppm)	1.65	2.37	1.86	1.52	1.06	1.43	1.82	4.86	4.25
Lu (ppm)	0.27	0.28	0.27	0.26	0.18	0.20	0.23	0.72	0.57
$(La/Sm)_N$	4.62	3.78	4.54	5.47	3.71	4.33	3.54	1.29	1.14
$(Gd/Yb)_N$	1.61	1.61	1.43	1.77	1.57	1.73	2.08	1.17	1.14
Nb/Nb*	0.09	0.08	0.08	0.05	0.12	0.07	0.07	0.31	0.66

Leta Arm group (Eastern zone)									
Sample name	TS23-18	TS23-19	TS23-30	TS23-31	TS23-32	TS23-33	TS23-34	TS23-35	TS23-36
Easting (UTM83-11N)	595358	595257	591343	590731	590932	591026	591105	591233	591578
Northing (UTM83-11N)	7145268	7145154	7140280	7140159	7140305	7140285	7140357	7140331	7140500
SiO_2 (wt%)	44.00	46.80	48.10	50.70	47.90	47.00	51.00	48.70	53.10
TiO_2 (wt%)	2.18	1.64	1.66	0.99	2.15	1.18	1.49	2.03	1.36
Al_2O_3 (wt%)	13.60	14.75	16.80	14.00	13.05	16.40	12.30	13.40	14.00
Fe_2O_3 (wt%)	20.70	16.85	14.95	15.10	18.50	15.25	17.70	16.95	12.55
MnO (wt%)	0.52	0.37	0.19	0.23	0.20	0.18	0.20	0.30	0.21
MgO (wt%)	4.46	4.59	7.69	5.82	7.08	4.41	3.93	5.95	3.72
CaO (wt%)	8.58	6.56	2.74	9.26	3.15	4.83	3.90	5.56	4.76
K_2O (wt%)	0.25	2.58	0.02	0.15	0.17	0.11	0.29	0.38	0.18
Na_2O (wt%)	2.71	3.02	3.67	2.50	2.35	5.06	3.43	3.95	4.52
P_2O_5 (wt%)	0.22	0.15	0.14	0.08	0.08	0.11	0.15	0.21	0.19
LOI	1.70	1.01	5.38	2.18	7.28	6.91	7.50	3.75	6.38
Mg#	0.30	0.35	0.50	0.50	0.43	0.43	0.36	0.31	0.41
Cr (ppm)	63.00	208.00	110.00	9.00	<5.00	7.00	15.00	88.00	39.00
Co (ppm)	39.00	58.00	58.00	51.00	60.00	48.00	52.00	46.00	32.00
Ni (ppm)	32.00	106.00	58.00	33.00	26.00	26.00	29.00	64.00	48.00
Sc (ppm)	39.00	40.00	39.00	39.00	51.00	28.00	41.00	34.00	23.00
V (ppm)	335.00	388.00	440.00	301.00	715.00	303.00	369.00	424.00	235.00
Ta (ppm)	0.60	0.30	0.30	0.20	0.20	0.20	0.30	0.50	0.60
Nb (ppm)	9.15	5.83	5.90	3.06	3.99	4.60	5.59	9.41	8.56
Zr (ppm)	183.00	117.00	123.00	60.00	71.00	79.00	124.00	199.00	178.00
Hf (ppm)	4.71	2.96	3.18	1.76	1.89	2.10	3.35	5.26	4.44
Th (ppm)	1.54	0.92	0.67	0.48	0.52	0.66	1.20	2.44	2.52
U (ppm)	0.49	0.29	0.17	0.13	0.15	0.19	0.31	0.43	0.64
Y (ppm)	46.50	34.90	32.00	18.40	23.10	26.20	31.70	50.10	30.90
La (ppm)	12.10	9.20	3.60	3.60	3.20	5.10	8.00	14.30	13.90
Ce (ppm)	30.70	21.00	11.10	9.60	8.10	12.50	19.00	33.30	30.80
Pr (ppm)	4.15	2.64	1.71	1.36	1.18	1.80	2.62	4.47	4.00
Nd (ppm)	20.50	13.30	8.90	6.80	5.80	8.40	13.00	20.90	17.20
Sm (ppm)	5.96	3.84	3.17	2.02	1.81	2.85	3.85	6.05	4.08
Eu (ppm)	2.10	1.20	1.04	0.88	0.68	0.83	1.26	1.80	1.36
Gd (ppm)	7.37	5.02	4.30	3.13	2.92	3.83	5.09	7.34	5.16
Tb (ppm)	1.31	0.90	0.81	0.53	0.61	0.72	0.83	1.32	0.94
Dy (ppm)	8.36	5.72	5.61	3.45	4.10	4.53	5.64	8.48	5.50
Ho (ppm)	1.84	1.28	1.30	0.79	0.95	1.02	1.27	1.94	1.24
Er (ppm)	5.61	4.05	3.76	2.38	2.60	2.93	3.73	5.68	3.31
Tm (ppm)	0.75	0.59	0.51	0.31	0.38	0.37	0.48	0.82	0.52
Yb (ppm)	5.16	3.63	3.57	2.11	2.65	2.51	3.56	5.39	3.03
Lu (ppm)	0.72	0.49	0.52	0.33	0.34	0.33	0.49	0.78	0.49
$(La/Sm)_N$	1.31	1.55	0.73	1.15	1.14	1.16	1.34	1.53	2.20
$(Gd/Yb)_N$	1.18	1.14	1.00	1.23	0.91	1.26	1.18	1.13	1.41
Nb/Nb*	0.28	0.25	1.17	0.56	0.84	0.49	0.30	0.22	0.20

Leta Arm group (Eastern zone)									
Sample name	TS23-37	TS23-38	TS23-39	TS23-40	TS23-41	TS23-42	TS23-43	TS23-44	TS23-45
Easting (UTM83-11N)	591775	593165	593047	592947	592762	592654	592536	592418	593259
Northing (UTM83-11N)	7140500	7141771	7141723	7141680	7141693	7141650	7141450	7141332	7143191
SiO_2 (wt%)	55.50	48.20	74.20	74.30	53.50	73.40	75.20	68.10	70.90
TiO_2 (wt%)	1.28	1.66	0.22	0.20	0.93	0.23	0.22	0.24	0.23
Al_2O_3 (wt%)	14.10	13.55	10.90	11.15	15.25	11.35	11.00	12.40	11.25
Fe_2O_3 (wt%)	8.87	16.30	3.61	4.59	10.05	3.87	3.85	4.91	4.26
MnO (wt%)	0.15	0.23	0.05	0.04	0.12	0.08	0.04	0.09	0.11
MgO (wt%)	4.05	5.06	1.28	1.42	5.63	0.60	0.54	0.33	0.66
CaO (wt%)	6.61	6.92	0.75	0.27	7.16	1.18	2.04	2.78	2.86
K_2O (wt%)	0.31	0.48	4.21	1.26	0.19	3.73	1.46	1.92	3.80
Na_2O (wt%)	4.41	2.98	0.41	4.45	2.93	2.98	4.00	5.50	0.82
P_2O_5 (wt%)	0.17	0.15	0.04	0.04	0.19	0.04	0.02	0.04	0.03
LOI	6.24	2.99	2.26	1.12	3.03	1.52	2.26	2.76	3.73
Mg#	0.47	0.38	0.41	0.38	0.53	0.24	0.22	0.12	0.23
Cr (ppm)	138.00	<5.00	5.00	12.00	169.00	10.00	11.00	12.00	<5.00
Co (ppm)	32.00	52.00	1.00	<1.00	32.00	1.00	4.00	1.00	1.00
Ni (ppm)	54.00	22.00	1.00	2.00	65.00	1.00	1.00	2.00	<1.00
Sc (ppm)	27.00	40.00	7.00	5.00	21.00	7.00	7.00	7.00	7.00
V (ppm)	298.00	376.00	<5.00	22.00	190.00	73.00	9.00	6.00	<5.00
Ta (ppm)	0.40	0.40	1.60	1.90	0.60	1.50	1.60	1.70	1.50
Nb (ppm)	6.87	6.18	22.10	29.00	9.29	23.40	24.00	23.50	22.90
Zr (ppm)	119.00	115.00	456.00	568.00	178.00	496.00	510.00	533.00	491.00
Hf (ppm)	2.74	3.11	11.50	14.15	4.22	11.85	12.30	12.95	12.15
Th (ppm)	1.88	1.26	10.30	10.50	2.44	11.00	11.50	11.85	10.85
U (ppm)	0.49	0.28	2.76	2.64	0.62	2.93	2.96	2.80	2.91
Y (ppm)	20.70	29.00	62.40	56.60	27.80	61.20	60.20	66.20	68.50
La (ppm)	13.80	8.00	40.40	38.40	15.40	46.40	44.20	35.80	42.70
Ce (ppm)	27.40	19.60	88.40	86.60	34.80	94.80	97.80	86.80	94.20
Pr (ppm)	3.20	2.65	10.65	10.20	4.15	11.20	11.30	10.55	11.05
Nd (ppm)	14.80	13.10	44.00	42.20	18.20	45.70	46.80	45.10	46.40
Sm (ppm)	3.32	3.54	10.15	9.04	3.97	9.71	10.20	10.70	10.05
Eu (ppm)	1.02	1.26	2.10	1.35	1.20	1.81	1.92	1.97	1.90
Gd (ppm)	3.85	4.70	11.00	9.06	4.80	10.60	10.10	12.50	11.55
Tb (ppm)	0.68	0.82	1.92	1.54	0.82	1.73	1.75	1.99	1.89
Dy (ppm)	3.85	5.22	11.55	10.30	4.76	11.00	10.60	11.95	12.05
Ho (ppm)	0.85	1.20	2.45	2.24	1.05	2.23	2.36	2.56	2.58
Er (ppm)	2.33	3.52	7.16	7.26	3.19	6.96	6.98	8.05	7.75
Tm (ppm)	0.30	0.49	0.98	1.11	0.45	0.98	1.02	1.10	1.06
Yb (ppm)	2.01	3.14	6.57	8.08	2.88	6.25	6.93	7.13	7.31
Lu (ppm)	0.32	0.45	0.91	1.19	0.46	0.91	1.06	1.08	1.07
$(La/Sm)_N$	2.69	1.46	2.57	2.75	2.51	3.09	2.80	2.16	2.75
$(Gd/Yb)_N$	1.58	1.24	1.38	0.93	1.38	1.40	1.21	1.45	1.31
Nb/Nb*	0.15	0.34	0.11	0.16	0.19	0.09	0.11	0.15	0.11

Leta Arm group (Eastern zone)									
Sample name	TS23-46	TS23-47	TS23-48	TS23-49	TS23-50	TS23-51	TS23-52	TS23-53	TS23-54
Easting (UTM83-11N)	593401	593541	593634	593730	593870	593987	594097	594192	594394
Northing (UTM83-11N)	7143298	7143366	7143444	7143381	7143404	7143477	7143465	7143439	7143586
SiO_2 (wt%)	47.20	49.00	51.80	71.10	47.00	55.30	46.60	48.20	52.20
TiO_2 (wt%)	1.64	1.64	1.71	0.68	1.42	1.32	1.31	1.28	1.25
Al_2O_3 (wt%)	12.20	12.05	15.30	13.00	13.65	12.85	13.70	13.40	13.40
Fe_2O_3 (wt%)	16.20	16.70	12.45	7.26	14.65	12.95	13.90	15.95	13.15
MnO (wt%)	0.22	0.18	0.28	0.06	0.20	0.19	0.18	0.20	0.17
MgO (wt%)	4.78	4.01	4.13	0.85	5.14	3.49	4.36	5.68	6.09
CaO (wt%)	5.67	5.28	9.07	0.70	6.65	6.42	9.52	5.20	8.12
K_2O (wt%)	1.80	0.27	0.25	1.20	0.51	0.20	0.11	0.23	0.11
Na_2O (wt%)	2.66	2.76	3.04	5.81	3.60	2.55	2.75	1.76	2.60
P_2O_5 (wt%)	0.18	0.17	0.14	0.12	0.12	0.13	0.11	0.12	0.11
LOI	5.85	6.51	1.44	0.70	7.85	6.32	7.56	7.15	1.90
Mg#	0.37	0.32	0.40	0.19	0.41	0.35	0.38	0.41	0.48
Cr (ppm)	<5.00	7.00	129.00	10.00	70.00	67.00	95.00	89.00	133.00
Co (ppm)	48.00	44.00	54.00	6.00	47.00	49.00	52.00	55.00	48.00
Ni (ppm)	19.00	22.00	77.00	1.00	54.00	56.00	75.00	66.00	87.00
Sc (ppm)	36.00	35.00	43.00	10.00	36.00	27.00	36.00	37.00	35.00
V (ppm)	371.00	324.00	388.00	22.00	339.00	286.00	330.00	333.00	315.00
Ta (ppm)	0.40	0.40	0.30	1.70	0.30	0.30	0.30	0.30	0.30
Nb (ppm)	7.09	6.45	4.82	23.30	4.39	4.28	4.25	4.75	4.76
Zr (ppm)	136.00	134.00	105.00	525.00	89.00	99.00	93.00	102.00	100.00
Hf (ppm)	3.48	3.57	2.71	13.05	2.24	2.41	2.44	2.68	2.71
Th (ppm)	1.38	1.93	0.81	9.47	1.17	1.15	1.15	1.37	1.34
U (ppm)	0.36	0.80	0.27	2.43	0.32	0.32	0.33	0.34	0.31
Y (ppm)	32.50	33.30	31.00	99.40	25.20	25.00	24.00	25.20	23.00
La (ppm)	8.80	11.00	6.30	39.60	7.60	6.50	7.00	6.60	6.00
Ce (ppm)	21.90	24.60	16.70	88.80	17.20	16.50	16.30	15.90	14.90
Pr (ppm)	3.04	3.26	2.38	11.50	2.34	2.29	2.33	2.23	2.08
Nd (ppm)	14.80	14.80	12.20	50.60	11.10	11.50	10.30	10.50	9.80
Sm (ppm)	3.96	4.04	3.56	12.90	3.20	3.17	2.84	3.16	2.73
Eu (ppm)	1.24	1.14	1.14	2.45	1.04	1.02	1.04	1.00	0.87
Gd (ppm)	5.44	4.94	4.90	14.10	3.97	4.29	3.92	3.63	3.44
Tb (ppm)	0.94	0.85	0.80	2.42	0.70	0.70	0.67	0.71	0.69
Dy (ppm)	5.91	5.60	5.49	16.80	4.53	4.30	4.68	4.75	4.27
Ho (ppm)	1.28	1.12	1.14	3.46	0.93	0.89	0.82	0.92	0.85
Er (ppm)	3.75	3.43	3.18	10.15	2.64	2.52	2.62	2.74	2.24
Tm (ppm)	0.50	0.51	0.51	1.52	0.40	0.38	0.40	0.41	0.38
Yb (ppm)	3.55	3.26	3.04	10.10	2.64	2.57	2.74	2.70	2.44
Lu (ppm)	0.51	0.47	0.45	1.60	0.39	0.38	0.40	0.39	0.41
$(La/Sm)_N$	1.44	1.76	1.14	1.98	1.53	1.33	1.59	1.35	1.42
$(Gd/Yb)_N$	1.27	1.25	1.33	1.15	1.24	1.38	1.18	1.11	1.17
Nb/Nb*	0.34	0.21	0.39	0.12	0.25	0.33	0.28	0.34	0.40

Leta Arm group (Eastern zone)										
Sample name	TS23-55	TS23-56	TS23-57	TS23-58	TS23-59	TS23-60	TS23-61	TS23-62	TS23-63	TS23-64
Easting (UTM83-11N)	594537	594645	594789	594886	594993	595095	595254	595255	595253	590863
Northing (UTM83-11N)	7143517	7143649	7143677	7143613	7143646	7143702	7143756	7143877	7144025	7140691
SiO_2 (wt%)	70.20	46.50	47.00	49.00	48.70	49.90	46.60	48.90	49.90	52.50
TiO_2 (wt%)	0.34	1.56	1.26	1.53	1.87	1.62	1.71	1.94	1.46	1.38
Al_2O_3 (wt%)	16.55	13.50	13.10	16.05	14.55	12.80	14.10	14.90	15.30	16.20
Fe_2O_3 (wt%)	3.67	15.15	13.05	14.80	14.55	10.55	14.35	11.10	11.60	7.82
MnO (wt%)	0.06	0.19	0.15	0.17	0.28	0.30	0.33	0.29	0.25	0.12
MgO (wt%)	1.12	6.12	7.03	6.84	3.91	2.92	3.47	5.11	6.52	2.27
CaO (wt%)	1.98	6.99	7.54	6.45	9.26	9.14	11.30	6.09	8.03	5.40
K_2O (wt%)	3.44	0.63	0.13	0.26	0.18	0.72	0.17	0.80	0.36	1.81
Na_2O (wt%)	2.23	1.72	2.37	2.53	2.82	2.66	2.46	3.57	3.55	4.31
P_2O_5 (wt%)	0.10	0.12	0.10	0.13	0.19	0.17	0.16	0.20	0.12	0.28
LOI	1.84	7.60	8.62	2.33	3.15	7.74	4.50	6.41	2.76	6.25
Mg#	0.38	0.44	0.52	0.48	0.35	0.35	0.32	0.48	0.53	0.37
Cr (ppm)	<5.00	86.00	172.00	191.00	134.00	117.00	121.00	137.00	195.00	87.00
Co (ppm)	2.00	52.00	48.00	34.00	59.00	46.00	54.00	63.00	58.00	30.00
Ni (ppm)	<1.00	74.00	78.00	78.00	81.00	69.00	74.00	92.00	95.00	58.00
Sc (ppm)	6.00	39.00	40.00	39.00	39.00	34.00	37.00	39.00	42.00	22.00
V (ppm)	12.00	356.00	347.00	407.00	372.00	314.00	358.00	389.00	401.00	207.00
Ta (ppm)	1.00	0.30	0.20	0.30	0.40	0.40	0.40	0.40	0.30	0.80
Nb (ppm)	10.75	4.58	3.81	4.54	7.04	6.25	6.51	6.70	4.10	12.00
Zr (ppm)	301.00	96.00	89.00	100.00	130.00	119.00	129.00	137.00	98.00	210.00
Hf (ppm)	7.41	2.50	2.35	2.67	3.33	3.02	3.37	3.35	2.62	5.03
Th (ppm)	9.11	0.76	0.63	0.72	1.14	1.01	1.08	1.09	0.72	3.10
U (ppm)	2.33	0.19	0.35	0.25	0.29	0.26	0.29	0.27	0.19	0.79
Y (ppm)	39.40	25.90	25.80	25.00	34.50	31.30	34.90	28.90	29.60	29.70
La (ppm)	25.30	5.50	4.80	4.90	8.70	8.60	8.30	8.20	5.70	19.90
Ce (ppm)	59.20	14.70	12.50	12.70	22.40	21.10	21.40	21.70	14.60	45.20
Pr (ppm)	6.53	2.14	1.83	1.91	3.27	3.00	3.14	2.98	2.11	5.68
Nd (ppm)	26.00	10.50	9.70	9.80	15.80	14.00	15.00	15.30	11.10	24.90
Sm (ppm)	6.08	3.10	2.77	2.85	4.57	3.95	4.42	3.99	3.67	5.74
Eu (ppm)	1.56	1.04	1.10	1.13	1.44	1.35	1.38	1.50	1.24	1.51
Gd (ppm)	6.53	4.19	4.09	3.80	5.59	5.17	5.65	5.17	4.50	5.91
Tb (ppm)	1.10	0.71	0.68	0.69	1.02	0.86	0.96	0.90	0.79	0.90
Dy (ppm)	7.04	4.93	4.73	4.81	6.34	5.40	6.31	5.74	5.36	6.03
Ho (ppm)	1.36	0.91	0.91	0.93	1.32	1.12	1.26	1.14	1.16	1.11
Er (ppm)	4.03	2.80	2.78	2.78	3.62	3.31	3.69	3.02	3.15	3.25
Tm (ppm)	0.57	0.43	0.39	0.41	0.59	0.49	0.58	0.47	0.46	0.46
Yb (ppm)	3.94	2.56	2.72	2.88	3.62	3.26	3.76	2.81	3.04	3.04
Lu (ppm)	0.58	0.44	0.39	0.40	0.65	0.50	0.53	0.43	0.47	0.47
$(La/Sm)_N$	2.69	1.15	1.12	1.11	1.23	1.41	1.21	1.33	1.00	2.24
$(Gd/Yb)_N$	1.37	1.35	1.24	1.09	1.28	1.31	1.24	1.52	1.22	1.61
Nb/Nb*	0.11	0.46	0.45	0.52	0.35	0.31	0.35	0.37	0.38	0.17

Leta Arm group (Eastern zone, 2024 samples)									
Sample name	TS24-02	TS24-03	TS24-06	TS24-08	TS24-09	TS24-10	TS24-11	TS24-12	TS24-13
Drillhole ID	GB21-16	NL21-15	NL21-08	GB21-26	GB21-26	GB21-26	GB21-26	GB21-26	GB21-26
Easting (UTM83-11N)	590493.50	593358	593093	590633.8	590633.8	590633.8	590633.80	590633.8	590633.80
Northing (UTM83-11N)	7140203	7143356	7142151	7140345	7140345	7140345	7140345	7140345	7140345
SiO_2 (wt%)	85.40	69.50	78.50	63.10	77.10	75.20	75.20	74.90	76.50
TiO_2 (wt%)	0.15	0.24	0.25	0.16	0.16	0.15	0.14	0.17	0.17
Al_2O_3 (wt%)	8.75	12.75	14.15	10.75	9.97	9.58	9.58	11.05	11.30
Fe_2O_3 (wt%)	1.27	3.24	0.60	4.32	3.94	3.97	3.72	3.20	2.72
MnO (wt%)	0.01	0.07	0.01	0.17	0.04	0.09	0.08	0.07	0.04
MgO (wt%)	0.24	1.20	0.21	0.93	0.34	0.39	0.46	0.35	0.33
CaO (wt%)	0.16	3.28	0.21	7.91	1.68	4.22	3.38	2.74	1.46
K_2O (wt%)	1.88	4.02	2.57	2.39	1.72	1.32	1.32	2.08	1.26
Na_2O (wt%)	2.05	0.27	1.16	1.82	2.67	2.79	2.94	2.87	4.08
P_2O_5 (wt%)	0.02	0.03	0.02	0.01	0.01	0.02	0.02	0.02	0.02
LOI	0.82	3.35	1.94	7.42	2.06	3.80	3.30	2.35	1.68
Mg#	0.27	0.42	0.41	0.30	0.15	0.16	0.20	0.18	0.19
Cr (ppm)	11.00	2.50	2.50	2.50	2.50	2.50	2.50	2.50	7.00
Co (ppm)	1.00	1.00	0.50	1.00	2.00	1.00	1.00	0.50	0.50
Ni (ppm)	1.00	0.50	0.50	1.00	1.00	0.50	1.00	1.00	0.50
Sc (ppm)	3.00	7.00	5.00	4.00	3.00	3.00	3.00	3.00	59.00
V (ppm)	2.50	2.50	8.00	2.50	2.50	2.50	2.50	2.50	2.50
Ta (ppm)	1.30	1.80	2.60	1.80	1.70	1.60	1.60	1.90	1.90
Nb (ppm)	18.45	24.20	39.50	26.30	25.00	22.50	23.40	26.50	24.50
Zr (ppm)	367.00	524.00	733.00	504.00	447.00	430.00	412.00	506.00	501.00
Hf (ppm)	9.34	13.25	19.40	12.85	11.40	11.55	11.85	13.30	13.70
Th (ppm)	8.32	12.10	10.80	10.85	9.89	9.73	10.50	11.15	11.85
U (ppm)	1.85	2.85	1.94	2.38	2.37	2.27	2.66	2.46	2.42
Y (ppm)	45.20	68.20	106.50	66.90	68.90	57.30	64.10	69.70	62.10
La (ppm)	27.30	46.10	32.80	47.40	40.80	38.50	45.90	49.30	44.50
Ce (ppm)	62.10	102.50	85.30	106.50	93.20	85.70	100.50	109.50	102.00
Pr (ppm)	7.58	12.35	11.90	13.30	11.40	10.45	12.25	13.05	12.30
Nd (ppm)	32.30	51.70	52.90	56.30	47.50	46.50	48.60	57.00	53.60
Sm (ppm)	7.29	12.05	14.85	13.45	10.65	10.20	11.40	13.50	12.45
Eu (ppm)	1.14	1.90	2.32	2.15	1.68	1.72	1.57	1.97	2.02
Gd (ppm)	7.55	12.60	16.15	13.90	11.05	10.55	10.30	13.80	11.50
Tb (ppm)	1.13	1.84	3.59	2.15	1.76	1.66	1.89	2.00	1.80
Dy (ppm)	7.47	12.35	22.30	13.90	11.45	10.85	12.30	13.10	11.80
Ho (ppm)	1.68	2.49	5.06	2.66	2.49	2.16	2.63	2.68	2.37
Er (ppm)	5.49	7.93	13.60	8.05	8.19	6.81	7.51	8.45	7.90
Tm (ppm)	0.81	1.23	1.76	1.23	1.19	1.05	1.13	1.26	1.19
Yb (ppm)	5.85	7.82	10.60	7.84	7.98	6.71	8.14	8.09	8.01
Lu (ppm)	0.90	1.17	1.64	1.19	1.30	1.12	1.02	1.30	1.20
$(La/Sm)_N$	2.42	2.47	1.43	2.28	2.48	2.44	2.60	2.36	2.31
$(Gd/Yb)_N$	1.07	1.33	1.26	1.47	1.15	1.30	1.05	1.41	1.19
Nb/Nb*	0.17	0.10	0.30	0.11	0.13	0.12	0.10	0.10	0.11

Leta Arm group (Western zone)									
Sample name	TS23-65	TS23-66	TS23-67	TS23-68	TS23-69	TS23-70	TS23-71	TS23-72	TS23-73
Easting (UTM83-11N)	585235	585317	585454	585539	585691	585884	585970	586145	586346
Northing (UTM83-11N)	7146844	7146751	7146678	7146558	7146443	7146431	7146537	7146485	7146528
SiO_2 (wt%)	38.00	51.90	49.30	60.70	47.70	45.20	44.60	44.90	47.20
TiO_2 (wt%)	1.15	1.60	1.32	1.40	1.42	0.92	1.04	1.20	1.00
Al_2O_3 (wt%)	15.10	13.60	15.70	17.05	16.15	14.25	14.25	13.75	15.10
Fe_2O_3 (wt%)	14.30	10.40	12.60	9.45	13.30	11.05	11.65	16.10	13.00
MnO (wt%)	0.41	0.27	0.23	0.18	0.20	0.24	0.28	0.20	0.21
MgO (wt%)	3.66	3.49	3.41	1.84	3.94	3.71	4.53	6.97	5.30
CaO (wt%)	12.00	7.92	7.01	3.68	5.92	12.30	10.80	9.42	11.15
K_2O (wt%)	0.59	1.01	0.51	0.28	0.40	0.07	0.08	0.12	0.13
Na_2O (wt%)	1.14	1.32	2.82	3.26	2.69	2.44	2.55	1.58	1.73
P_2O_5 (wt%)	0.08	0.13	0.08	0.11	0.10	0.06	0.07	0.08	0.07
LOI	11.70	9.24	7.50	2.19	6.62	8.61	9.70	3.87	3.43
Mg#	0.34	0.40	0.35	0.28	0.37	0.40	0.44	0.46	0.45
Cr (ppm)	242.00	39.00	235.00	244.00	305.00	259.00	272.00	151.00	274.00
Co (ppm)	50.00	39.00	41.00	27.00	50.00	47.00	50.00	56.00	51.00
Ni (ppm)	114.00	23.00	94.00	46.00	80.00	138.00	128.00	115.00	150.00
Sc (ppm)	43.00	27.00	45.00	29.00	48.00	37.00	41.00	41.00	39.00
V (ppm)	304.00	420.00	421.00	332.00	422.00	302.00	322.00	415.00	325.00
Ta (ppm)	0.20	0.30	0.20	0.20	0.20	0.20	0.10	0.20	0.20
Nb (ppm)	2.74	5.24	2.84	7.33	5.37	3.29	3.11	3.41	2.79
Zr (ppm)	56.00	92.00	71.00	73.00	76.00	60.00	62.00	62.00	62.00
Hf (ppm)	1.51	2.61	1.92	2.01	2.13	1.63	1.61	1.68	1.72
Th (ppm)	0.20	0.48	0.24	0.54	0.44	0.26	0.30	0.26	0.32
U (ppm)	0.06	0.13	0.06	0.08	0.08	0.07	0.08	0.08	0.08
Y (ppm)	16.90	24.30	22.30	20.60	22.30	20.70	21.30	22.80	21.40
La (ppm)	2.90	4.90	3.20	5.80	4.50	3.40	3.50	3.90	3.20
Ce (ppm)	8.40	13.20	8.90	14.90	12.10	9.40	9.70	10.20	8.80
Pr (ppm)	1.31	1.97	1.45	2.14	1.76	1.40	1.41	1.59	1.38
Nd (ppm)	7.30	10.10	7.60	9.50	8.90	7.70	7.80	7.80	7.40
Sm (ppm)	2.16	3.20	2.42	2.82	2.74	2.51	2.26	2.56	2.28
Eu (ppm)	0.83	1.08	0.90	1.10	1.04	0.87	0.95	0.97	0.92
Gd (ppm)	3.04	4.11	3.15	3.24	3.54	3.29	3.40	3.47	3.52
Tb (ppm)	0.51	0.68	0.58	0.54	0.57	0.58	0.54	0.60	0.54
Dy (ppm)	3.23	4.56	4.01	3.73	4.43	3.85	4.05	3.99	3.97
Ho (ppm)	0.64	0.91	0.85	0.74	0.87	0.75	0.82	0.86	0.80
Er (ppm)	1.77	2.72	2.48	2.21	2.75	2.42	2.33	2.27	2.29
Tm (ppm)	0.26	0.42	0.37	0.31	0.44	0.34	0.34	0.34	0.34
Yb (ppm)	1.71	2.53	2.36	2.16	2.71	2.18	2.08	2.28	2.31
Lu (ppm)	0.29	0.41	0.38	0.28	0.46	0.33	0.33	0.32	0.35
$(La/Sm)_N$	0.87	0.99	0.85	1.33	1.06	0.88	1.00	0.98	0.91
$(Gd/Yb)_N$	1.47	1.34	1.10	1.24	1.08	1.25	1.35	1.26	1.26
Nb/Nb*	0.72	0.62	0.63	0.66	0.72	0.67	0.60	0.55	0.61

Leta Arm group (Western zone)									
Sample name	TS23-74	TS23-75	TS23-76	TS23-77	TS23-78	TS23-79	TS23-80	TS23-81	TS23-82
Easting (UTM83-11N)	586494	586596	586822	587108	587210	587310	587451	587556	587643
Northing (UTM83-11N)	7146475	7146346	7145150	7145306	7145322	7145298	7145215	7145165	7145034
SiO_2 (wt%)	48.60	47.50	43.30	46.60	46.30	47.60	58.00	48.40	60.60
TiO_2 (wt%)	1.22	0.96	1.15	1.08	2.19	1.24	0.83	1.10	0.78
Al_2O_3 (wt%)	15.20	14.70	15.80	15.45	14.25	14.00	16.70	13.60	15.70
Fe_2O_3 (wt%)	10.20	13.45	13.75	13.15	15.50	15.40	8.07	14.20	6.33
MnO (wt%)	0.22	0.17	0.19	0.19	0.23	0.16	0.09	0.20	0.14
MgO (wt%)	3.42	7.76	6.68	8.28	4.61	8.49	3.52	6.68	1.66
CaO (wt%)	10.40	4.73	9.25	9.72	6.52	3.74	2.39	10.20	8.29
K_2O (wt%)	0.04	0.01	0.13	0.05	0.01	0.03	0.07	0.07	0.80
Na_2O (wt%)	2.28	2.39	1.44	1.73	2.83	0.75	6.54	2.11	2.65
P_2O_5 (wt%)	0.09	0.06	0.09	0.07	0.22	0.09	0.16	0.08	0.17
LOI	6.32	7.61	7.50	3.45	8.08	7.07	3.55	2.93	2.88
Mg#	0.40	0.53	0.49	0.56	0.37	0.52	0.46	0.48	0.34
Cr (ppm)	233.00	184.00	294.00	281.00	24.00	149.00	27.00	132.00	24.00
Co (ppm)	47.00	46.00	58.00	47.00	41.00	52.00	27.00	46.00	16.00
Ni (ppm)	113.00	80.00	105.00	135.00	37.00	67.00	43.00	73.00	25.00
Sc (ppm)	41.00	44.00	38.00	28.00	43.00	38.00	15.00	42.00	13.00
V (ppm)	344.00	321.00	343.00	333.00	449.00	345.00	139.00	318.00	114.00
Ta (ppm)	0.20	0.10	0.20	0.10	0.50	0.20	0.60	0.10	0.50
Nb (ppm)	3.34	2.44	2.94	2.66	7.08	3.24	7.87	3.21	7.80
Zr (ppm)	70.00	48.00	69.00	55.00	165.00	81.00	176.00	63.00	156.00
Hf (ppm)	1.92	1.38	1.82	1.48	4.13	2.26	4.24	1.73	3.85
Th (ppm)	0.30	0.19	0.37	0.27	0.75	0.32	5.02	0.26	4.82
U (ppm)	0.09	0.05	0.06	0.08	0.21	0.09	1.22	0.06	1.12
Y (ppm)	22.10	18.10	23.00	20.90	48.20	22.50	17.70	21.70	18.20
La (ppm)	3.70	1.70	3.60	3.00	9.10	3.40	15.20	3.10	20.00
Ce (ppm)	10.40	5.30	10.40	8.20	24.60	9.70	32.10	9.00	40.30
Pr (ppm)	1.60	0.91	1.48	1.17	3.65	1.50	3.74	1.42	4.70
Nd (ppm)	8.50	4.60	8.20	6.60	19.60	7.80	15.10	7.30	19.20
Sm (ppm)	2.66	1.77	2.43	2.06	6.14	2.78	3.48	2.16	3.64
Eu (ppm)	1.04	0.63	1.02	0.90	1.98	0.82	1.12	0.91	1.14
Gd (ppm)	3.67	2.42	3.42	2.99	8.02	3.71	3.33	3.26	3.72
Tb (ppm)	0.66	0.48	0.65	0.51	1.35	0.66	0.51	0.58	0.54
Dy (ppm)	4.07	3.27	4.22	3.78	9.21	4.23	3.24	3.72	3.20
Ho (ppm)	0.79	0.67	0.84	0.74	1.86	0.93	0.67	0.84	0.68
Er (ppm)	2.33	1.98	2.54	2.11	5.15	2.47	1.88	2.45	1.85
Tm (ppm)	0.34	0.31	0.38	0.31	0.80	0.36	0.28	0.36	0.28
Yb (ppm)	2.38	1.90	2.39	2.23	4.78	2.42	1.78	2.25	1.73
Lu (ppm)	0.32	0.30	0.39	0.33	0.81	0.39	0.30	0.37	0.25
$(La/Sm)_N$	0.90	0.62	0.96	0.94	0.96	0.79	2.82	0.93	3.55
$(Gd/Yb)_N$	1.28	1.05	1.18	1.11	1.39	1.27	1.55	1.20	1.78
Nb/Nb*	0.60	1.43	0.56	0.64	0.34	0.67	0.16	0.76	0.10

Leta Arm group (Western zone)									
Sample name	TS23-83	TS23-84	TS23-85	TS23-86	TS23-87	TS23-88	TS23-89	TS23-90	TS23-91
Easting (UTM83-11N)	587735	587867	587993	588102	588245	588386	588549	588828	588942
Northing (UTM83-11N)	7145904	7145788	7145802	7145670	7145597	7145507	7145508	7145793	7145782
SiO_2 (wt%)	58.20	48.20	48.90	66.90	66.40	60.80	59.10	58.80	51.10
TiO_2 (wt%)	1.05	0.88	1.39	0.74	0.36	0.71	0.71	1.04	1.53
Al_2O_3 (wt%)	15.60	16.30	12.75	18.00	15.30	15.90	17.15	14.40	12.85
Fe_2O_3 (wt%)	9.58	11.05	15.70	5.23	4.08	6.29	6.36	6.63	18.30
MnO (wt%)	0.12	0.15	0.20	0.05	0.05	0.08	0.08	0.10	0.25
MgO (wt%)	2.82	6.75	6.47	1.28	1.06	2.36	2.44	4.86	4.36
CaO (wt%)	5.85	12.45	7.81	1.22	3.90	4.06	5.30	6.01	6.71
K_2O (wt%)	1.14	0.08	0.07	3.19	2.81	0.71	1.40	0.40	0.50
Na_2O (wt%)	3.38	1.76	1.70	2.09	2.19	5.28	3.07	4.68	2.51
P_2O_5 (wt%)	0.22	0.08	0.11	0.21	0.09	0.18	0.19	0.29	0.14
LOI	2.25	3.30	4.64	2.64	5.15	3.83	4.27	1.93	2.41
Mg#	0.37	0.55	0.45	0.33	0.34	0.43	0.43	0.59	0.32
Cr (ppm)	7.00	263.00	74.00	6.00	55.00	40.00	159.00	377.00	44.00
Co (ppm)	30.00	39.00	47.00	12.00	12.00	18.00	20.00	26.00	46.00
Ni (ppm)	15.00	107.00	53.00	10.00	30.00	25.00	63.00	123.00	41.00
Sc (ppm)	17.00	29.00	44.00	14.00	7.00	13.00	12.00	17.00	43.00
V (ppm)	184.00	276.00	415.00	122.00	57.00	204.00	109.00	150.00	459.00
Ta (ppm)	0.70	0.20	0.20	0.70	0.80	0.60	0.80	0.60	0.30
Nb (ppm)	8.37	2.40	4.10	8.83	7.49	8.13	10.70	9.82	5.13
Zr (ppm)	166.00	54.00	80.00	211.00	160.00	171.00	194.00	182.00	102.00
Hf (ppm)	4.12	1.52	2.29	4.75	4.00	4.07	4.55	4.23	2.89
Th (ppm)	5.75	0.26	0.41	7.52	10.50	5.62	6.82	4.95	0.43
U (ppm)	1.59	0.07	0.10	1.95	2.33	1.49	1.77	1.19	0.12
Y (ppm)	23.90	17.60	27.80	18.70	10.70	19.10	16.30	22.30	35.80
La (ppm)	21.40	3.80	5.10	14.20	13.30	21.30	20.30	25.70	5.30
Ce (ppm)	45.90	9.30	12.70	31.10	24.90	40.60	40.70	57.90	14.10
Pr (ppm)	5.47	1.34	2.02	3.31	2.74	4.48	4.40	7.06	2.10
Nd (ppm)	24.20	6.80	10.80	13.90	10.30	18.30	18.80	30.20	11.90
Sm (ppm)	4.92	2.07	3.09	3.12	1.98	3.47	3.75	6.01	3.74
Eu (ppm)	1.30	0.77	1.13	0.73	0.49	1.12	1.24	1.62	1.19
Gd (ppm)	4.55	2.84	4.42	3.33	1.95	3.57	3.66	4.82	5.10
Tb (ppm)	0.71	0.45	0.78	0.51	0.29	0.53	0.54	0.72	0.88
Dy (ppm)	4.33	3.30	4.77	3.23	1.90	3.25	3.02	4.21	6.05
Ho (ppm)	0.91	0.68	1.04	0.69	0.38	0.70	0.59	0.91	1.35
Er (ppm)	2.54	1.99	3.03	2.01	1.04	1.97	1.66	2.47	4.00
Tm (ppm)	0.35	0.30	0.40	0.29	0.15	0.27	0.25	0.35	0.58
Yb (ppm)	2.22	1.76	2.67	1.91	0.95	1.70	1.35	2.09	3.59
Lu (ppm)	0.40	0.31	0.44	0.30	0.15	0.27	0.22	0.31	0.62
$(La/Sm)_N$	2.81	1.19	1.07	2.94	4.34	3.97	3.50	2.76	0.92
$(Gd/Yb)_N$	1.70	1.33	1.37	1.44	1.70	1.74	2.24	1.91	1.18
Nb/Nb*	0.10	0.39	0.44	0.20	0.17	0.10	0.14	0.10	0.54

Leta Arm group (Western zone)					
Sample name	TS23-92	TS23-93	TS23-94	TS23-95	TS23-96
Easting (UTM83-11N)	589070	589364	589551	589695	589806
Northing (UTM83-11N)	7145727	7145726	7145740	7145654	7145621
SiO_2 (wt%)	60.50	54.00	55.00	59.90	58.80
TiO_2 (wt%)	0.57	0.74	0.58	0.52	0.34
Al_2O_3 (wt%)	14.90	13.85	14.15	13.90	11.75
Fe_2O_3 (wt%)	5.09	9.48	6.95	7.87	4.62
MnO (wt%)	0.14	0.15	0.18	0.12	0.12
MgO (wt%)	2.68	5.99	3.22	4.34	2.89
CaO (wt%)	5.89	4.61	8.16	4.63	9.26
K_2O (wt%)	0.62	0.96	1.28	1.08	1.52
Na_2O (wt%)	4.45	1.94	2.59	2.98	1.61
P_2O_5 (wt%)	0.10	0.21	0.13	0.10	0.08
LOI	5.24	7.78	7.27	4.90	9.74
Mg#	0.51	0.56	0.48	0.52	0.55
Cr (ppm)	226.00	286.00	457.00	196.00	127.00
Co (ppm)	17.00	30.00	23.00	22.00	16.00
Ni (ppm)	90.00	134.00	112.00	83.00	72.00
Sc (ppm)	16.00	16.00	21.00	14.00	7.00
V (ppm)	142.00	140.00	146.00	115.00	54.00
Ta (ppm)	0.50	0.60	0.50	0.40	0.40
Nb (ppm)	6.72	9.34	6.28	5.99	5.08
Zr (ppm)	142.00	175.00	142.00	144.00	119.00
Hf (ppm)	3.42	4.14	3.22	3.52	2.95
Th (ppm)	4.46	3.81	3.65	4.53	5.62
U (ppm)	1.01	0.94	0.86	0.91	1.02
Y (ppm)	17.30	20.20	15.80	14.90	13.40
La (ppm)	17.00	18.60	15.60	15.80	25.10
Ce (ppm)	34.30	41.30	32.40	32.20	48.60
Pr (ppm)	3.84	4.88	3.62	3.73	5.35
Nd (ppm)	15.50	21.00	15.00	13.60	19.40
Sm (ppm)	3.69	4.19	2.95	3.02	3.75
Eu (ppm)	1.00	1.03	1.00	0.85	0.88
Gd (ppm)	3.19	4.10	3.03	2.75	3.18
Tb (ppm)	0.51	0.63	0.49	0.46	0.41
Dy (ppm)	3.14	3.77	2.91	2.72	2.46
Ho (ppm)	0.63	0.74	0.62	0.52	0.52
Er (ppm)	1.83	2.08	1.68	1.66	1.28
Tm (ppm)	0.24	0.30	0.27	0.22	0.19
Yb (ppm)	1.41	1.97	1.47	1.31	1.16
Lu (ppm)	0.26	0.26	0.23	0.20	0.18
$(La/Sm)_N$	2.98	2.87	3.42	3.38	4.33
$(Gd/Yb)_N$	1.87	1.72	1.71	1.74	2.27
Nb/Nb*	0.11	0.15	0.12	0.11	0.05

Whole-rock geochemistry data not used in the thesis.

Hewitt Lake group (Southwestern zone)									
Sample name	TS23-01	TS23-02	TS23-03	TS23-04	TS23-05	TS23-06	TS23-07	TS23-08	TS23-09
Easting (UTM83-11N)	582363	582538	583016	583386	583765	583720	583868	584334	584654
Northing (UTM83-11N)	7133501	7133566	7133597	7133647	7133740	7133719	7134073	7135056	7135938
Cr_2O_3	0.01	0.03	0.03	0.02	0.03	0.02	0.03	0.00	0.01
SrO	0.02	0.02	0.04	0.02	0.03	0.01	0.01	0.01	0.03
BaO	0.03	0.02	0.03	<0.01	0.15	0.01	0.08	0.01	0.03
Sr	132.5	128.5	290.00	135.00	245.00	128.50	108.50	103.00	264.00
Ba	266.00	136.50	249.00	26.30	1280.00	52.80	737.00	124.00	295.00
Li	40.00	10.00	20.00	20.00	50.00	30.00	50.00	20.00	10.00
Rb	46.90	11.20	56.50	3.80	80.40	5.50	104.00	5.10	35.80
Cs	1.90	0.30	0.32	0.15	4.85	0.71	3.04	0.55	0.88
S	0.01	0.01	0.06	0.05	0.32	0.02	<0.01	0.15	0.02
C	0.04	0.02	0.20	0.05	0.17	0.13	0.22	0.54	0.26
Ga	15.60	15.60	19.40	15.00	23.20	17.40	27.40	18.30	16.20
Ge	0.80	1.10	1.30	1.30	1.20	1.90	1.20	1.70	1.00
As	0.60	<0.10	0.40	0.10	46.60	0.60	90.20	58.40	0.90
Sb	<0.05	<0.05	<0.05	0.10	0.12	0.24	0.10	0.16	0.10
Te	0.01	<0.01	<0.01	0.02	0.05	0.02	0.02	0.03	<0.01
In	0.02	0.01	0.01	0.01	0.05	0.02	0.01	0.03	0.03
Sn	0.90	1.50	1.20	0.50	1.20	0.50	1.60	1.10	1.80
Tl	0.09	<0.02	0.05	<0.02	0.72	<0.02	0.06	0.02	0.02
Bi	0.03	0.01	0.02	<0.01	0.22	<0.01	0.12	0.04	0.03
W	0.50	<0.50	8.80	0.80	1.40	0.60	5,00	1.90	0.80
Re	0.00	0.00	0.00	0.00	0.00	0.00	0.00	0.00	0.00
Hg	<0.01	<0.01	<0.01	<0.01	<0.01	<0.01	<0.01	<0.01	<0.01
Se	<0.20	<0.20	0.20	0.30	0.40	0.20	0.20	0.80	0.30
Cu	46.00	59.00	37.00	103.00	42.00	116.00	4.00	102.00	21.00
Mo	<1.00	<1.00	<1.00	<1.00	1.00	<1.00	<1.00	<1.00	1.00
Pb	<2.00	<2.00	2.00	<2.00	12.00	<2.00	<2.00	3.00	4.00
Zn	73.00	87.00	87.00	100.00	132.00	97.00	52.00	122.00	42.00
Au	<0.01	<0.01	<0.01	<0.01	<0.01	<0.01	<0.01	<0.01	<0.01
Ag	<0.50	<0.50	<0.50	<0.50	<0.50	<0.50	<0.50	<0.50	<0.50
Cd	<0.50	<0.50	<0.50	<0.50	<0.50	<0.50	<0.50	<0.50	<0.50
Leta Arm group (Southern zone)									
Sample name	TS23-10	TS23-11	TS23-12	TS23-20	TS23-21	TS23-22	TS23-23	TS23-24	TS23-25
Easting (UTM83-11N)	584658	584798	584915	585074	585175	585287	585543	585628	585899
Northing (UTM83-11N)	7136007	7136103	7136124	7136209	7136316	7136441	7136709	7136732	7136824
Cr_2O_3	0.01	0.00	0.02	0.01	0.02	0.01	0.00	0.00	0.00
SrO	0.03	0.02	0.01	0.01	0.02	0.02	0.03	0.01	0.01
BaO	0.06	0.04	0.01	0.03	0.04	0.07	0.07	0.04	0.03
Sr	224.00	195.5	91.60	76.20	161.5	153.5	279	123.50	87.70
Ba	486.00	339.00	122.50	240.00	329.00	540.00	542.00	366.00	245.00
Li	10.00	10.00	20.00	20.00	30.00	10.00	20.00	10.00	10.00
Rb	71.10	36.80	24.70	48.90	50.8	76.2	58.6	54.9	56.7
Cs	2.22	9.68	0.94	1.04	1.20	1.88	1.91	1.18	0.96
S	0.06	0.02	0.01	0.01	0.01	0.01	0.02	0.01	0.01
C	0.21	0.45	0.63	0.77	0.48	0.19	0.17	0.83	0.49
Ga	22.20	20.70	17.70	15.20	19.8	22.9	21.1	17.2	16.2
Ge	0.80	1.00	1.10	0.90	1.00	0.80	1.20	0.90	0.90
As	<0.10	0.90	0.60	0.70	0.70	0.20	1.60	<0.10	0.80
Sb	0.13	0.33	0.08	0.18	0.07	<0.05	0.18	<0.05	<0.05
Te	0.01	0.01	0.02	0.01	<0.01	<0.01	<0.01	0.01	<0.01
In	0.04	0.03	0.02	0.01	0.016	0.005	0.011	0.007	0.006
Sn	2.10	2.20	1.50	0.90	1.60	2.40	1.90	1.60	1.80
Tl	0.03	0.02	0.02	0.03	0.02	0.03	0.03	0.03	<0.02
Bi	0.04	0.04	0.02	0.11	0.05	0.01	0.06	0.07	0.06
W	1.00	0.60	0.50	1.20	1.00	1.20	0.90	47.80	0.90
Re	0.00	0.00	0.00	0.00	0.00	0.00	0.00	0.00	0.00
Hg	<0.01	<0.01	<0.01	<0.01	<0.01	<0.01	<0.01	<0.01	<0.01
Se	<0.20	<0.20	<0.20	0.2	<0.20	<0.20	0.20	<0.20	0.20
Cu	20.00	28.00	1.00	15.00	20.00	22.00	28.00	11.00	14.00
Mo	<1.00	1.00	<1.00	<1.00	<1.00	<1.00	<1.00	<1.00	<1.00
Pb	4.00	6.00	<2.00	4.00	8.00	8.00	11.00	8.00	4.00
Zn	81.00	86.00	82.00	72.00	84.00	34.00	72.00	52.00	26.00
Au	<0.01	<0.01	<0.01	<0.01	<0.01	<0.01	<0.01	<0.01	<0.01
Ag	<0.50	<0.50	<0.50	<0.50	<0.50	<0.50	<0.50	<0.50	<0.50
Cd	<0.50	<0.50	<0.50	<0.50	<0.50	<0.50	<0.50	<0.50	<0.50

Leta Arm group (Southern zone)					Leta Arm group (Eastern zone)				
Sample name	TS23-26	TS23-27	TS23-28	TS23-29	TS23-13	TS23-14	TS23-15	TS23-16	TS23-17
Easting (UTM83-11N)	586012	586264	586417	586670	595877	595854	595565	595523	595431
Northing (UTM83-11N)	7136814	7136853	7136861	7136895	7145371	7145308	7145147	7145233	7145242
Cr_2O_3	0.00	0.00	0.00	0.00	0.02	0.02	0.02	0.01	0.03
SrO	0.02	0.01	0.01	0.01	0.02	0.03	0.03	0.02	0.02
BaO	0.05	0.04	0.03	0.04	0.05	0.03	0.03	0.02	0.04
Sr	161.50	93.40	111.50	75.40	195.00	240.00	280.00	170.00	179.5
Ba	430.00	306.00	241.00	358.00	445.00	244.00	253.00	188.00	316.00
Li	10.00	30.00	50.00	20.00	40.00	30.00	50.00	40.00	90.00
Rb	66.1	39.70	37.50	57.30	67.00	60.60	17.40	4.60	27.00
Cs	1.65	1.50	1.76	2.34	4.00	3.83	0.98	0.27	2.22
S	0.01	0.01	0.01	0.01	0.04	0.16	0.01	0.05	0.08
C	0.85	0.85	0.74	1.37	0.14	0.14	0.09	0.42	0.12
Ga	17.4	15.00	15.60	15.50	17.60	16.80	19.70	21.20	33.00
Ge	0.90	1.00	0.70	0.90	1.10	1.20	1.10	1.40	1.80
As	0.40	0.30	<0.10	0.10	17.30	21.30	27.30	43.60	>250.00
Sb	0.20	0.06	0.18	<0.05	<0.05	<0.05	<0.05	<0.05	0.08
Te	<0.01	<0.01	<0.01	<0.01	0.03	0.05	0.01	0.02	0.07
In	0.01	0.01	0.01	0.01	0.01	0.02	0.02	0.04	0.14
Sn	1.50	2.00	1.90	1.60	0.90	0.80	0.90	2.10	3.50
Tl	0.02	<0.02	0.02	0.02	0.28	0.4	0.14	0.05	0.35
Bi	0.09	0.04	0.03	0.03	0.21	0.26	0.01	0.01	0.02
W	0.70	0.70	1.00	1.90	1.10	1.00	0.50	3.90	2.20
Re	0.00	0.00	0.00	0.00	0.00	0.00	0.00	0.00	0.00
Hg	<0.01	<0.01	<0.01	<0.01	0.00	0.00	0.00	0.00	0.00
Se	<0.20	0.20	0.20	<0.20	0.40	0.20	0.20	<0.20	0.30
Cu	20.00	22.00	5.00	10.00	24.00	41.00	6.00	7.00	8.00
Mo	<1.00	1.00	<1.00	<1.00	2.00	1.00	<1.00	1.00	<1.00
Pb	8.00	4.00	5.00	6.00	12.00	14.00	14.00	2.00	7.00
Zn	50.00	88.00	67.00	54.00	73.00	75.00	112.00	193.00	398.00
Au	<0.01	<0.01	<0.01	<0.01	<0.01	<0.01	<0.01	0.01	<0.01
Ag	<0.50	<0.50	<0.50	<0.50	<0.50	<0.50	<0.50	<0.50	<0.50
Cd	<0.50	<0.50	<0.50	<0.50	<0.50	<0.50	<0.50	<0.50	<0.50
Leta Arm group (Eastern zone)									
Sample name	TS23-18	TS23-19	TS23-30	TS23-31	TS23-32	TS23-33	TS23-34	TS23-35	TS23-36
Easting (UTM83-11N)	595358	595257	591343	590731	590932	591026	591105	591233	591578
Northing (UTM83-11N)	7145268	7145154	7140280	7140159	7140305	7140285	7140357	7140331	7140500
Cr_2O_3	0.01	0.03	0.013	0.00	0.00	0.00	0.00	0.01	0.00
SrO	0.01	0.01	0.01	0.02	<0.01	0.01	0.01	0.01	0.01
BaO	0.01	0.05	<0.01	<0.01	<0.01	<0.01	0.01	0.01	0.01
Sr	106.50	77.90	44.6	140.50	54.10	89.40	64.10	105.50	75.00
Ba	50.20	403.00	11.80	39.70	45.20	39.90	78.20	96.50	54.70
Li	20.00	40.00	50.00	10.00	30.00	20.00	20.00	20.00	20.00
Rb	2.70	79.10	0.30	4.10	5.90	1.90	6.10	10.40	6.20
Cs	0.18	3.56	0.21	0.14	0.61	0.11	0.85	0.41	0.31
S	0.07	0.03	0.02	0.02	0.03	0.02	0.07	0.01	0.02
C	0.08	0.10	0.30	0.070	1.01	1.06	1.56	0.46	1.11
Ga	22.40	18.50	22.70	18.80	19.80	25.80	20.20	21.90	18.20
Ge	2.00	1.40	1.20	1.80	1.80	1.20	1.40	1.80	1.20
As	17.30	143.00	0.80	3.70	0.40	1.90	3.70	0.20	0.40
Sb	<0.05	<0.05	0.28	0.05	<0.05	<0.05	0.05	0.06	<0.05
Te	0.03	0.07	0.01	0.01	<0.01	0.01	0.02	<0.01	<0.01
In	0.04	0.03	0.079	0.01	0.067	0.072	0.091	0.054	0.074
Sn	2.50	3.10	1.20	0.60	0.50	0.90	0.80	2.20	1.60
Tl	0.03	0.64	<0.02	<0.02	0.03	<0.02	0.03	0.06	0.02
Bi	0.02	0.05	0.01	<0.01	0.01	0.01	0.01	0.03	0.02
W	1.60	1.90	1.10	0.50	1.90	10.00	1.40	328.00	1.90
Re	0.00	0.00	0.001	0.001	0.001	<0.001	0.001	0.001	<0.001
Hg	<0.005	<0.01	<0.01	<0.01	<0.01	<0.01	<0.01	<0.01	<0.01
Se	<0.20	0.30	0.20	0.30	0.30	0.40	0.40	0.30	0.2
Cu	18.00	12.00	184.00	108.00	201.00	207.00	140.00	51.00	18.00
Mo	<1.00	<1.00	<1.00	<1.00	<1.00	<1.00	<1.00	1.00	<1.00
Pb	3.00	<2.00	8.00	7.00	15.00	7.00	9.00	10.00	5.00
Zn	181.00	172.00	181.00	104.00	128.00	125.00	159.00	212.00	191.00
Au	<0.01	0.01	<0.01	<0.01	<0.01	0.01	<0.01	<0.01	<0.01
Ag	<0.50	<0.50	<0.50	<0.50	<0.50	<0.50	<0.50	<0.50	<0.50
Cd	<0.50	<0.50	<0.50	<0.50	<0.50	<0.50	<0.50	<0.50	<0.50

Leta Arm group (Eastern zone)									
Sample name	TS23-37	TS23-38	TS23-39	TS23-40	TS23-41	TS23-42	TS23-43	TS23-44	TS23-45
Easting (UTM83-11N)	591775	593165	593047	592947	592762	592654	592536	592418	593259
Northing (UTM83-11N)	7140500	7141771	7141723	7141680	7141693	7141650	7141450	7141332	7143191
Cr_2O_3	0.02	0.00	0.00	0.00	0.00	0.00	0.00	0.00	0.00
SrO	0.01	0.02	0.01	<0.01	0.03	<0.01	<0.01	0.01	0.02
BaO	0.01	0.02	0.09	0.04	0.01	0.07	0.08	0.03	0.05
Sr	81.40	158.50	60.20	30.80	219.00	20.40	32.00	84.60	133.50
Ba	79.30	148.50	773.00	360.00	73.90	590.00	713.00	261.00	424.00
Li	20.00	20.00	10.00	20.00	20.00	10.00	10.00	20.00	20.00
Rb	11.00	12.00	128.00	22.80	2.80	63.60	28.00	41.50	134.00
Cs	0.17	1.50	1.08	0.95	0.06	0.53	0.54	0.58	1.98
S	0.01	0.06	0.02	0.19	0.01	0.01	0.03	0.01	0.01
C	1.07	0.36	0.15	0.09	0.11	0.27	0.44	0.70	0.65
Ga	15.40	21.80	19.80	21.20	19.30	18.90	17.80	14.30	20.70
Ge	0.90	1.60	1.20	0.80	1.20	1.00	1.20	1.10	1.40
As	1.10	0.40	<0.10	0.40	0.60	<0.10	1.00	<0.10	<0.10
Sb	<0.05	0.09	<0.05	<0.05	0.11	<0.05	<0.05	<0.05	<0.05
Te	<0.01	0.03	<0.01	0.02	0.01	<0.01	<0.01	<0.01	0.01
In	0.01	0.02	0.03	0.04	0.02	0.03	0.03	0.07	0.02
Sn	0.90	1.10	4.10	2.70	1.10	4.00	5.20	3.40	4.50
Tl	0.05	0.05	0.08	0.09	<0.02	0.16	0.06	0.14	0.22
Bi	0.01	0.02	0.09	0.05	0.02	0.04	0.06	0.12	0.08
W	1.90	1.10	1.90	0.70	1.20	2.50	2.70	1.30	1.40
Re	0.00	0.00	0.00	0.00	0.00	0.00	0.00	0.00	0.00
Hg	<0.01	<0.01	<0.01	<0.01	<0.01	<0.01	<0.01	<0.01	<0.01
Se	0.40	0.50	<0.20	1.00	<0.20	<0.20	0.30	0.20	<0.20
Cu	57.00	190.00	18.00	19.00	60.00	7.00	29.00	7.00	9.00
Mo	<1.00	<1.00	2.00	4.00	<1.00	1.00	3.00	1.00	2.00
Pb	5.00	11.00	5.00	4.00	8.00	4.00	7.00	11.00	7.00
Zn	99.00	160.00	42.00	48.00	109.00	86.00	44.00	130.00	103.00
Au	<0.01	<0.01	<0.01	<0.01	0.01	<0.01	<0.01	<0.01	<0.01
Ag	<0.50	<0.50	<0.50	<0.50	<0.50	<0.50	<0.50	<0.50	<0.50
Cd	<0.50	<0.50	<0.50	<0.50	<0.50	<0.50	<0.50	<0.50	<0.50
Leta Arm group (Eastern zone)									
Sample name	TS23-46	TS23-47	TS23-48	TS23-49	TS23-50	TS23-51	TS23-52	TS23-53	TS23-54
Easting (UTM83-11N)	593401	593541	593634	593730	593870	593987	594097	594192	594394
Northing (UTM83-11N)	7143298	7143366	7143444	7143381	7143404	7143477	7143465	7143439	7143586
Cr_2O_3	<0.002	<0.002	0.017	<0.002	0.009	0.009	0.012	0.012	0.018
SrO	0.02	0.01	0.01	0.01	0.01	<0.01	0.02	0.01	0.02
BaO	0.03	0.01	0.01	0.05	0.02	0.02	<0.01	0.01	<0.01
Sr	137.50	90.80	107.50	58.30	99.40	25.00	173.50	36.10	179.50
Ba	233.00	45.8	68.7	423	188.5	137.5	17.6	74.8	29.30
Li	30.00	20.00	10.00	10.00	10.00	10.00	10.00	30.00	10.00
Rb	66.3	6.00	5.00	18.00	21.00	6.00	0.9	5.50	0.50
Cs	4.13	0.36	0.18	0.86	2.31	0.32	0.04	0.23	0.03
S	0.01	0.10	0.03	0.02	0.05	0.02	0.07	0.01	0.01
C	1.18	1.14	0.37	0.09	1.49	1.12	1.46	0.99	0.19
Ga	20.30	16.40	17.10	21.80	16.80	14.50	15.20	17.00	15.40
Ge	1.50	1.20	1.30	1.20	1.70	1.00	1.20	0.70	1.40
As	0.30	0.40	0.30	0.50	0.50	0.30	0.20	<0.10	0.20
Sb	<0.05	<0.05	<0.05	<0.05	<0.05	<0.05	0.06	<0.05	<0.05
Te	0.01	0.01	<0.01	<0.01	0.01	<0.01	<0.01	<0.01	<0.01
In	0.05	0.09	0.03	0.12	0.07	0.03	0.01	0.02	0.02
Sn	0.80	0.70	0.90	2.90	1.10	0.60	1.20	0.50	1.00
Tl	0.30	0.03	0.03	0.05	0.22	0.03	<0.02	0.02	<0.02
Bi	0.01	0.03	<0.01	0.03	0.02	<0.01	<0.01	<0.01	0.01
W	1.00	0.80	<0.50	0.90	1.30	<0.50	<0.50	0.80	0.70
Re	0.00	0.00	0.00	0.00	0.00	0.00	0.00	0.00	0.00
Hg	<0.01	<0.01	<0.01	<0.01	<0.01	<0.01	<0.01	<0.01	<0.01
Se	0.30	0.20	0.20	0.20	0.40	0.20	0.40	<0.20	<0.20
Cu	89.00	55.00	67.00	5.00	98.00	83.00	107.00	65.00	95.00
Mo	<1.00	<1.00	1.00	2.00	<1.00	<1.00	<1.00	<1.00	<1.00
Pb	8.00	9.00	11.00	4.00	7.00	8.00	8.00	7.00	6.00
Zn	79.00	132.00	123.00	86.00	116.00	109.00	108.00	145.00	105.00
Au	<0.01	<0.01	<0.01	<0.01	<0.01	<0.01	<0.01	<0.01	<0.01
Ag	<0.50	<0.50	<0.50	<0.50	<0.50	<0.50	<0.50	<0.50	<0.50
Cd	<0.50	<0.50	<0.50	<0.50	<0.50	<0.50	<0.50	<0.50	<0.50

Leta Arm group (Eastern zone)										
Sample name	TS23-55	TS23-56	TS23-57	TS23-58	TS23-59	TS23-60	TS23-61	TS23-62	TS23-63	TS23-64
Easting (UTM83-11N)	594537	594645	594789	594886	594993	595095	595254	595255	595253	590863
Northing (UTM83-11N)	7143517	7143649	7143677	7143613	7143646	7143702	7143756	7143877	7144025	7140691
Cr_2O_3	0.00	0.01	0.02	0.03	0.02	0.02	0.02	0.02	0.01	0.01
SrO	0.02	0.02	0.01	0.03	0.01	0.01	0.02	0.01	0.01	0.01
BaO	0.05	<0.01	<0.01	<0.01	<0.01	0.02	0.01	0.03	0.03	0.03
Sr	204.00	162.00	82.00	255.00	127.50	108.50	180.00	132.50	104.50	67.80
Ba	432.00	40.80	23.90	36.30	36.10	151.50	52.30	266.00	177.00	267.00
Li	10.00	20.00	30.00	30.00	20.00	30.00	30.00	40.00	30.00	20.00
Rb	109.50	25.50	3.00	3.80	0.70	13.00	0.8	15.7	14.20	45.00
Cs	1.22	1.71	0.46	0.16	0.05	0.32	0.04	1.04	2.18	0.93
S	<0.01	0.05	0.02	0.04	0.16	0.03	0.05	0.01	0.03	0.01
C	0.09	1.22	1.54	0.07	0.73	1.72	1.16	1.11	1.17	1.17
Ga	22.4	17.2	17.5	20.2	18.6	16.8	19.2	19.7	18.00	19.80
Ge	1.20	1.70	1.50	2.00	1.50	1.30	1.60	1.20	1.40	1.00
As	<0.10	0.40	0.20	0.20	0.10	0.10	1.10	3.20	0.10	21.00
Sb	<0.05	0.27	0.05	0.10	<0.05	0.05	0.06	<0.05	<0.05	0.12
Te	<0.01	0.01	0.01	0.01	0.01	0.01	<0.01	0.01	0.02	<0.01
In	0.027	0.042	0.029	0.021	0.023	0.052	0.021	0.08	0.03	0.03
Sn	3.40	0.80	0.60	0.70	1.00	1.00	1.20	1.40	0.90	1.70
Tl	0.17	0.10	<0.02	<0.02	<0.02	0.06	<0.02	0.08	0.07	0.03
Bi	0.09	0.05	<0.01	0.01	0.01	0.01	0.01	0.02	0.02	0.02
W	1.60	1.10	0.80	1.00	0.60	0.60	0.60	1.00	1.20	1.20
Re	0.00	0.00	0.00	0.00	0.00	0.00	0.00	0.00	0.00	0.00
Hg	<0.01	<0.01	<0.01	<0.01	<0.01	<0.01	<0.01	<0.01	<0.01	<0.01
Se	0.20	0.20	<0.20	0.30	0.60	0.40	0.30	<0.20	0.20	0.20
Cu	15.00	121.00	47.00	173.00	147.00	87.00	73.00	109.00	131.00	59.00
Mo	<1.00	<1.00	<1.00	<1.00	<1.00	<1.00	<1.00	<1.00	<1.00	<1.00
Pb	6.00	10.00	6.00	9.00	8.00	8.00	8.00	8.00	<2.00	<2.00
Zn	86.00	120.00	80.00	104.00	138.00	102.00	134.00	140.00	126.00	126.00
Au	<0.01	<0.01	<0.01	<0.01	<0.01	<0.01	<0.01	0.01	0.01	0.01
Ag	<0.50	<0.50	<0.50	<0.50	<0.50	<0.50	<0.50	<0.50	<0.50	<0.50
Cd	<0.50	<0.50	<0.50	<0.50	<0.50	<0.50	<0.50	<0.50	<0.50	<0.50

Leta Arm group (Eastern zone, 2024 samples)									
Sample name	TS24-02	TS24-03	TS24-06	TS24-08	TS24-09	TS24-10	TS24-11	TS24-12	TS24-13
Drillhole ID	GB21-16	NL21-15	NL21-08	GB21-26	GB21-26	GB21-26	GB21-26	GB21-26	GB21-26
Easting (UTM83-11N)	590493.50	593358	593093	590633.8	590633.8	590633.8	590633.80	590633.8	590633.80
Northing (UTM83-11N)	7140203	7143356	7142151	7140345	7140345	7140345	7140345	7140345	7140345
Cr2O3	0.00	0.00	0.00	0.00	0.00	0.00	0.00	0.00	0.00
SrO	0.01	0.02	0.01	0.03	0.02	0.02	0.02	0.02	0.01
BaO	0.04	0.13	0.19	0.04	0.04	0.03	0.04	0.06	0.04
Sr	14.00	58.90	65.90	170.50	67.80	97.90	80.90	72.50	50.90
Ba	373.00	1170.00	1760.00	400.00	358.00	303.00	325.00	522.00	316.00
Li	5.00	20.00	10.00	10.00	10.00	10.00	10.00	10.00	10.00
Rb	36.70	84.60	61.00	78.20	52.10	33.00	32.50	43.20	28.40
Cs	0.52	1.06	0.89	2.18	2.32	1.06	1.26	1.04	0.59
S	0.01	0.01	0.06	0.06	0.03	0.01	0.10	0.68	0.05
C	0.07	0.55	0.03	1.80	0.42	0.87	0.78	0.63	0.32
Ga	20.90	22.40	4.90	20.70	18.40	17.30	17.90	21.10	18.60
Ge	1.00	1.20	0.70	1.30	1.20	1.20	1.30	1.30	1.30
As	0.70	0.20	0.20	0.40	0.50	0.30	3.70	>250.00	1.50
Sb	0.03	0.03	0.03	0.03	0.03	0.03	0.03	0.15	0.03
Te	0.02	0.01	0.05	0.02	0.01	0.01	0.01	0.09	0.01
In	0.00	0.04	0.00	0.10	0.02	0.02	0.03	0.03	0.02
Sn	3.20	5.10	6.00	4.70	3.50	3.50	2.30	4.80	4.20
Tl	0.02	0.13	0.04	0.11	0.15	0.06	0.08	0.03	0.02
Bi	0.03	0.13	0.01	0.15	0.06	0.02	0.05	0.21	0.03
W	1.30	1.70	1.20	2.00	1.10	0.70	1.00	3.00	1.30
Re	0.00	0.00	0.00	0.00	0.00	0.00	0.00	0.00	0.00
Hg	0.00	0.00	0.00	0.01	0.00	0.00	0.00	0.00	0.00
Se	0.10	0.20	0.10	0.10	0.10	0.10	0.30	0.50	0.20
Cu	3.00	35.00	3.00	15.00	5.00	8.00	6.00	27.00	2.00
Mo	0.50	3.00	2.00	1.00	1.00	1.00	0.50	1.00	0.50
Pb	4.00	12.00	5.00	9.00	4.00	5.00	4.00	4.00	4.00
Zn	15.00	202.00	15.00	416.00	58.00	49.00	76.00	118.00	46.00
Au	0.01	0.01	0.01	0.01	0.01	0.01	0.01	0.15	0.05
Ag	0.25	0.25	0.25	0.25	0.25	0.25	0.25	0.25	0.25
Cd	0.25	0.50	0.25	1.90	0.25	0.25	0.25	0.25	0.25

Leta Arm group (Western zone)									
Sample name	TS23-65	TS23-66	TS23-67	TS23-68	TS23-69	TS23-70	TS23-71	TS23-72	TS23-73
Easting (UTM83-11N)	585235	585317	585454	585539	585691	585884	585970	586145	586346
Northing (UTM83-11N)	7146844	7146751	7146678	7146558	7146443	7146431	7146537	7146485	7146528
Cr_2O_3	0.03	0.00	0.03	0.03	0.04	0.03	0.04	0.02	0.04
SrO	0.01	0.01	0.01	0.03	0.01	0.02	0.01	0.02	0.02
BaO	0.02	0.03	0.05	0.01	0.01	<0.01	<0.01	<0.01	<0.01
Sr	116.00	104.00	98.80	270.00	92.00	168.50	106.00	192.00	172.00
Ba	165.00	300.00	484.00	92.60	88.90	20.90	32.90	41.90	40.40
Li	50.00	40.00	30.00	20.00	30.00	20.00	20.00	20.00	10.00
Rb	14.40	25.00	19.60	8.20	10.80	0.80	1.10	3.00	2.20
Cs	1.06	2.22	1.04	0.88	0.79	0.11	0.13	0.13	0.22
S	0.03	0.01	0.04	0.05	0.11	0.02	0.01	0.16	0.07
C	2.50	1.97	1.36	0.17	1.07	1.70	1.88	0.34	0.39
Ga	17.30	18.00	18.20	15.80	19.80	15.20	18.00	18.60	18.00
Ge	1.20	1.40	1.60	1.00	1.50	1.40	1.10	1.90	1.60
As	59.00	41.90	10.70	17.50	7.60	21.10	14.40	20.00	0.70
Sb	0.17	0.08	0.14	0.17	0.34	0.17	0.14	0.26	0.07
Te	0.03	<0.01	0.01	0.01	0.01	0.01	0.01	0.02	<0.01
In	0.07	0.05	0.04	0.03	0.04	0.01	0.01	0.01	0.01
Sn	0.50	1.50	0.70	0.80	0.60	0.50	<0.5	0.70	0.60
Tl	0.02	0.03	<0.02	<0.02	<0.02	<0.02	<0.02	<0.02	0.02
Bi	0.01	0.01	0.01	<0.01	0.01	<0.01	0.01	0.01	<0.01
W	1.20	2.80	0.60	<0.5	0.60	0.60	0.50	1.20	<0.5
Re	0.00	0.00	0.00	0.00	0.00	0.00	0.00	0.00	0.00
Hg	<0.01	<0.01	<0.01	<0.01	<0.01	0.01	<0.01	<0.01	<0.01
Se	0.40	0.20	0.30	0.20	0.30	0.20	0.20	0.50	0.30
Cu	217.00	46.00	77.00	109.00	51.00	118.00	88.00	116.00	109.00
Mo	<1.00	<1.00	<1.00	<1.00	<1.00	<1.00	<1.00	<1.00	<1.00
Pb	<2.00	<2.00	<2.00	<2.00	<2.00	2.00	<2.00	<2.00	<2.00
Zn	100.00	116.00	120.00	66.00	114.00	85.00	97.00	114.00	105.00
Au	0.01	0.01	<0.01	0.01	0.01	<0.01	<0.01	<0.01	<0.01
Ag	<0.50	<0.50	<0.50	<0.50	<0.50	<0.50	<0.50	<0.50	<0.50
Cd	<0.50	<0.50	<0.50	<0.50	<0.50	<0.50	<0.50	<0.50	<0.50
Leta Arm group (Western zone)									
Sample name	TS23-74	TS23-75	TS23-76	TS23-77	TS23-78	TS23-79	TS23-80	TS23-81	TS23-82
Easting (UTM83-11N)	586494	586596	586822	587108	587210	587310	587451	587556	587643
Northing (UTM83-11N)	7146475	7146346	7145150	7145306	7145322	7145298	7145215	7145165	7145034
Cr_2O_3	0.03	0.02	0.04	0.04	0.00	0.02	0.00	0.02	0.00
SrO	0.03	0.01	0.01	0.01	0.01	0.01	0.01	0.02	0.04
BaO	<0.01	<0.01	<0.01	<0.01	<0.01	<0.01	<0.01	<0.01	0.03
Sr	234.00	77.30	118.00	131.50	61.70	72.60	67.40	179.50	341.00
Ba	10.40	6.00	39.30	20.80	18.50	19.70	11.80	24.20	249.00
Li	10.00	20.00	20.00	10.00	20.00	30.00	10.00	10.00	10.00
Rb	0.20	<0.2	2.10	1.40	2.90	0.20	0.40	2.40	25.10
Cs	0.04	0.11	0.17	0.09	0.27	0.07	0.09	0.16	1.01
S	0.18	0.02	0.09	0.02	0.02	0.13	0.01	0.05	0.01
C	1.17	0.88	1.02	0.15	1.36	0.61	0.37	0.20	0.40
Ga	19.10	15.10	18.30	16.60	21.00	16.50	18.20	16.80	18.20
Ge	1.70	1.60	1.30	1.70	1.60	1.20	1.00	1.60	1.30
As	9.50	4.50	14.90	39.00	0.50	1.10	1.00	39.70	4.10
Sb	1.17	0.33	0.17	0.39	<0.05	0.09	0.13	0.79	0.31
Te	0.01	0.02	0.01	0.01	<0.01	0.03	<0.01	0.02	<0.01
In	0.01	0.04	0.02	0.01	0.04	0.02	0.03	0.01	0.01
Sn	0.60	0.50	0.60	0.60	1.10	0.50	1.30	0.60	1.20
Tl	<0.02	<0.02	0.03	<0.02	<0.02	<0.02	<0.02	<0.02	0.07
Bi	0.01	0.01	0.01	0.01	0.01	0.05	0.01	<0.01	0.03
W	<0.5	0.60	<0.5	<0.5	0.50	<0.5	0.60	1.00	0.70
Re	0.00	0.00	0.00	0.00	0.00	0.00	0.00	0.00	0.00
Hg	<0.01	<0.01	0.01	<0.01	<0.01	0.01	<0.01	<0.01	<0.01
Se	0.80	<0.20	0.50	<0.20	<0.20	0.50	<0.20	0.40	0.20
Cu	126.00	115.00	222.00	102.00	109.00	119.00	1.00	128.00	39.00
Mo	<1.00	<1.00	<1.00	<1.00	<1.00	<1.00	<1.00	<1.00	1.00
Pb	<2.00	<2.00	<2.00	<2.00	<2.00	<2.00	<2.00	<2.00	7.00
Zn	84.00	140.00	107.00	114.00	154.00	147.00	89.00	108.00	65.00
Au	<0.01	0.01	<0.01	<0.01	<0.01	<0.01	<0.01	0.01	<0.01
Ag	<0.50	<0.50	<0.50	<0.50	<0.50	<0.50	<0.50	<0.50	<0.50
Cd	<0.50	<0.50	<0.50	<0.50	<0.50	<0.50	<0.50	<0.50	<0.50

Leta Arm group (Western zone)							
Sample name	TS23-83	TS23-84	TS23-85	TS23-86	TS23-87	TS23-88	TS23-89
Easting (UTM83-11N)	587735	587867	587993	588102	588245	588386	588549
Northing (UTM83-11N)	7145904	7145788	7145802	7145670	7145597	7145507	7145508
Cr_2O_3	0.00	0.04	0.01	0.00	0.01	0.01	0.02
SrO	0.01	0.03	0.01	0.01	<0.01	0.02	0.03
BaO	0.03	<0.01	<0.01	0.05	0.05	0.02	0.05
Sr	115.00	219.00	120.00	109.50	49.10	152.00	280.00
Ba	300.00	19.70	27.40	433.00	443.00	216.00	491.00
Li	10.00	10.00	20.00	10.00	10.00	10.00	20.00
Rb	26.50	1.70	1.40	83.50	93.70	21.90	47.50
Cs	1.78	0.17	0.35	2.25	2.16	0.62	1.18
S	0.01	0.04	0.11	0.01	0.01	0.01	0.01
C	0.14	0.23	0.43	0.10	0.86	0.56	0.56
Ga	20.20	15.00	19.50	22.80	18.60	18.30	22.20
Ge	1.20	1.40	1.40	0.90	0.80	1.00	1.10
As	3.20	15.60	13.40	0.30	0.40	2.60	0.70
Sb	0.16	0.91	0.35	0.13	<0.05	0.09	0.26
Te	<0.01	0.01	0.02	<0.01	<0.01	<0.01	<0.01
In	0.01	0.01	0.02	0.01	0.01	0.02	0.01
Sn	1.60	<0.5	0.90	1.90	1.40	1.10	1.40
Tl	0.13	<0.02	<0.02	0.03	0.03	<0.02	<0.02
Bi	0.02	0.01	0.01	0.02	0.03	0.02	0.04
W	0.60	0.90	0.90	1.10	1.00	2.00	1.20
Re	0.00	0.00	0.00	0.00	0.00	0.00	0.00
Hg	<0.01	<0.01	<0.01	<0.01	<0.01	<0.01	<0.01
Se	<0.20	0.20	0.50	<0.20	<0.20	<0.20	<0.20
Cu	25.00	77.00	148.00	19.00	2.00	8.00	53.00
Mo	1.00	<1.00	<1.00	<1.00	<1.00	<1.00	<1.00
Pb	8.00	<2.00	2.00	4.00	3.00	3.00	8.00
Zn	107.00	66.00	133.00	70.00	51.00	71.00	82.00
Au	<0.01	<0.01	0.01	<0.01	<0.01	<0.01	<0.01
Ag	<0.50	<0.50	<0.50	<0.50	<0.50	<0.50	<0.50
Cd	<0.50	<0.50	<0.50	<0.50	<0.50	<0.50	<0.50
Leta Arm group (Western zone)							
Sample name	TS23-90	TS23-91	TS23-92	TS23-93	TS23-94	TS23-95	TS23-96
Easting (UTM83-11N)	588828	588942	589070	589364	589551	589695	589806
Northing (UTM83-11N)	7145793	7145782	7145727	7145726	7145740	7145654	7145621
Cr_2O_3	0.05	0.01	0.03	0.04	0.06	0.02	0.02
SrO	0.01	0.01	0.02	0.01	0.02	0.01	0.02
BaO	0.01	0.02	0.03	0.02	0.03	0.02	0.03
Sr	130.00	128.50	219.00	70.40	207.00	126.50	179.00
Ba	127.50	137.00	310.00	171.50	241.00	180.50	274.00
Li	10.00	10.00	20.00	30.00	30.00	30.00	40.00
Rb	9.90	13.90	22.30	26.20	31.70	28.30	34.40
Cs	0.47	2.32	0.59	0.78	1.06	1.68	1.44
S	0.03	0.11	0.01	0.01	0.01	0.01	0.01
C	0.13	0.16	0.95	1.18	1.39	0.66	2.14
Ga	17.60	22.00	17.00	17.60	16.60	17.00	11.40
Ge	1.00	1.50	0.70	0.90	1.10	1.00	1.00
As	1.30	0.70	0.10	1.10	0.40	0.50	9.60
Sb	0.13	0.20	0.10	0.05	0.12	0.09	<0.05
Te	<0.01	0.01	<0.01	<0.01	<0.01	<0.01	<0.01
In	0.01	0.02	0.02	0.03	0.02	0.02	0.01
Sn	1.30	0.90	1.20	1.60	1.50	1.00	0.90
Tl	0.05	0.04	<0.02	<0.02	0.05	0.05	<0.02
Bi	0.02	0.01	0.02	0.02	0.02	0.02	0.03
W	0.80	<0.5	0.70	0.90	1.00	0.60	0.70
Re	0.00	0.00	0.00	0.00	0.00	0.00	0.00
Hg	0.01	0.01	0.01	0.01	0.01	0.01	0.01
Se	0.20	0.60	<0.20	<0.20	<0.20	<0.20	<0.20
Cu	51.00	91.00	35.00	43.00	1.00	47.00	41.00
Mo	<1.00	<1.00	<1.00	<1.00	<1.00	<1.00	<1.00
Pb	3.00	<2.00	<2.00	<2.00	<2.00	4.00	4.00
Zn	98.00	139.00	61.00	112.00	63.00	79.00	61.00
Au	<0.01	<0.01	<0.01	0.02	<0.01	<0.01	0.01
Ag	<0.50	<0.50	<0.50	<0.50	<0.50	<0.50	<0.50
Cd	<0.50	<0.50	<0.50	<0.50	<0.50	<0.50	<0.50

Appendix III: Electron Probe Microanalyzer data for amphiboles

Sample TS23-08

All tables include formula assignments (A, B, C, T, O and W site). The amount of H_2O total is (100 - analytical total).

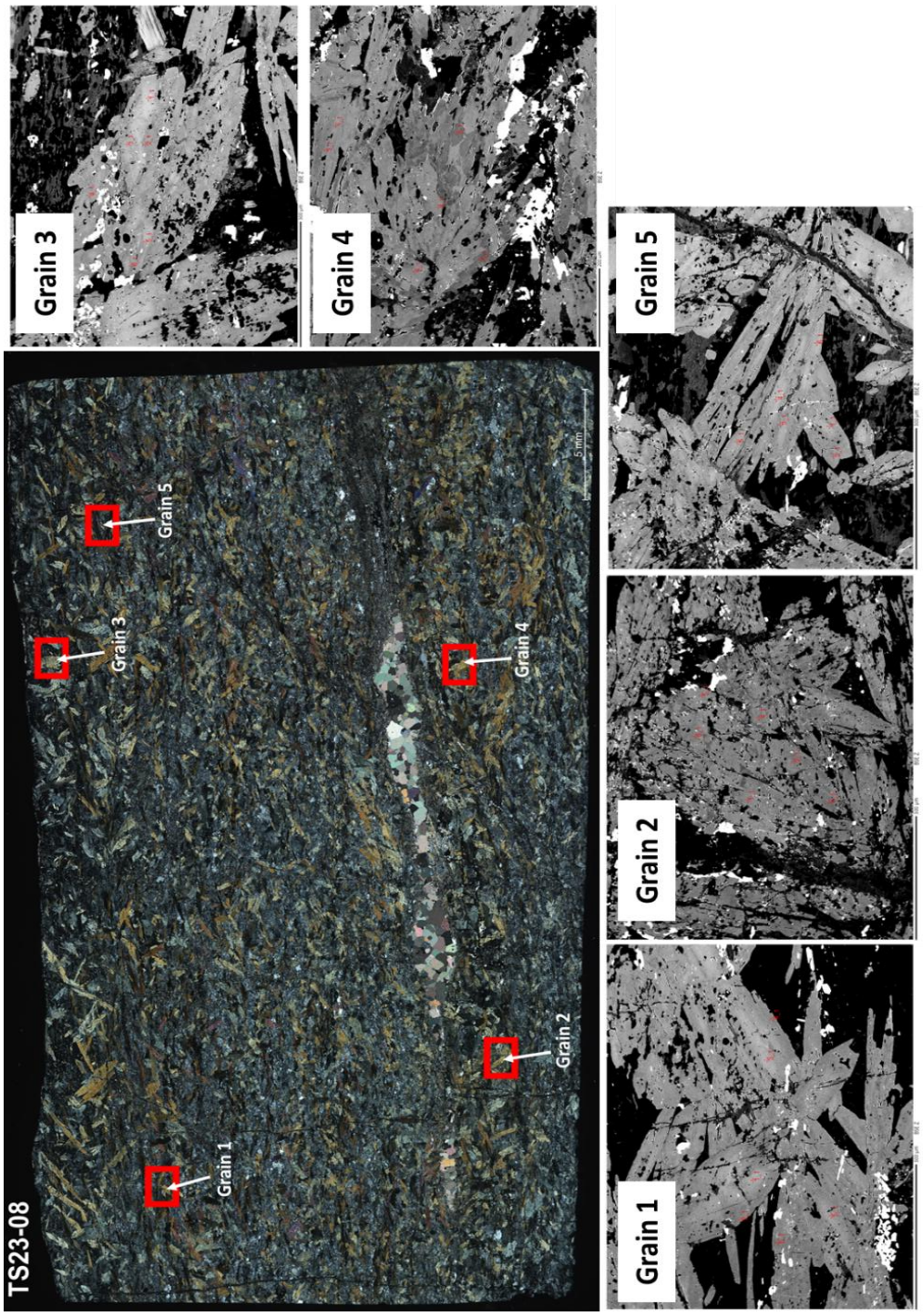

		Grain1-1	Grain1-2	Grain1-3	Grain1-4	Grain1-5	Grain1-6
Weight%	F	0.09	0.10	0.00	0.08	0.09	0.04
	Na	0.90	1.01	0.91	1.04	0.90	0.99
	Mg	4.24	5.35	4.77	5.45	4.63	5.28
	Al	7.89	7.83	7.02	7.90	7.75	7.57
	Si	19.65	20.16	20.05	20.01	19.74	20.25
	K	0.29	0.19	0.25	0.21	0.25	0.19
	Ti	0.22	0.26	0.20	0.23	0.21	0.29
	Cl	0.00	0.01	0.01	0.00	0.00	0.01
	Ca	8.41	8.12	8.29	8.23	8.32	8.16
	Fe	15.09	13.01	14.96	12.64	14.32	13.19
	Mn	0.31	0.27	0.30	0.27	0.35	0.29
	O	42.64	43.40	42.92	43.61	43.11	43.43
	H	0.27	0.29	0.32	0.34	0.33	0.31
	Total	100.00	100.00	100.00	100.00	100.00	100.00
Oxide	F	0.09	0.10	0.00	0.08	0.09	0.04
	Na_2O	1.21	1.36	1.23	1.40	1.21	1.34
	MgO	7.03	8.88	7.90	9.04	7.68	8.75
	Al_2O_3	14.91	14.80	13.27	14.92	14.65	14.31
	SiO_2	42.04	43.13	42.90	42.80	42.23	43.32
	K_2O	0.35	0.23	0.30	0.25	0.31	0.23
	TiO_2	0.37	0.43	0.34	0.38	0.35	0.48
	Cl	0.00	0.01	0.01	0.00	0.00	0.01
	CaO	11.76	11.36	11.60	11.51	11.64	11.42
	FeO	19.41	16.73	19.24	16.26	18.42	16.97
	MnO	0.40	0.34	0.39	0.35	0.45	0.37
	H_2O	2.43	2.62	2.82	2.99	2.98	2.76
	Total	100.00	100.00	100.00	100.00	100.00	100.00
	X	16362.00	16227.00	16777.00	16916.00	16240.00	16148.00
	Y	32906.00	32942.00	32863.00	32844.00	32666.00	32830.00
	Z	-20.00	-20.00	-21.00	-21.00	-19.00	-19.00
Formula Assignments	**T** (ideally 8 apfu)						
	Si	6.31	6.43	6.44	6.36	6.34	6.43
	Al	1.69	1.57	1.56	1.64	1.66	1.57
	Fe^{3+}						
	T subtotal	8.00	8.00	8.00	8.00	8.00	8.00
	C (ideally 5 apfu)						
	Ti	0.04	0.05	0.04	0.04	0.04	0.05
	Al	0.95	1.03	0.79	0.97	0.93	0.94
	Fe^{3+}	0.36		0.42	0.32	0.38	0.29
	Mn^{2+}						
	Fe^{2+}	2.08	1.94	1.99	1.67	1.94	1.78
	Mg	1.57	1.97	1.77	2.00	1.72	1.94
	C subtotal	5.00	5.00	5.00	5.00	5.00	5.00
	B (ideally 2 apfu)						
	Mn^{2+}	0.05	0.04	0.05	0.04	0.06	0.05
	Fe^{2+}		0.14	0.01	0.03	0.00	0.04
	Ca	1.89	1.82	1.87	1.83	1.87	1.82
	Na	0.06		0.07	0.09	0.07	0.10
	B subtotal	2.00	2.00	2.00	2.00	2.00	2.00
	A (from 0 to 1 apfu)						
	Ca		0.00				
	Na	0.29	0.39	0.29	0.31	0.28	0.29
	K	0.07	0.04	0.06	0.05	0.06	0.04
	A subtotal	0.36	0.44	0.34	0.36	0.34	0.33
	O (non-W)	22.00	22.00	22.00	22.00	22.00	22.00
	W (ideally 2 apfu)						
	OH	1.96	1.95	2.00	1.96	1.96	1.98
	F	0.04	0.05		0.04	0.04	0.02
	Cl		0.00	0.00			0.00
	W subtotal	2.00	2.00	2.00	2.00	2.00	2.00
	Sum **T,C,B,A**	15.36	15.44	15.34	15.36	15.34	15.33

		Grain2-1	Grain2-2	Grain2-3	Grain2-4	Grain2-5	Grain2-6
Weight%	F	0.03	0.04	0.03	0.05	0.07	0.00
	Na	0.59	0.72	0.83	0.81	0.82	0.75
	Mg	5.32	5.00	4.99	4.63	4.37	5.22
	Al	5.39	6.17	7.15	7.09	7.35	6.12
	Si	21.36	20.69	20.27	20.05	19.76	20.86
	K	0.17	0.19	0.21	0.20	0.26	0.18
	Ti	0.22	0.23	0.22	0.20	0.25	0.20
	Cl	0.00	0.00	0.01	0.00	0.00	0.00
	Ca	8.44	8.44	8.38	8.39	8.39	8.39
	Fe	14.53	14.62	13.95	14.74	14.83	14.32
	Mn	0.45	0.41	0.45	0.45	0.45	0.45
	O	43.18	43.16	43.19	43.04	43.07	43.19
	H	0.31	0.34	0.31	0.34	0.37	0.32
	Total	100.00	100.00	100.00	100.00	100.00	100.00
Oxide	F	0.03	0.04	0.03	0.05	0.07	0.00
	Na_2O	0.80	0.97	1.12	1.09	1.11	1.01
	MgO	8.82	8.29	8.27	7.68	7.25	8.65
	Al_2O_3	10.19	11.65	13.51	13.39	13.89	11.56
	SiO_2	45.70	44.27	43.37	42.88	42.27	44.62
	K_2O	0.21	0.22	0.25	0.24	0.31	0.22
	TiO_2	0.37	0.38	0.38	0.33	0.42	0.33
	Cl	0.00	0.00	0.01	0.00	0.00	0.00
	CaO	11.81	11.81	11.72	11.75	11.74	11.74
	FeO	18.70	18.81	17.95	18.97	19.08	18.42
	MnO	0.59	0.53	0.58	0.58	0.58	0.58
	H_2O	2.80	3.02	2.81	3.02	3.28	2.85
	Total	100.00	100.00	100.00	100.00	100.00	100.00
	X	12608.00	12763.00	12598.00	12940.00	13031.00	12865.00
	Y	19796.00	19631.00	19502.00	19755.00	19962.00	19983.00
	Z	9.00	9.00	9.00	8.00	7.00	8.00
Formula Assignments	**T** (ideally 8 apfu)						
	Si	6.83	6.65	6.48	6.45	6.40	6.67
	Al	1.17	1.35	1.52	1.55	1.60	1.33
	Fe^{3+}						
	T subtotal	8.00	8.00	8.00	8.00	8.00	8.00
	C (ideally 5 apfu)						
	Ti	0.04	0.04	0.04	0.04	0.05	0.04
	Al	0.63	0.72	0.86	0.83	0.87	0.71
	Fe^{3+}	0.30	0.33	0.34	0.39	0.35	0.33
	Mn^{2+}	0.02	0.02	0.02	0.03	0.03	0.02
	Fe^{2+}	2.04	2.04	1.90	1.99	2.06	1.97
	Mg	1.97	1.86	1.84	1.72	1.64	1.93
	C subtotal	5.00	5.00	5.00	5.00	5.00	5.00
	B (ideally 2 apfu)						
	Mn^{2+}	0.05	0.05	0.06	0.05	0.05	0.06
	Fe^{2+}						
	Ca	1.89	1.90	1.88	1.90	1.90	1.88
	Na	0.06	0.05	0.07	0.06	0.05	0.06
	B subtotal	2.00	2.00	2.00	2.00	2.00	2.00
	A (from 0 to 1 apfu)						
	Ca						
	Na	0.17	0.23	0.26	0.26	0.27	0.23
	K	0.04	0.04	0.05	0.05	0.06	0.04
	A subtotal	0.21	0.27	0.31	0.31	0.33	0.27
	O (non-W)	22.00	22.00	22.00	22.00	22.00	22.00
	W (ideally 2 apfu)						
	OH	1.99	1.98	1.98	1.98	1.97	2.00
	F	0.01	0.02	0.01	0.02	0.03	
	Cl			0.00			
	W subtotal	2.00	2.00	2.00	2.00	2.00	2.00
	Sum **T,C,B,A**	15.21	15.27	15.31	15.31	15.33	15.27

		Grain3-1	Grain3-2	Grain3-3	Grain3-4	Grain3-5	Grain3-6
Weight%	F	0.03	0.08	0.00	0.00	0.02	0.09
	Na	0.93	0.61	0.89	0.93	0.93	0.92
	Mg	4.42	7.03	4.91	4.93	5.65	5.26
	Al	7.55	4.25	7.71	7.80	6.80	6.88
	Si	19.46	22.64	20.12	20.13	20.52	20.42
	K	0.29	0.12	0.25	0.22	0.22	0.23
	Ti	0.20	0.14	0.18	0.16	0.31	0.23
	Cl	0.00	0.00	0.01	0.00	0.01	0.00
	Ca	8.41	8.31	8.32	8.26	8.21	8.31
	Fe	14.91	12.66	13.77	13.57	13.23	14.06
	Mn	0.29	0.26	0.26	0.28	0.24	0.27
	O	43.10	43.63	43.27	43.40	43.53	43.04
	H	0.39	0.26	0.31	0.32	0.34	0.28
	Total	100.00	100.00	100.00	100.00	100.00	100.00
Oxide	F	0.03	0.08	0.00	0.00	0.02	0.09
	Na_2O	1.26	0.82	1.20	1.25	1.25	1.23
	MgO	7.33	11.66	8.14	8.17	9.37	8.73
	Al_2O_3	14.27	8.03	14.57	14.74	12.84	13.00
	SiO_2	41.63	48.42	43.04	43.07	43.89	43.68
	K_2O	0.36	0.14	0.30	0.27	0.27	0.28
	TiO_2	0.34	0.23	0.30	0.26	0.51	0.38
	Cl	0.00	0.00	0.01	0.00	0.01	0.00
	CaO	11.77	11.63	11.65	11.55	11.49	11.63
	FeO	19.18	16.29	17.72	17.46	17.01	18.09
	MnO	0.38	0.34	0.33	0.36	0.32	0.34
	H_2O	3.46	2.34	2.74	2.86	3.01	2.53
	Total	100.00	100.00	100.00	100.00	100.00	100.00
	X	-7587.00	-7768.00	-7769.00	-7971.00	-8156.00	-8252.00
	Y	36144.00	36155.00	36219.00	36354.00	36154.00	36204.00
	Z	24.00	25.00	25.00	25.00	26.00	26.00
Formula Assignments	**T** (ideally 8 apfu)						
	Si	6.31	7.09	6.41	6.42	6.53	6.51
	Al	1.69	0.91	1.59	1.58	1.47	1.49
	Fe^{3+}						
	T subtotal	8.00	8.00	8.00	8.00	8.00	8.00
	C (ideally 5 apfu)						
	Ti	0.04	0.03	0.03	0.03	0.06	0.04
	Al	0.86	0.48	0.97	1.01	0.79	0.79
	Fe^{3+}	0.40	0.31	0.29	0.27	0.34	0.36
	Mn^{2+}	0.01					
	Fe^{2+}	2.03	1.64	1.89	1.88	1.74	1.87
	Mg	1.66	2.55	1.81	1.82	2.08	1.94
	C subtotal	5.00	5.00	5.00	5.00	5.00	5.00
	B (ideally 2 apfu)						
	Mn^{2+}	0.04	0.04	0.04	0.05	0.04	0.04
	Fe^{2+}		0.04	0.02	0.03	0.04	0.02
	Ca	1.91	1.82	1.86	1.84	1.83	1.86
	Na	0.05	0.09	0.08	0.08	0.09	0.08
	B subtotal	2.00	2.00	2.00	2.00	2.00	2.00
	A (from 0 to 1 apfu)						
	Ca						
	Na	0.32	0.14	0.27	0.28	0.27	0.28
	K	0.07	0.03	0.06	0.05	0.05	0.05
	A subtotal	0.39	0.17	0.33	0.33	0.32	0.33
	O (non-W)	22.00	22.00	22.00	22.00	22.00	22.00
	W (ideally 2 apfu)						
	OH	1.99	1.96	2.00	2.00	1.99	1.96
	F	0.01	0.04			0.01	0.04
	Cl			0.00		0.00	
	W subtotal	2.00	2.00	2.00	2.00	2.00	2.00
	Sum **T,C,B,A**	15.39	15.16	15.33	15.33	15.32	15.33

		Grain4-1	Grain4-2	Grain4-3	Grain4-4	Grain4-5	Grain4-6
Weight%	F	0.11	0.14	0.05	0.09	0.00	0.00
	Na	0.84	0.34	0.83	0.84	0.31	0.79
	Mg	4.87	6.58	5.00	4.16	6.79	4.72
	Al	6.98	2.99	6.98	7.13	2.84	6.39
	Si	20.18	23.09	20.29	19.77	23.16	20.19
	K	0.22	0.05	0.22	0.24	0.06	0.21
	Ti	0.20	0.12	0.20	0.24	0.13	0.23
	Cl	0.03	0.00	0.00	0.00	0.01	0.00
	Ca	8.26	8.60	8.37	8.43	8.61	8.42
	Fe	14.64	14.12	14.31	15.56	13.73	15.16
	Mn	0.42	0.44	0.36	0.43	0.41	0.46
	O	42.94	43.25	43.08	42.76	43.62	43.06
	H	0.31	0.27	0.31	0.34	0.32	0.37
	Total	100.00	100.00	100.00	100.00	100.00	100.00
Oxide	F	0.11	0.14	0.05	0.09	0.00	0.00
	Na_2O	1.14	0.46	1.12	1.14	0.42	1.07
	MgO	8.08	10.90	8.30	6.89	11.26	7.83
	Al_2O_3	13.18	5.66	13.18	13.47	5.36	12.07
	SiO_2	43.16	49.40	43.41	42.29	49.56	43.19
	K_2O	0.27	0.06	0.27	0.29	0.08	0.26
	TiO_2	0.34	0.20	0.33	0.40	0.22	0.38
	Cl	0.03	0.00	0.00	0.00	0.01	0.00
	CaO	11.55	12.04	11.72	11.80	12.05	11.78
	FeO	18.83	18.17	18.40	20.02	17.66	19.50
	MnO	0.54	0.56	0.47	0.56	0.53	0.59
	H_2O	2.76	2.40	2.75	3.04	2.86	3.32
	Total	100.00	100.00	100.00	100.00	100.00	100.00
	X	-6786.00	-6806.00	-6850.00	-6993.00	-7125.00	-7156.00
	Y	22195.00	21921.00	22218.00	21964.00	21868.00	22017.00
	Z	48.00	48.00	48.00	49.00	49.00	49.00
Formula Assignments	**T** (ideally 8 apfu)						
	Si	6.47	7.31	6.49	6.42	7.34	6.54
	Al	1.53	0.69	1.51	1.59	0.66	1.46
	Fe^{3+}						
	T subtotal	8.00	8.00	8.00	8.00	8.00	8.00
	C (ideally 5 apfu)						
	Ti	0.04	0.02	0.04	0.05	0.03	0.04
	Al	0.80	0.30	0.81	0.82	0.28	0.69
	Fe^{3+}	0.43	0.30	0.38	0.37	0.29	0.42
	Mn^{2+}	0.00	0.03	0.00	0.03	0.03	0.03
	Fe^{2+}	1.93	1.95	1.92	2.17	1.90	2.05
	Mg	1.81	2.40	1.85	1.56	2.49	1.77
	C subtotal	5.00	5.00	5.00	5.00	5.00	5.00
	B (ideally 2 apfu)						
	Mn^{2+}	0.07	0.04	0.06	0.04	0.04	0.04
	Fe^{2+}						
	Ca	1.86	1.91	1.88	1.92	1.91	1.91
	Na	0.08	0.05	0.07	0.04	0.05	0.05
	B subtotal	2.00	2.00	2.00	2.00	2.00	2.00
	A (from 0 to 1 apfu)						
	Ca						
	Na	0.25	0.08	0.26	0.29	0.07	0.27
	K	0.05	0.01	0.05	0.06	0.02	0.05
	A subtotal	0.31	0.09	0.31	0.35	0.09	0.32
	O (non-W)	22.00	22.00	22.00	22.00	22.00	22.00
	W (ideally 2 apfu)						
	OH	1.94	1.93	1.98	1.96	2.00	2.00
	F	0.05	0.07	0.02	0.04		
	Cl	0.01				0.00	
	W subtotal	2.00	2.00	2.00	2.00	2.00	2.00
	Sum **T,C,B,A**	15.31	15.09	15.31	15.35	15.09	15.32

		Grain5-1	Grain5-2	Grain5-3	Grain5-4	Grain5-5	Grain5-6
Weight%	F	0.02	0.04	0.02	0.00	0.11	0.00
	Na	0.85	0.92	0.87	0.77	0.84	0.80
	Mg	5.16	5.16	6.03	5.52	5.00	5.34
	Al	7.11	7.45	6.44	5.63	7.46	6.55
	Si	20.30	20.30	21.02	20.87	20.06	20.45
	K	0.22	0.23	0.17	0.17	0.23	0.20
	Ti	0.19	0.18	0.20	0.21	0.13	0.23
	Cl	0.00	0.00	0.00	0.00	0.00	0.00
	Ca	8.31	8.34	8.34	8.30	8.29	8.39
	Fe	14.09	13.26	12.66	14.65	13.79	14.03
	Mn	0.24	0.23	0.25	0.36	0.32	0.26
	O	43.19	43.53	43.69	43.19	43.41	43.38
	H	0.31	0.34	0.32	0.34	0.36	0.36
	Total	100.00	100.00	100.00	100.00	100.00	100.00
Oxide	F	0.02	0.04	0.02	0.00	0.11	0.00
	Na_2O	1.15	1.24	1.17	1.04	1.14	1.08
	MgO	8.55	8.56	10.00	9.15	8.29	8.85
	Al_2O_3	13.44	14.07	12.17	10.65	14.09	12.38
	SiO_2	43.43	43.43	44.96	44.66	42.91	43.76
	K_2O	0.27	0.28	0.21	0.20	0.28	0.25
	TiO_2	0.32	0.30	0.33	0.35	0.22	0.38
	Cl	0.00	0.00	0.00	0.00	0.00	0.00
	CaO	11.63	11.67	11.67	11.61	11.60	11.74
	FeO	18.13	17.06	16.28	18.85	17.75	18.04
	MnO	0.31	0.30	0.33	0.46	0.41	0.34
	H_2O	2.75	3.02	2.87	3.05	3.21	3.17
	Total	100.00	100.00	100.00	100.00	100.00	100.00
	X	-15122.00	-15230.00	-15118.00	-15029.00	-15178.00	-14832.00
	Y	35382.00	35368.00	35535.00	35548.00	35672.00	35422.00
	Z	47.00	47.00	48.00	46.00	47.00	47.00
Formula Assignments	**T** (ideally 8 apfu)						
	Si	6.47	6.48		6.71	6.56	6.48
	Al	1.53	1.52		1.29	1.44	1.52
	Fe^{3+}						
	T subtotal	8.00	8.00		8.00	8.00	8.00
	C (ideally 5 apfu)						
	Ti	0.04	0.03		0.04	0.02	0.04
	Al	0.83	0.96		0.58	1.00	0.69
	Fe^{3+}	0.39	0.22		0.45	0.24	0.49
	Mn^{2+}						
	Fe^{2+}	1.84	1.88		1.90	1.93	1.79
	Mg	1.90	1.91		2.04	1.82	1.99
	C subtotal	5.00	5.00		5.00	5.00	5.00
	B (ideally 2 apfu)						
	Mn^{2+}	0.04	0.04		0.06	0.05	0.04
	Fe^{2+}	0.03	0.03		0.01	0.02	0.00
	Ca	1.86	1.87		1.86	1.83	1.90
	Na	0.08	0.07		0.08	0.11	0.05
	B subtotal	2.00	2.00		2.00	2.00	2.00
	A (from 0 to 1 apfu)						
	Ca						
	Na	0.26	0.29		0.22	0.22	0.26
	K	0.05	0.05		0.04	0.05	0.05
	A subtotal	0.31	0.34		0.26	0.27	0.31
	O (non-W)	22.00	22.00		22.00	22.00	22.00
	W (ideally 2 apfu)						
	OH	1.99	1.98		2.00	1.95	2.00
	F	0.01	0.02			0.05	
	Cl						
	W subtotal	2.00	2.00		2.00	2.00	2.00
	Sum **T,C,B,A**	15.31	15.34		15.26	15.27	15.31

Sample TS23-31

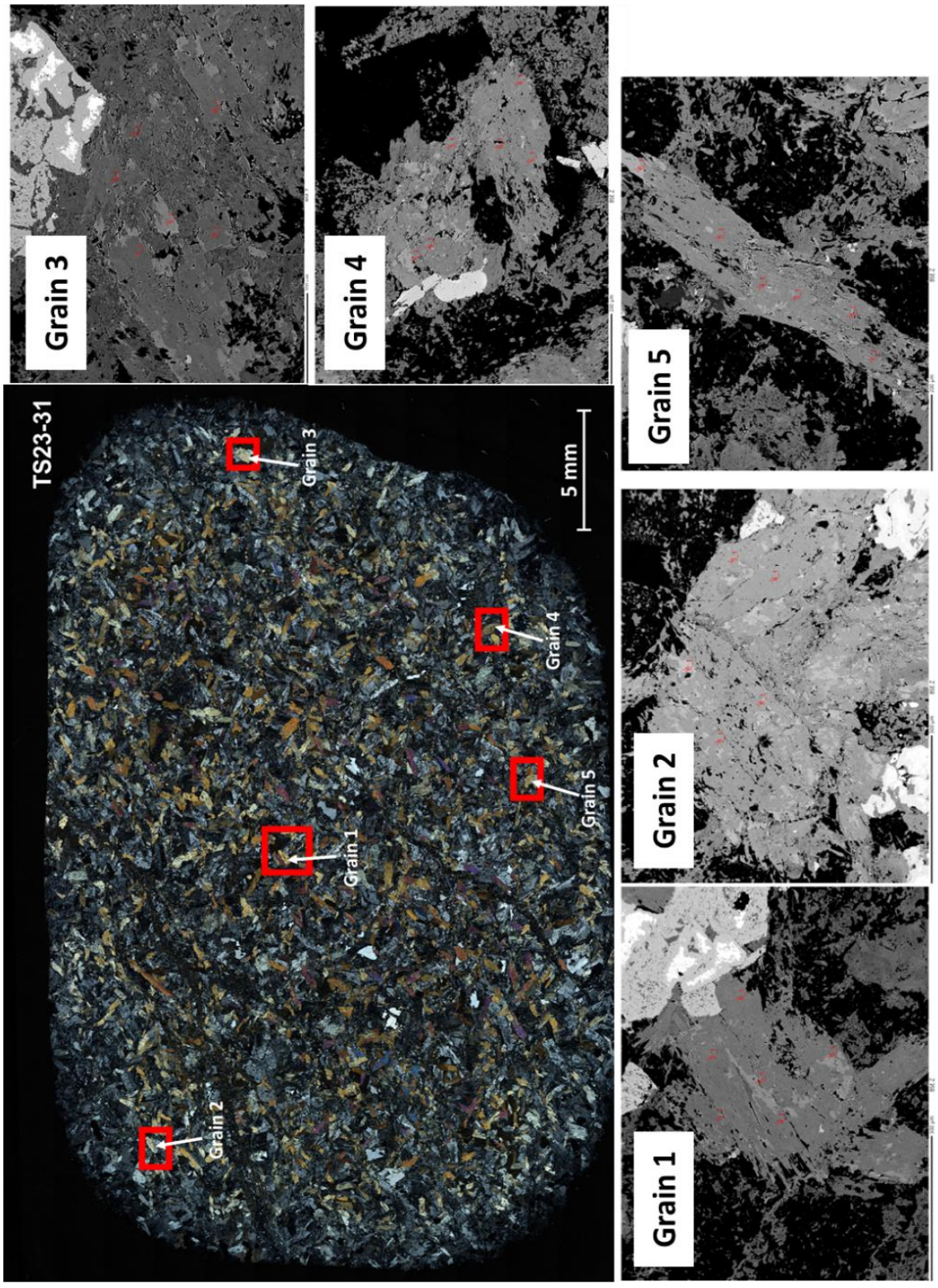

		Grain1-1	Grain1-2	Grain1-3	Grain1-4	Grain1-5	Grain1-6
Weight%	F	0.00	0.01	0.04	0.00	0.01	0.00
	Na	0.21	0.10	0.76	0.19	0.82	0.15
	Mg	7.23	7.23	4.48	6.86	4.00	6.68
	Al	1.73	0.97	5.67	1.81	6.19	1.58
	Si	24.10	24.59	20.77	24.03	20.11	24.14
	K	0.10	0.07	0.24	0.16	0.40	0.12
	Ti	0.04	0.01	0.18	0.05	0.17	0.02
	Cl	0.00	0.01	0.00	0.00	0.00	0.00
	Ca	8.79	8.87	8.31	8.80	8.32	8.84
	Fe	13.80	14.15	16.38	14.37	16.99	14.75
	Mn	0.34	0.33	0.34	0.29	0.33	0.27
	O	43.41	43.40	42.55	43.21	42.34	43.20
	H	0.25	0.25	0.30	0.23	0.32	0.25
	Total	100.00	100.00	100.00	100.00	100.00	100.00
Oxide	F	0.00	0.01	0.04	0.00	0.01	0.00
	Na_2O	0.28	0.14	1.03	0.26	1.11	0.20
	MgO	11.99	11.98	7.42	11.38	6.63	11.07
	Al_2O_3	3.27	1.83	10.71	3.42	11.69	2.98
	SiO_2	51.56	52.61	44.43	51.41	43.02	51.65
	K_2O	0.12	0.09	0.28	0.19	0.48	0.15
	TiO_2	0.06	0.02	0.29	0.08	0.29	0.04
	Cl	0.00	0.01	0.00	0.00	0.00	0.00
	CaO	12.30	12.42	11.62	12.31	11.64	12.37
	FeO	17.75	18.20	21.08	18.48	21.86	18.97
	MnO	0.44	0.42	0.44	0.38	0.43	0.35
	H_2O	2.22	2.27	2.65	2.09	2.85	2.22
	Total	100.00	100.00	100.00	100.00	100.00	100.00
	X	-1218.00	-1010.00	-1091.00	-1231.00	-1002.00	-806.00
	Y	-24379.00	-24354.00	-24515.00	-24578.00	-24749.00	-24448.00
	Z	27.00	26.00	24.00	25.00	24.00	25.00
Formula Assignments	**T** (ideally 8 apfu)						
	Si	6.99	7.76	6.72	7.59	6.56	7.65
	Be						
	Al	0.62	0.24	1.28	0.41	1.44	0.35
	Ti	0.01					
	Fe^{3+}	0.39					
	T subtotal	8.00	8.00	8.00	8.00	8.00	8.00
	C (ideally 5 apfu)						
	Ti		0.00	0.03	0.01	0.03	0.00
	Al		0.08	0.63	0.18	0.66	0.17
	Fe^{3+}	0.89	0.16	0.36	0.16	0.39	0.12
	Mn^{2+}	0.06	0.04	0.00	0.02	0.01	0.03
	Fe^{2+}	1.09	2.09	2.31	2.12	2.39	2.23
	Mg	2.85	2.63	1.67	2.50	1.51	2.45
	C subtotal	4.90	5.00	5.00	5.00	5.00	5.00
	B (ideally 2 apfu)						
	Mn^{2+}		0.01	0.06	0.03	0.05	0.02
	Mg						
	Ca	2.00	1.96	1.88	1.95	1.90	1.96
	Na		0.03	0.06	0.03	0.05	0.02
	B subtotal	2.00	2.00	2.00	2.00	2.00	2.00
	A (from 0 to 1 apfu)						
	Ca	0.11					
	Na	0.09	0.01	0.24	0.05	0.28	0.04
	K	0.02	0.02	0.05	0.04	0.09	0.03
	A subtotal	0.22	0.03	0.29	0.08	0.37	0.07
	O (non-W)	22.00	22.00	22.00	22.00	22.00	22.00
	W (ideally 2 apfu)						
	OH	2.00	1.99	1.98	2.00	2.00	2.00
	F		0.01	0.02		0.01	
	Cl		0.00				
	W subtotal	2.00	2.00	2.00	2.00	2.00	2.00
	Sum **T,C,B,A**	15.11	15.03	15.30	15.08	15.37	15.07

		Grain2-1	Grain2-2	Grain2-3	Grain2-4	Grain2-5	Grain2-6
Weight%	F	0.00	0.00	0.00	0.05	0.01	0.00
	Na	0.13	0.19	0.11	0.15	0.18	0.93
	Mg	7.10	6.98	7.45	7.44	7.32	3.37
	Al	1.23	1.59	0.89	1.22	1.36	7.39
	Si	24.33	24.08	24.71	24.57	24.29	19.06
	K	0.10	0.13	0.07	0.08	0.11	0.40
	Ti	0.02	0.02	0.00	0.04	0.03	0.26
	Cl	0.00	0.00	0.00	0.00	0.00	0.02
	Ca	8.82	8.79	8.80	8.84	8.83	8.36
	Fe	14.08	14.09	13.59	13.54	13.56	16.83
	Mn	0.34	0.33	0.31	0.30	0.30	0.35
	O	43.56	43.51	43.77	43.52	43.70	42.62
	H	0.30	0.29	0.30	0.25	0.30	0.41
	Total	100.00	100.00	100.00	100.00	100.00	100.00
Oxide	F	0.00	0.00	0.00	0.05	0.01	0.00
	Na_2O	0.17	0.25	0.15	0.21	0.25	1.25
	MgO	11.77	11.58	12.36	12.34	12.15	5.60
	Al_2O_3	2.32	3.00	1.68	2.31	2.56	13.97
	SiO_2	52.05	51.51	52.87	52.56	51.96	40.77
	K_2O	0.12	0.16	0.08	0.09	0.13	0.48
	TiO_2	0.04	0.04	0.01	0.06	0.04	0.44
	Cl	0.00	0.00	0.00	0.00	0.00	0.02
	CaO	12.34	12.31	12.31	12.36	12.36	11.70
	FeO	18.11	18.12	17.48	17.42	17.45	21.66
	MnO	0.43	0.42	0.40	0.39	0.39	0.45
	H_2O	2.64	2.60	2.66	2.20	2.69	3.68
	Total	100.00	100.00	100.00	100.00	100.00	100.00
	X	-14489.00	-14458.00	-13847.00	-13911.00	-14329.00	-14213.00
	Y	-18572.00	-18693.00	-18738.00	-18871.00	-18828.00	-18591.00
	Z	84.00	82.00	80.00	81.00	82.00	82.00
Formula Assignments	**T** (ideally 8 apfu)						
	Si	7.71	7.64	7.81	7.72	7.68	6.29
	Be						
	Al	0.29	0.37	0.19	0.28	0.32	1.71
	Ti						
	Fe^{3+}						
	T subtotal	8.00	8.00	8.00	8.00	8.00	8.00
	C (ideally 5 apfu)						
	Ti	0.00	0.00	0.00	0.01	0.00	0.05
	Al	0.11	0.16	0.10	0.12	0.13	0.84
	Fe^{3+}	0.16	0.14	0.08	0.15	0.13	0.37
	Mn^{2+}	0.04	0.03	0.02	0.03	0.03	0.03
	Fe^{2+}	2.08	2.10	2.08	1.99	2.03	2.43
	Mg	2.60	2.56	2.72	2.70	2.68	1.29
	C subtotal	5.00	5.00	5.00	5.00	5.00	5.00
	B (ideally 2 apfu)						
	Mn^{2+}	0.01	0.02	0.03	0.02	0.02	0.03
	Mg						
	Ca	1.96	1.96	1.95	1.95	1.96	1.94
	Na	0.03	0.02	0.02	0.04	0.02	0.04
	B subtotal	2.00	2.00	2.00	2.00	2.00	2.00
	A (from 0 to 1 apfu)						
	Ca						
	Na	0.02	0.05	0.02	0.02	0.05	0.34
	K	0.02	0.03	0.02	0.02	0.03	0.10
	A subtotal	0.04	0.08	0.04	0.04	0.07	0.43
	O (non-W)	22.00	22.00	22.00	22.00	22.00	22.00
	W (ideally 2 apfu)						
	OH	2.00	2.00	2.00	1.98	2.00	2.00
	F				0.02	0.01	
	Cl						0.01
	W subtotal	2.00	2.00	2.00	2.00	2.00	2.00
	Sum **T,C,B,A**	15.04	15.08	15.04	15.04	15.07	15.44

		Grain3-1	Grain3-2	Grain3-3	Grain3-4	Grain3-5	Grain3-6
Weight%	F	0.07	0.04	0.00	0.07	0.00	0.03
	Na	0.22	0.13	0.94	0.15	0.20	0.14
	Mg	7.00	7.08	3.19	7.10	7.32	6.91
	Al	1.71	1.27	7.79	1.35	1.54	1.38
	Si	23.65	23.79	18.81	23.97	24.10	23.79
	K	0.12	0.10	0.44	0.10	0.10	0.12
	Ti	0.04	0.01	0.21	0.02	0.12	0.02
	Cl	0.00	0.00	0.00	0.00	0.00	0.01
	Ca	8.77	8.81	8.26	8.79	8.78	8.89
	Fe	14.07	14.31	17.04	14.18	13.56	14.43
	Mn	0.32	0.30	0.32	0.31	0.29	0.28
	O	43.67	43.76	42.57	43.61	43.68	43.64
	H	0.36	0.39	0.41	0.34	0.30	0.37
	Total	100.00	100.00	100.00	100.00	100.00	100.00
Oxide	F	0.07	0.04	0.00	0.07	0.00	0.03
	Na_2O	0.29	0.18	1.27	0.21	0.27	0.19
	MgO	11.61	11.75	5.29	11.77	12.14	11.46
	Al_2O_3	3.23	2.40	14.72	2.55	2.91	2.61
	SiO_2	50.60	50.89	40.23	51.28	51.55	50.89
	K_2O	0.15	0.11	0.53	0.12	0.12	0.14
	TiO_2	0.06	0.02	0.35	0.04	0.19	0.04
	Cl	0.00	0.00	0.00	0.00	0.00	0.01
	CaO	12.27	12.33	11.56	12.30	12.29	12.43
	FeO	18.10	18.41	21.93	18.25	17.45	18.56
	MnO	0.42	0.38	0.41	0.41	0.38	0.36
	H_2O	3.20	3.48	3.69	3.01	2.69	3.27
	Total	100.00	100.00	100.00	100.00	100.00	100.00
	X	16094.00	16134.00	16163.00	16257.00	16359.00	16411.00
	Y	-24360.00	-24522.00	-24426.00	-24309.00	-24353.00	-24523.00
	Z	2.00	1.00	0.00	2.00	2.00	0.00
Formula Assignments	**T** (ideally 8 apfu)						
	Si	7.55	7.61	6.22	7.63	7.62	7.61
	Be						
	Al	0.45	0.39	1.79	0.37	0.38	0.39
	Ti						
	Fe^{3+}						
	T subtotal	8.00	8.00	8.00	8.00	8.00	8.00
	C (ideally 5 apfu)						
	Ti	0.01	0.00	0.04	0.00	0.02	0.01
	Al	0.12	0.04	0.90	0.08	0.13	0.08
	Fe^{3+}	0.25	0.30	0.42	0.24	0.17	0.23
	Mn^{2+}	0.04	0.04	0.01	0.03	0.02	0.04
	Fe^{2+}	2.01	2.01	2.42	2.03	1.99	2.09
	Mg	2.58	2.62	1.22	2.61	2.68	2.56
	C subtotal	5.00	5.00	5.00	5.00	5.00	5.00
	B (ideally 2 apfu)						
	Mn^{2+}	0.02	0.01	0.04	0.02	0.03	0.00
	Mg						
	Ca	1.96	1.98	1.91	1.96	1.95	1.99
	Na	0.02	0.01	0.05	0.02	0.03	0.00
	B subtotal	2.00	2.00	2.00	2.00	2.00	2.00
	A (from 0 to 1 apfu)						
	Ca						
	Na	0.06	0.04	0.33	0.04	0.05	0.05
	K	0.03	0.02	0.10	0.02	0.02	0.03
	A subtotal	0.09	0.06	0.44	0.06	0.07	0.08
	O (non-W)	22.00	22.00	22.00	22.00	22.00	22.00
	W (ideally 2 apfu)						
	OH	1.97	1.98	2.00	1.97	2.00	1.98
	F	0.03	0.02		0.03		0.01
	Cl						0.00
	W subtotal	2.00	2.00	2.00	2.00	2.00	2.00
	Sum **T,C,B,A**	15.09	15.06	15.44	15.06	15.07	15.08

		Grain4-1	Grain4-2	Grain4-3	Grain4-4	Grain4-5	Grain4-6
Weight%	F	0.03	0.05	0.00	0.01	0.00	0.04
	Na	0.93	0.04	0.11	0.14	0.23	0.19
	Mg	3.44	7.74	7.41	7.33	7.14	6.89
	Al	7.35	0.33	1.07	1.20	1.76	1.74
	Si	19.37	25.16	24.39	24.44	24.07	23.86
	K	0.38	0.02	0.07	0.09	0.11	0.18
	Ti	0.22	0.02	0.01	0.02	0.04	0.03
	Cl	0.01	0.00	0.01	0.00	0.00	0.00
	Ca	8.32	9.00	8.88	8.81	8.79	8.71
	Fe	17.06	13.46	13.84	13.93	14.00	14.26
	Mn	0.33	0.29	0.29	0.33	0.32	0.30
	O	42.24	43.63	43.62	43.45	43.31	43.47
	H	0.32	0.25	0.29	0.26	0.24	0.31
	Total	100.00	100.00	100.00	100.00	100.00	100.00
Oxide	F	0.03	0.05	0.00	0.01	0.00	0.04
	Na_2O	1.25	0.06	0.14	0.19	0.30	0.26
	MgO	5.70	12.84	12.30	12.15	11.84	11.43
	Al_2O_3	13.89	0.62	2.02	2.26	3.32	3.29
	SiO_2	41.45	53.83	52.18	52.29	51.50	51.04
	K_2O	0.46	0.03	0.09	0.11	0.13	0.21
	TiO_2	0.37	0.03	0.02	0.03	0.06	0.06
	Cl	0.01	0.00	0.01	0.00	0.00	0.00
	CaO	11.64	12.59	12.43	12.33	12.31	12.19
	FeO	21.95	17.32	17.81	17.92	18.01	18.35
	MnO	0.43	0.38	0.37	0.43	0.41	0.39
	H_2O	2.82	2.26	2.63	2.29	2.12	2.73
	Total	100.00	100.00	100.00	100.00	100.00	100.00
	X	8434.00	8469.00	8751.00	8931.00	8712.00	8751.00
	Y	-31732.00	-31773.00	-31831.00	-32019.00	-32051.00	-31962.00
	Z	-11.00	-9.00	-10.00	-10.00	-10.00	-11.00
Formula Assignments	**T** (ideally 8 apfu)						
	Si	6.34	7.91	7.70	7.70	7.58	7.58
	Be						
	Al	1.66	0.09	0.30	0.30	0.42	0.42
	Ti						
	Fe^{3+}						
	T subtotal	8.00	8.00	8.00	8.00	8.00	8.00
	C (ideally 5 apfu)						
	Ti	0.04	0.00	0.00	0.00	0.01	0.01
	Al	0.84	0.02	0.06	0.09	0.16	0.16
	Fe^{3+}	0.38	0.07	0.23	0.21	0.21	0.19
	Mn^{2+}	0.01	0.04	0.04	0.04	0.02	0.02
	Fe^{2+}	2.43	2.06	1.97	2.00	2.01	2.09
	Mg	1.30	2.81	2.71	2.67	2.60	2.53
	C subtotal	5.00	5.00	5.00	5.00	5.00	5.00
	B (ideally 2 apfu)						
	Mn^{2+}	0.04	0.01	0.01	0.02	0.03	0.03
	Mg						
	Ca	1.91	1.98	1.97	1.95	1.94	1.94
	Na	0.05	0.01	0.03	0.04	0.03	0.03
	B subtotal	2.00	2.00	2.00	2.00	2.00	2.00
	A (from 0 to 1 apfu)						
	Ca						
	Na	0.32	0.01	0.02	0.02	0.05	0.04
	K	0.09	0.01	0.02	0.02	0.02	0.04
	A subtotal	0.41	0.01	0.03	0.04	0.08	0.08
	O (non-W)	22.00	22.00	22.00	22.00	22.00	22.00
	W (ideally 2 apfu)						
	OH	1.98	1.98	2.00	2.00	2.00	1.98
	F	0.02	0.02		0.01		0.02
	Cl	0.00		0.00			
	W subtotal	2.00	2.00	2.00	2.00	2.00	2.00
	Sum **T,C,B,A**	15.41	15.01	15.03	15.04	15.08	15.08

		Grain5-1	Grain5-2	Grain5-3	Grain5-4	Grain5-5	Grain5-6
Weight%	F	0.05	0.00	0.03	0.00	0.00	0.04
	Na	0.18	0.18	0.13	0.16	0.18	0.82
	Mg	7.37	7.17	7.51	7.11	7.30	3.81
	Al	1.39	1.57	1.05	1.41	1.49	6.81
	Si	24.17	24.03	24.36	24.15	23.99	19.86
	K	0.11	0.14	0.08	0.11	0.11	0.33
	Ti	0.03	0.03	0.01	0.02	0.03	0.07
	Cl	0.00	0.01	0.01	0.00	0.01	0.01
	Ca	8.84	8.78	8.84	8.82	8.73	8.36
	Fe	13.70	14.15	13.74	14.19	13.74	16.73
	Mn	0.31	0.30	0.31	0.29	0.32	0.31
	O	43.58	43.37	43.64	43.46	43.76	42.50
	H	0.29	0.27	0.30	0.28	0.34	0.34
	Total	100.00	100.00	100.00	100.00	100.00	100.00
Oxide	F	0.05	0.00	0.03	0.00	0.00	0.04
	Na_2O	0.24	0.25	0.18	0.22	0.25	1.10
	MgO	12.23	11.88	12.46	11.79	12.11	6.33
	Al_2O_3	2.62	2.98	1.98	2.66	2.82	12.87
	SiO_2	51.71	51.40	52.12	51.67	51.31	42.48
	K_2O	0.13	0.16	0.09	0.14	0.13	0.40
	TiO_2	0.05	0.04	0.02	0.03	0.04	0.11
	Cl	0.00	0.01	0.01	0.00	0.01	0.01
	CaO	12.36	12.29	12.36	12.34	12.21	11.70
	FeO	17.62	18.21	17.67	18.25	17.67	21.53
	MnO	0.40	0.39	0.40	0.38	0.42	0.40
	H_2O	2.59	2.38	2.68	2.53	3.02	3.02
	Total	100.00	100.00	100.00	100.00	100.00	100.00
	X	1837.00	1952.00	1996.00	2028.00	2155.00	2335.00
	Y	-33395.00	-33343.00	-33201.00	-33115.00	-33009.00	-32810.00
	Z	-5.00	-5.00	-4.00	-4.00	-4.00	-4.00
Formula Assignments	**T** (ideally 8 apfu)						
	Si	7.64	7.59	7.69	7.65	7.61	6.48
	Be						
	Al	0.36	0.41	0.31	0.35	0.39	1.52
	Ti						
	Fe^{3+}						
	T subtotal	8.00	8.00	8.00	8.00	8.00	8.00
	C (ideally 5 apfu)						
	Ti	0.01	0.00	0.00	0.00	0.00	0.01
	Al	0.10	0.11	0.04	0.11	0.10	0.79
	Fe^{3+}	0.21	0.25	0.26	0.19	0.25	0.40
	Mn^{2+}	0.03	0.02	0.04	0.03	0.03	0.01
	Fe^{2+}	1.97	2.00	1.92	2.06	1.94	2.35
	Mg	2.69	2.62	2.74	2.60	2.68	1.44
	C subtotal	5.00	5.00	5.00	5.00	5.00	5.00
	B (ideally 2 apfu)						
	Mn^{2+}	0.02	0.03	0.01	0.02	0.03	0.04
	Mg						
	Ca	1.96	1.94	1.96	1.96	1.94	1.91
	Na	0.02	0.03	0.03	0.02	0.03	0.05
	B subtotal	2.00	2.00	2.00	2.00	2.00	2.00
	A (from 0 to 1 apfu)						
	Ca						
	Na	0.05	0.04	0.02	0.04	0.04	0.28
	K	0.02	0.03	0.02	0.03	0.03	0.08
	A subtotal	0.07	0.07	0.04	0.07	0.07	0.36
	O (non-W)	22.00	22.00	22.00	22.00	22.00	22.00
	W (ideally 2 apfu)						
	OH	1.98	2.00	1.98	2.00	2.00	1.98
	F	0.02		0.01			0.02
	Cl		0.00	0.00		0.00	0.00
	W subtotal	2.00	2.00	2.00	2.00	2.00	2.00
	Sum **T,C,B,A**	15.07	15.07	15.04	15.07	15.07	15.36

Sample TS23-61

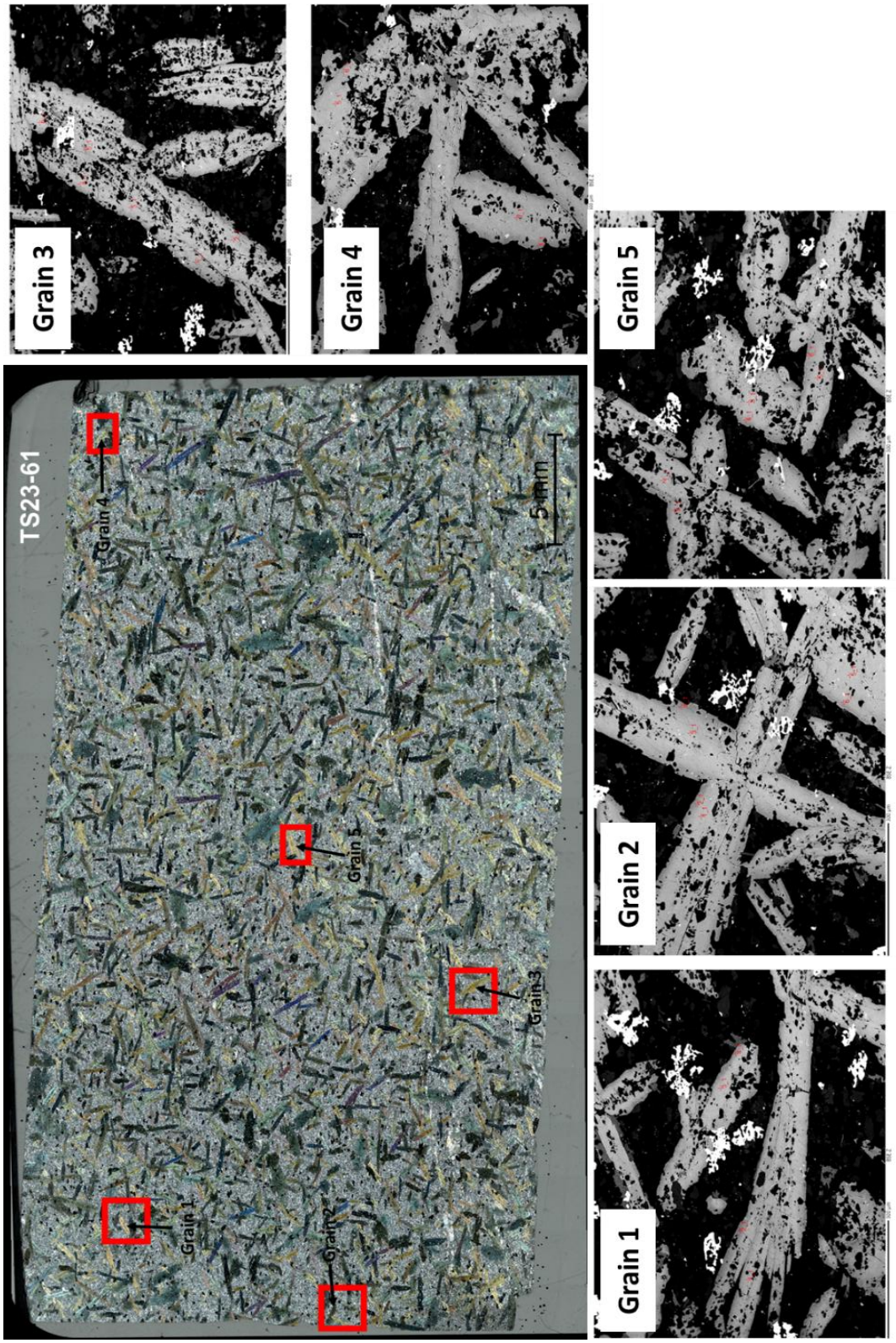

		Grain1-1	Grain1-2	Grain1-3	Grain1-4	Grain1-5	Grain1-6
Weight%	F	0.06	0.12	0.07	0.07	0.05	0.08
	Na	0.98	0.98	0.96	0.95	0.99	0.94
	Mg	3.19	4.68	3.15	4.76	3.13	5.16
	Al	7.91	7.28	8.04	6.80	7.97	6.59
	Si	18.90	20.07	19.01	20.48	19.04	20.68
	K	0.31	0.14	0.33	0.13	0.34	0.12
	Ti	0.19	0.18	0.17	0.20	0.18	0.19
	Cl	0.00	0.00	0.00	0.00	0.01	0.00
	Ca	8.10	8.25	8.18	8.26	8.13	8.23
	Fe	17.45	14.56	17.35	14.66	17.34	14.34
	Mn	0.30	0.30	0.32	0.31	0.32	0.30
	O	42.27	43.11	42.12	43.06	42.19	43.07
	H	0.35	0.33	0.30	0.31	0.32	0.29
	Total	100.00	100.00	100.00	100.00	100.00	100.00
Oxide	F	0.06	0.12	0.07	0.07	0.05	0.08
	Na_2O	1.32	1.32	1.30	1.28	1.34	1.27
	MgO	5.29	7.76	5.23	7.90	5.19	8.55
	Al_2O_3	14.95	13.76	15.18	12.86	15.07	12.46
	SiO_2	40.44	42.94	40.68	43.82	40.73	44.25
	K_2O	0.37	0.17	0.39	0.15	0.41	0.15
	TiO_2	0.31	0.30	0.29	0.34	0.30	0.32
	Cl	0.00	0.00	0.00	0.00	0.01	0.00
	CaO	11.33	11.54	11.44	11.56	11.37	11.52
	FeO	22.45	18.73	22.32	18.86	22.30	18.44
	MnO	0.39	0.39	0.41	0.40	0.41	0.39
	H_2O	3.10	2.97	2.69	2.76	2.82	2.57
	Total	100.00	100.00	100.00	100.00	100.00	100.00
	X	-14967.00	-14759.00	-14155.00	-14011.00	-15032.00	-14886.00
	Y	-7924.00	-7892.00	-7814.00	-7875.00	-7490.00	-7495.00
	Z	70.00	70.00	69.00	68.00	70.00	69.00
Formula Assignments	**T** (ideally 8 apfu)						
	Si	6.20	6.45	6.21	6.57	6.23	6.60
	Al	1.81	1.55	1.79	1.43	1.77	1.40
	T subtotal	8.00	8.00	8.00	8.00	8.00	8.00
	C (ideally 5 apfu)						
	Ti	0.04	0.03	0.03	0.04	0.04	0.04
	Zr						
	Al	0.90	0.89	0.94	0.85	0.94	0.79
	Fe^{3+}	0.52	0.32	0.47	0.26	0.43	0.32
	Mn^{2+}						
	Fe^{2+}	2.34	2.01	2.37	2.09	2.41	1.96
	Mg	1.21	1.74	1.19	1.77	1.18	1.90
	C subtotal	5.00	5.00	5.00	5.00	5.00	5.00
	B (ideally 2 apfu)						
	Mn^{2+}	0.05	0.05	0.05	0.05	0.05	0.05
	Fe^{2+}	0.02	0.02	0.01	0.02	0.01	0.03
	Ca	1.86	1.86	1.87	1.86	1.86	1.84
	Sr						
	Na	0.08	0.08	0.07	0.08	0.07	0.09
	B subtotal	2.00	2.00	2.00	2.00	2.00	2.00
	A (from 0 to 1 apfu)						
	Na	0.32	0.31	0.32	0.30	0.32	0.28
	K	0.07	0.03	0.08	0.03	0.08	0.03
	A subtotal	0.39	0.34	0.39	0.33	0.40	0.31
	O (non-W)	22.00	22.00	22.00	22.00	22.00	22.00
	W (ideally 2 apfu)						
	OH	1.97	1.94	1.97	1.97	1.97	1.96
	F	0.03	0.06	0.03	0.03	0.02	0.04
	Cl					0.00	
	W subtotal	2.00	2.00	2.00	2.00	2.00	2.00
	Sum **T,C,B,A**	15.39	15.34	15.39	15.33	15.40	15.31

		Grain2-1	Grain2-2	Grain2-3	Grain2-4	Grain2-5	Grain2-6
Weight%	F	0.13	0.09	0.00	0.02	0.01	0.05
	Na	0.96	0.92	0.89	0.90	0.83	0.92
	Mg	3.07	4.77	2.93	4.64	3.23	4.22
	Al	7.86	6.74	7.88	6.92	7.78	7.62
	Si	18.96	20.24	18.91	20.28	19.13	19.75
	K	0.32	0.13	0.36	0.15	0.33	0.17
	Ti	0.19	0.22	0.18	0.13	0.17	0.07
	Cl	0.01	0.00	0.00	0.01	0.00	0.00
	Ca	8.20	8.22	8.17	8.16	8.32	8.17
	Fe	17.46	15.04	17.70	15.08	16.92	15.30
	Mn	0.34	0.34	0.33	0.33	0.26	0.31
	O	42.17	42.97	42.29	43.05	42.63	43.05
	H	0.33	0.33	0.36	0.33	0.39	0.36
	Total	100.00	100.00	100.00	100.00	100.00	100.00
Oxide	F	0.13	0.09	0.00	0.02	0.01	0.05
	Na_2O	1.30	1.25	1.19	1.21	1.12	1.24
	MgO	5.09	7.91	4.86	7.70	5.35	7.00
	Al_2O_3	14.85	12.74	14.89	13.07	14.70	14.40
	SiO_2	40.57	43.31	40.45	43.40	40.92	42.25
	K_2O	0.38	0.16	0.44	0.19	0.40	0.21
	TiO_2	0.32	0.36	0.31	0.21	0.29	0.12
	Cl	0.01	0.00	0.00	0.01	0.00	0.00
	CaO	11.47	11.50	11.43	11.41	11.64	11.44
	FeO	22.46	19.35	22.77	19.40	21.76	19.68
	MnO	0.44	0.43	0.43	0.43	0.34	0.40
	H_2O	2.98	2.92	3.24	2.97	3.47	3.22
	Total	100.00	100.00	100.00	100.00	100.00	100.00
	X	1383.00	1429.00	1694.00	1796.00	1913.00	1811.00
	Y	-694.00	-680.00	-656.00	-625.00	-1224.00	-1201.00
	Z	42.00	43.00	42.00	43.00	42.00	41.00
Formula Assignments	**T** (ideally 8 apfu)						
	Si	6.23	6.51	6.22	6.52	6.28	6.38
	Al	1.77	1.49	1.78	1.48	1.72	1.62
	T subtotal	8.00	8.00	8.00	8.00	8.00	8.00
	C (ideally 5 apfu)						
	Ti	0.04	0.04	0.04	0.02	0.03	0.01
	Zr						
	Al	0.91	0.77	0.92	0.84	0.94	0.94
	Fe^{3+}	0.45	0.40	0.47	0.38	0.39	0.40
	Mn^{2+}	0.00		0.00		0.01	
	Fe^{2+}	2.43	2.02	2.46	2.04	2.41	2.06
	Mg	1.16	1.77	1.11	1.73	1.23	1.58
	C subtotal	5.00	5.00	5.00	5.00	5.00	5.00
	B (ideally 2 apfu)						
	Mn^{2+}	0.05	0.06	0.05	0.06	0.04	0.05
	Fe^{2+}		0.01		0.02		0.02
	Ca	1.89	1.85	1.88	1.84	1.92	1.85
	Sr						
	Na	0.06	0.08	0.06	0.09	0.05	0.08
	B subtotal	2.00	2.00	2.00	2.00	2.00	2.00
	A (from 0 to 1 apfu)						
	Na	0.33	0.29	0.29	0.27	0.29	0.28
	K	0.07	0.03	0.09	0.04	0.08	0.04
	A subtotal	0.40	0.32	0.38	0.30	0.37	0.32
	O (non-W)	22.00	22.00	22.00	22.00	22.00	22.00
	W (ideally 2 apfu)						
	OH	1.93	1.96	2.00	1.99	2.00	1.98
	F	0.06	0.04		0.01	0.01	0.02
	Cl	0.00			0.00		
	W subtotal	2.00	2.00	2.00	2.00	2.00	2.00
	Sum **T,C,B,A**	15.40	15.32	15.38	15.30	15.37	15.32

		Grain4-1	Grain4-2	Grain4-3	Grain4-4	Grain4-5	Grain4-6
Weight%	F	0.11	0.00	0.00	0.04	0.09	0.02
	Na	0.96	0.94	0.89	0.94	0.88	0.95
	Mg	3.26	4.57	3.49	4.85	3.07	4.03
	Al	7.85	7.15	7.00	6.72	7.76	7.39
	Si	19.00	20.43	19.57	19.77	19.10	19.59
	K	0.30	0.14	0.27	0.13	0.35	0.21
	Ti	0.19	0.18	0.21	0.17	0.18	0.19
	Cl	0.00	0.00	0.00	0.00	0.00	0.00
	Ca	8.14	8.30	8.15	8.35	8.26	8.17
	Fe	17.25	14.65	17.46	14.62	17.77	16.06
	Mn	0.30	0.27	0.30	0.29	0.29	0.30
	O	42.28	43.08	42.32	43.62	41.94	42.73
	H	0.34	0.30	0.33	0.48	0.29	0.34
	Total	100.00	100.00	100.00	100.00	100.00	100.00
Oxide	F	0.11	0.00	0.00	0.04	0.09	0.02
	Na_2O	1.29	1.26	1.20	1.26	1.19	1.28
	MgO	5.41	7.57	5.78	8.05	5.09	6.69
	Al_2O_3	14.84	13.50	13.22	12.70	14.67	13.97
	SiO_2	40.66	43.71	41.87	42.30	40.87	41.91
	K_2O	0.36	0.17	0.33	0.16	0.43	0.25
	TiO_2	0.31	0.30	0.35	0.29	0.31	0.32
	Cl	0.00	0.00	0.00	0.00	0.00	0.00
	CaO	11.40	11.61	11.41	11.68	11.56	11.43
	FeO	22.19	18.85	22.46	18.81	22.87	20.66
	MnO	0.39	0.34	0.39	0.38	0.37	0.38
	H_2O	3.04	2.68	2.98	4.33	2.56	3.07
	Total	100.00	100.00	100.00	100.00	100.00	100.00
	X	16587.00	16606.00	16857.00	16767.00	17260.00	17371.00
	Y	-7000.00	-6944.00	-7577.00	-7649.00	-6974.00	-7001.00
	Z	29.00	29.00	28.00	29.00	28.00	28.00
Formula Assignments	**T** (ideally 8 apfu)						
	Si	6.22	6.55	6.40	6.45	6.24	6.35
	Al	1.78	1.45	1.60	1.55	1.76	1.65
	T subtotal	8.00	8.00	8.00	8.00	8.00	8.00
	C (ideally 5 apfu)						
	Ti	0.04	0.03	0.04	0.03	0.04	0.04
	Zr						
	Al	0.90	0.93	0.78	0.73	0.89	0.85
	Fe^{3+}	0.49	0.21	0.46	0.45	0.48	0.45
	Mn^{2+}				0.01		
	Fe^{2+}	2.34	2.14	2.40	1.95	2.44	2.15
	Mg	1.23	1.69	1.32	1.83	1.16	1.51
	C subtotal	5.00	5.00	5.00	5.00	5.00	5.00
	B (ideally 2 apfu)						
	Mn^{2+}	0.05	0.04	0.05	0.04	0.05	0.05
	Fe^{2+}	0.01	0.02	0.01		0.00	0.02
	Ca	1.87	1.86	1.87	1.91	1.89	1.86
	Sr						
	Na	0.07	0.08	0.07	0.05	0.06	0.08
	B subtotal	2.00	2.00	2.00	2.00	2.00	2.00
	A (from 0 to 1 apfu)						
	Na	0.31	0.29	0.29	0.32	0.30	0.30
	K	0.07	0.03	0.06	0.03	0.08	0.05
	A subtotal	0.38	0.32	0.35	0.35	0.38	0.35
	O (non-W)	22.00	22.00	22.00	22.00	22.00	22.00
	W (ideally 2 apfu)						
	OH	1.95	2.00	2.00	1.98	1.96	1.99
	F	0.05			0.02	0.04	0.01
	Cl						
	W subtotal	2.00	2.00	2.00	2.00	2.00	2.00
	Sum **T,C,B,A**	15.38	15.32	15.35	15.35	15.38	15.35

		Grain5-1	Grain5-2	Grain5-3	Grain5-4	Grain5-5	Grain5-6
Weight%	F	0.00	0.00	0.00	0.06	0.09	0.00
	Na	0.94	1.01	0.92	0.93	0.94	0.95
	Mg	3.27	4.44	3.18	4.36	3.23	4.48
	Al	7.59	7.14	7.67	7.31	7.55	6.87
	Si	19.12	20.15	19.10	20.02	19.03	20.08
	K	0.28	0.14	0.31	0.15	0.30	0.14
	Ti	0.20	0.18	0.20	0.20	0.20	0.20
	Cl	0.00	0.00	0.00	0.00	0.00	0.00
	Ca	8.12	8.18	8.16	8.20	8.18	8.15
	Fe	17.45	15.30	17.61	15.09	17.37	15.78
	Mn	0.30	0.33	0.31	0.32	0.33	0.31
	O	42.37	42.83	42.21	43.02	42.40	42.74
	H	0.36	0.30	0.33	0.33	0.38	0.31
	Total	100.00	100.00	100.00	100.00	100.00	100.00
Oxide	F	0.00	0.00	0.00	0.06	0.09	0.00
	Na_2O	1.27	1.36	1.24	1.26	1.27	1.28
	MgO	5.42	7.36	5.27	7.23	5.36	7.43
	Al_2O_3	14.34	13.49	14.48	13.80	14.26	12.98
	SiO_2	40.91	43.11	40.86	42.84	40.72	42.96
	K_2O	0.34	0.17	0.38	0.18	0.37	0.17
	TiO_2	0.34	0.30	0.33	0.34	0.33	0.33
	Cl	0.00	0.00	0.00	0.00	0.00	0.00
	CaO	11.36	11.45	11.42	11.47	11.44	11.40
	FeO	22.45	19.69	22.66	19.42	22.35	20.30
	MnO	0.39	0.43	0.41	0.41	0.42	0.41
	H_2O	3.19	2.64	2.96	2.99	3.39	2.76
	Total	100.00	100.00	100.00	100.00	100.00	100.00
	X	-17568.00	-17689.00	-17255.00	-17328.00	-17157.00	-17072.00
	Y	2449.00	2407.00	2124.00	2137.00	1867.00	1900.00
	Z	76.00	75.00	75.00	75.00	75.00	75.00
Formula Assignments	**T** (ideally 8 apfu)						
	Si	6.27	6.48	6.25	6.46	6.27	6.46
	Al	1.73	1.53	1.75	1.54	1.73	1.54
	T subtotal	8.00	8.00	8.00	8.00	8.00	8.00
	C (ideally 5 apfu)						
	Ti	0.04	0.03	0.04	0.04	0.04	0.04
	Zr						
	Al	0.86	0.86	0.87	0.91	0.85	0.77
	Fe^{3+}	0.50	0.33	0.50	0.32	0.47	0.46
	Mn^{2+}					0.00	
	Fe^{2+}	2.37	2.12	2.40	2.12	2.40	2.07
	Mg	1.24	1.65	1.20	1.62	1.23	1.67
	C subtotal	5.00	5.00	5.00	5.00	5.00	5.00
	B (ideally 2 apfu)						
	Mn^{2+}	0.05	0.06	0.05	0.05	0.05	0.05
	Fe^{2+}	0.01	0.02	0.01	0.02		0.02
	Ca	1.87	1.84	1.87	1.85	1.89	1.84
	Sr						
	Na	0.07	0.08	0.07	0.08	0.06	0.09
	B subtotal	2.00	2.00	2.00	2.00	2.00	2.00
	A (from 0 to 1 apfu)						
	Na	0.31	0.31	0.30	0.29	0.32	0.29
	K	0.07	0.03	0.07	0.04	0.07	0.03
	A subtotal	0.37	0.35	0.37	0.32	0.39	0.32
	O (non-W)	22.00	22.00	22.00	22.00	22.00	22.00
	W (ideally 2 apfu)						
	OH	2.00	2.00	2.00	1.97	1.96	2.00
	F				0.03	0.04	
	Cl						
	W subtotal	2.00	2.00	2.00	2.00	2.00	2.00
	Sum **T,C,B,A**	15.37	15.35	15.37	15.33	15.39	15.32

Appendix IV: U-Pb zircon ID-TIMS data

2023 geochronology sample (TS23-40)

TS23-40							
	Fraction	1-2	1-4	1-5	1-9	1-10	1-15
	Pb^T (pg)	262.96	366.22	423.04	369.97	199.11	248.75
	Pb_C (pg)	0.13	0.22	0.28	0.12	0.33	0.29
	Th/U	0.63	0.63	0.56	0.53	0.51	0.52
	$^{206}Pb/^{204}Pb$	14076.64	19609.76	22952.93	20202.51	10924.03	13618.70
	$^{206}Pb/^{238}U$	0.51	0.51	0.51	0.51	0.51	0.51
	± 2s	0.04	0.04	0.04	0.04	0.04	0.04
	$^{207}Pb/^{235U}$	12.92	12.91	12.91	12.91	12.91	12.91
	± 2s	0.06	0.06	0.05	0.06	0.06	0.06
	$^{207}Pb/^{206}Pb$	0.18	0.18	0.18	0.18	0.18	0.18
	± 2s	0.02	0.02	0.02	0.02	0.02	0.02
Ages (Ma)	**$^{206}Pb/^{238}U$**	2673.35	2672.35	2672.55	2673.20	2673.40	2672.72
	± 2s	0.95	0.93	0.91	0.97	0.96	0.92
	$^{207}Pb/^{235}U$	2673.54	2672.90	2673.16	2673.27	2673.30	2673.03
	± 2s	0.54	0.52	0.51	0.54	0.54	0.53
	$^{207}Pb/^{206}Pb$	2673.68	2673.31	2673.61	2673.33	2673.22	2673.27
	± 2s	0.39	0.35	0.32	0.38	0.39	0.38
	Correlation coefficient	0.93	0.94	0.95	0.93	0.93	0.93
	Weighted mean $^{207}Pb/^{206}Pb$ age	**2673.42 ± 0.15 [2.33] Ma (2s); MSWD = 1.11 (n=6)**					

Model Th/U ratio iteratively calculated from the radiogenic $^{208}Pb/^{206}Pb$ ratio and $^{206}Pb/^{238}U$ age.

Pb* and Pbc represent radiogenic and common Pb, respectively; mol % $^{206}Pb^*$ with respect to radiogenic, blank and initial common Pb.

Measured ratio corrected for spike and fractionation only. Pb fractionation of 0.13 ± 0.03 %/amu (1 sigma; absolute) calculated from NBS-982 measurements, Uranium fractionation determined from double spike U.

Corrected for fractionation, spike, and common Pb; all common Pb was assumed to be procedural blank: $^{206}Pb/^{204}Pb$ = 18.24 ± 0.74%; $^{207}Pb/^{204}Pb$ = 15.74 ± 0.62%;

$^{208}Pb/^{204}Pb$ = 37.886 ± 0.83% (all uncertainties 1-sigma).

Errors are 2-sigma, propagated using the algorithms of Schmitz and Schoene (2007).

Calculations are based on the decay constants of Jaffey et al. (1971) and $^{238}U/^{235}U$ = 137.82 ± 0.05.

2024 geochronology samples (TS24-01, TS24-05 and TS24-07)

Schematic sections of drillholes GB21-16 and NL21-08 correlated with samples TS24-01 and TS24-05.

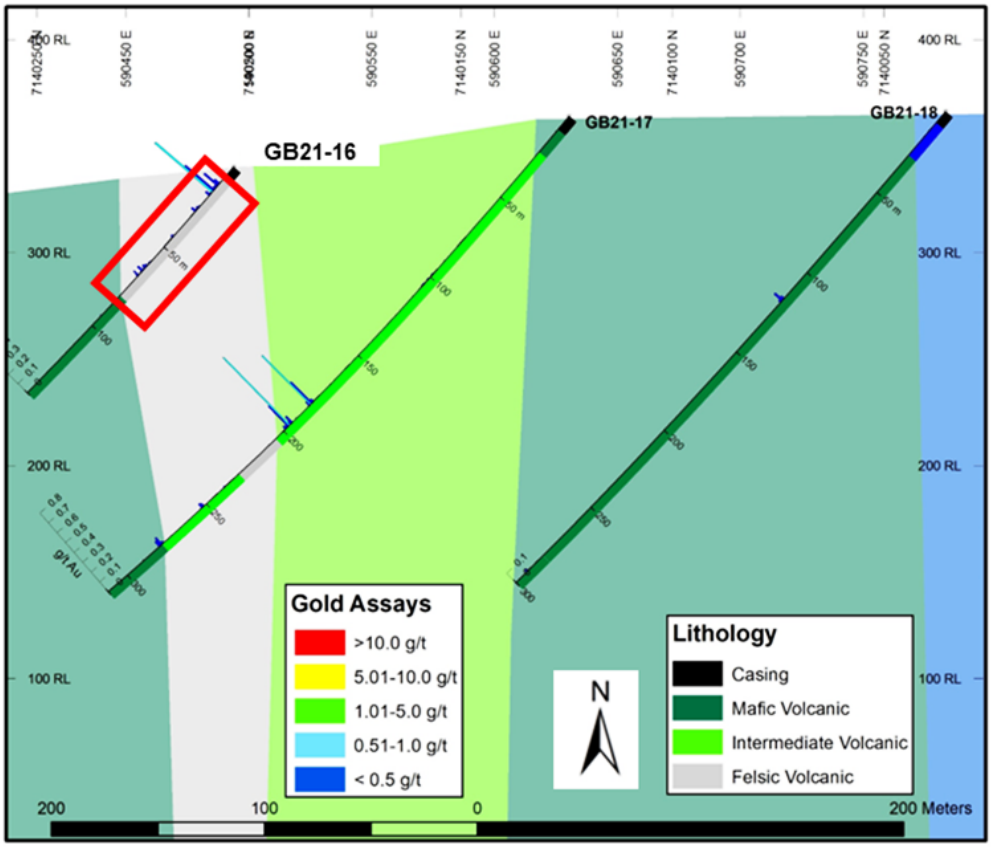

		TS24-01 Felsic volcanic, DDH GB21-16		
	Fraction	Z1	Z2	Z3
	Description	1 clr, cls, Sharp, 3:1 euh pr	1 clr, cls, sharp, brkn pr	1 clr. Cls, thick, sharp, brkn pr
	U (ppm)	95.87	129.98	201.32
	Pb^T (pg)	55.94	135.23	252.63
	Pb_C (pg)	1.02	0.56	0.43
	Th/U	0.51	0.54	0.53
	$^{206}Pb/^{204}Pb$	3097.38	13599.64	32656.93
	$^{206}Pb/^{238}U$	0.51	0.51	0.51
	± 2s	0.00	0.00	0.00
	$^{207}Pb/^{235U}$	12.89	12.91	12.89
	± 2s	0.04	0.03	0.03
	$^{207}Pb/^{206}Pb$	0.18	0.18	0.18
	± 2s	0.00	0.00	0.00
Ages (Ma)	$^{206}Pb/^{238}U$	2668.70	2671.95	2669.38
	± 2s	4.98	4.97	4.13
	$^{207}Pb/^{235}U$	2671.31	2672.86	2671.90
	± 2s	2.68	2.48	2.16
	$^{207}Pb/^{206}Pb$	2673.29	2673.54	2673.82
	± 2s	2.04	1.40	1.33
	Discordance (%)	0.21	0.07	0.20

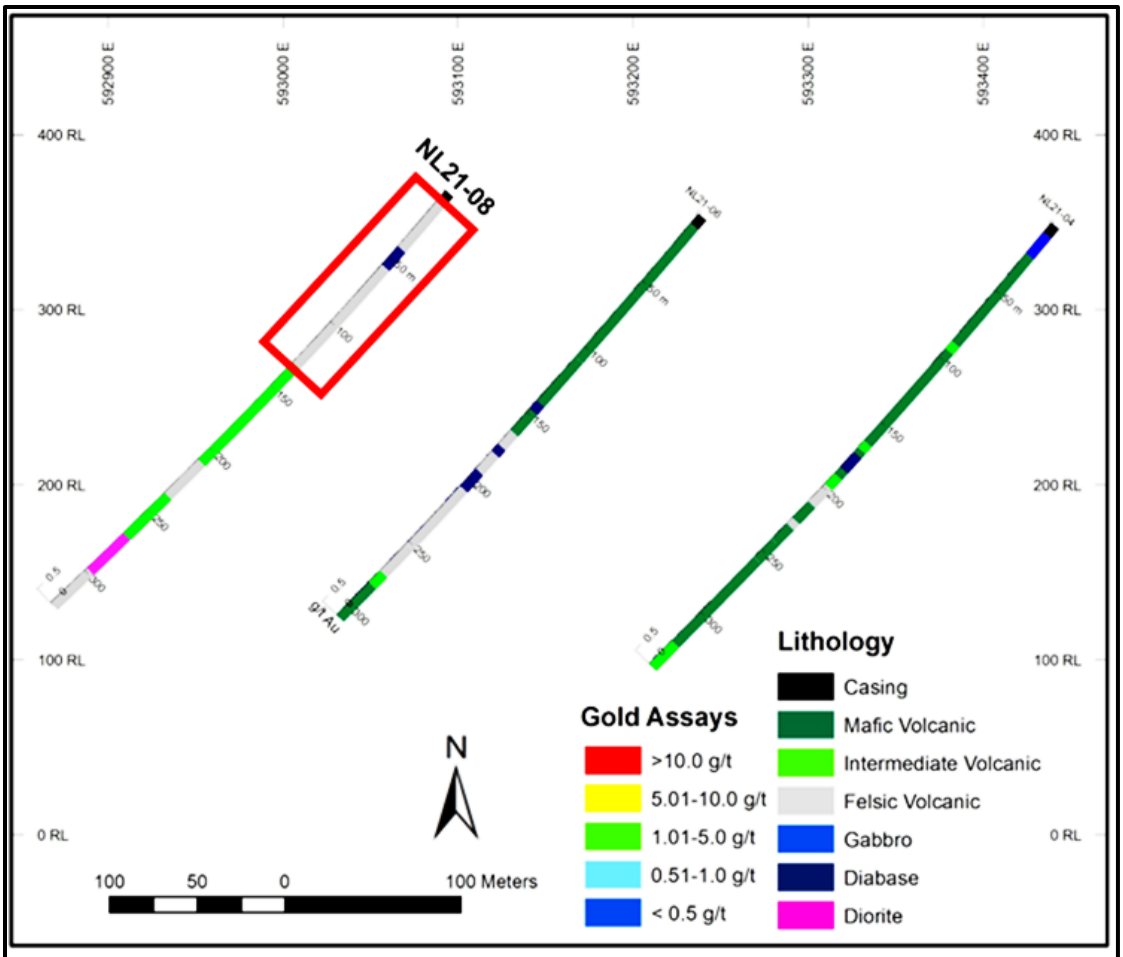

		TS24-05 Felsic volcanic, DDH NL21-08		
	Fraction	Z1	Z2	Z3
	Description	1 clr, cls, brkn el pr	1 clr, cls, brkn el pr	1 clr, cls, crkd, stubby euh pr
	U (ppm)	47.59	53.24	71.55
	Pb^T (pg)	28.32	31.52	41.81
	Pb_C (pg)	0.44	0.89	0.30
	Th/U	0.60	0.61	0.52
	$^{206}Pb/^{204}Pb$	3602.34	1965.58	7778.03
	$^{206}Pb/^{238}U$	0.51	0.51	0.51
	± 2s	0.00	0.00	0.00
	$^{207}Pb/^{235U}$	12.89	12.80	12.86
	± 2s	0.05	0.05	0.04
	$^{207}Pb/^{206}Pb$	0.18	0.18	0.18
	± 2s	0.00	0.00	0.00
Ages (Ma)	**$^{206}Pb/^{238}U$**	2672.03	2655.83	2664.60
	± 2s	6.96	7.70	5.66
	$^{207}Pb/^{235}U$	2671.74	2665.02	2669.57
	± 2s	3.35	3.87	2.74
	$^{207}Pb/^{206}Pb$	2671.53	2672.00	2673.33
	± 2s	1.97	3.07	1.63
	Discordance (%)	-0.02	0.74	0.40

TS24-07 Felsic volcanic, DDH GB21-26				
	Fraction	Z1	Z2	Z3
	Description	1 clr, cls, sharp, brkn el pr; ap incl	1 clr, cls, stubby sharp euh pr; ap incl	1 clr, cls, brkn 2:1 euh pr; melt/fluid incl?
	U (ppm)	156.31	111.35	162.89
	Pb^T (pg)	91.16	65.05	95.25
	Pb_C (pg)	0.71	1.03	1.04
	Th/U	0.50	0.53	0.52
	$^{206}Pb/^{204}Pb$	7223.46	3558.57	5162.57
	$^{206}Pb/^{238}U$	0.51	0.51	0.51
	± 2s	0.00	0.00	0.00
	$^{207}Pb/^{235U}$	12.88	12.83	12.86
	± 2s	0.03	0.04	0.04
	$^{207}Pb/^{206}Pb$	0.18	0.18	0.18
	± 2s	0.00	0.00	0.00
Ages (Ma)	**$^{206}Pb/^{238}U$**	2672.34	2661.68	2670.38
	± 2s	4.88	6.18	6.56
	$^{207}Pb/^{235}U$	2670.62	2667.05	2669.72
	± 2s	2.47	3.08	3.11
	$^{207}Pb/^{206}Pb$	2669.32	2671.12	2669.21
	± 2s	1.58	1.96	2.03
	Discordance (%)	-0.14	0.43	-0.05
Note:				
All analyzed fractions represent best optical quality (crack-, inclusion-, core-free), fresh (least altered) grains of zircon. Zircons were chemically abraded (modified after Mattinson, 2005).				
Abbreviations: Z - zircon; clr - clear; cls - colourless; crkd - cracked; el- elongate; pr - prism/prismatic; euh - euhedral; brkn - broken; incl - inclusion; ap - apatite.				
Pb^T is total amount (in picograms) of Pb.				
Pb_C is total measured common Pb (in picograms) assuming the isotopic composition of laboratory blank: 206/204 - 18.49±0.4%; 207/204 - 15.59±0.4%; 208/204 - 39.36±0.4%				
Pb/U atomic ratios are corrected for spike, fractionation, blank, and, where necessary, initial common Pb; 206Pb/204Pb is corrected for spike and fractionation.				
Th/U is model value calculated from radiogenic 208Pb/206Pb ratio and 207Pb/206Pb age, assuming concordance.				
Disc. (%) - per cent discordance for the given 207Pb/206Pb age.				
Uranium decay constants are from Jaffey et al. (1971).				